THERMAL ENVIRONMENT MODELING AND OPTIMIZATION OF GREENHOUSE IN COLD REGIONS

A Thesis Submitted to the College of

Graduate and Postdoctoral Studies

In Partial Fulfillment of the Requirements

For the Degree of Doctor of Philosophy

In the Division of Environmental Engineering

University of Saskatchewan

Saskatoon, Saskatchewan

By

MD SHAMIM AHAMED

PERMISSION TO USE

In presenting this thesis in partial fulfillment of the requirements for a post-graduate degree from the University of Saskatchewan, I agree that the libraries of this University may make it freely available for inspection. I further agree that permission for copying of this thesis in any manner, in whole or in part, for scholarly purposes may be granted by the professor or professors who supervised my thesis work or, in their absence, by the Head of the Department or the Dean of the College in which my thesis work was done. It is understood that any copying or publication or use of this thesis or parts thereof for financial gain shall not be allowed without my written permission. It is also understood that due recognition shall be given to me and to the University of Saskatchewan in any scholarly use which may be made of any material in my thesis.

Requests for permission to copy or to make other uses of materials in this thesis in whole or part should be addressed to:

Head of the Department of Chemical and Biological Engineering
University of Saskatchewan, 57 Campus Drive
Saskatoon, Saskatchewan, S7N 5A9
Canada
or
Dean of the College of Graduate and Postdoctoral Studies
University of Saskatchewan, 110 Science Place
Saskatoon, Saskatchewan, S7N 5C9
Canada.

ABSTRACT

Thermal simulation models for the time-dependent heating requirement of greenhouses are very important for the evaluation of various energy-saving technologies, and energy-efficient design of greenhouses based on local climates. A quasi-steady state thermal model "GREENHEAT" was developed using the programing language MATLAB for simulation heating requirement in conventional greenhouses. The model could predict the hourly heating requirement based on the input of hourly weather data, indoor environmental parameters, and physical and thermal properties of greenhouse building materials. The model was validated with measured data from a commercial greenhouse located in Saskatoon, Canada, and the monthly average error in prediction was found to be less than 5.0%. This study also reviewed various energy-saving technologies used in greenhouses in cold climate, and the GREENHEAT model allowed selections of commonly used ones in the simulation. The GREENHEAT model was used for evaluating the impact of various geometrical parameters on the heating requirement of the single span and multiple-span conventional greenhouses located in Saskatoon. Results showed that the east-west oriented gable roof greenhouse could be more energy-efficient for the multi-span gutter connected greenhouse whereas quonset shape as a free-standing single span greenhouse. The large span width could be beneficial for the single-span greenhouses, but the impact of increased span width could be negligible on the heating demand of multi-span greenhouses. The model was also used for an economic feasibility analysis of year-round vegetable production (tomato, cucumber, and pepper) in northern Saskatchewan, and tomato was found to be the most economical vegetable as compared to the cucumber and pepper.

Another heating simulation model CSGHEAT was developed to estimate of the supplemental heating requirement of mono-slope Chinese-style solar greenhouses (CSGs). This model is also a quasi-steady state thermal model using the programming language MATLAB, and it can simulates the hourly heating requirement of CSGs. The model was validated with experimental data from a CSG located in Winnipeg, Manitoba. The average error for prediction of the hourly heating requirement was found to be less than 8.7%. The model sensitivities to various geometrical and thermal parameters were studied. The results indicated that the thermal properties of cover, thermal blanket, and parameter insulation were the most important design parameters in CSGs.

Finally, the heating requirement in CSGs was modeled using TRNSYS simulation tool, and the predictions were compared with that of CSGHEAT. The result indicated that TRNSYS had serious limitations for modeling of greenhouse thermal environment, thereby high uncertainties could occur, thus was not suitable for greenhouse simulation.

Keywords: Heating simulation model; conventional greenhouse, Chinese-style solar greenhouse; energy-efficient design, TRNSYS.

CO-AUTHORSHIP STATEMENT

This thesis includes eight individual manuscripts, which form the core of this thesis, the candidate (Md Shamim Ahamed) developed conceptual ideas and theoretical frameworks of the developed models (GREENHEAT and CSGHEAT), carried out simulations and performed various analyses, and designed and prepared all manuscripts. I am or will be, the first author of all eight manuscripts.

The manuscripts presented in Chapter 2-5 and Chapter 7-8 are co-authored by Md Shamim Ahamed, Professor Huiqing Guo, and Professor Karen Tanino. The co-authors (Prof. Huiqing Guo and Prof. Karen Tanino) provided financial and laboratory support, guidance on various aspects of the research and critical reviews of the results and analysis presented in the manuscripts.

The sixth manuscript entitled 'Heating demand and economic feasibility analysis for year-round vegetable production in Canadian Prairies' greenhouses' (Chapter 6) is under review in the Journal of Information Processing in Agriculture. This manuscript is co-authored with Professor Huiqing Guo, Lisa Taylor, and Professor Karen Tanino. The co-authors (Prof. Huiqing Guo and Prof. Karen Tanino) provided valuable support and advice on various aspects of the research and manuscript preparation. Another co-author (Lisa Taylor) contributed to select the suitable crop species for greenhouse production in high northern latitudes, and also collected data about the yield rates, market prices, and vegetable consumption rates by average Canadian.

ACKNOWLEDGMENTS

First and foremost, I am proud to express my earnest and heartfelt gratitude and appreciation to thank my supervisor, Prof. Huiqing Guo for her guidance and advice throughout this dissertation. Her input has been invaluable and contributed immensely to the success of this research. I also would like to thank my co-supervisor Prof. Karen Tanino for her invaluable support and advice. I extend my sincere thanks to my committee Chair Prof. Oon-Doo Baik, and others committee members Prof. Chris Zhang, Prof. Lope G. Tabil, Prof. Carey J. Simonson, and Dr. Warren Helgason.

I would like to acknowledge Grandora Gardens for providing the data for validation of the GREENHEAT model. Special thanks go to the owner of Wenkai Greenhouse, Winnipeg for allowing us to experiment with his Chinese-style solar greenhouse, and also thanks to RLee Prokopishyn for helping to install the experimental setup in the greenhouse. I also would like to thanks all members of my research groups for their help, suggestions, and appreciation to my research work.

I wish to thank all lovely people in Bangladesh who graciously supported my 18 years of education in different institutes of Bangladesh. I also would like to express my gratitude to the College of Graduates and Postdoctoral Studies (CGPS), University of Saskatchewan, and Innovation Saskatchewan for providing funding for this research work.

Last but not least, I need to thank my parents and family members who helped me a lot unconditionally throughout my life. I would like to thank my parents Abdur Rashid Bapery and Rowshnara Begum, my elder brother Md Jane Alam, my family members, teachers, and friends for encouraging me and believing in me in every single step. Endless support, sacrifice, and encouragement from my lovely wife, Arifun Nahar, is highly acknowledged. Without her support, I might not have been able to finish this research work. Thank you, my sweet and lovely son, Saifan Ahamed, who brought a notable change in my life with lots of happiness.

DEDICATION

This thesis is dedicated to

My parents (late Abdur Rashid Bapery and Rowshnara Begum),

Wife (Arifun Nahar Mithila),

Son (Saifan Ahamed) and

My family members

TABLE OF CONTENTS

LIST OF TABLES

LIST OF FIGURES

CHAPTER 1

INTRODUCTION

A greenhouse is a building, an enclosed structure that creates a favorable micro-climate for crop production. Greenhouse technology has been used for around two centuries around the world for crop production (Gupta and Chandra, 2002). Crop production in greenhouses became popular to meet the food demand of an increasing number of world population because of much higher crop yields with more consistent crop quality than field crops. However, the greenhouse industry is one of the most energy demanding agricultural sectors as it requires control and creation of optimum environments for increased yield (Vadiee, 2011). The production costs in cold region greenhouses are extremely high because of high energy demand; thereby the growers might experience the marginal profit or high produce price at the consumer level. The heating and cooling costs in the greenhouse at northern latitudes including Canada could be about 75-85% of the total operating costs excluding cost associated with labor (Rorabaugh et al., 2002), whereas the heating energy demand represents about 70-80% of the total greenhouse energy demand (Sanford, 2011). The heating cost in Canadian greenhouse accounts about 15-20% of total greenhouse operational cost (Statistics Canada, 2008). Therefore, the greenhouse in cold regions such as the Canadian Prairies is highly energy inefficient and economically less profitable. As a result, Canadian Prairies including Saskatchewan mainly relies on the produce transported from southern U.S.A, British Columbia, and Ontario, which leads to higher product price and quality of product deteriorate over long-distance transportation. Therefore, energy efficient design of greenhouses and use of alternative energy such as industrial waste heat or solar energy can minimize the heating energy demand for greenhouse production at high northern latitudes. Also, Saskatchewan has the highest number of sunshine hours of any province that can be effectively capitalized through solar greenhouse technology, which can offset the need for high supplemental heating demand in conventional style greenhouses. The Chinese-style solar greenhouse (CSG) is typically an unheated envelope with transparent south facing covering and an insulated wall in the North, East, and West sides. CSGs are highly energy-efficient, and vegetables can grow without supplying

additional heat even when the average daily temperature falls below -10˚C in China (Tong et al., 2013). However, a significant amount of additional heating could be required under Canadian Prairies' weather conditions (Beshada et al., 2006).

Greenhouse thermal model for energy simulation is important for optimizing the energy-efficient designs and economic feasibility analysis of greenhouse production. Numerous studies have been performed to develop greenhouse thermal models to describe the heat and mass transfer process in greenhouses. Greenhouse thermal models can be classified into three groups such as: static, dynamic, and intermediate. Static models (Chiapale and Kittas, 1981; Morris, 1964) were mainly developed to determine the capacities of heating and cooling equipment and based on the approximated thermal gain and losses, and these models require yearly or monthly meteorological data. Intermediate models (Chandra and Albright, 1981; Garzoli, 1985; Jolliet et al., 1991; Tunc et al., 1985) are the improved versions of simple static models taking into account solar contributions; however, the validity is restricted to certain types of greenhouses and climates. Complex dynamic models (Cooper and Fuller, 1983; Sethi, 2009; Vanthoor et al., 2011) were mostly developed based on several energy balance equations of greenhouse interactive components such as cover, plants, floor, and indoor air. These models show good accuracy but need very complicated modification to estimate the heating energy requirement over long periods or for a greenhouse with different configurations. Also, most previous models did not consider the effect of plant evapotranspiration and environmental control systems on the energy balance of greenhouses. The environmental control systems including supplemental lighting, CO_2 supply system, and air circulation system are very important to maintain the optimum indoor environment for higher yield and better quality of crop production in northern greenhouses. Also, these environmental control systems have a significant contribution to the greenhouse heating requirement (Brault et al., 1989; Yang et al., 2015).

Structural design and operation techniques in the Chinese-style solar greenhouse are different than the conventional greenhouses, so the heat and mass transfer mechanisms in the CSGs are quite different. CSGs are relatively small with a large thermal mass in the north and side walls and in the ground which has important influences on the energy balance of greenhouses. A couple of thermal models (Guo et al., 1994; Meng et al., 2009; Tong et al., 2009; Yu et al., 2016) have been developed for evaluation of temperature variation at different components in the CSGs. Most of

these models are suitable to evaluate the temperature fluctuations in the greenhouse interactive components, but very complicated to simulate the heating requirement.

Also, the commercial building energy simulation tools such as TRNSYS, EnergyPlus, and DOE usually need complicated modifications for simulation of greenhouse heating requirements, and the existing greenhouse models have various limitations for simulation of the time-dependent heating requirement in greenhouses. In this study, two thermal models (GREENHEAT and CSGHEAT) were developed to simulate the heating requirement in the conventional and Chinese-style solar greenhouses. The developed models were also used for analysis of different energy saving measures and an economic feasibility study of greenhouse production at high northern latitudes.

1.1 Research purpose

1.1.1 Knowledge gaps

The following are the main knowledge gaps:

1. Many mathematical models have been developed for predicting the thermal environment of the conventional greenhouses. Most of these models were developed by using individual energy balance equations for the interactive components (plants, soil, cover, and air) of greenhouses. These models are very complex for long-term simulation because of large number of input parameters, and also need a significant modification for different types of greenhouses. On the other hand, simplified models based on the lumped estimation of the greenhouse heat sources and sinks are not precise because of some significant sources of heat exchange such as plant transpiration, supplemental lighting, CO_2 generator were neglected. Therefore, an accurate simplified model is needed for simulation of the time-dependent heating requirement in the conventional greenhouses.
2. There is no unique design for the conventional greenhouses because the performance of greenhouses varies based on location, size, and types of crops grown. A large number of studies have been conducted for the energy-efficient design of the conventional greenhouses based on local weather conditions in different parts of the world. However, very limited information is available about energy-efficient design of the conventional greenhouses for Canadian Prairies. Also, very limited information is available about the economic feasibility of greenhouse production in Canadian Prairies regions.

3. A few mathematical models have been developed to evaluate the thermal performance of Chinese-style solar greenhouse, and most of these models are developed based on the energy balance equation of the different components of the greenhouses. However, the existing models need very complicated modification for estimation of the time-dependent heating requirement in CSGs. Also, very limited information is available on energy-efficient design features of CSGs under Canadian weather conditions.

1.1.2 Objectives

The overall objective of this research was to develop the heating simulation models for greenhouses (conventional greenhouse, and Chinese-style solar greenhouse), and also analyze the heating requirements for different settings in greenhouses under Candain Prairies weather conditions. The following were the detailed objectives of the study:

1. Develop a thermal model with a solar radiation sub-model for simulation of time-dependent heating requirements in conventional greenhouses based on the input of local weather data, indoor environmental control parameters, and physical and thermal properties of greenhouse building materials and plants.
2. Identify the different techniques of heating energy saving options for the conventional greenhouses and the energy-efficient design of greenhouse parameters which vary depending on the location of greenhouses. Analyze the heating energy saving potential of the selected design parameters of the conventional greenhouses under the weather conditions of Saskatchewan.
3. Conduct the economic feasibility study of year-round production of common vegetables in a conceptually designed conventional greenhouse in northern Saskatchewan.
4. Develop a thermal model for simulation of the supplemental heating requirement in the Chinese-style solar greenhouses, and validate the model with experimental data from a typical Chinese-style solar greenhouse.
5. Analyze the sensitivity of the developed heating simulation model of the Chinese-style solar greenhouse, and evaluate the heating requirement for different settings in the study greenhouse.
6. Configure TRANSYS for predicting the heating requirement of CSGs, and also compare the performance of heating simulation model (CSGHEAT) with the commercial building simulation software TRANSYS.

1.2 Thesis outline

This thesis follows a manuscript based structure according to the College of Graduate and Postdoctoral Studies (CGPS) guidelines. After an introduction in Chapter 1, Chapters 2-9 represent eight individual manuscripts that been published, accepted, submitted or ready to submit for publication. Chapter 2 provides the background of the solar radiation sub-model which is a very important part of the modeling of greenhouse thermal environment. Chapter 3 describes the detailed principle of the GREENHEAT model for simulation of heating requirement in the conventional greenhouses, and also the validation of the model and the analysis of heating transfer in a conventional greenhouse under cold climate. Chapters 4 and 5 address the second objective of the study. Chapter 4 includes the comprehensive review of heating energy saving techniques for conventional greenhouses. Based on the developed model in Chapter 3, Chapter 5 presents the energy-saving potential of some design features of the conventional greenhouses in Saskatchewan. To address the objective 3, Chapter 6 incorporates the economic feasibility of greenhouse production in northern Saskatchewan.

Chapter 7 provides the comprehensive background of the heating simulation model and validation for the CSGHEAT model. Based on the developed model in Chapter 7, Chapter 8 includes the sensitivity of the CSGHEAT model for simulation of the heating requirement in CSGs. This chapter also includes the sensitivity of the different design features and environmental control parameters on the heating requirement in a typical Chinese-style solar greenhouse. Chapter 9 addresses the objective 6 and presents detailed description of a heating simulation model for CSG using the commercial building simulation tool TRNSYS. The performance of the TRNSYS model was compared with the developed thermal model (CSGHEAT) described in Chapter 7.

Finally, Chapter 10 summarizes the conclusions from the present study and also discusses opportunities for the future research on this topic.

1.3 Copyright and author permissions

Chapters 2 through 9 of this thesis consist of manuscripts that have been published, submitted or ready to submit for publication. Consistent with the copyright and author rights of each publisher, the manuscript citations are provided below. Permission to use or author rights from each publisher allowing the use of the manuscripts in this thesis is included in Appendix B. For all manuscripts,

as per the guidelines of the College of Graduate and Postdoctoral Studies, for manuscript-style theses, the student is the first author and supervisor (s) the second author (s).

Chapter 2: Ahamed, M. S., Guo, H., and Tanino, K. (2018). Evaluation of a cloud cover based model for estimation of hourly global solar radiation in Western Canada. International Journal of Sustainable Energy, 1-10. DOI: https://doi.org/10.1080/14786451.2018.1443934

Chapter 3: Ahamed, M. S., Guo, H., and Tanino, K. (2017). A quasi-steady state model for predicting the heating requirement of conventional greenhouses in cold region. Information Processing in Agriculture, 1-13. DOI: https://doi.org/10.1016/j.inpa.2017.12.003

Chapter 4: Ahamed, M. S., Guo, H., and Tanino, K. (2018). A review of different techniques for reducing the heating cost of conventional winter greenhouses. Submitted to the International Journal of Energy Research; submission no. ER_18_9421.

Chapter 5: Ahamed, M. S., Guo, H., and Tanino, K. (2018). Energy efficient design of greenhouse for Canadian Prairies using a heating simulation model. International Journal of Energy Research, 1-10. DOI: https://doi.org/10.1002/er.4019

Chapter 6: Ahamed, M. S., Guo, H., Taylor, L., and Tanino, K. (2018). Heating demand and economic feasibility analysis for year-round vegetable production in Canadian Prairies' greenhouses. Submitted to the Information Processing in Agriculture; submission no. IPA_2018_15.

Chapter 7: Ahamed, M. S., Guo, H., and Tanino, K. (2018). A thermal model for simulating supplemental heating requirements in Chinese-style solar greenhouses. Submitted to the Computers and Electronics in Agriculture; submission no. COMPAG_2018_106.

Chapter 8: Ahamed, M. S., Guo, H., and Tanino, K. (2018). Sensitivity analysis of CSGHEAT model for estimation of heating energy consumption in a Chinese-style solar greenhouse. Submitted to the Computers and Electronics in Agriculture; submission no. COMPAG_2018_316.

Chapter 9: Ahamed, M. S., Guo, H., and Tanino, K. (2018). Modeling of heating demand in the Chinese-style solar greenhouse using transient building energy simulation model TRNSYS. The manuscript is ready to submit to the Journal.

CHAPTER 2

EVALUATION OF A CLOUD COVER BASED MODEL FOR ESTIMATION OF HOURLY GLOBAL SOLAR RADIATION IN WESTERN CANADA

(The manuscript presented in this chapter has been published in the International Journal of Sustainable Energy, DOI: https://doi.org/10.1080/14786451.2018.1443934)

Overview

The simulation of solar radiation is a very important part of the development of greenhouse thermal models. The input of solar radiation data for simulation of greenhouse microclimates could be difficult since the solar radiation data are not easily available for most locations, especially in remote areas. In this chapter, the performance of the cloud cover based solar radiation model (Kasten-Czeplak model) was evaluated for four different locations in Western Canada. The simulated solar radiation from the Kasten-Czeplak model was compared with the data from the National Solar Radiation Database (NSRDB). The estimation of solar radiation is one of the very important part for modeling of greenhouse thermal environment. Results presented in this chapter fulfill part of the first and fourth objectives of this thesis and more configurations are studied in Chapters 3 and 7. The Kasten-Czeplak model was used as a sub-model of the developed thermal models for the conventional (Chapter 3) and Chinese-style solar greenhouses (Chapter 7). As the lead author of this manuscript, I conducted the research, analyzed the results, prepared the manuscript, incorporated co-authors comments, and addressed the reviewers' comments. The coauthors (Professor Huiqing Guo, and Professor Karen Tanino) have contributed to this manuscript through providing technical guidance to conduct the research and constructive review to improve the quality of research.

Abstract

Cloud cover based solar radiation models are relatively simple and convenient as the models require the input of cloud cover data which are mostly available from the meteorological stations. In this study, the performance of a cloud cover based solar radiation model (Kasten-Czeplak model) with original or locally fitted coefficients was evaluated for estimating the hourly global solar radiation for four different locations in Western Canada. The average value of R^2, mean bias error, and root mean square error are 0.69, -61.6 W m^{-2}, and 157.9 W m^{-2}, respectively, for the model with original coefficients, whereas 0.82, 4.4 W m^{-2}, 107.1 W m^{-2} with locally fitted coefficients. Results show that the Kasten-Czeplak model with locally fitted coefficients satisfactorily estimated the hourly solar radiation of four different locations in Western Canada. Also, the results indicate that the model with original coefficients has very limited accuracy under intermediate cloud cover conditions.

2.1 Introduction

Continuous time series data of solar radiation are very important for the evaluation of building thermal performance and analysis the potential of different solar application systems. However, the time series solar radiation data are mainly available in the developed countries, whereas very limited resources in the developing countries. Although the solar radiation stations do exist in the developing countries, there are uncertainties regarding the quality of data obtained. Also, the measured data from a given solar station become less accurate for a location that is beyond 50 km from the measuring station (Younes and Muneer, 2007). The surface weather stations which recording the solar radiation data is very small compared to the number of meteorological stations that record meteorological data including temperature, precipitation, relative humidity, sunshine duration, and cloud cover. Also, the observational records for solar radiation are usually short and often have missing data because of equipment malfunction (Cutforth and Judiesch, 2007). Therefore, many empirical models have been developed for estimation of global solar radiation by using commonly available meteorological data such as sunshine duration, temperature, precipitation, relative humidity, and cloud cover. The sunshine based solar radiation models (Al-Mostafa et al., 2012; Bakirci, 2008; Trnka et al., 2005) are usually considered to be more reliable because the sunshine data are precisely recorded by a sunshine recorder whereas cloud cover data are based on the visual estimation and satellite image. Also, the variation of solar radiation explained by sunshine duration is 70-85% whereas 50% quoted against the cloud amount (Bennett, 1969). However, the sunshine duration data are not easily available from the weather stations. Conversely, the temperature-based models (Spokas and Forcella, 2006; Supit and van Kappel, 1998) could be the most convenient tool for estimation of solar radiation because of the wide availability of air temperature data, but accuracy is limited for hourly simulation as these models estimate the solar radiation based on the daily maximum and minimum temperature. However, the cloud cover based models can provide comparatively accurate predictions, and cloud cover data are relatively easy to access from weather stations (Kim et al., 2014).

Previous studies (El-Metwally, 2004; Younes and Muneer, 2007) shows that the performance of solar radiation models could be significantly different depending on the location of the study area. Hence, it is very important to evaluate the performance of these models against the local dataset, and also need to determine the local coefficients for estimation of solar radiation with good accuracy. De Jong & Stewart (1993) estimated the daily total solar radiation of Western Canada

by using temperature and precipitation based model. Similarly, Barr et al. (1996) evaluated the solar radiation model by using sunshine duration and temperature data. Kahimba et al. (2009) evaluated the SolarCalc model developed by Spokas & Forcella (2006) for estimating the hourly incoming solar radiation of different locations in Western Canada by using daily total precipitation (mm), and daily maximum and minimum air temperatures. Jeong et al. (2016) used several empirical models to simulate daily solar radiation in Quebec using two meteorological inputs such as daily temperature and relative humidity. To the best of our knowledge, no previous studies are found related to the prediction of solar radiation from cloud cover data in Canada. Therefore, the objective of this study is to evaluate the selected cloud cover based solar radiation models for different locations in Western Canada. The preliminary results from this study were presented in the CSBE/SCGAB Annual Conference, Winnipeg, Canada (Ahamed et al., 2017a).

2.2 Cloud cover solar radiation models (CRM)

Different types of empirical models have been developed for estimating the daily/hourly solar radiation using cloud cover information. Most of these models (Black 1956; Sarkar 2016; Badescu 1999; Bennett 1969) are used for estimating the daily average total solar radiation using cover cloud data. Kasten and Czeplak (1980) developed a cloud cover based solar radiation model by using ten-years (1964–1973) of continuous hourly data from Hamburg, Germany. The model used the cloud amount in Oktas which ranges from 0 to 8; zero Oktas indicate a completely clear sky and 8 Oktas means a completely overcast sky. Younes and Muneer (2007) evaluated the performance of several cloud cover based models for estimation of hourly global solar radiation for different locations in England. Results show that the Kasten-Czeplak model performed relatively better than the other models. Also, the Kasten-Czeplak model has been tested against the dataset for different locations over the world (Younes and Muneer 2007; Badescu and Dumitrescu 2014a; Kim, Baltazar, and Haberl 2014; Badescu and Dumitrescu 2014b), but the model has not been evaluated against the dataset from high northern latitudes. Therefore, the Kasten-Czeplak models with the original coefficients and locally fitted coefficients were considered for evaluating their performance against the dataset of four different locations in Western Canada. For this analysis, the original Kasten-Czeplak model is referred to as M1. According to the Kasten & Czeplak (1980), the global solar radiation (I_g) on any horizontal surface under cloud cover condition can be estimated by using the following equation:

$$I_g = I_{gc}(1 - 0.75\left(\frac{N}{8}\right)^{3.4}) \quad (2.1)$$

where I_{gc} is the clear sky global solar radiation (W m^{-2}); N is the cloud cover (Oktas).

The Kasten-Czeplak model with locally fitted coefficients can be written as follows:

$$I_g = I_{gc}(1 - A\left(\frac{N}{8}\right)^{B}) \quad (2.2)$$

where A and B are the local coefficients. The model with locally fitted coefficients is referred to as M2 for this analysis.

The Katen-Czeplak model estimates the clear sky solar radiation based on empirical equation related to the solar altitude angle which is relatively simple as the model avoids the atmospheric attenuation of solar radiation (Orsini et al., 2002). The clear sky solar radiation on the earth surface depends on the solar altitude angle and local atmospheric turbidity. By considering the atmospheric turbidity, the clear sky global solar radiation on the horizontal surfaces, and the direct normal irradiance (I_N) on any terrestrial region can be calculated as follows (Tiwari, 2003):

$$I_{gc} = I_N \cos\theta_z + \frac{1}{3}(I_{ex} - I_N)\cos\theta_z \quad (2.3)$$

$$I_N = I_{ex} \exp\left[\frac{-T_R}{(0.9+9.4\sin\alpha)}\right], \alpha = 90 - \theta_z \quad (2.4)$$

where θ_z is the zenith angle (degrees), α is the solar altitude angle (degrees).

According to Spencer (1971), the extraterrestrial radiation from the sun on a surface normal to the sun's rays on the n^{th} day of the year is given by:

$$I_{ex} = I_{sc}\left[1 + 0.033 \times \cos\left(360 \times \frac{n-3}{365}\right)\right] \quad (2.5)$$

where I_{sc} is the solar constant (1367 W m^{-2}), n is the day of the year.

2.3 Meteorological data for the study

Four representative locations in Western Canada including Saskatoon, Winnipeg, Fort McMurray, and Vancouver, were considered for this study. Twelve years (2004-2015) of hourly meteorological data including solar radiation and cloud cover data were collected from the National Solar Radiation Data Base (NSRDB). Hubbard (1994) reported that the length of the dataset should be more than one year to characterize the seasonal pattern of special variability. Gueymard (2000) recommended that a minimum of three-year datasets are needed to validate the solar radiation models. Previous studies (Badescu, 2002; Muneer and Gul, 2000; Younes and

Muneer, 2007) used continuous time series data for validation of solar radiation models, and reported that more than one-year data would be logical enough to characterize the temporal evolution of metrological data. Hence, the data from the NSRDB were grouped into two datasets such as 75% as training dataset and 25% as a test dataset. The training dataset (2004-2012) was used for estimation of the local coefficients by fitting against the local dataset for all selected locations, and the test dataset (2013-2015) was considered for validation of the models. The details of geographical information of the selected locations and the estimated local coefficients are listed in Table 2.1.

Table 2.1: The description of sample location in Western Canada and local coefficients of the Kasten-Czeplak model.

Locations	Latitude (˚N)	Longitude (˚W)	Altitude (m)	Coefficient A	Coefficient B	Data period
Saskatoon	52.13	106.66	456	0.54	0.43	2004-2012
Winnipeg	49.89	97.18	232	0.57	0.48	2004-2012
Fort McMurray	56.73	111.38	261	0.55	0.32	2004-2012
Vancouver	49.25	123.06	45	0.61	0.36	2004-2012

2.4 Statistical indicators for model evaluation

The statistical indices including the coefficient of determination (R^2), mean bias error (MBE), root mean square error (RMSE), and t-statistic (t-stat) were considered to evaluate the adequacy of the cloud cover based solar radiation models. The MBE can be the indicator to figure out the tendency of overestimation or underestimation of the model, and the RMSE can be used to figure out the degree of dispersion of the estimated radiation against the measured radiation (Kim et al., 2014). Another statistical indicator (t-statistic) was proposed by Stone (1993) for evaluation of solar radiation model, and the indicator allows models to be compared for performance evaluation with other models. The negative value of MBE would indicate the overestimation while the positive indicates underestimation, and low values of RMSE and t-stat are desirable for higher accuracy of the model. The MBE, RMSE, and t-stat can be estimated by the following equations (Stone, 1993):

$$\mathrm{MBE} = \frac{\sum(I_o - I_e)}{n} \quad (2.6)$$

$$\mathrm{RMSE} = \sqrt{\frac{\sum(I_o - I_e)^2}{n}} \quad (2.7)$$

$$t - \mathrm{stat} = \sqrt{\frac{\mathrm{MBE}^2(n-1)}{\mathrm{RMSE}^2 - \mathrm{MB}^2}} \quad (2.8)$$

where I_o is the observed/measured solar radiation (W m^{-2}); I_e is the estimated solar radiation (W m^{-2}); and n is the number of data points.

Dimensionless qualities rMBE and rRMSE are defined by (Badescu and Dumitrescu 2014a):

$$\mathrm{rMBE} = \frac{\mathrm{MBE}}{\check{I}} \quad (2.9)$$

$$\mathrm{rRMSE} = \frac{\mathrm{RMSE}}{\check{I}} \quad (2.10)$$

where $\check{I}$ is the mean value of measured global solar irradiation (W m^{-2}).

2.5 Results and discussion

2.5.1 Cloud cover

Hourly cloud cover data (2013-2015) from the NSRDB for four different locations in Western Canada were analyzed, and the frequency of cloud cover occurrence is shown in Figure 2.1. The peak frequency of occurrence is observed at the value of 0 and 4 Oktas. The maximum occurrence of 26.9% is observed at the value of 0 Oktas in Vancouver, and the minimum 21.7% in Fort McMurray. The peak frequency of 4 Oktas accounting 29.9% is observed in Fort McMurray and the minimum value of 21.1% in Winnipeg. The second most frequent cloud cover is 7 Oktas, accounting for 24.1%, 22.1%, 24.6%, and 18.4%, respectively, for Saskatoon, Winnipeg, Fort McMurray, and Vancouver. The lowest frequency of occurrence of cloud cover less than 2.0% is observed for the value of 2 and 5 Oktas.

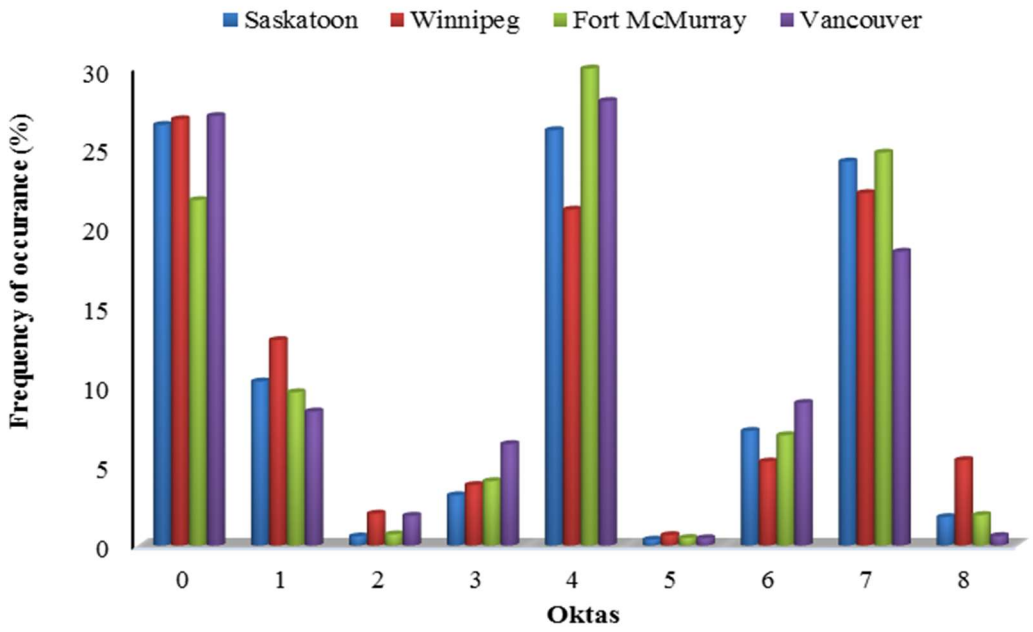

Figure 2.1: Hourly frequency of occurrence of cloud cover.

2.5.2 Solar radiation

The estimated global solar radiation from the Kasten-Czeplak model was compared with the solar radiation data of 2013-2015 from the NSRDB. Figure 2.2-2.5 show the comparative performance of the Kasten-Czeplak model with original and locally fitted coefficients for four different locations in Western Canada. The scatterplots indicate that the cloud cover model (M2) with locally fitted coefficients performs well as compared the model (M1) with the original coefficients. Also, the figures indicate that the model with the original coefficients has a relatively higher tendency to overestimate solar radiation as compared the model with the locally fitted coefficients. The overdispersion in estimation from the model with original coefficients is reduced for using of local coefficients because the local coefficients were estimated based on the measured dataset. The estimated solar radiation from the model (M1) is over-dispersed because the effect of local atmospheric composition, cloud composition, and height, and elevation of location, were not considered in solar radiation estimation.

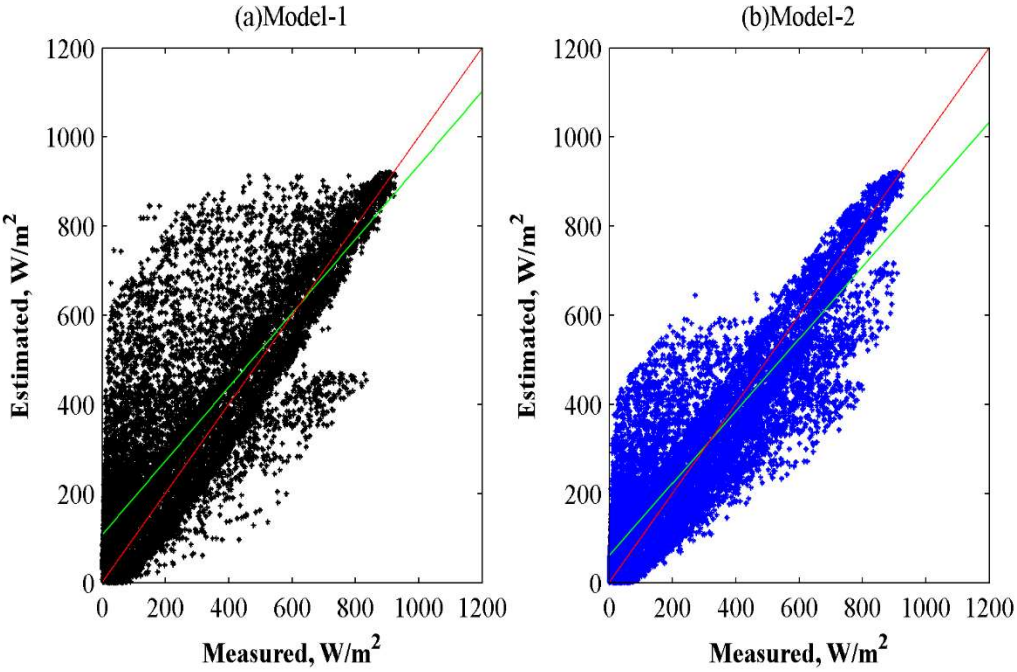

Figure 2.2: Scatterplots between measured and estimated global solar radiation by the Kasten-Czeplak models, (a) with the original coefficients (b) locally fitted coefficients in Saskatoon.

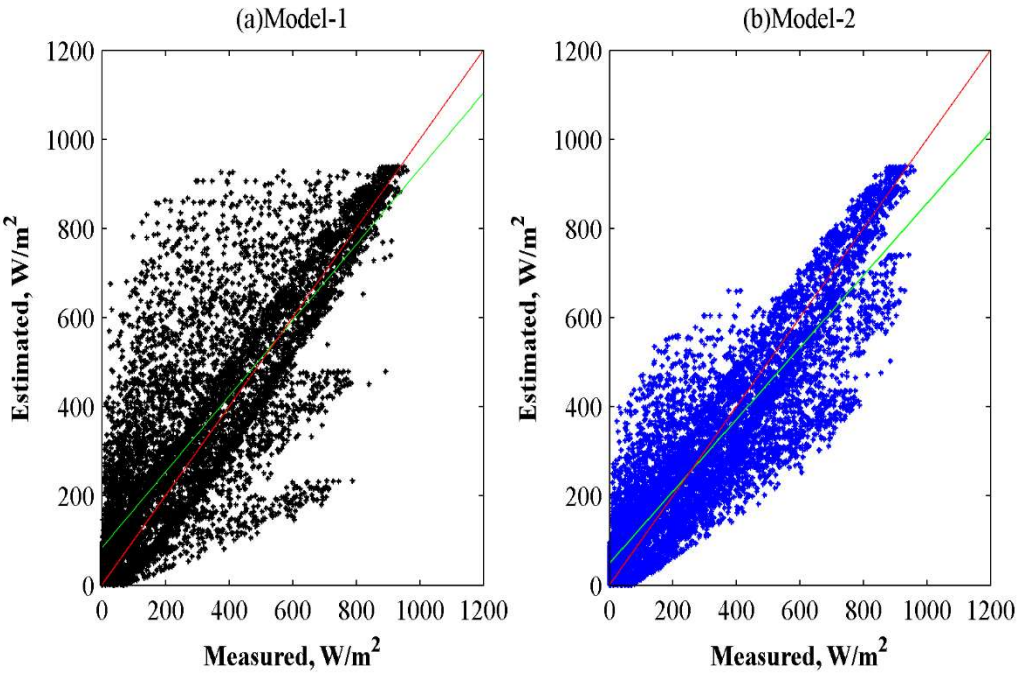

Figure 2.3: Scatterplots between measured and estimated global solar radiation by the Kasten-Czeplak models, (a) with the original coefficients (b) locally fitted coefficients in Winnipeg.

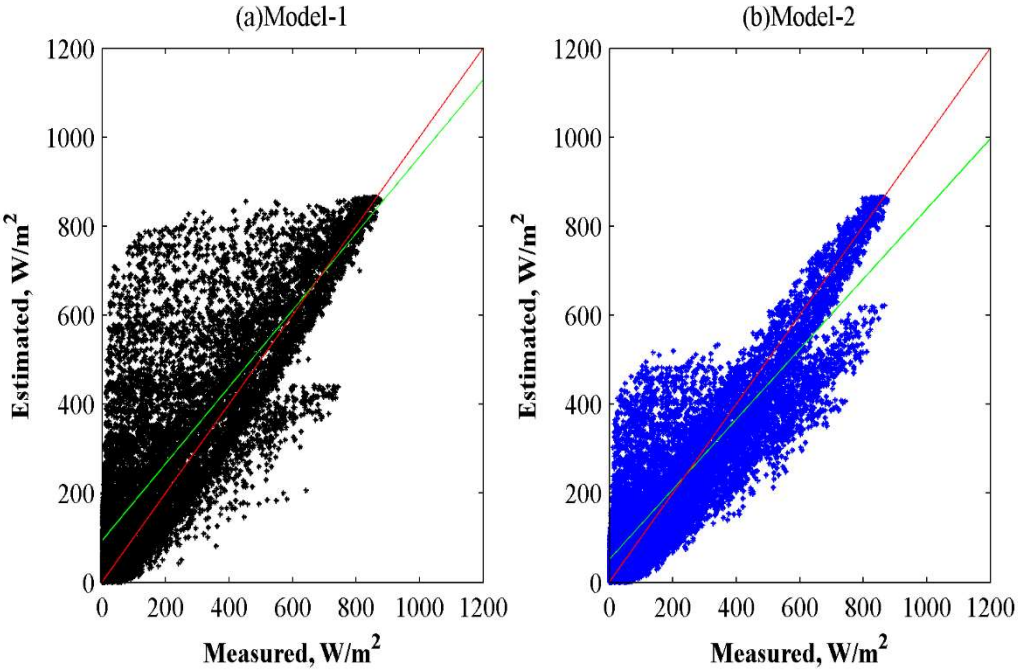

Figure 2.4: Scatterplots between measured and estimated global solar radiation by the Kasten-Czeplak models, (a) with the original coefficients (b) locally fitted coefficients in Fort McMurray.

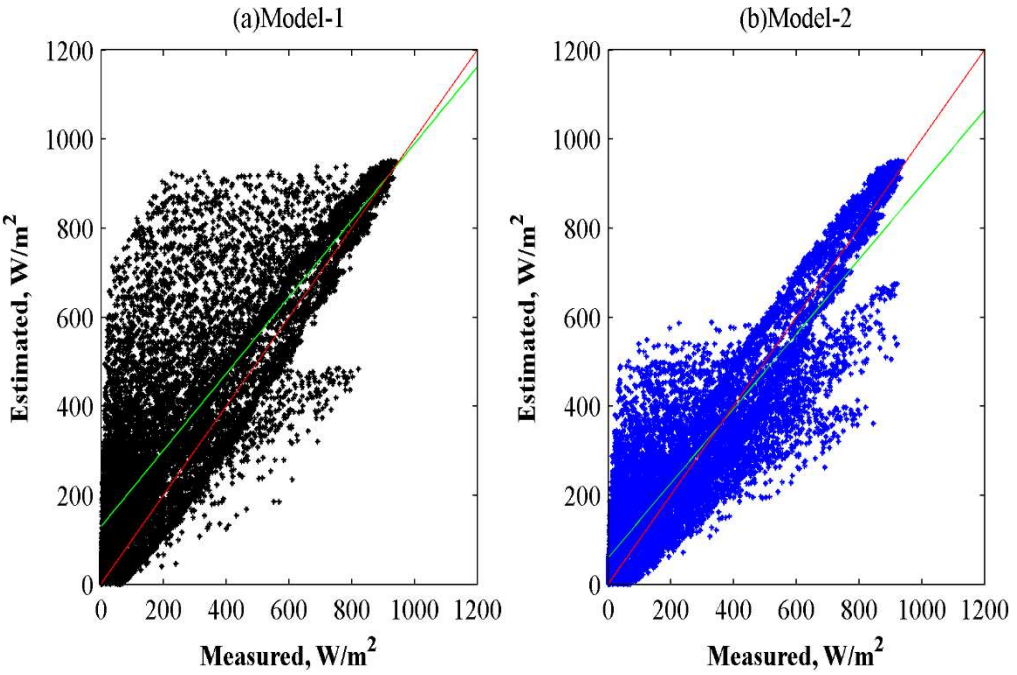

Figure 2.5: Scatterplots between measured and estimated global solar radiation by the Kasten-Czeplak models, (a) with the original coefficients (b) locally fitted coefficients in Vancouver.

Table 2.2 shows the statistical indicators obtained for four different locations of the model with original coefficients and locally fitted coefficients. The relative difference between the average measured and estimated solar radiation is less than 5.0% for the Kasten-Czeplak model with local coefficients whereas more than 14% for the model with original coefficients. The coefficient of determination (R^2) value is ranging from 0.81 to 0.83 for the model with the local coefficients, whereas from 0.68 to 0.70 with the original coefficients. The negative value of MBE indicates the model with the original coefficients has greater tendency to overestimate solar radiation for all the selected locations. The RMSE and t-stat values are noticeably lower for the Kasten-Czeplak model with the locally fitted coefficients. The RMSE value with the local coefficients varies between 101.0 and 111.0 W m^{-2}, with an average RMSE of 107.1 W m^{-2}, whereas from 150.0 to 177.0 W m^2, with an average value of 157.9 W m^{-2} for the model with original coefficients. Based on the results of statistical indicators, it shows that the estimation of hourly solar radiation from the model with local coefficients is more consistent with the measured data. Also, the performance of the model with local coefficients is close enough to the results from other studies (Ahamed et al., 2017b; Badescu and Dumitrescu, 2016, 2014b; Kim et al., 2014; Younes and Muneer, 2007) for evaluation of the Kasten-Czeplak model with locally fitted coefficients. The statistical indicators value for the model with original coefficients is also quite close to the results from other types of models (Spokas and Forcella, 2006; Younes and Muneer, 2007) with their site-specific coefficients. Badescu and Dumitrescu (2014b) also adopted accuracy criteria for evaluation of solar radiation models for estimation of cloudy sky global irradiation. A threshold value of rMBE (±5-10%) and rRMSE (35-45%) was considered as good enough for computation of hourly solar irradiance. Based on the accuracy criteria, the model (M2) with local coefficients could be considered as good because the rMBE and rRMSE values are less than 5.0% and 40.0%, respectively. However, the rMBE value varies between 12.0% and 33.0% for the model (M1) with original coefficients, and the rRMSE value between 49.0% and 64.0%. Therefore, the performance of the model with local coefficients could be considered as poor for computation of solar radiation at high northern latitudes.

Table 2.2: Comparison of statistical indicators for estimating the hourly solar radiation for four different cities in Western Canada.

Location	Model	Observed average hourly solar radiation (W m^{-2})	Estimated average hourly solar radiation (W m^{-2})	R^2	MBE (W m^{-2})	RMSE (W m^{-2})	t-stat
Saskatoon	M1	284.6	354.9	0.69	-56.7	154.1	43.9
	M2		291.9	0.82	-7.3	108.9	7.7
Winnipeg	M1	304.7	348.5	0.70	-38.3	150.7	30.1
	M2		295.4	0.82	9.3	110.4	9.7
Fort McMurray	M1	243.6	304.2	0.68	-60.2	150.5	49.8
	M2		242.9	0.81	0.6	101.0	0.67
Vancouver	M1	274.4	365.7	0.69	-91.0	176.2	68.9
	M2		289.6	0.83	15.1	107.9	16.2

As the cloud cover is the only input parameter for the model; therefore, the good quality of cloud cover data is important to get a relatively better result from the model. The cloud cover observer has general tendency to underestimate cloud cover under low overcast condition but overestimates under high overcast condition (Brinsfield et al., 1984). Therefore, the evaluation of the model's performance under different cloud condition would be helpful for understanding their limitation for simulation of the global solar radiation. The cloud cover data were separated into three groups such as clear skies ($N \leq 1$), intermediate skies ($1< N <7$), and overcast skies ($N \geq 7$). The performance evaluation indicators value for selected the models under different sky conditions is given in Table 2.3. Sometimes, it becomes difficult to decide better performed solar radiation models from the statistical indicators. Therefore, a scoring system recommended by Muneer & Gul (2000) was used for better understanding of each model's performance. The score is the sum of absolute values of MBE and RMSE for different skies conditions, and the lowest score would be the best.

Table 2.3: Evaluation of cloud cover model based on different sets of cloud cover data.

Location	Model	Cloud cover (Oktas)	R^2	MBE (W m^{-2})	RMSE (W m^{-2})	Scores (W m^{-2})
Saskatoon	M1	$N \leq 1$	0.94	6.6	60.7	67.3
		$1< N <7$	0.60	-164.6	225.0	389.6
		$N \geq 7$	0.62	11.3	125.4	136.7
	M2	$N \leq 1$	0.94	14.9	79.8	94.7
		$1< N <7$	0.61	-30.9	129.9	160.8
		$N \geq 7$	0.64	9.0	117.2	126.2
Winnipeg	M1	$N \leq 1$	0.95	-1.9	62.1	64.0
		$1< N <7$	0.66	-150.7	211.5	362.2
		$N \geq 7$	0.58	59.1	152.8	211.9
	M2	$N \leq 1$	0.93	23.4	90.7	114.1
		$1< N <7$	0.68	-15.7	119.6	135.3
		$N \geq 7$	0.70	21.2	126.2	147.4
Fort McMurray	M1	$N \leq 1$	0.96	9.3	52.8	62.1
		$1< N <7$	0.61	-149.6	210.9	360.5
		$N \geq 7$	0.68	8.3	101.8	110.1
	M2	$N \leq 1$	0.94	22.7	76.6	79.72
		$1< N <7$	0.61	-14.1	118.1	132.2
		$N \geq 7$	0.67	-4.2	97.3	101.5
Vancouver	M1	$N \leq 1$	0.95	-10.9	63.6	74.5
		$1< N <7$	0.59	-188.9	248.5	437.4
		$N \geq 7$	0.60	-23.9	119.5	143.4
	M2	$N \leq 1$	0.93	4.2	80.7	84.9
		$1< N <7$	0.59	-30.4	125.8	156.2
		$N \geq 7$	0.60	20.2	112.9	133.1

The results indicate that the model performs better under clear skies both with original and local coefficients. However, the model with original coefficients performs poorly under intermediate skies conditions because original coefficients do not consider the local atmospheric effect on solar

radiation. The average score with original coefficients under intermediate skies conditions is 387.4 W m^{-2}, whereas about 146.1 W m^{-2} with the locally fitted coefficients. The performance of the model with local coefficients is relatively poor under intermediate and overcast skies conditions compared to the clear skies conditions because the cloud cover observation is a relative measurement so the higher error in estimation could be occurred due to the error in cloud cover observation. The MBE values indicate both models have a general tendency to underestimate the solar radiation for high overcast conditions and an opposite trend for low overcast conditions because the cloud cover observer usually underestimates cloud cover under low overcast condition but overestimates under high overcast condition.

2.6 Conclusions

In this study, the cloud cover model based Kasten-Czeplak model was evaluated for estimation of hourly global solar radiation of four different locations in Western Canada. The results show that the observed solar radiation data from the NSRDB is better consistent with the estimated solar radiation from the Kasten-Czeplak model using locally fitted coefficients. The results also indicate that the model with original coefficients performs poorly under intermediate skies condition which could be improved significantly using local coefficients. Henceforth, it is recommended to use the Kasten–Czeplak model with local coefficients for estimation of hourly global solar irradiation.

Acknowledgement

The preliminary results from this study were published in the CSBE/SCGAB Annual Conference, Winnipeg, Canada, and 6-10 August 2017. The authors are very thankful to the College of Graduate and Postdoctoral Studies (CGPS) at the University of Saskatchewan, and Innovation Saskatchewan for their financial support to this research.

CHAPTER 3

A QUASI-STEADY STATE MODEL FOR PREDICTING THE HEATING REQUIREMENTS OF CONVENTIONAL GREENHOUSES IN COLD REGIONS

(The manuscript presented in this chapter has been published in the Journal of Information Processing in Agriculture, DOI: https://doi.org/10.1016/j.inpa.2017.12.003)

Overview

Thermal model for simulation of greenhouse heating requirement is essential for studying the energy-efficient design and economic feasibility of greenhouse production under particular weather conditions. This chapter includes the detailed theoretical principle for the development of the heating simulation model for the conventional greenhouses (Objective 1), and also the analysis of different heat sources and sinks in a typical conventional style greenhouse at high northern latitudes. The developed model (GREENHEAT) presented in this chapter was used for the energy-efficient design of conventional greenhouse for Canadian Prairies (Chapter 5) and economic feasibility study of year-round greenhouse production (Chapter 6). As the lead author of this manuscript, I conducted the research, analyzed the results, prepared the manuscript, incorporated co-authors comments, and addressed the reviewers' comments. The coauthors (Professor Huiqing Guo, and Professor Karen Tanino) have contributed to this manuscript through providing technical guidance to conduct the research and constructive review to improve the quality of research.

Abstract

A time-dependent, quasi-steady state thermal model (GREENHEAT) based on the lumped estimation of heat transfer parameters of greenhouses has been developed to predict the hourly heating requirements of conventional greenhouses. The model was designed to predict the hourly heating requirements based on the input of greenhouse indoor environmental control parameters, physical and thermal properties of crops and construction materials, and hourly weather data including temperature, relative humidity, wind speed, and cloud cover. The model includes all of the heat transfer parameters in greenhouses including the heat loss for plant evapotranspiration, and the heat gain from environmental control systems. Results show that the predicted solar radiation data from the solar radiation sub-model are a reasonable fit with the data from the National Solar Radiation Database (NSRDB). Thermal analysis indicates environmental control systems could reduce 13-56% of the total heating requirements over the course of a year in the study greenhouse. During the winter season, the highest amount of greenhouse heat is lost due to conduction and convection, and the heat used for evapotranspiration is dominant in the summer. Finally, the model was validated with actual heating data collected from a commercial greenhouse located in Saskatoon, and the results show that the model satisfactorily predicts the greenhouse heating requirements.

Nomenclature

A_c, A_f, A_p	area of cover, floor, and plant, m^2
A_n, A_t	area of non-transparent and transparent surfaces, m^2
CF	cloud cover factor, Oktas
C_{pa}	specific heat of air, J kg^{-1} K^{-1}
E_m	motor efficiency, %
F_c, F_{sk}	cover view factor and sky view factor, dimensionless
F_p	perimeter heat loss factor, W m^{-1} K^{-1}
F_{hc}, F_a	heat conversion factor, and lighting allowance factor, dimensionless
F_{um}, F_{ul}	motor load factor, and motor use factor, dimensionless
G_r	Grashof number, dimensionless
g	acceleration of gravity, m s^{-2}
H	depth of underground soil for constant temperature, m
h_a	thermal air conductance, W m^{-2} K^{-1}
h_i, h_o	convection coefficient for indoor and outdoor surfaces, W m^{-2} K^{-1}
I_b, I_d	direct beam radiation, and diffuse radiation on horizontal surfaces, W m^{-2}
I_{bc}, I_{dc}	clear sky direct beam radiation and diffuse radiation, W m^{-2}
I_g	global solar radiation on horizontal surface, W m^{-2}
I_{gc}	clear sky global solar radiation on horizontal surface, W m^{-2}
I_{ex}, I_N, I_{sc}	extraterrestrial solar radiation, sky beam normal radiation, and solar constant (Wm^{-2})
k_a, k_c, k_s	thermal conductivity of air, cover, and soil, W m^{-1} K^{-1}
k	thermal conductivity of i^{th} section in composite wall, W m^{-1} K^{-1}
L_c, L_f	characteristic length of convective surfaces and plant leaves, m
L_v	latent heat of water vaporization, J kg^{-1}
MFR	carbon dioxide supply rate in greenhouse, kg m^{-2} hr^{-1}
M_T	moisture transfer rate, kg s^{-1}
n	day of the year, n=1, for January 1^{st}
N	number of air exchange per hour
N_c	number of layer in covering
N_f	number of re-circulation fans
Nu	Nusselt number, dimensionless

NHV	net heating value of fuel, MJ kg^{-1}
P	perimeter of greenhouse, m
P_m	motor power rating, W
P_r	Prandtl number, dimensionless
PR	CO_2 production rate, kg/kg fuel
p	atmospheric pressure, kPa
p_w	partial pressure of the water vapor, kPa
p_{ws}	partial pressure at saturation, kPa
Q	Heat transfer rate, W
R_a, R_s	aerodynamic resistance and stomatal resistance, s m^{-1}
R_e	Reynold number, dimensionless
S	total solar radiation entering the greenhouse, W
T_c, T_i, T_o	cover temperature, indoor temperature, and outdoor temperature, K
T_s, T_{sk}	underground soil temperature and sky temperature, K
T_R	turbidity Factor, dimensionless
U_t, U_n	heat transfer coefficient for transparent and non-transparent surfaces, W m^{-1} K^{-1}
V	volume of greenhouse, m^3
v_i, v_o	indoor airspeed, and outdoor airspeed, m s^{-1}
W	installed power of lamp, W m^{-2}
w_{ps}	saturated humidity ratio of air at plant temperature, kg kg^{-1}
w_i	humidity ratio of air at indoor temperature, kg kg^{-1}

Greek letters

α_s	factor for estimation of effective solar radiation, dimensionless
β	angle of inclined surface with horizontal, degrees
γ	surface azimuth angle, degrees
δ	declination angle of sun, degrees
ε_c, ε_i	emissivity of cover and indoor components, dimensionless
ε_{sky}, ε_{clear}	cloud cover sky emissivity and clear sky emissivity, dimensionless
θ	angle between two radiative surfaces, degrees
θ_z	zenith angle of sun, degrees
θ_i	angle of incidence of surfaces, degrees

ρ	air density, kg m^{-3}
ρ_r	reflectivity of outdoor ground, dimensionless
τ	transmissivity of cover, dimensionless
τ_l	transmissivity of cover to long-wave radiation, dimensionless
μ	dynamic viscosity of air, kg m^{-1} s^{-1}
φ	local latitudes, degrees
∂	volumetric thermal expansion coefficient, K^{-1}
σ	Stefan-Boltzmann Constant, W m^{-2} K^{-4}
ω	hour angle, degrees
Δx	thickness of i^{th} section in composite wall, m
ΔT	temperature difference, ˚C

Subscripts

sr, sw	south roof and south wall
nr, nw	north roof and north wall
er, ew	east roof and east wall
wr, ww	west roof and west wall

3.1 Introduction

Greenhouse production of vegetables can enable people living in cold regions to enjoy fresh healthy food during the winter season. The harvested area of greenhouse production in Canada has been increasing steadily despite high heating costs (Statistics Canada, 2008). At high northern latitudes, heating of a greenhouse for about eight months of the year is essential to ensure the growth and development of crops grown therein. In Canada, heating accounts for 10–35% of the total greenhouse production costs; the amount of heat necessary depends on the building envelope, the location of the greenhouse, and the kind of crops grown (Spencer, 2009). Different types of thermal models are available that can be used for studying the greenhouse heating requirement, but the approaches of modeling are different depending on the application of these models. Static models (Chiapale and Kittas, 1981; Morris, 1956) were initially developed by considering the heat transfer by conduction, convection, and radiation through the greenhouse cover, but the precision of the static models is very limited ($\pm$25% error) (Sethi et al., 2013). Reasons include the lack of consideration of the effect of solar radiation in the model, and the prediction is often based on yearly or monthly average meteorological data. Improved static models (Breuer and Short, 1985; Chandra and Albright, 1981; Fitz-Rodríguez et al., 2010; Hill, 2006; Jolliet et al., 1991; Tunc et al., 1985) have been developed to increase the accuracy of the simple static models, however, they are valid only for certain types of greenhouses and requires the input of hourly solar radiation data. These intermediate models neglect the heat addition from environmental control systems such as supplemental lighting, CO_2 generators, and various electric motors that contribute significantly to heating in commercial greenhouses. It was estimated the supplemental lighting with high-pressure sodium (HPS) lamps contributed about 25-41% of the total heating requirement of a double-poly greenhouse located in Quebec City (Brault et al., 1989). Conversely, complex dynamic models (Avissar and Mahrer, 1982; Cooper and Fuller, 1983; De Zwart, 1996; Kindelan, 1980; Sengar and Kothari, 2008; Sethi, 2009; Singh et al., 2006; Singh and Tiwari, 2000; Vanthoor et al., 2011) have been developed by forming individual energy balance equations for greenhouse interactive components including cover, plant, floor, and indoor air. These models show good precision for predicting the temperature variation of different interactive components in greenhouses, but require complicated modifications to simulate greenhouse heating with a different configuration. For example, Vanthoor et al. (2011) developed a dynamic model based on solving the individual energy balance equation of the indoor air, cover, soil, plant, and thermal screen, however, these

energy balance equations need complicated modifications for a greenhouse without a thermal screen, or with multilayer of glazing, and that had nontransparent wall. Also, these complex dynamic models neglect the heating contribution of different environmental control systems, and require hourly solar radiation data that are not easily available in some locations.

Energy simulation software including EnergyPlus, EE4, and TRNSYS is available for simulation of energy requirements in different types of buildings. These tools have limitations such as not accurately accounting for the dynamic heat and mass transfer process caused by plant evapotranspiration and other environmental control systems used in greenhouses. Building simulation tools need to be modified to account for heat and mass transfer in a greenhouse, and often need additional models to increase the prediction accuracy (Lee et al., 2012). As such, these building simulation tools have limitations for simulation of greenhouse thermal environments, and existing greenhouse lumped estimation models have limitations to consider all of the heat transfer parameters involved in greenhouses. This study develops a time-dependent quasi-steady state thermal model named GREENHEAT to simulate the heating requirement in conventional greenhouses in cold regions.

3.2 Principles of modelling

The GREENHEAT model was designed to predict the heating requirements of conventional greenhouses under heating mode when greenhouse temperature and relative humidity (RH) are controlled at a set-point. This model did not consider the cooling mode of the greenhouse, which allows the temperature to rise above the set-point and where RH may be higher or lower than the set-point, because greenhouses in cold regions mostly control indoor temperature through natural ventilation. A greenhouse is a complex physical and biological system including the dynamic heat and mass transfer process and the process of plant photosynthesis. Therefore, several assumptions were considered when developing the model for simulation of heating requirements in conventional greenhouses. The major assumptions for simplification of the model are as follows:

1. Greenhouse air is considered to be well-mixed, which means that there is no spatial difference in air temperature because the mechanical air-circulation system is used to avoid air stratification in modern commercial greenhouses.

2. Radiative heat exchange between walls and roofs is assumed to be negligible because the temperature is not significantly different when indoor temperature is controlled at the set-point and the air is well circulated.
3. The fluctuation of indoor relative humidity is considered to be negligible since the modern commercial greenhouses control relative humidity at an optimum set-point during heating mode.
4. The ground heat loss from floor to the depth-ground is considered in a steady state mode since the fluctuation of underground soil temperature is negligible after a certain depth.

The model was developed based on the lumped-system analysis of heat sources and sinks in greenhouses because the indoor temperature and relative humidity in modern commercial greenhouses are usually well controlled and uniform during heating mode. The heat sources in a conventional commercial greenhouse include solar radiation and heat from environmental control systems including supplemental lighting, CO_2 generators, and recirculating fans. The possible heat sinks in greenhouses include heat loss by conduction and convection, heat loss with air exchange, floor and perimeter heat loss, long-wave radiation heat loss, and heat used in the process of plant evapotranspiration.

The general form of heat balance for conventional greenhouses can be given by:

$$Q_h = \text{Sources} - \text{Sinks} = \left(Q_s + Q_{sl} + Q_{co_2} + Q_m\right) - \left(Q_t + Q_i + Q_g + Q_p + Q_r + Q_e\right) \quad (3.1)$$

where Q_h is the heating requirement; Q_s is the net heat gain from solar radiation; $Q_{sl,}$ Q_{CO_2}, and Q_m are the heat gain from supplemental lighting, CO_2 generators, and motors, respectively; Q_t is the heat transfer by conduction and convection; Q_i is the heat transfer caused with air exchange; Q_g is the heat transfer through the greenhouse floor; Q_p is the heat transfer along the perimeter; Q_r is the heat loss by transfer of long-wave radiation; and Q_e is the heat used in the process of plant evapotranspiration.

A negative value (Q_h) from simulation would indicate supplemental heating is needed in the greenhouse, while a positive value indicates cooling needs. A detailed description of the modeling principle for estimation of heat sources and sinks in conventional greenhouses is given in the following sections.

3.2.1 Heat gain from solar radiation

The solar radiation that passes through the greenhouse cover can be absorbed by greenhouse indoor components; the remaining portion is lost outside of the greenhouse. It is very complicated to estimate the amount of solar insolation effectively used in a greenhouse. As a rough rule, one-half of the available insolation in the greenhouse is converted immediately to sensible heat added to the air, one-quarter is added as latent heat to the greenhouse air, and the last quarter is usually lost (Al-Helal and Abdel-Ghany, 2011; Albright, 1990). The net heat gain from solar radiation can be estimated as follows:

$$Q_s = \alpha_s S \tag{3.2}$$

The total solar radiation available in the greenhouse depends on several factors, mainly on the transmissivity and orientation of the transparent cover surface. The transparent cover surface area available to receive solar radiation is different depending on the type of greenhouse. Therefore, the solar radiation through different surfaces is estimated separately based on the orientation of the surfaces. Finally, the total solar radiation in greenhouses is the sum of the incoming solar radiation through different surfaces exposed to the outside and can be given by Sethi (2009):

$$S = \sum \tau_i A_i I_i \tag{3.3}$$

where τ_i, and $A_{i,}$ are the solar transmissivity and area of i^{th} section; and I_i is the total solar radiation available on i^{th} section.

$$\sum \tau_i A_i I_i = \tau_{sr} A_{sr} I_{sr} + \tau_{sw} A_{sw} I_{sw} + \tau_{nr} A_{nr} I_{nr} + \tau_{nw} A_{nw} I_{nw} + \tau_{ew} A_{ew} I_{ew} + \tau_{ww} A_{ww} I_{ww} + \tau_{er} A_{er} I_{er} + \tau_{wr} A_{wr} I_{wr} \tag{3.3a}$$

3.2.1.1 Hourly solar radiation through the inclined surface

The solar radiation on any inclined surface includes the beam component from direct beam radiation and the diffuse radiation. The diffuse component composed of isotropic diffuse component received uniformly from the skydome, circumsolar diffuse component resulting from forward scattering of solar radiation and concentrated in an area close to the sun, horizon brightening component concentrated in a band near the horizon and most pronounced in clear skies, and a reflected component that quantifies the radiation reflected from the ground to the tilted surface. Different models (Isotropic sky model, Klucher model, Hay and Davies model, Reindl model, Muneer model, and Perez model) are available for estimating solar radiation on an inclined surface. The isotropic sky model is the simplest model for predicting the solar radiation on the inclined surface with reasonable accuracy as compared to the other more complicated models

(Loutzenhiser et al., 2007). According to Liu and Jordan (1963), the total solar radiation on an inclined surface with an angle (β) is given by the isotropic diffuse model:

$$I_i = I_b \frac{\cos\theta_i}{\cos\theta_z} + I_d \left(\frac{1+\cos\beta}{2}\right) + (I_b + I_d)\rho_r \left(\frac{1-\cos\beta}{2}\right) \quad (3.4)$$

The angle of incidence of beam radiation on a surface and the zenith angle of the sun can be expressed as follows (Duffie and Beckman, 2006):

$$\cos\theta_i = \sin\delta \sin\varphi \cos\beta - \sin\delta \cos\varphi \sin\beta \cos\gamma + \cos\delta \cos\varphi \cos\beta \cos\omega + \cos\delta \sin\varphi \sin\beta \cos\gamma \cos\omega + \cos\delta \sin\beta \sin\gamma \sin\omega \quad (3.5)$$

$$\cos\theta_z = \cos\varphi \cos\delta \cos\omega + \sin\varphi \sin\delta \quad (3.6)$$

The declination angle (δ) depends on the n^{th} day of the year, and the hour angle (ω) depends on the time of the day; the required values of these parameters have been calculated according to the ASHRAE Fundamental (ASHRAE, 2013).

3.2.1.2 Cloud cover solar radiation

The solar radiation data are very important for the analysis of solar application systems and building thermal performance. However, the continuous time series solar radiation data are mainly available in developed countries, whereas very limited resources in the developing countries. Also, the measured data available from a solar station become less accurate for a distance of 50 km from the measuring station (Younes and Muneer, 2007). Therefore, the estimation of solar radiation by using cloud cover solar radiation models are convenient because the cloud cover data can be easily obtained from meteorological stations. The solar radiation transmitted through the clouds depends on a number of factors such as the degree of cloudiness, cloud thickness (or height), water content per unit of volume, and the distribution of clouds in relation to the position of the sun in the sky. Cloud cover can significantly affect the availability of solar radiation; about 80-90% of solar radiation intensity can be reduced by thick, low-level, and layered cloud (Matuszko, 2012). A few empirical models (Kasten and Czeplak, 1980; Lam and Li, 1998; Muneer and Gul, 2000) have been developed to estimate solar radiation based on cloud cover information. Previous studies (Badescu and Dumitrescu, 2014a; Younes and Muneer, 2007) have reported that the Kasten-Czeplak model is relatively simple and accurate compared to other cloud cover models. These studies also indicate the Kasten-Czeplak model performs significantly better at estimating global solar radiation with local coefficients (A, B). Therefore, the global solar radiation, diffuse

radiation, and direct beam radiation on a horizontal surface under cloud cover can be given as follows (Kasten and Czeplak, 1980):

$$I_g = I_{gc}\left(1 - A\left(\frac{CF}{8}\right)^B\right) \quad (3.7)$$

$$I_d = I_g\left(0.3 + 0.7\left(\frac{CF}{8}\right)^2\right) \quad (3.8)$$

$$I_b = (I_g - I_d) \quad (3.9)$$

Clear sky global solar radiation on a horizontal surface (I_{gc}) is the sum of the clear sky direct beam radiation (I_{bc}) and the diffuse radiation component (I_{dc}). Several solar radiation models (ASHRAE, 2013; Hottel, 1976; Iqbal, 1983; Tiwari, 2003) have been used for estimating clear sky direct and diffuse radiation on a horizontal surface. The solar radiation model using the turbidity factor is comparatively simple and convenient for estimating clear sky solar radiation. The clear sky beam and diffuse radiation on any horizontal surfaces and the direct normal irradiance on any terrestrial region can be calculated using the turbidity factor (Tiwari, 2003):

$$I_{bc} = I_N \cos\theta_z \quad (3.10)$$

$$I_{dc} = \frac{1}{3}(I_{ex} - I_N)\cos\theta_z \quad (3.11)$$

$$I_N = I_{ex} \exp\left[\frac{-T_R}{(0.9+9.4\sin\alpha)}\right], \alpha = 90 - \theta_z \quad (3.12)$$

According to Spencer (1971), the extraterrestrial heat from the sun on a surface normal to the sun's ray on the n^{th} day of the year is given by:

$$I_{ex} = I_{sc}\left[1 + 0.033 \times \cos\left(360 \times \frac{n-3}{365}\right)\right] \quad (3.13)$$

3.2.2 Heat gain from environmental control systems

Greenhouses can receive a significant amount of heat from environmental control systems such as supplemental lighting, air circulation fans, and carbon dioxide enrichment equipment. Depending on the types of lamps, the supplemental lighting can return about 75-100% of thermal energy as heat to the greenhouses (Castilla, 2013). The heat addition from supplemental lighting can be estimated by the following equation (ASHRAE, 2013):

$$Q_{sl} = WF_{hc}F_a A_f \quad (3.14)$$

Recirculation of indoor air is very important for reducing air stratification in greenhouses because air stagnation may cause abnormal growth of plants and also increase heating requirements. Therefore, recirculation fans are needed in greenhouses in the direction of plant rows at distances not less than 30 times of the diameter of the fan (ASABE, 2006). The instantaneous heat gain from the motors of recirculating fans can be estimated by the following equation (ASHRAE, 2013):

$$Q_m = N_f \frac{P_m}{E_m} F_{um} F_{lm} \quad (3.15)$$

The heat gains from CO_2 generators depend on the types of equipment used for carbon dioxide enrichment in greenhouses. A significant amount of heat can be added to a greenhouse when CO_2 is produced from the combustion of fuel in greenhouses. The amount of heat from the CO_2 generators can be estimated by the following equation (ASHRAE, 2013):

$$Q_{co_2} = 0.278 \times NHV \times MFR \times \frac{A_f}{PR} \quad (3.16)$$

3.2.3 Heat transfer by conduction and convection

Conduction and convection are two of the major heat transfer phenomena in greenhouses. Heat transfer through the processes of conduction and convection in transparent and non-transparent envelopes can be calculated as follows:

$$Q_t = (U_t A_t + U_n A_n) \times (T_i - T_o) \quad (3.17)$$

Depending on the types of greenhouse envelopes, two different approaches have been applied to the estimation of the overall conduction and convection heat transfer coefficient. The overall heat transfer coefficient for transparent surfaces and non-transparent surfaces can be given as (Tiwari, 2003):

$$U_t = \left[\frac{1}{h_i} + N_c \times \frac{l_c}{k_c} + (N_c\text{-}1) \times \frac{1}{h_a} + \frac{1}{h_o}\right]^{-1} \quad (3.18)$$

$$U_n = \left[\frac{1}{h_i} + \sum \frac{k}{\Delta x} + \frac{1}{h_o}\right]^{-1} \quad (3.19)$$

The estimation of thermal air conductance of air spaces (h_a) for a double-layer greenhouse cover is very complicated. The thermal resistance of air spaces depends on several factors including temperature difference, the direction of heat flow, orientation, the thickness of air spaces, and the emissivity coefficient of the surface that encloses the air spaces (ASHRAE, 2013). The air gap of greenhouse covers varies between 8-12 mm depending on the type of cover; and the emissivity of covers range from 0.2-0.9 (Hill, 2006). Depending on the temperature difference and orientation,

the thermal resistance of a 13 mm air spaces varies from 0.45-0.13 for an emittance range of 0.2-0.82 (ASHRAE, 2013). Garzoli and Blackwell (Garzoli and Blackwell, 1987) determine the thermal resistance of the air spaces for double-layer polyethylene-covered greenhouses by analyzing the rate of heat loss through the cover under different climatic conditions. A value of 3.85 (W $m^{-2} \cdot K^{-1}$) for the thermal air conductance of the air spaces (h_a) has been found to give very good agreement between the predicted and the measured rate of heat loss. Therefore, the thermal air conductance of the air spaces is assumed to be 3.85 (W $m^{-2} \cdot K^{-1}$) for calculating the overall heat transfer coefficient of a multi-layer greenhouse cover.

Several empirical equations (Bot, 1983; Garzoli and Blackwell, 1981; Kindelan, 1980; Kittas, 1994; Papadakis et al., 1992) have been developed to determine the convection coefficient for greenhouse covering surfaces, but these equations are only valid for certain conditions. Therefore, the following equation derived from the Nusselt number can be used to estimate the convective heat transfer coefficient for different surfaces (Tiwari, 2003):

$$h = \frac{N_u k_a}{L_c} \tag{3.20}$$

Indoor air velocity in greenhouses is usually very low compared to the outside, so the heat convection between the cover and the indoor components mainly occurs due to the thermal difference between the surfaces. Therefore, the convection heat transfer at the cover inside surface is considered to be a free convection. The indoor convection coefficient of the transparent surfaces under turbulent flow conditions can be estimated using following relation (Tiwari, 2003):

$$h_i = \left(\frac{k_a}{L_c}\right) 0.1(G_r P_r)^{0.33} \quad (10^9 < G_r P_r < 10^{13}) \tag{3.21}$$

$$G_r = \frac{g \partial L c^3 \Delta T}{\mu^2} \tag{3.22}$$

$$P_r = \frac{\mu C_{pa}}{k_a} \tag{3.23}$$

For nontransparent vertical surfaces, the indoor convection coefficient is estimated by the following equation (Tiwari, 2003):

$$h_i = \left(\frac{k_a}{L_c}\right) 0.1\ (10^{11})^{0.33} \tag{3.24}$$

On the other hand, the heat convection between the greenhouse enclosed surface and the outside air is considered to be forced convection; because outdoor airspeed is the dominant force for heat convection from an outside surface. For forced convection, the outdoor convection coefficient under turbulent flow along a plane surface can be expressed as follows (Wong, 1977):

$$h_o = (\frac{k_a}{L_c})0.037\ (R_e^{0.8}\ P_r^{0.33}) \quad (R_e > 5 \times 10^5) \tag{3.25}$$

$$R_e = \frac{\rho v_o L_c}{\mu} \tag{3.26}$$

3.2.4 Heat transfer by air exchange

The air exchange in greenhouses transfers a large amount of heat to the outside during the winter season. Depending on airtightness, wind speed, and inside-outside temperature differences, infiltration represents about 20% of the total heat loss from greenhouses (Jolliet et al., 1991). However, the air exchange caused by ventilation was not considered in the model because the forced ventilation system is shut down during the winter season to minimize heat loss when heating is needed. A natural ventilation system usually operates in greenhouses when the indoor temperature is greater than the set-point temperature and, cooling is needed, but natural ventilation of cooling is not considered in this study since the objective is to estimate heating needs. Thus, the heat loss from greenhouses caused by infiltration can be calculated from the following relation (Sethi and Sharma, 2007):

$$Q_i = 0.33\ N\ V(T_i - T_o) \tag{3.27}$$

3.2.5 Heat transfer through floor and perimeter

A large amount of heat can be lost through the greenhouse floor including conduction through the ground and heat transfer along the perimeter. The floor surface temperature is considered to be the same as the indoor temperature. Also, the fluctuation of underground soil temperature over the year at a certain depth becomes negligible, so the steady-state method is applied to estimate heat conduction through the floor (Florides and Kalogirou, 2004). Based on steady-state, one-dimensional heat conduction, the heat transfer through the floor can be estimated by the following equation (Tunc et al., 1985):

$$Q_s = \frac{k_s}{H} A_f\ (T_i - T_s) \tag{3.28}$$

The perimeter heat loss can be calculated using the given equation (ASHRAE, 2013):

$$Q_p = F_p\ P\ (T_i - T_o) \tag{3.29}$$

3.2.6 Long-wave radiation transfer from greenhouses

The exchange of long-wave radiation through the transparent cover is responsible for a significant amount of heat loss in greenhouses. The thermal radiation emitted from indoor greenhouse

components can be transmitted to the sky or absorbed in the cover, and part of the radiation can reflect back to the greenhouses. The use of a thermal curtain at night reflects the radiative heat back to the greenhouse. Therefore, it is assumed long-wave radiation loss through a transparent roof would be negligible when the reflective thermal curtain is in operation. This transmitted radiative heat loss from a greenhouse can be expressed as follows (Hill, 2006):

$$Q_r = \left[\sigma \varepsilon_c A_c F_c \left(T_i^4 - T_c^4\right) + \sigma \varepsilon_i \tau_l A_f F_{sk} \left(T_i^4 - T_{sk}^4\right)\right] \quad (3.30)$$

The view factor between the greenhouse and the sky (F_{sk}) is considered to be 1.0 because the greenhouse is enclosed by the sky, which can be considered a black hemisphere (Vadiee, 2011). The view factor between the ground and the cover (F_c) can be estimated as follows (Liu and Jordan, 1961):

$$F_c = \frac{1+\cos}{2} \quad (3.31)$$

The cover temperature is typically a linear function of the indoor and the outdoor temperature (Hill, 2006). The following linear function can be used to solve cover temperature (Bakker, 1995):

$$T_c = \frac{2}{3} T_o + \frac{1}{3} T_i \quad (3.32)$$

The effective sky temperature is usually estimated by using the different empirical equations based on the measured ground meteorological parameters including air temperature, air-water vapor tension, and sky cloud cover. However, most of the existing greenhouse thermal models used the simplest models (Swinbank, 1963; Whillier, 1967) based on the outside air temperature without taking into account cloud cover. The estimation of sky temperature taking cloud cover into consideration is more accurate than simple correlations based on air temperature. According to Clark and Allen (1978) the effective sky temperature can be estimated as follows:

$$T_{sk} = T_o \varepsilon_{sk}^{0.25} \quad (3.33)$$

$$\varepsilon_{sk} = (1 + 0.0224\,CF - 0.0035\,CF^2 + 0.00028\,CF^3)\,\varepsilon_{clear} \quad (3.34)$$

$$\varepsilon_{clear} = 0.787 + 0.7641 \ln\left(\frac{T_{dp}}{273}\right) \quad (3.35)$$

The dew point temperature of the outside air (T_{dp}) based on the outdoor relative humidity (RH_o) and the dry bulb temperature (T_o) can be calculated by the following equation (Martin et al., 1997):

$$T_{dp} = \left(\frac{RH_o}{100}\right)^{0.125}(112 + 0.9 \times T_o) + 0.1 \times T_o - 112 \quad (3.36)$$

3.2.7 Heat used in evapotranspiration

Evapotranspiration represents evaporation from the floor or growth media and transpiration from the plants, and it is responsible for a significant amount heat loss in greenhouses. The evaporation from the floor is very complicated to model, and this study considers it to be included in plant evapotranspiration. Evapotranspiration from plant leaves is an evaporative cooling process that reduces the canopy surface temperature. Therefore, greenhouse plants get heat from the solar radiation/indoor air to recover the reduced temperature of the leaf surface. The heat used by plants in the process of plant evapotranspiration can be estimated as follows (Nobel, 1974):

$$Q_e = M_T L_v \tag{3.37}$$

$$M_T = A_p \rho \frac{w_{ps} - w_i}{(R_a + R_s)} \tag{3.38}$$

The plant surface area can be calculated from the leaf area index of plants. The saturated humidity ratio at plant temperature and the humidity ratio at indoor air temperature can be calculated as follows (Albright, 1990):

$$w_{ps} = 0.6219 \frac{P_{ws}}{(P - P_{ws})} \tag{3.39}$$

$$w_i = 0.6219 \frac{P_w}{(P - P_w)} \tag{3.40}$$

Previous studies (Singh et al., 2006; Singh and Tiwari, 2010) show that a negligible temperature difference exists between the plant and the indoor air. Therefore, the water vapor saturation pressure at plant temperature is calculated by assuming plant temperature to be the same as the indoor temperature. The actual vapor pressure can be calculated from the relative humidity and the saturated vapor pressure.

The aerodynamic resistance and stomatal resistance in plant evapotranspiration can be calculated from the following relationships (Boulard et al., 1991; Boulard and Wang, 2000):

$$R_a = 220 \times \frac{L_f^{0.2}}{v_i^{0.8}} \tag{3.41}$$

$$R_s = 200 \left(1 + \frac{1}{\exp(0.05(\tau I_g - 50))}\right) \tag{3.42}$$

3.3 Program design

The programming flow chart for simulating the greenhouse heating requirement for the model (GREENHEAT) developed in this study is shown in Figure 3.1. The programming language MATLAB was used to develop this computer program for simulation of heating requirements of

conventional greenhouses. The input parameters for simulation include latitude and longitude of the study area, the indoor set-point temperature, relative humidity, air exchange rate, physical and thermal properties of crops and construction materials, and hourly weather data including temperature, relative humidity, cloud cover, and wind speed.

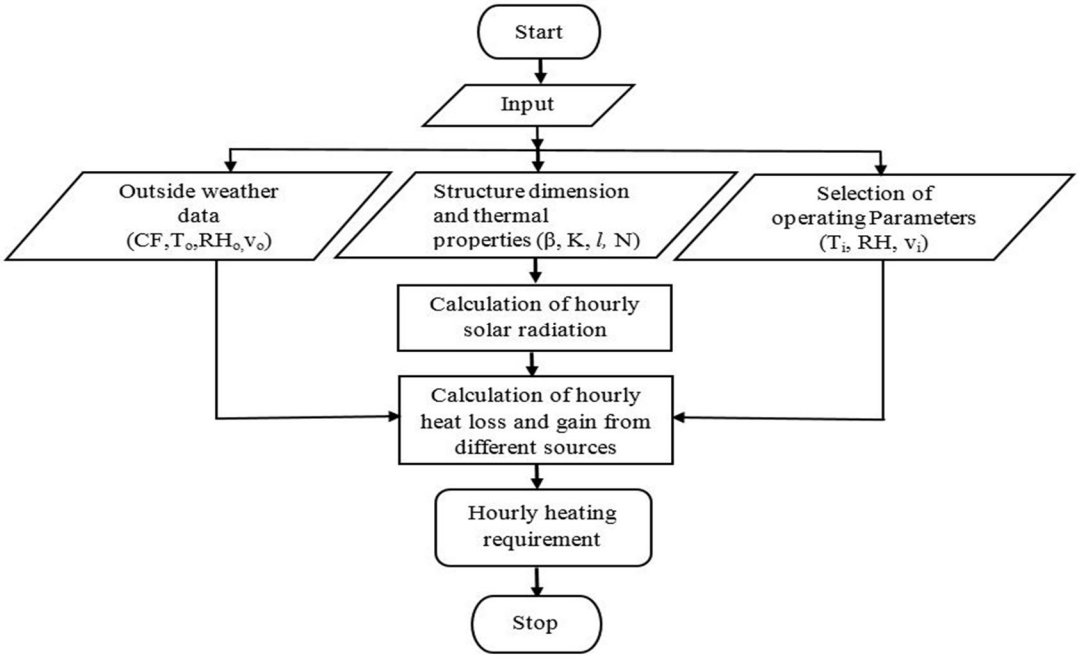

Figure 3.1: Flowchart of the computer program GREENHEAT for simulation of the greenhouse heating requirement.

3.4 Description of the model commercial greenhouse

A four-span gable roof greenhouse with east-west orientation (1125 m^2) located near the city of Saskatoon (52.09^{o}N latitude, 106.82^{o}W longitude, and 428 m elevation), covered with air-inflated, double-layer polyethylene film was selected for this study. The north wall of the greenhouse was non-transparent and insulated with extruded polystyrene board and plywood sheathing. A similar non-transparent composite wall was constructed 2.43 m from the ground on the east and west section of the sidewall, and 1.65 m on the south section of wall; twin-wall polycarbonate panels (8 mm) were used for the remaining portion of the sidewall. The hourly weather data (temperature, relative humidity, cloud cover, and wind speed) in Saskatoon for 2014 as collected by the National Solar Radiation Database (NSRDB) were used for simulation of the heating requirements in the study greenhouse. Tomato plants were grown in the greenhouse, so the indoor set-point temperatures were maintained at 21˚C during the daytime and 18˚C during the night. The relative

humidity in the study greenhouse was controlled at 75% using the mechanical dehumidifier. Depending on the types of crops, the supplemental lighting is usually turned on when the greenhouse solar radiation reaches below 240-300 W/m^2 (Dorais, 2003), and a photoperiod about 14-h was found to be best for optimum growth of tomatoes in greenhouses (Demers et al., 1998). Therefore, it was considered that the supplemental lighting would be turned on when solar radiation in the greenhouse was reduced to 250 W m^{-2}, and artificial lighting was turned off between 10 PM to 7 AM to maintain the optimal 14-h photoperiod. The CO_2 generator was considered to be in operation only during the daytime, and a thermal curtain was used at night. Other constant values used in the simulation are listed in Table 3.1.

Table 3.1: Constant values of different parameters used in the simulation.

Parameters	Value
Greenhouse characteristics	
Infiltration rate per hour (N) (ASABE, 2006)	1.0
Thermal conductivity of plywood (19 mm)	0.12 (W m^{-1} K^{-1})
Thermal conductivity of polystyrene insulation (65 mm)	0.03 (W m^{-1} K^{-1})
Perimeter heat loss factor (F_p) (ASHRAE, 2013)	0.85 (W m^{-1} K^{-1})
Angle of roof (β)	26˚
Soil characteristics	
Thermal conductivity of soil (k_s) (ASHRAE, 2013)	1.4 (W m^{-1} K^{-1})
Soil temperature (T_s) (Florides and Kalogirou, 2004)	15 (˚C)
Plant characteristics (Rincón et al., 2012)	
Average leaf area index of tomato (LAI)	2.0
Characteristic length of tomato leaf (L_f)	0.027 (m)
Emissivity coefficient of plants (ε_i)	0.9
Covering characteristics (Sanford, 2011)	
Poly cover (6 mils)	
Emissivity of IR barrier poly cover (ε_c)	0.2
Transmissivity to solar radiation (τ)	0.75
Transmissivity to long-wave radiation (τ_l)	0.29
Thermal conductivity (k_c)	0.33 (W m^{-1} K^{-1})

Polycarbonate (8 mm twin-wall)	
Emissivity of polycarbonate (ε_c)	0.65
Thermal conductivity (k_c)	0.2 (W m^{-1} K^{-1})
Transmissivity to solar radiation (τ)	0.78
Transmissivity coefficient to long-wave radiation (τ_l)	0.03
Other parameters	
Indoor air velocity (Castilla, 2013)	0.2 (m/s)
Latent heat of water vaporization (L_v) (ASHRAE, 2013)	2450 (kJ kg^{-1})
Installed lighting wattage (W) (Dorais, 2003)	100 (W m^{-2})
Heat conversion factor (F_{hc}) (Castilla, 2013)	0.75
Lighting allowance factor (F_a) (ASHRAE, 2013)	1.2
Number of recirculating fans (N_f)	8
Rated power of motors (P_m)	375 (W)
Motor efficiency (E_m)	0.9
Motor load factor (F_{um}) (ASHRAE, 2013)	1.0
Motor use factor (F_{ul}) (ASHRAE, 2013)	1.0
Net heating value of fuel (NHV) (ASHRAE, 2013)	38 (MJ m^{-3} of gas)
Rate of CO_2 supply in greenhouse (MFR) (Castilla, 2013)	4.5 (g m^{-2} hr^{-1})
CO_2 production rate (PR) (EIA, 2016)	2.7 (kg kg^{-1} of fuel)
Stefan-Boltzmann Constant (σ)	5.67×10^{-8} (W m^{-2} K^{-4})
Reflectivity of outdoor ground (ρ_r)	0.5

3.5 Results and discussion

3.5.1 Evaluation of solar radiation sub-model

The model estimated the hourly solar radiation based on the input of hourly cloud cover data from the NSRDB. Figure 3.2 shows the scatter plot of the estimated hourly solar radiation from the model versus the data from the NSRDB. The statistical indices including the coefficient of determination (R^2) and the root mean square error (RMSE) were used to evaluate the adequacy of the solar radiation sub-model. The R^2 and RMSE values are 0.78 and 112.61 W m^{-2}, respectively, which is very close to the results obtained in other studies (Badescu and Dumitrescu, 2014a; Kim et al., 2014; Younes and Muneer, 2007) to estimate global solar radiation. Based on the statistical

indicators, it can be concluded that the estimation of hourly solar radiation from the solar radiation sub-model is reasonably fit with the data from the NSRDB.

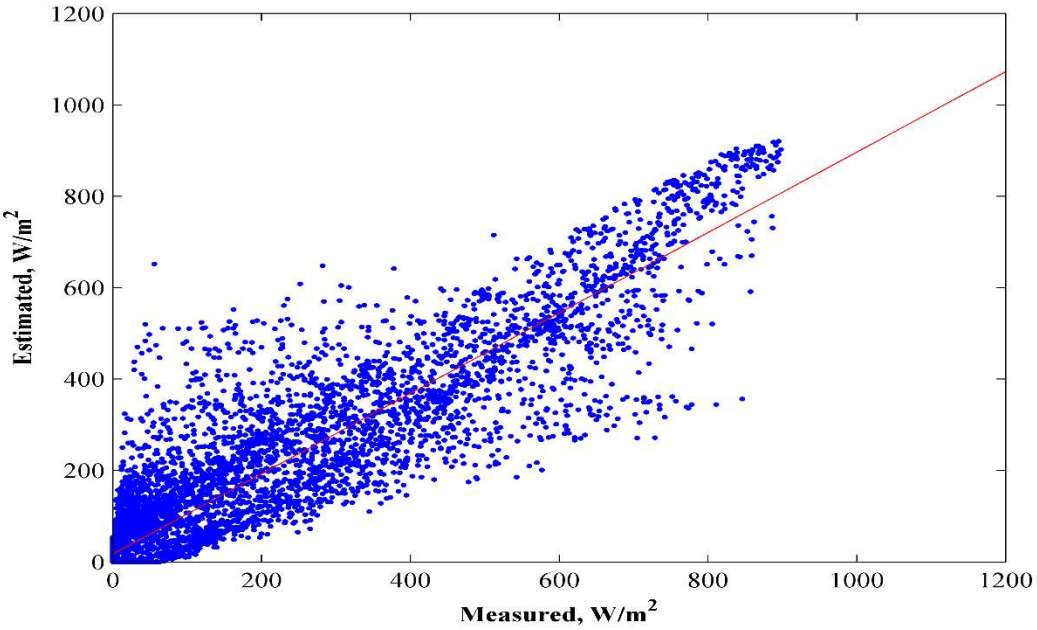

Figure 3.2: The scatter plot of estimated and measured value of global solar radiation on the horizontal surface in Saskatoon.

3.5.2 Simulation of the model greenhouse

Figure 3.3 shows the annual variation of the simulated heating requirements in the study greenhouse and the monthly average temperature in Saskatoon (52.09˚N, -106.82˚W) in 2014. The annual total estimated heating requirement in the study greenhouse was about 1380 MJ m^{-2}. The peak heating requirement occurred in February, and was 15.6% higher than the value in January (the lowest average temperature was recorded in February at -19.2˚C). Figure 3.3 shows that the average temperature in March and November was -8.0˚C and -8.03˚C, respectively, but the average daily heating requirement in November was about 5.8% higher than the heating requirement in March because the average daily solar heat gain in March was about three times higher than the solar heat gain in November.

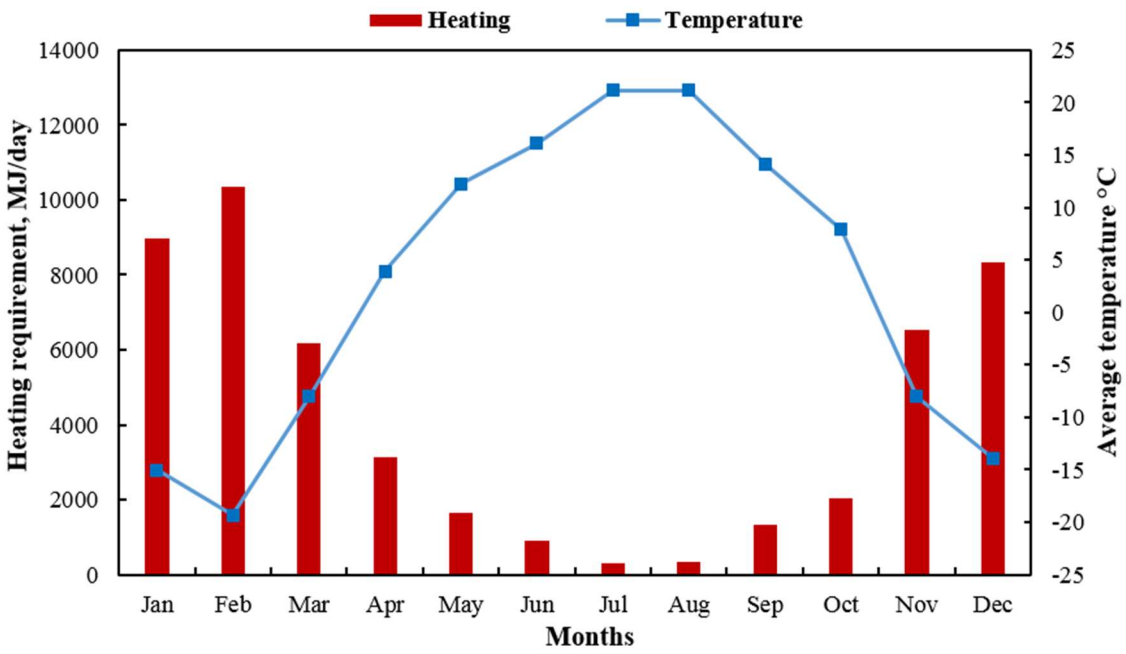

Figure 3.3: Annual variation of the heating requirements in the study greenhouse, and the outside average temperature in Saskatoon.

3.5.2.1 Analysis of heat transfers in the greenhouse

Greenhouse heat gain includes the heat from solar radiation and the heat from environmental control systems, including supplemental lighting, CO_2 supply system, and air circulation system. Figure 3.4 shows the variation of heating contributions from solar radiation compared to the total heat gain in the greenhouse. Based on the simulation results, solar radiation contributed about 44-65% of the total heat gain in the greenhouse during the three coldest months (January, February, and December), whereas about 83-86% during the summer months (June-August).

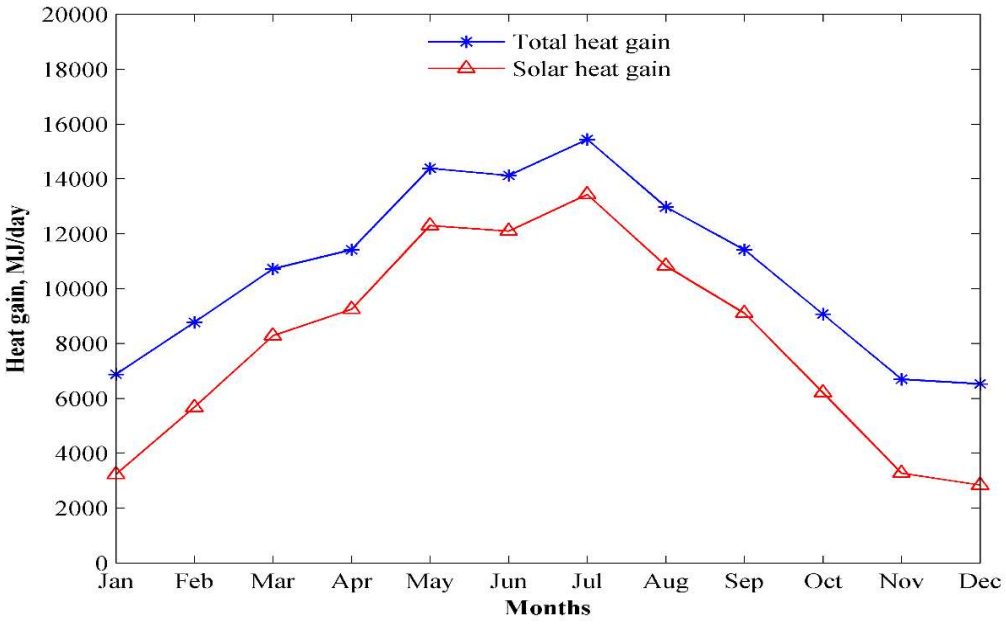

Figure 3.4: Annual variation of heating contribution from solar radiation compared to the total heat gain.

The heating contribution of different environmental control systems is shown in Figure 3.5. The predicted heat gains from environmental control systems were about 13-56% of the total greenhouse heat gain over the year. Figure 3.5 indicates the heat gain from supplemental lighting decreased with the increase of day length because the artificial photoperiod decreased with the increase of day length in summer; an opposite trend was true for the CO_2 supply system because the operating time of CO_2 generator increased with an increase in day length. However, the heat gain from electric motors was constant for the entire simulation period since the recirculating fans were considered to be in operation all the time. The heat contribution from supplemental lighting mainly depends on the installed wattage of the lighting system and the period of artificial lighting. At winter solstice in 2014, the HSP lamp with an installed capacity of 100 W m^{-2} contributed about 38.0% of the total heating requirement in the study greenhouse with eight hours of artificial lighting. Brault et al. (Brault et al., 1989) reported similar heating contributions from HPS lamps in a double-polyethylene greenhouse in Quebec, Canada. The CO_2 generators contributed about 6.5% of the total heating requirement when operating for seven hours during the daytime, whereas 24-hour operation of recirculating fans contributed about 3.8% of the total heating demand. The predicted result indicates environmental control systems can supply a significant amount of heat

to a greenhouse, which can significantly reduce heating demands. However, most of the previous models ignore the heat gain from these environmental control systems, so that a significant error arises in simulation when the heat addition from these environmental systems is neglected.

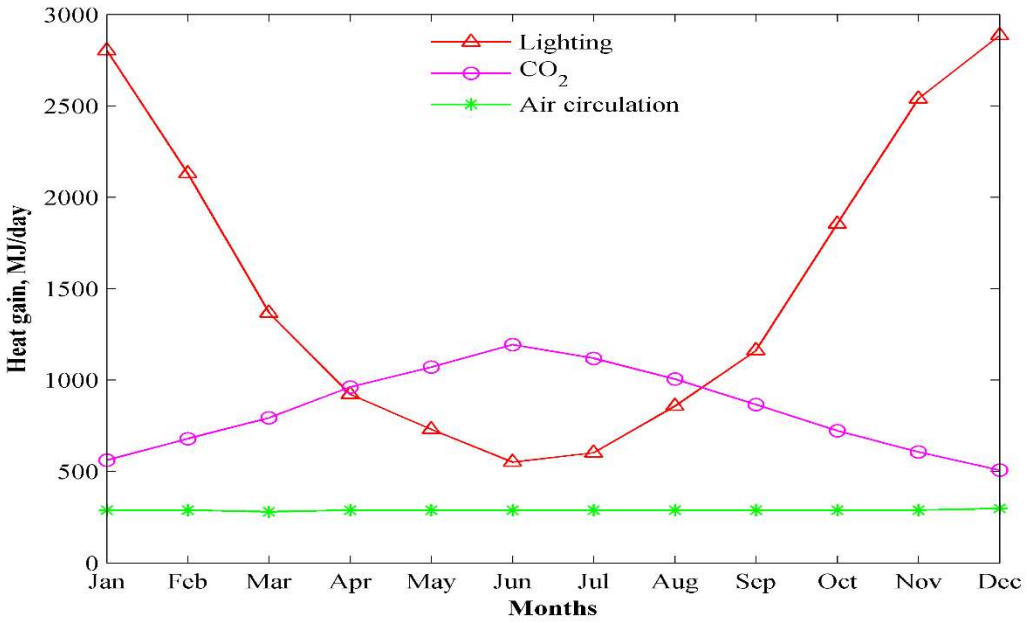

Figure 3.5: Annual variation of the heat gains from different environmental control systems.

Figure 3.6 shows the annual variation of heat loss from the study greenhouse by different heat transfer mechanisms such as transmission heat loss, infiltration loss, long-wave radiation loss, heat loss through the ground, and heat loss for evapotranspiration. The similar trend of heat losses was found in a conventional greenhouse in the UK (Al-Hussaini and Suen, 1998), however, the magnitude of heat loss by different mechanisms would be different depending on the greenhouse envelope and their location. Since February was the coldest month in 2014 (Figure 3), the amount of heat loss from the greenhouse was highest in February. About 40% of the total heat from the study greenhouse was lost through conduction and convection during the coldest three months of the year. The heat loss caused by infiltration was the second largest source of heat loss (up to 32%) in the greenhouse, followed by the heat loss caused by long-wave radiation (up to 21%). After March, the long-wave radiation loss increased because the operation hour of the energy curtain decreased with an increase in day length. The heat loss caused by the process of evapotranspiration from plants accounted for about 9.0% during extremely cold periods, while the heat used in the process of evapotranspiration was found to be the highest in summer and spring because

evapotranspiration depends greatly on solar radiation. The heat loss along the perimeter and the vertical conduction through the soil fluctuated mildly over the year because the underground temperature was considered to be constant over the year. A very small amount of heat (about 3.0%) was lost through the floor of the study greenhouse. The thermal analysis indicates more than 80% of greenhouse heat is lost by transmission, infiltration, and exchange of long-wave radiation. Therefore, the use of insulation and construction materials with a high thermal resistance, infrared radiation (IR) barrier glazing, and reflective thermal screens at night would significantly reduce greenhouse heating requirements at high northern latitudes. The intensity of heat loss through different mechanisms could be different depending on the type of structure, materials used for construction, management of environmental control systems, and also, importantly, the location of the greenhouse. However, the thermal analysis of different heat sources and sinks in the greenhouse at high northern latitudes would be helpful for greenhouse growers and researchers for analyzing the energy efficient greenhouse production under similar cold climates.

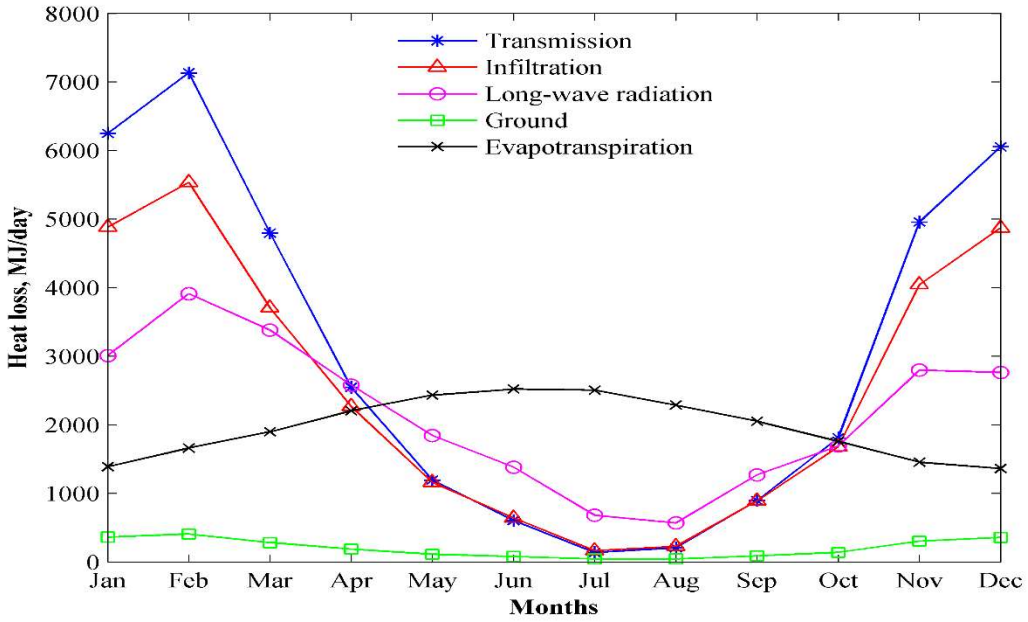

Figure 3.6: Annual variation of heat loss by different heat transfer mechanisms from the study greenhouse during heating mode.

3.5.3 Validation of the model

The actual heating requirement in the study greenhouse for the year of 2014 from March to October was calculated based on the data collected from the commercial greenhouse. The data for the four

coldest months were ignored for validation because the greenhouse started its operation in mid-February and continued until mid-November. The monthly heating requirement was calculated based on the heating value (38 MJ kg^{-1}) and the retail rate (CAD 0.286 m^{-3}) of natural gas. The predicted heating requirement was calculated without considering the heating contribution from the supplemental lighting because no supplemental lighting was provided in the greenhouse in 2014. The comparison of the predicted and the actual heating requirement is shown in Figure 3.7. Figure 3.7 shows that the predicted heating requirement in the greenhouse is close to the actual heating requirement, except for the summer months when the natural ventilation system was in operation very frequently to control the indoor relative humidity instead of the mechanical dehumidifier. Therefore, the air-exchange rate during summer months (July-August) could be relatively higher that draws the cool outside air into the greenhouse, thereby increasing the greenhouse heating requirement. Also, the actual heating requirement during the summer months is very close to the heating requirement in May, but the average temperature during the summer months was relatively high compared to the average temperature in May. Hence, the conclusion regarding the model validation was made without considering the data from June to August. The validation of the model shows that the errors in heating prediction for the winter months is less than 9.0%, and 4.6% is the average simulation error. Previous studies (Jolliet et al., 1991; Sethi et al., 2013; Singh and Tiwari, 2010) reported that the average percent error in simulation of about 10% is reasonably acceptable for greenhouse thermal modeling. The percent error of the simple static models (Chiapale and Kittas, 1981; Morris, 1956) is about 25% , and close to 11% for the improved static models (Jolliet et al., 1984; Pieters and Deltour, 1997), whereas error is less than 10% for the complex dynamic models (Bot, 1983; Sethi, 2009; Singh and Tiwari, 2000; Trigui et al., 2001). Therefore, it can be concluded that GREENHEAT can predict the heating requirement of conventional greenhouses with good accuracy.

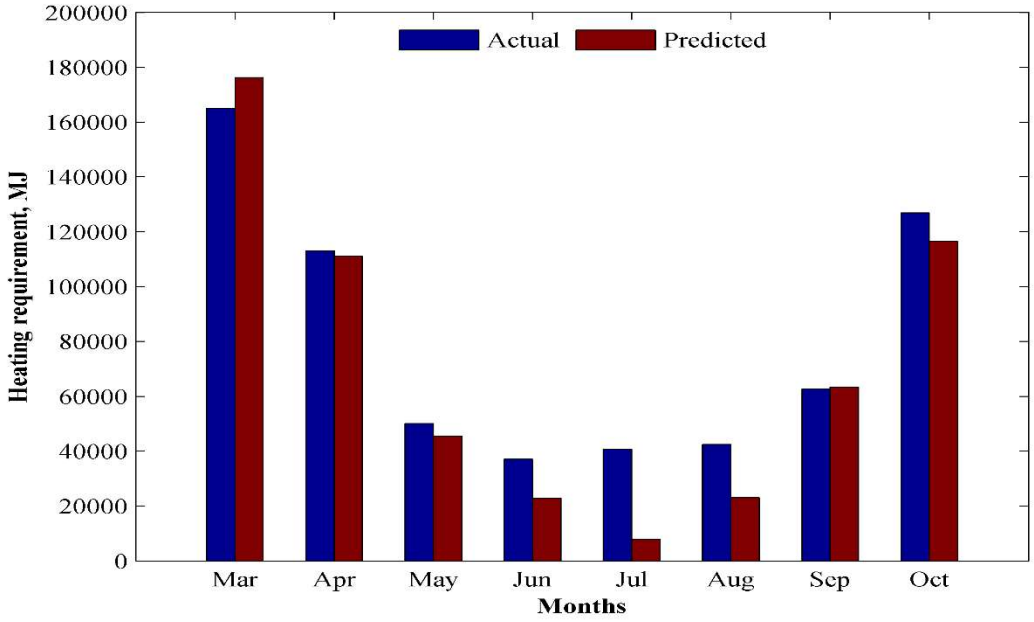

Figure 3.7: Comparison of predicted and actual heating requirements in the study greenhouse.

3.6 Conclusions

In this study, a quasi-steady state thermal model named GREENHEAT was developed based on the lumped estimation of heat sources and sinks in greenhouses. The developed model considered most of the heat sources and sinks in a conventional greenhouse, including the hourly variation of solar radiation, heat gain from environmental control systems, and heat used for plant evapotranspiration. The simulated results indicate that the environmental control systems (supplemental lighting, CO_2 generators, and motors of recirculating fans) contribute up to 56% of heating requirements in the study greenhouse. The transmission heat loss by conduction and convection is the largest component of heat loss (40%) during the winter periods followed by the infiltration and long-wave radiation loss, respectively. Validation shows that the average error in prediction is less than 5%, therefore, the model can be considered sufficiently accurate for simulation of heating requirements in conventional greenhouses. The model will be beneficial for researchers, engineers, and growers to assist with their decision-making regarding energy-efficient designs and feasibility analysis of greenhouse production in cold northern climates.

Acknowledgements

The authors are very thankful to the College of Graduate Studies and Research (CGSR) at the University of Saskatchewan, Innovation Saskatchewan, for their support and funding of the research. The authors are also thankful to the owners of Grandora Gardens for the support the research.

CHAPTER 4

A REVIEW OF ENERGY SAVING TECHNIQUES FOR REDUCING HEATING COST OF CONVENTIONAL GREENHOUSES

(The manuscript presented in this chapter was submitted to the International Journal of Energy Research, submission no: ER_18_9421)

Overview

Knowledge of heating energy saving potential is essential to study the energy-efficient design of greenhouses. This chapter includes the comprehensive review of different techniques to reduce the heating cost of the conventional-style greenhouse in cold regions. Results presented in this chapter fulfill part of the second objective of this thesis (i.e., to identify the different techniques of heating energy saving options for the conventional greenhouses), and more configurations are studied in Chapter 5 to address this objective completely. As the lead author of this manuscript, I conducted the research and prepared the manuscript for submission to the journal. The co-authors (Professor Huiqing Guo, and Professor Karen Tanino) have contributed to this manuscript through providing technical guidance to conduct the research and constructive review to improve the quality of research.

Abstract

Reducing heating cost is the major challenge for greenhouses growers especially the greenhouses located at high northern latitudes. Several techniques have been applied to reduce the heating cost in winter greenhouses. This study presents a comprehensive review of different energy saving techniques for reducing the heating cost of the conventional winter greenhouses including energy-efficient design of greenhouses, use of energy-efficient greenhouse cover, use of thermal curtain, energy-efficient management of indoor microclimates, selection of energy-efficient heating system, and potential of using alternative energy sources. Previous studies indicate energy saving potential of design parameters (shape, orientation) highly depend on the locations of greenhouses, and the energy-saving potential of most passive heating systems (water tanks, rock bed) might not be feasible for commercial greenhouses production in high northern latitudes. The reviewed also indicates that the alternative energy such as industrial waste heat, geothermal energy, and wood biomass could be a suitable option to reduce the greenhouse heating cost for large-scale production. However, it is very important to consider the trade-offs between the agronomic need of greenhouse plants and energy saving potential of various energy saving techniques, also the economic feasibility of energy saving systems in greenhouses. It can be concluded that the study would be useful for greenhouse growers, researchers, and manufacturer for creating the sustainable energy-efficient greenhouse production in cold regions.

4.1 Introduction

Control environment agriculture such as crop production in greenhouses is becoming very popular because of very high output which is 10 to 20 times higher than the outdoor production (Nederhoff and Houter, 2007). However, the higher energy cost in greenhouse production is the major challenge for the greenhouse industry. The energy cost is the second largest operating cost after labor for greenhouse production in cold regions. About 65-85% of the total energy consumed in greenhouses is used for heating, and the remaining portion is used for electricity and transportation (Runkle and Both, 2012). The cost for heating (mainly) and cooling in northern greenhouses represents about 70-85% of total operating costs excluding cost associated with labor (Anifantis et al., 2017; Rorabaugh et al., 2002), and the heating energy could be up to 90 % of the total energy demand (Kristinsson, 2006). Therefore, reducing greenhouse heating cost would make the greenhouse production more economical and sustainable. To reduce heating cost, the greenhouses must be energy-efficient and enable the use of renewable resources such as solar, biomass, and geothermal heat. Many studies have been conducted to reduce heating cost of greenhouses; several strategies such as energy-efficient structural design, use of energy-efficient cover, improved heating and ventilation systems, energy-efficient management of indoor micro-climates, and use of renewable energy sources, can be applied depending on the location of greenhouses. The principles of these techniques are mostly to increase the solar heat gain of the greenhouse and reduce heat loss from the greenhouses. However, its very important that there are trade-offs between the agronomic need of the plants and energy saving potential of various energy saving techniques (Sanford, 2011). Hence, the information related to the energy-efficient strategies and their effect on plants and the economic feasibility of the existing heating energy-saving technologies for the conventional greenhouses would be useful for the greenhouse growers, researchers, and manufacturer. Sethi and Sharma (2008) reviewed and evaluated the various passive heating technologies available for worldwide agricultural greenhouses. Anifantis et al. (2017) reviewed key strategies of energy saving using renewable and sustainable based solutions such as photovoltaic (PV) modules, solar thermal collectors, and hybrid PV/T collectors and systems. To our best knowledge, there is no recent literature review about the energy saving techniques for reduction of heating cost in the conventional greenhouses. Therefore, the objective of this study is to present a comprehensive review of the potential techniques to reduce the heating cost of the conventional-style winter greenhouses.

4.2 Energy-efficient design of greenhouses

The energy-efficient design of greenhouse envelope is very important to reduce the heating cost of the conventional greenhouses located in cold regions. The goal of energy-efficient design is to increase solar energy gain and energy retention in the greenhouses. The design parameters of greenhouse envelope that greatly affect the heating requirement include the greenhouse shape, orientation, and north wall.

4.2.1 Greenhouse shape

Greenhouse shape influences the amount of solar radiation received by the greenhouse, as well as amount heat transfer with the outsides. In general, greenhouses are distinguished into two types: (i) single module or mono-span; and (ii) multi-module or multi-span. Djevic & Dimitrijevic (2008) studied the energy consumption for various types of double-layered plastic film covered greenhouses in Serbia region and reported 4-10% less heating energy consumption in the multi-span greenhouse as compared to the different types of single-span greenhouses. The multi-span greenhouses are more energy efficient as compared to the single-span greenhouse because less surface exposes to the outside per unit floor area (Boodley, 1998; Hanan, 1998a). Also, the geometry of greenhouse roof has a significant effect on solar energy gain and heat loss in winter greenhouses. Five different shapes including even-span gable roof, uneven-span gable roof, gothic arch shape, vinery shape, and quonset shape are usual practice for crop production (Figure 4.1). A few studies have been conducted for selecting the energy-efficient greenhouse shape for different locations because the energy-saving potential of greenhouse shape greatly depends on the locations of greenhouses. Chandra (1976) theoretically studied the thermal performance of three types of single-span greenhouses (even-span gable roof, gothic arch roof, and quonset shape) under weather condition of Winnipeg (49˚N) in Canada. It was observed that the gothic arch roof greenhouse required about l5-25% less heating as compared to the gable roof and quonset type of greenhouses. Gupta & Chandra (2002) evaluated the heating requirement of three types of greenhouses under cold climate condition of northern India (28˚N). The simulated heating requirement in the gothic arch shaped greenhouse was about 2.6% and 4.2% less as compared to the gable roof and the quonset shape, respectively. Similarly, Cakır and Sahin (2015) studied five different greenhouse shapes (Figure 4.1) for selecting the optimum shape based on the availability of solar radiation; they reported that the gothic arch shape as the optimum type in the studied region (40.3˚N) in Turkey. Conversely, Singh and Tiwari (2010) studied the thermal performance of similar five

different greenhouse shapes under weather condition in New Delhi, India. The results indicated that the uneven-span gable roof greenhouse received the highest solar radiation because uneven-span shape has a highest surface area for receiving the solar radiation, and quonset shape received the lowest solar radiation; therefore, the uneven-span shape gable roof greenhouse required the lowest additional heating to keep the optimum indoor temperature. Similarly, Sethi (2009) theoretically studied the availability of solar radiation in five different greenhouse shapes under three different climate conditions (10˚N, 31˚N, and 50˚N) of India and obtained a similar result in all three different latitudes. Other similar studies (Kumari, Tiwari, & Sodha, 2007; Malquori, Pellegrini, & Tesi, 1993; Tiwari & Gupta, 2002) conducted under different climate condition also recommended that the uneven-span gable roof greenhouse is the most suitable from the heating point of view. Ahamed et al. (2018a) also optimized the greenhouse shape based on the additional heating requirement in five different greenhouse shapes (Figure 4.1) in Saskatoon (52.13˚N), Canada. The results showed that the uneven-span gable roof shape received the highest solar radiation, but no significant difference in the heating requiement as compared to the even-span gable roof shape; whereas the quonset shape received the lowest solar radiation; however, the quonset shape greenhouse required about 7.6% less annual heating as compared to the even-span gable roof shape, but the quonset shape cannot be adopted as multi-span greenhouses. Hence, the even-span gable roof greenhouse was considered as energy-efficient for the multi-span gutter connected greenhouses whereas quonset shape as a free-standing single span greenhouses. Ghasemi et al. (2016) investigated the energy saving potential of six different greenhouse shapes including: even span, uneven span, vinery, single span (mono roof), gothic arch, and quonset type, under the climatic condition of Tabriz, Iran. The results showed that the single span shape received the highest solar radiation and the vinery shape received the lowest solar radiation in a typical winter day, whereas the vinery shape showed the least supplemental heating requirement and the highest heating was required for the gothic arch shape to reach desired plant temperature.

Based on the outcome of previous studies, it shows that the energy-efficient greenhouse shape could be different depending on the location and physical dimensions of greenhouses. Therefore, it is very important to study the energy-saving potential of greenhouse shape based on local weather conditions because the heat gain from solar radiation per unit area of cover could be lower than the rate of heat loss under extreme cold weather conditions (Ahamed et al., 2018a).

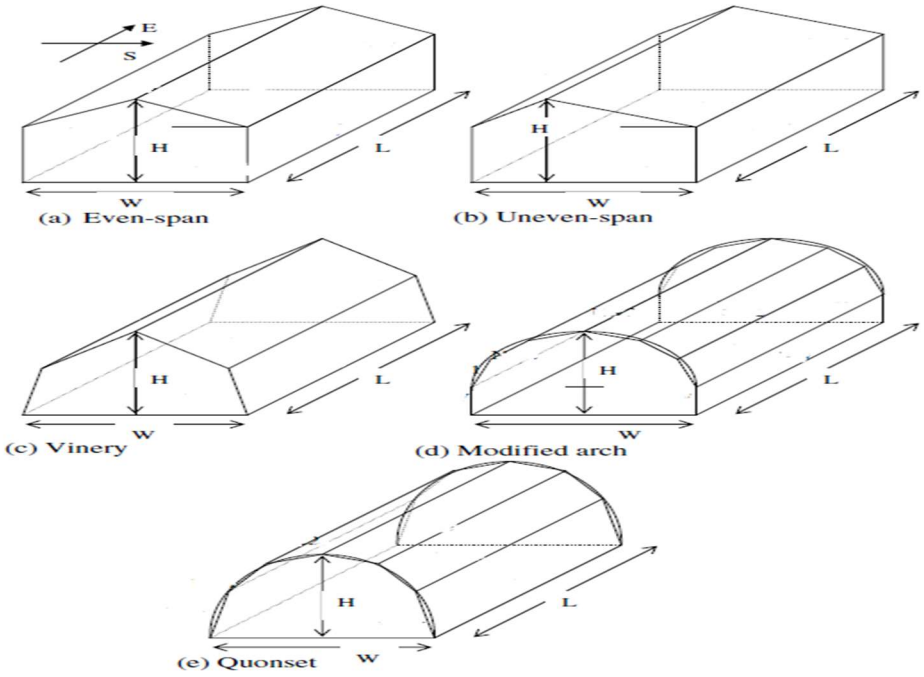

Figure 4.1: View of the common conventional greenhouse shape (Sethi et al. 2009).

4.2.2 Orientation

The orientation of a greenhouse (ridge direction) has a significant contribution to reducing the heating energy of winter greenhouses and its effect is location dependent. Chandra (1976) theoretically studied the energy-saving potential of an east-west (E-W) oriented free-standing gothic arch shaped greenhouse under northern latitudes of Canada (49.25°N). It was observed that east-west (E-W) oriented greenhouse required about 20% less heating as compared to the same size of greenhouse with a north-south (N-S) orientation. Gupta & Chandra (2002) simulated the heating requirement of a gothic arch shape greenhouse (1200 m^2) with E-W and N-S orientation in India (28.8˚N); the heating requirement with E-W orientation was only 2% less than the N-S oriented one. Stanciu et al. (2016) evaluated the effect of orientation on the heating and cooling requirement in a greenhouse (180 m^2) located in Romania (44.25˚N). They found the cooling energy saving was about 125 kWh/day in June and 87 kWh/day of heating energy saving in January, with the E-W orientation as compared to the N-S oriented one. Conversely, Ghasemi et al. (2016) reported that the N-S orientated greenhouse required less additional heating in a typical winter day as compared to E-W orientated one in Iran. Facchini et al. (1983) evaluated the energy efficiency of a greenhouse with different orientations and concluded that the longer side should face the south, i.e. E-W orientation, for lower energy consumption in a greenhouse located in

northern Italy. Similarly, a few studies have been conducted to select the optimum orientation of a greenhouse based on the availability of solar radiation in the greenhouse. The solar transmissivity of a single-span greenhouse was studied experimentally using scale model with E-W and N-S orientation at 37.58°N latitude of Greece (Papadakis et al., 1998). The study proved that the E-W orientation is preferable since the average solar energy gain for the E-W orientation was higher than the N-S orientation. Sethi (2009) theoretically studied the availability of solar radiation in an even-span gable roof greenhouse at three different latitudes (10°N, 31°N, and 50°N) in India. At 10°N latitudes, it was found that the N-S orientation receives more solar radiation over the year as compared to the E-W orientation. However, the comparison of orientation at 31°N latitude showed that the E-W oriented greenhouse received about 5.4% higher solar radiation in December and 15.8% less solar radiation in June. The difference of solar radiation gain with E-W orientation and N-S one was significantly higher at greater northern latitudes (50°N), with 14.2% higher solar radiation in December whereas it was 8% less in June. Similarly, Ahamed et al. (2018a) reported about 51.8% more solar radiation in December with a single span E-W orientated greenhouse in Saskatoon, Canada, whereas about 20.1% less in June with N-S orientation. A similar result was also found from the theoretical study conducted by Dragićević (2011) for different latitudes (24˚N, 34˚N, 44˚N, and 54˚N) in Serbia. Most of these previous studies have been conducted for the single-span greenhouse. Harnett et al. (1979) reported the consistent benefit regarding the solar light transmission in a multi-span E-W orientated greenhouse as compared to the N-W one; however, the uniformity of light transmittance can be reduced in an E-W oriented multi-span greenhouse because shadow could occur on the plants from the gutters of greenhouses. Conversely, Ahamed et al. (2018a) reported that the solar heat gain with E-W orientation could be reduced by a large margin for a multi-span greenhouse when the length-width ratio become greater than one.

In summary, a greenhouse with E-W orientation receives higher solar radiation during the winter season at higher northern latitudes because of lower altitudes angle of the sun. Thereby, the long south facing surface receives the high direct solar radiation during the winter time. Hence, the length-width ratio of a multi-span greenhouse need to be maintained greater than one to obtain the maximum benefit of E-W orientation in northern greenhouses.

4.2.3 North wall

The design of north wall is very important because most incoming solar radiation in greenhouses is received by the south wall and south roof and mostly leaves through the transparent north wall. The thermal performance of a northern greenhouse can be improved by using the reflective north wall and the massive thermal mass in the north wall or using heat storing materials.

4.2.3.1 Non-transparent north wall

The concept of the opaque north wall is practiced for greenhouses in northern hemisphere because of lower altitude angle of the sun in the winter season. The transparent north wall has a high potential of losing solar energy because the direct incoming solar radiation usually leaves through the transparent north wall. Chandra (1976) observed that a very little solar heat gain (around 3%) from the transparent north wall in an east-west oriented greenhouse. In another study, it was reported that about 24% of solar radiation loss can be decreased with the nontransparent north wall in a greenhouse in India (Tiwari et al., 2002). The north wall insulation in a N–S oriented greenhouse in India (28˚N) resulted a little reduction in the heating requirements (approx. 5%), whereas the reduction was about 30% in an E–W oriented greenhouse. This difference in the reduction with greenhouse orientation could be the direct consequence of the area available for insulation such as the north wall area in a N–S oriented greenhouse was only 39.18 m^2 while the area available in an E–W oriented greenhouse was 1584.0 m^2 (Gupta and Chandra, 2002). Different techniques such as the use of color coated film, aluminized polyester film, and air proof polyethylene film coated with aluminum, have been practiced to prevent direct solar radiation loss through the north wall. Heartz & Lewis (1982) observed about 14% less heating requirement with the reflective north wall (white coating) as compared to the conventional greenhouse with the transparent north wall. Aluminized polyester sheet was used as a reflector in the north wall of a 121 m^2 glass-covered greenhouse at Silsoe Bedfordshire (52.05˚N), UK, to reduce the loss of direct solar radiation through the north wall (Bailey and Critten, 1982); the lighting intensity in the greenhouse was about 20-25% higher than the greenhouse with a transparent north wall. In another application, a 30-mm thick of glass wool wrapped in airproof polyethylene film with aluminum coating was used to make the opaque north wall in a glass-covered greenhouse (Andersson and Nielsen, 2000). About 28% of the heating requirement was reduced as compared to the uninsulated greenhouse, but electrical energy consumption was increased by 35% for the additional supplemental lighting to increase the lighting intensity in the greenhouse. The overall reduction in

energy consumption was about 25% less as compared to the uninsulated greenhouse (Andersson and Nielsen, 2000). In another application, the thermal performance of opaque north wall in a 340 m^2 single polyethylene covered greenhouse was tested in Gard Andure, France (Banboul and Banbouserale, 1987), and a similar study also performed in a 104 m^2 polycarbonate greenhouse at Lozere, France (Francois, 1987). In both studies, the opaque north walls were able to maintain about 7-9˚C higher indoor temperature than the outside air.

On the other hand, the inclination of the reflective north wall could increase the illumination level on the floor. Pucar (2002) observed that the inclined reflective north wall enhanced the illumination level about 50% as compared to the vertical wall. Similarly, Gupta & Tiwari (2005) concluded that a 15˚ inclined reflective north wall would be more efficient in utilizing solar radiations as compared to a vertical wall, as shown in Figure 4.2.

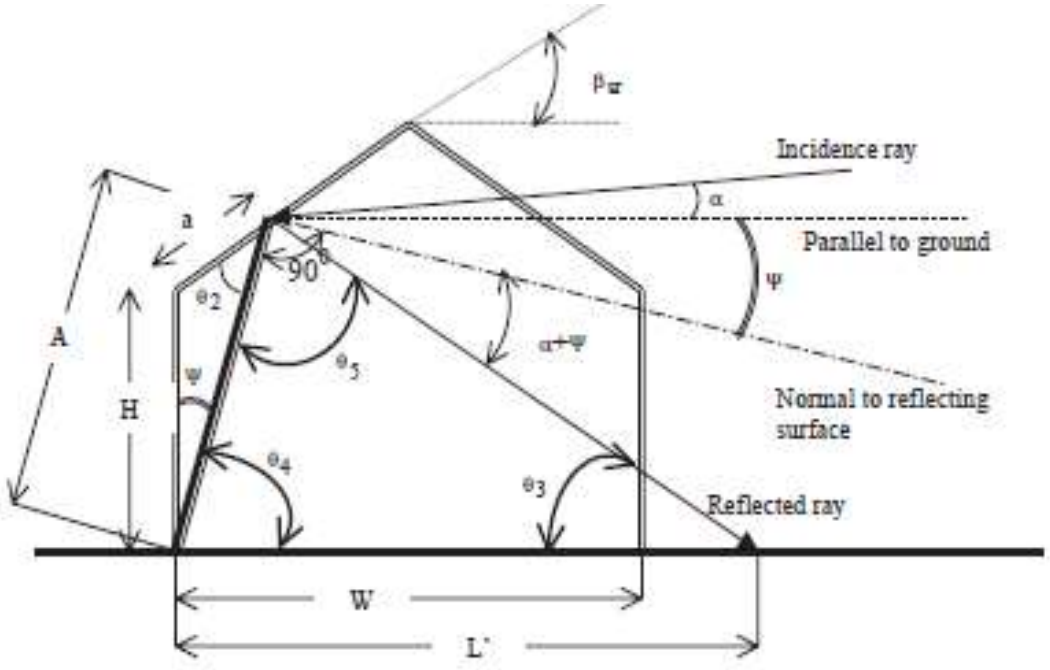

Figure 4.2: Schematic representation of reflective inclined surface attached to the north wall (Gupta and Tiwari, 2005a).

4.2.3.2 Heat storage with north wall

A significant amount of heating requirement can be reduced by using massive thermal mass in the north wall that can store solar energy during the daytime and release at night. The massive thick thermal mass is usually made of brick or cement blocks filled with different materials having high

heat capacity including sand, concrete, and phase change material (PCM). Santamouris (1993) reviewed the thermal performance of different heat storing north wall for greenhouse heating, and the reduction of heating demand was reported about 35-50% depending on the location and type of greenhouses. In another study, Santamouris et al. (1994) reported about 82% saving of heating energy with a 60-cm thick insulated north wall in a 30 m^2 glass-covered greenhouse with E-W orientation in France (46.85˚N), when the average daily temperature was 3.4˚C and 5.4˚C in December and January, respectively. Ghasemi et al. (2016) studied the energy saving potential of the north wall constructed of bricks covered with concrete for different greenhouse shapes in Iran. The results showed that the use of the brick north wall in the greenhouses on an average could reduce 13.4% of energy consumption. Gupta and Tiwari (2005b) studied the thermal performance of a greenhouse with the north wall made of brick, concrete, and mud; they concluded that concrete wall as the suitable one since more energy could be stored during sunshine hours. The study also reported that the variation of wall thickness had a negligible effect on the plant and room temperature.

Also, the heat storing north wall was used in combination with other thermal storage systems including the ground air collector (GAC), photovoltaic/thermal (PV/T) collector, and earth-to-air heat exchanger (EAHE) system to improve the greenhouse heating performance. In GAC, the solar radiation is absorbed in the blackened sand, concrete, and rock bed, and the absorbed heat is circulated in the greenhouse, and cool greenhouse air returned to the collector. Singh & Tiwari (2000) studied the thermal performance of a greenhouse (24 m^2) in India (28.40˚N) with massive north wall and ground air collector. The system was able to maintain the indoor temperature 5-6˚C above the outside air temperature. Similarly, Jain & Tiwari (2003) found that the stored thermal energy in the 12 m^2 GAC in a greenhouse (24 m^2) located in Delhi, India, gave a rise of temperature of 6–7˚C from the ambient during the night. Nayak and Tiwari (2008) studied the thermal performance of a greenhouse (48 m^2) with brick north wall integrated with two 76 W photovoltaic (PV) panels to store the solar energy in Delhi, India; they reported the yearly net electrical energy saving was about 716 kWh. Tiwari et al. (2006) studied the thermal performance of a greenhouse (24 m^2) with brick north wall integrated with the EAHE under same weather conduction, and the temperature of the greenhouse increased 4˚C for typical winter night due to use of an EAHE. Also, the potential of using stored thermal energy with the help of a GAC and EAHE was investigated for a greenhouse (24 m^2) in Delhi, India (Ghosal et al., 2005). The total

length of the buried pipes in both arrangements was kept same; and the temperatures of greenhouse air with GAC were observed to be 2–3˚C higher than those with EAHE.

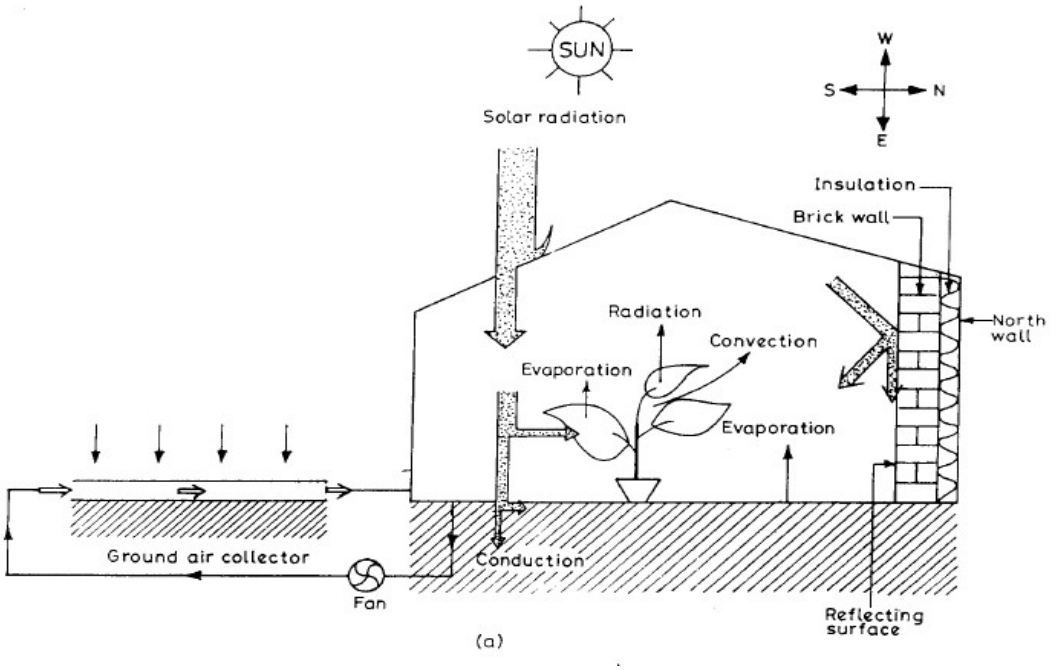

Figure 4.3: Greenhouse with heat-storing north wall integrated with the ground air collector (Jain and Tiwari, 2003).

Sensible heat storage systems such as massive north wall have low initial cost and require less technical knowledge as compared to the latent heat storage system by using the phase change materials (PCMs). However, the sensible heat storage systems such as massive north wall require a high volume of thermal mass and greater temperature difference. Therefore, the latent thermal storage system using PCM have many advantages over the sensible one including high heat capacity, low volume, low temperature, thermal energy stored and released at an almost constant temperature (Berroug et al. 2011). PCM use chemical bonds to store and release heat, it can store a large amounts of heat in phase change from solid to liquid (latent heat of fusion) at a constant temperature corresponding to the phase transition temperature and the circulating fluid (air or water) can extract heat from the storage unit causing the phase change material to solidify (Sethi and Sharma, 2008). There are two types of PCM: organic (paraffin wax, vegetable extract, polyethylene glycol) and inorganic (salt hydrates). The most commonly used PCM in the greenhouses are $CaCl_2 \cdot 6H2O$, $Na_2SO4 \cdot 10H_2O$, polyethylene glycol (PEG), and paraffin. Sethi and Sharma (2008) reviewed the different techniques of using PCMS for greenhouse heating and

reported that the use of $CaCl_2$ $6H_2O$ as a latent heat storage material could satisfy 30–75% of the annual heating needs of greenhouses situated at various locations. Later, Berroug et al. (2011) also theoretically studied the inside temperature of a greenhouse with a $CaCl_2$ $6H_2O$ filled a north wall, and the temperature of plants and indoor air were found to be 6–12˚C high during a winter night as compared to the greenhouse without the PCM filled north wall. Bouadila et al. (2014) studied the thermal performance of a greenhouse (14.8 m^2) in Tunisia (36.4˚N) with a solar air heater with PCM using a packed bed of spherical capsules as a latent heat storage system. Results showed that the night time temperature was about 5°C higher as compared to the controlled greenhouse. However, more technology development is still required for application of this technology in greenhouses. The major barriers to use PCM include the super-cooling, low thermal conductivity, phase segregation, fire safety, and costs (Bland et al., 2017). The super-cooling and phase segregation could cause thermal cycling degradation thereby limiting the useful lifecycle of the material. Also, the sensitivity towards the moisture causes serious disadvantages for long-term usage. Moreover, there is a big research gap about the economic feasibility of using PCM for large-scale greenhouse production and also the maintenance needed for PCM systems once they have been installed in greenhouses.

4.3 Use of energy-efficient greenhouse cover

The selection of covering materials for greenhouse depends on several factors such as capital cost and maintenance cost, its effect on plant growth and yield, and local climate and technical support (Papadopoulos and Hao, 1997). The greenhouse cover or glazing is the basic factor that greatly influences the energy consumption in greenhouses (Papadakis et al., 2000). Good covering materials must have high transparency to global solar radiation, especially within the photosynthetically active radiation (PAR) range, should be as opaque as possible to the long-wave infrared radiation (IR). A good covering material also must have higher diffusive radiation, good insulation, and anti-condensation properties (Castilla, 2013). Greenhouse covering materials are mainly two types such as plastic film and rigid panels (glass, polycarbonate, fiberglass, and acrylic). There is no ideal greenhouse cover; each has pros and cons and influence the plant microclimates in unique ways. The high transmissivity to the short-wave solar radiation and low transmissivity to the long-wave radiation, as well as low thermal conductivity are the important properties of greenhouse cover for energy conservation in winter greenhouses. The important thermal properties of common greenhouse covering material are presented in Table 4.1. The

traditional glass and acrylic panels allow high solar radiation transmission into the greenhouses as compared to other covering materials, but the infiltration rates are higher in the rigid panel covered greenhouses because the infiltration rates are proportional to the number of joints/connections which are typically higher in rigid panels. On the other hand, polyethylene film covered greenhouses have low infiltration rate and transmit the light in a fairly scattered manner, but usually have greater heat loss for exchange of long-wave radiation. On the other hand, diffusive glass has advantages to scatter the light as well as transmission of photosynthetic light as good as non-treated glass when the antireflection coating is used. Hence, the improvement of light transmission with diffusive cover could result in less supplemental lighting thereby increasing potential energy saving (Victoria et al., 2012).

Table 4.1: Thermal properties of different greenhouse cover materials (Sanford, 2011; [b]Papadakis et al. 2000; Hill, 2006; [c]Zhao et al. 2011).

Covering Material		Solar transmission (%)	Long-wave transmission (%)	Emissivity coefficient	Thermal conductivity (W m^{-1} K^{-1})	Infiltration rate (ACH)
Glass (3.2 mm)	Single	88-93	3	0.9	0.76	1.10
Low emissivity glass (3.2 mm)	Single	78	<3	0.3[a]	0.76	1.10
Diffusive glass (3.2 mm)	Single	8-85	<3	-	-	1.10
Polyethylene film (6-8 mil, UV-stabilized)	Single	87	50	0.2	0.33	0.85
	Double	78	<50			0.75
Polyethylene film (6-8 mil, IR-barrier)	Single	87	20	0.2[b]	0.33	0.85
	Double	78	<20			0.75
Poly-carbonate (6-8 mm)	Single	90	<3	0.65[c]	0.17	1.10
	Double	78-82	<3			0.85
Acrylic panel (8 mm)	Single	90	<5	0.65[c]	0.2	1.10
	Double	84	<3			0.85

The condensation of water vapor on the inner surface of cover could reduce the solar transmissivity thereby reducing the solar heat gain in greenhouses (Papadakis et al., 2000). Eggers (1975) reported that about 15-18% less solar radiation transmitted under the untreated plastic covered greenhouse as compared to the greenhouse cover having anti-condensation property. Also, the characteristics of a water droplet on the cover influence the rate of heat transfer through the cover. The condensation on the glass and rigid plastic materials usually form as water film or spread drops, whereas sphere shape droplets form on the polyethylene film sheet. Holman (2010) reported that the overall heat transfer rate from a surface with dropwise condensation (sphere shape) could be as much as ten times higher than that of film condensation (spread drops), because the film condensation formed on the glass and the rigid plastic material improve the insulation to reduce radiation heat transfer from the greenhouses (Feuilloley et al., 1994). So, the condensation on the cover has advantage and disadvantage in term of heat transfer from the greenhouses. However, most studies agreed that the heat loss caused by condensation exceeds the heat transfer prevented by film condensation (Delwich and Willits, 1984; Garzoli, 1986; Weimann, 1986). Another serious problem with condensation is plant disease, dripping water from condensation on plant surfaces promotes fungal diseases such as botrytis and powdery mildew. Also, dripping water spreads plant pathogens from plant to plant by splashing soil and plant debris. The new plastic cover usually has the anti-dripping property which prevent condensation or allows the condensate flow down on the side that can reduce the problem associated with condensation.

A few studies have been conducted to evaluate the energy-saving potential of different types of greenhouse covers. Previous studies (Dieleman and Hemming, 2009; Hill, 2006; Tantau et al., 2009; Van't Ooster et al., 2008) concluded that the most promising methods of reducing heating energy demand in greenhouses is the use of double layer cover instead of single layer cover. Cemek et al. (2006) studied the effect of different type of polyethylene film covers on aubergine growth, productivity, and energy requirement. The monthly average air temperature in the double-poly greenhouse and the IR-barrier polyethylene were higher than the UV stabilized and the untreated polyethylene cover. The overall heat transfer coefficient of different types of glass covered greenhouse was studied by using MatLight computer model (Swinkels et al., 2001). The study reported that the total heat transfer coefficient of the double-layer glass is about 16% lower as compared to the single-glass cover. The heating requirement of a 4,000 m^2 double layer PE covered Venlo-type greenhouse was simulated using Transient System Simulation (TRNSYS) software

program, and compared the heating requirement with the single and double glass-covered greenhouse (Semple et al., 2017). The heating demand in the double layer PE covered greenhouse was about 27% less as compared to the single layer glass-covered greenhouse whereas about 21% higher as compared to the greenhouse covered with double layered glass. Fabrizio (2012) studied the energy saving potential of a twin-wall polycarbonate covered greenhouse as compared to the traditional glass greenhouse, and the simulated results indicated that the polycarbonate cover greenhouse required 30-35% less heating than the glass-covered greenhouse. Researchers also trying to improve optical and thermal properties of existing greenhouse cover. High-quality polyethylene and glass are now available to reduce the condensation and heat loss problems associated with the traditional covering materials. A new double-layer glass panel with different anti-reflection coatings has similar transmissivity (84%), and lower heat transfer coefficient (3.6 W m^{-2} K^{-1}) as compared to the traditional single glass (7.6 W m^{-2} K^{-1}) (Hemming et al., 2011). Another study was conducted in a 500 m^2 greenhouse in the western Netherlands, the results showed that the new double layer glass also has transmissivity about 88%, and the heat transfer coefficient was 1.2 W m^{-2} K^{-1}, whereas 6.7 W m^{-2} K^{-1} for the traditional single glass (Hemming et al., 2012). Kempkes et al. (2014) also found that the use of this new double layered glass cover had energy savings up to 60% without affecting the production level in a commercial nursery greenhouse in the western Netherlands. Hemming et al. (2017) reported about 10-20% more natural light in greenhouses could be achieved during winter months through use of diffuse coverings with anti-reflective coatings and hydrophilic condensation properties on light transmission. So, the use of newly developed covering materials (diffusive glass, rigid plastic cover) could reduce a significant amount of heating requirement in greenhouses and also could minimize the problems associated with the tradition covering materials.

4.4 Energy saving potential of thermal screen

Thermal screen or night curtain is often used to reduce the loss of thermal radiation to the sky during the winter nights. The use of thermal screen can reduce about 40-70% of night-time long-wave radiation loss from the greenhouse (Andersson, 2010; Bakker, 2006; Chandra and Albright, 1981). Sethi & Sharma (2008) reported that the use of thermal screen in greenhouses could save about 23-60% of heating energy depending on the location and types of thermal screens, and the heating energy saving could be up to 90% by using thermal curtain with other passive heating systems such as rock bed heat storage system. De Zwart (1996) studied the energy saving potential

of the thermal screen in a Venlo type greenhouse (768 m^2) located in the Netherland, and the annual energy consumption was reported about 20% less as compared to the greenhouse without a thermal screen. Different types of thermal screens (aluminized thermal screen, isotex 60, polyester screen, black polyethylene, polypropylene monofilaments, and ethylene thermal screen) have been used to reduce the greenhouse heating requirement. A large number of studies (Andersson, 2010; Bailey, 1981; Bailey & Winspear, 1975; Dawson & Winspear, 1976; Goebertus, 1988; Rebuck, Aldrich, & White, 1977; Teitel, Peiper, & Zvieli, 1996; Zhang et al., 1996) have been conducted to evaluate the energy-saving potential of various types of thermal screens. Coulon & Wacquant (1984) experimented with two types of thermal screens namely permeable thermal screen (isotex 60) and aluminized thermal screen. The total fuel consumption per unit area was reduced by 24.48 % with isotex 60, and about 42.9% with aluminized thermal screen as compared to the greenhouse without a thermal screen. Sethi et al. (2003) used aluminized polyester sheet as a night screen in a 21 m^2 glasshouse in India (30.56°N), and observed 3-4˚C higher indoor temperature as compared to the unscreened greenhouse. The aluminized thermal screen is more efficient because of high reflectivity as compared to the other screens such as polyethylene, polyester, polypropylene, and polystyrene. Fuller et al. (1984) reported about 30% of energy saving in a greenhouse by using a molded polyester screen with mixture of aluminum. In addition, the polyethylene sheet and the inflated polyethylene tube also used to increase the roof insulation at night. Abak et al. (1993) reported that the night temperature in a single skinned plastic greenhouse with PE made night screen was 3.4˚C higher as compared to the unscreened greenhouse. Öztürk & Başçetinçelik (2003) used thermal screens made of PE and polyester material, and the thermal screen effectiveness for energy saving was 16% and 19.8%, respectively, for the PE and polyester screens. Roberts et al. (1981) used polypropylene monofilaments thermal screen in a double-layered PE covered greenhouse and obtained the energy savings up to 58%. Jolliet et al. (1984) reported that an ethylene thermal screen (EVA) and chrome coated one reduced the nighttime thermal transmittance through the roof by 35 % and 47 %, respectively, and whereas about 52 % if they installed simultaneously. The experimental study conducted by Short & Shah (1981) indicated that the night time heat loss from a double acrylic greenhouse could minimize by 60–70% with the polystyrene pellet shading system. An additional thermal blanket over the plant mass and below the thermal screen was recommended for winter greenhouses, and the air temperature surrounding the plant mass was recorded 2-5°C higher than air temperature between the cover and the thermal

screen (Ghosal and Tiwari, 2004; Shukla et al., 2006a, 2006b). Also, double layer thermal screen also recommended instead of single layer thermal screen to improve the effectiveness of thermal screen (Cui and Wang, 2002). From previous studies, it shows that at least 20% of heating energy could be saved by drawing any thermal screen at night in the winter greenhouses.

4.5 Energy saving potential of insulation

Greenhouse envelopes have little insulation as the maximum light transmittance become beneficial for the plants. The energy saving from insulation in the conventional greenhouses including the air gap insulation in double-layered cover, insulation in the side wall and basement wall, is reviewed in this section.

4.5.1 Insulation between two layers of cover

Greenhouse heat loss could be greatly reduced by providing the insulation between two layers of cover such as air layer insulation, liquid foam insulation, air bubble insulation, and pellet insulation. Inflated air layer insulation is the most common and affordable technique for the double layer polyethylene covered greenhouses. An electric blower is usually used to maintain an internal air layer which form a heat insulation barrier to reduce the transmission heat loss through the cover. It is recommended to draw the air from outside to prevent the condensation between the sheets because outside air is usually drier than the indoor air (Sanford, 2011). Also, the pellets of polystyrene beads and the liquid foam have been experimented to provide insulation in the double layer polyethylene covered greenhouses. The former is one of the most energy efficient insulation systems in the greenhouses (Short and Shah, 1981), and it can reduce the cover heat loss by 90% (Elwell et al., 1984). However, the pellet insulation system did not become popular for large commercial greenhouses because of difficulty in conveying and distributing the pellets (Enshayan, 1984). The liquid foam insulation system is very convenient regarding the handling of foam between two layers of cover. The liquid foam is generated and injected into the gap between two layers of the cover, and the collapsed foam is drained to the storage tank. The use of liquid foam techniques in greenhouses firstly reported during the late 1970s (Groh, 1977; Wells, 1980). The theoretical analysis proved that the maximum energy saving potential of this technique was up to 80% (Groh, 1977), but the experimental study found the energy saving potential about 20-40% (Wells, 1980). Villeneuve et al. (2005) studied the heating energy saving potential of using dynamic liquid foam in a conventional prototype greenhouse (24 m^2) in Montreal, Canada. Results

showed that the system could lead to energy savings of more than 50% at night, it was also noticed that the solar radiation measured inside the greenhouse was about 5.0% lower than the reference greenhouse since the presence of foam or solution residues on the membranes could reduce the transmissivity of cover. Similarly, Aberkani et al. (2006) found that the use of the liquid foam system reduced energy consumption by 62 % without reducing tomato yields. The thermal performance of liquid foam insulation technique also investigated for a greenhouse in Canada (42˚N) and reported up to 62% reduction of roof heat loss at night in April, and at least 29% reduction in January (Aberkani et al., 2011). The energy saving potential of liquid film can be decreased by the outside cold air temperature, and the extremely low outside temperature might freeze the liquid foam (Aberkani et al., 2011; Roberts & Mears, 1978). Also, air bubble plastic film along the inside surface of the cover could reduce the heating demand in greenhouses. Depending on the location, the film can reduce the heating demand up to 50% when applied along a single layer PE covered greenhouse (Duncan et al., 1979). Most of these insulation techniques except the air layer insulation were studied for the small or prototype greenhouses. The main barrier for using the liquid foam and pellet insulation system is the maintenance and operation of the system. Also, limited information is available about the economic feasibility of these systems for the commercial-scale greenhouse production.

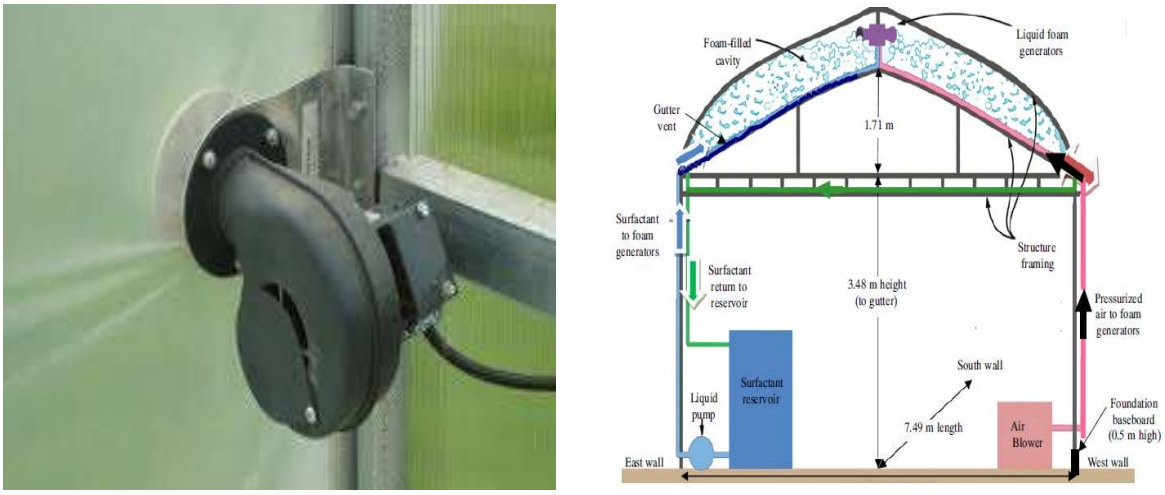

Figure 4.4: (a) A electrical blower for providing insulation in double layer polyethylene covered greenhouses, and (b) liquid foam insulation between two layers of cover (Aberkani et al., 2011; Runkle and Both, 2012).

4.5.2 Foundation and sidewall insulation

Insulation to the foundation around the perimeter of greenhouses, to the side walls up to the height of the plants can reduce a significant amount of conduction heat loss from greenhouses. Foundation heat loss can be reduced by 50% through the installation of 2.5-5 cm of polyurethane or polystyrene insulation (Latimer, 2009). Installation of polyurethane or polystyrene board (2-5 cm thickness) vertically around the entire perimeter to a depth of 0.6 m can increase the soil temperature near the sidewall as much as 10˚C in the winter season (Bartok, 2001). Gauthier et al. (1997) evaluated the energy-saving potential of perimeter insulation (0.76 m thick polystyrene) in a polycarbonate panel covered greenhouse (60 m^2) in La Pocatiere, Canada. Results show that the energy recovery ratio for the installed soil heat exchanger-storage system (SHESS) in the greenhouse is approximately 73% with insulation around the perimeter and falls to 67% without perimeter insulation. Similarly, extruded polystyrene insulation board, aluminum faced building paper, and foam insulation can be installed to the sidewall up to bench height or height of plants to reduce the heat loss. A study proved that the installation of 4-5 cm thick foam insulation up to 1 m height of side wall in a greenhouse (250 m^2) saved about 1514 liters of fuel oil or 1526 m^3 of natural gas over a heating session under northern climates (Bartok, 2001).

4.6 Energy saving potential of indoor microclimates management

Optimum climate control in greenhouses is very important for better plant growth, yield and quality, and also for energy saving. A significant amount of heating energy can be saved by effective management of indoor greenhouse microclimates including indoor set-point temperature and relative humidity.

4.6.1 Integration of indoor set-point temperature

A significant amount of greenhouse energy consumption can be reduced through lower the set-point temperatures. Also, extreme suboptimal temperatures may delay plant development and also affect other plant characteristics such as dry matter distribution (Körner and Challa, 2003a). So, the temperature integration (TI) is probably a better option for most greenhouse crops. Previous studies reported that the temperature effects on plant growth are relatively high under daylight conditions (Challa et al., 1995; Heuvelink, 1989). Also, Tantau (1998) reported that the night time energy consumption in a single layer glass-covered greenhouse is about 70% of the total energy consumption for 15°C indoor set-point temperature (Figure 4.5). So, the dropping of night

temperature (1-2˚C lower than the daytime temperature) could reduce the heating energy consumption up to 30% in winter greenhouses (Elings et al., 2005; Gilli et al., 2017; Langton and Hamer, 2003; Spanomitsios, 2001).

Conversely, several studies indicated that most crops respond to the longtime average temperature rather than fixed day/night temperature integration (Langhans et al., 1985; Miller et al., 1985). Therefore, dynamic temperature integration (DTI) over a longer period can compensate the cold spell during one of the following days that can accelerate the higher saving energy in greenhouses. Several studies tried to study the energy-saving potential of DTI between sub-optimal (lowest critical) and supra-optimal (top critical) temperature, and maintain the desired average for any user-defined period. Sigrimis et al. (2000) studied the energy-saving potential of varying the heating set-points temperature using past information to achieve the desired average for a particular period. The study allowed the temperature drop by 1-2°C below 17˚C for a couple of hours over three days and maintained the desired average temperature similar to the average temperature in FTI strategy (17˚C for the night and 22˚C for daytime) for 30 days. As compared to the fixed temperature integration (FTI), the DTI strategies for the long time (1-3 days) reduced the energy consumption up to 23%. Similarly, Körner and Challa (2003b) reported about 4.5% annual energy saving for the short time DTI strategy or up to 9% for the long time (6 days) as compared with the FTI. Körner and Van Straten (2008) also found that the DTI for six days period reduced annual energy consumption by 13.4% as compared to fixed TI, whereas 7.8% for the 24 hour DTI strategy. However, TI could have effect on plant growth and development, and fruit quality. Langton and Horridge (2006) showed that DTI between sub-optimal (14°C) and supra-optimal temperatures (24°C) delayed flowering in chrysanthemum when compared with plants grown at FTI (19°C average temperature). Conversely, Truffault et al. (2015) reported that DTI did not affect tomato fruit size and composition (sugars, acids, vitamin C), but leaf area slightly decreased by 11%. DTI strategies are mostly applied with a temperature margin between 4-8 °C and an averaging period of 24 h (Körner and Van Straten, 2008). Some studies (Körner and Challa, 2004; Langton and Horridge, 2006) reported that DTI for an extended period (6 days) caused short flowering delays for chrysanthemum as compared to the 24 hour DTI.

A few studies have conducted to evaluate energy saving potential of TI with the temperature drop for certain hours. Borhan (2007) studied the energy-saving potential of TI with a pre-night (6 to 9 pm) temperature of 13°C as compared to the TI with a pre-night temperature of 17°C for tomato

production, and about 3-5% of reduced energy consumption was reported. Similarly, Hao et al. (2011) evaluated the energy-saving potential of TI with pre-morning (3 to 6 am) temperature drop at 13˚C, but the reduced the energy use from March to May was about 6-8%. Hao et al. (2015) studied energy saving potential with temperature drop for a certain period in the greenhouse for cucumber production. The air temperature was allowed to drop to 12°C during the pre-night period (6-9 pm) from March 6 to April 20 and 13°C during the pre-morning period (3 to 6 am) from April 27 to May 27, while it was maintained at 19°C or 18°C. The new temperature integration strategy (TI-drop) could be an energy efficient climate control strategy in greenhouse production; however some plants could be sensitive to the kind of temperature control practice in greenhouses.

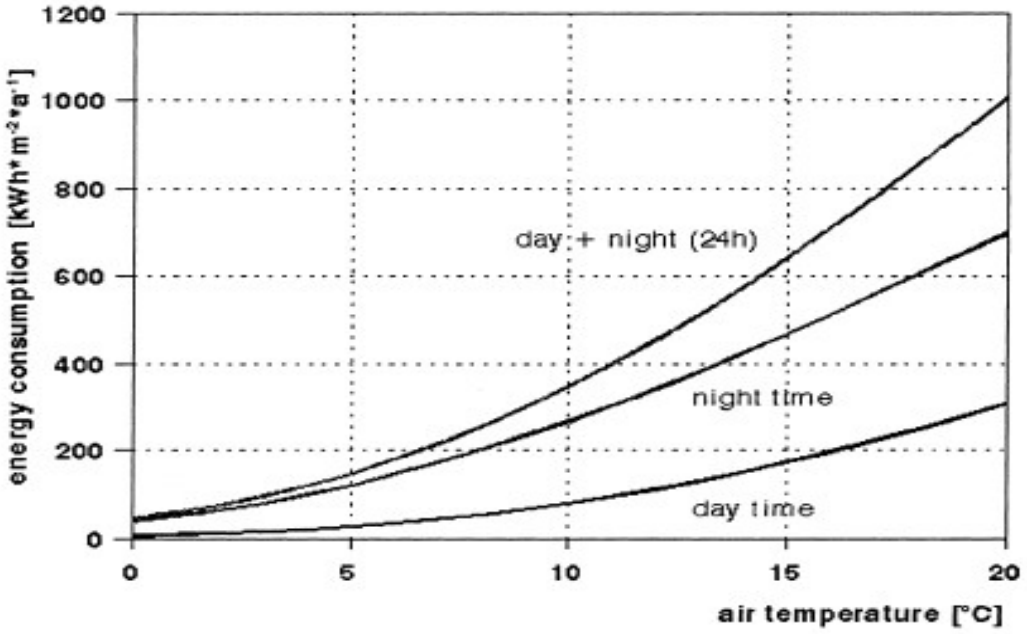

Figure 4.5: Specific energy consumption in greenhouses as a function of inside air temperature (Tantau, 1998).

Another approach for greenhouse energy saving with temperature integration is the control of set-point temperature based on the outdoor wind speed. The wind speed-based temperature control technique is such as dropping of set-point temperature below the required average value when outdoor wind velocity is higher than the average speed and increasing up to optimum set-point when wind speed is lower as compared to the average value. This practice would reduce heat loss from greenhouses as low temperature gradient would cause low the relative heat loss. The temperature integration in response to the outdoor wind speed gave a reduction of 5-10% in the

annual heating requirement in a study greenhouse as compared to a greenhouse heated at a constant 15˚C (Bailey, 1985). However, the energy saving potential in wind speed depending temperature control is comparatively low as compared to the temperature integration based on day-night integral (Tantau, 1998).

4.6.2 Control of indoor relative humidity

The control of high relative humidity (RH) is very important to prevent the fungal growth in plants in a fully closed greenhouse. The main reason for RH control is to prevent condensation, high RH caused plant disease. Also, the control of relative humidity may have an impact on the energy consumption in greenhouses. If the relative humidity exceeds a certain limit, then heating set-point will be increased because the control of humidity or the saturation deficit can be achieved by heating and/or ventilation so that energy consumption will be high (Tantau, 1998). However, greenhouse industry in cold region does not practice this strategy for RH control since high heat loss occurs during the heating season, so other dehumidification methods (heat exchanger, chilled water condensation, chemical dehumidification, and mechanical dehumidification) are used for commercial production. Campen et al. (2003) compared different dehumidification methods (air-to-air heat exchangers, ventilation, chilled water condensation) for a commercial greenhouse and suggested that the most promising and economical method would be the use of heat exchangers. Gao (2012) evaluated four dehumidification methods (air-to-air heat exchangers, ventilation, chilled water condensation, and mechanical dehumidifier) in a greenhouse located in the Canadian Prairies. Results showed that the mechanical dehumidification could be effective and energy-efficient dehumidification method for year-round. Similarly, other studies (De Zwart, 2014; Han et al., 2015) also reported that the internal mechanical dehumidifier is more energy efficient and effective for year-round operation.

On the other hand, the energy saving in greenhouses with temperature integration is comparatively high when the indoor air has high RH. Energy saving with the temperature integration was increased when the RH was over 90% as compared to the RH fixed at 85%. However, high RH (above 90%) could cause the condensation in greenhouse thereby plant disease would increase (Körner and Challa, 2003b). Körner and Challa (2004) showed that yearly energy consumption could be reduced by 18% for TI with RH control between 80 and 85% as compared to a fixed set-point of 80% RH. The study also reported that the dynamic RH within 80-85% had no negative

consequences on crop development, but there was a strong increase in the dry weight of all plant organs. Hence, TI with process-based humidity control (flexible humidity control regime) would be more energy efficient as compared to the fixed RH in greenhouses.

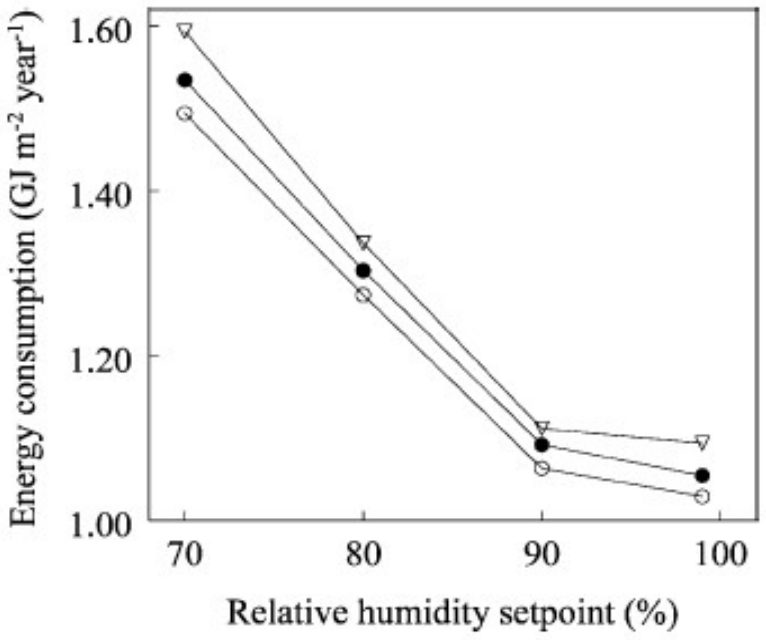

Figure 4.6: Energy consumption as a function of fixed RH set point for simulations with different temperature integrations scheme (Körner and Challa, 2003b).

4.7 Heating contribution of supplemental lighting

Supplemental lighting is very important for a modern greenhouse in northern latitudes because the shorter day length and reduced solar radiation affect the plant growth in greenhouses (Nelson, 1985). The supplemental lighting for greenhouses depends on the daily light integral which varies due to location and time of the year, and crop species; the lighting selection is also affected by lamp cost, electrical cost, and heating requirement (Dorais, 2003). The operating cost and the energy use efficiency are the major challenges of artificial lighting in greenhouses. The common types of lamps for artificial lighting in greenhouses are: (i) incandescent; (ii) fluorescent; and (iii) high-intensity discharge lamps (Castilla, 2013). Incandescent lamps have very low energy efficiency in converting electricity into photosynthetically active radiation (PAR) (around 6%), emitting most of the energy in the IR range. Fluorescent and high-intensity discharge lamp (halogen and sodium) have high energy efficiency 20%, and 26-27%, respectively (Baille, 1993). High-pressure sodium (HPS) lamp for supplemental lighting is more efficient for converting the

electrical energy into the useful light for photosynthesis. Besides, LED lamp is more energy efficient than HPS lamp, but the capital cost for LED is extremely high as compared to other lamps and no heating contribution in greenhouses. The energy efficiency of artificial lighting can increase by using inter-lighting (combination of HPS and LED) or more efficient lamps, as it is expected from light emitting diodes (LED) in the future (Castilla, 2013). Singh et al. (2015) reviewed the research work done on energy-efficient greenhouse lighting with LEDs and concluded that LEDs can significantly reduce the electricity cost and investment will be returned in long-term operations in greenhouse industry although it has high capital cost. However, more research is needed to understand the plant response to LED as a supplemental lighting source in greenhouse industries (Singh et al., 2015).

Although the main purpose of supplemental lighting is to increase the photosynthesis rate by extending the day length (photoperiod), it can provide a significant amount of heating in greenhouses depending on the types of lamps used. In general, about 75-100% of the consumed electrical energy by supplemental lighting systems (except LEDs) can be converted into the sensible heat (Castilla, 2013; Fisher et al., 2001). About 25-30% of the heating contribution was reported from high-intensity discharge (HID) lamp for a greenhouse located in the Netherlands (Mpelkas, 1981). Brault et al. (1989) reported about 25-41% of the heating requirement in a double poly greenhouse in Quebec City, was provided from the light level of 30 W/m^2 (PAR). Another study was conducted in a twin wall polycarbonate (8 mm thick) covered greenhouse located at the University of Laval, Quebec (46.47ºN). The heating contribution was reported up to 100% with supplemental lighting (25 W/m^2 of PAR) when the temperature difference between inside and outside was between 10-12ºC, and the heating contribution decreased to 30% when temperature difference was greater than 25°C (Zhang et al., 1996). Another study was conducted to evaluate the heating contribution from 21 high-pressure sodium lamps of 250 W which were used for supplemental lighting in a 100 m^2 glass-covered greenhouse in Seoul, North Korea (Yang et al., 2015). The greenhouse was operated with thermal screens at night. The heat contribution from lighting for five hours a day was evaluated up to 91.3 MJ, and the effective contributions of lighting for heating were between 12.8% and 72.2%. Ahamed et al. (2017) reported that the HPS lamp (100 W m^{-2}) contributed about 38.0% of the total heating requirement with eight hours of artificial photoperiod at the winter solstice. Similarly, White & Sherry (1981) suggested that the supplemental lighting with HID lamps (15 W m^{-2} PAR) met the heating requirement in the study

greenhouse when the temperature difference is less than 12ºC. Hence, the use of supplemental lighting could be an option to reduce the greenhouse heating requirement. Also, the supplemental lighting with HPS lamps could increase the operating costs depending on the rate of electricity, and LED has high initial cost, so the detailed economic feasibility evaluation would be beneficial for decision making about supplemental lighting system for greenhouse operation in cold regions.

4.8 Energy saving potential of heating systems

The heating system in greenhouses can be in the active or passive mode, and sometimes a combination of active and passive mode. Active mode of heating systems means the supply of heat from other sources for increasing indoor temperatures. In passive mode, the solar energy is used to heat the greenhouse by storing the heat using different heat storage materials. The passive heating systems are suitable for the small size of greenhouses located in moderate climates, and the active mode of the heating system is usually used for commercial greenhouse production at high northern latitudes.

4.8.1 Active heating

Active heating systems include the hot water pipe heating system, hot air heating system, and infrared radiation (IR) radiation heating system. In general, the water heating system is very common practice for large commercial greenhouses, and hot air heating system and infrared radiation heating system are mostly used for the small size of greenhouses or the Mediterranean greenhouses where heating needs are relatively low. In water heating, the plants are usually warmer than the surrounding air because the heating pipe is often placed at crop level and warms up the crops both by convectively heating the air and by radiating heat directly to the plants. Conversely, the main advantage of air heating is to promptly responses to control the air temperature, but additional energy electrical energy requires for the heaters (Bartzanas et al., 2005). Mavrogianopulos et al. (1993) reported that higher heat loss occurs in a small size greenhouse with pipe heating system as compared to the hot air heating system because the half of the total length of heating pipes was located near the side walls. Conversely, Teitel et al. (1999) found no significant difference between these two types of the heating systems regarding the energy use if the pipes and ducts are positioned between the plant rows, but the hot air heating system requires additional electrical energy that accounts 10% of the energy required for heating. However, the pipe heating system maintains higher plants temperature than the surrounding air so that indoor

set-point can be lower than the optimal temperature range. Therefore, the hot water heating system indirectly could reduce the greenhouse heating requirement by proving the heat closer to plants surfaces (Runkle and Both, 2012). The location of heating pipe in greenhouses was investigated by Popovski (1986), the study recommended the lower height of pipe mesh to reduce the radiation loss to cover, and to increase the radiation to crop canopy. The position of heating pipes closes to the plant canopy or on the soil could provide a uniform vertical temperature distribution by avoiding air stratification in greenhouses. This system can minimize the heating demand by 15-25% as compared to the conventional fan assisted convector heater (Jolliet et al., 1991). In general, the position of heating pipe at the middle height of crop canopy found the best practice for maximizing the efficiency of the heating system (Teitel and Tanny, 1998). However, the combination of the heating pipe and the air heater more suitable for optimum control of air temperature and relative humidity, but the heating energy consumption was increased by 19% (Bartzanas et al., 2005). Kurpaska & Slipek (2000) also studied the energetic efficiency assessment of two types of pipe heating systems such as the buried pipes heating system and vegetation heating system. The result indicated that the vegetation heating required 3K higher water temperature than buried pipe heating, and heat loss also found higher in vegetation heating system. Fabrizio (2012) studied the thermal performance of a polycarbonate-covered greenhouse with the underground heating system. In this system, the hot water (40°C) was passed through a hollow polypropylene sheet placed at 15 cm below the ground cultivation level. The system reduced the heating requirement up to 26% as compared to the overhead tube air heaters.

The use of infrared radiation heating system can be an alternative option for reducing the greenhouse energy consumption. The use of long-wave radiation heating sources could directly heat the greenhouse plants without moving air, so air and cover temperature remain relatively low and thereby heat loss could be reduced significantly. In the greenhouse with infrared radiation heating system, plant and greenhouse soil temperature could be 1.7˚C or higher than the surrounding air temperature (Stone and Youngsman, 2006). Caouette et al. (1990) compared the temperature distribution in an infrared radiation heated greenhouse with the greenhouse heated by the hot air heating system. The results showed that the infrared radiation heating system allowed to reduce the set-point temperature by 3˚C and still maintained the comparable leaf temperature. In another study, about 33-41% of heating energy savings was reported for using a long-wave radiation heating system as compared to the conventional air heating system (Blom et al., 1981).

Similarly, the heating energy saving potential of the infrared heating system was evaluated by comparing with the conventional water pipes heating system for a 285 m^2 Swedish greenhouses (Näslund et al., 2002). The heating energy saving potential was reported about 11.8%, and the heating saving could be increased by 15-20% for using the overhead heating system. Similarly, Kavga et al. (2007) reported that the heating efficiency of the longwave radiation heating system was about 45% higher as compared to the hot water pipe heating system for a 500 m^2 glass-covered greenhouse located in Greece. Teitel et al. (2000) used a 500 W microwave generator to heat a small greenhouse which was used to grow tomato and pepper plants. The experimental results showed that the microwave generator could be used for the greenhouse heating without visible plant damage. The energy required for microwave heating system was about 45% less as compared to the hot air heating system. Although the infrared heating system has advantages over conventional hot air and pipe heating system, but the infrared heating system cloud cause the greater temperature differences at various location in the greenhouse, so crops development may not be as uniform as in the conventional heating system (Näslund et al., 2002). However, more details studies about the use of radiant heaters for greenhouse heating might require as there is risk of burning the plant leaves. However, the radiant heater can be more suitable for loading ducks, header houses, and work areas of greenhouses (Sanford, 2011). Previous studies indicate the infrared radiation heating system could be more energy efficient among active mode of heating systems but also has some major consequences on plant growth, so hot water pipe heating system mostly practices for large-scale greenhouse production.

4.8.2 Passive heating

The passive mode of greenhouse heating system used solar energy for heating by using different heat storage materials such as water, rock bed, and phase change material (PCM). Sethi & Sharma (2008) reviewed and evaluated several types of passive heating for greenhouse application and concluded that this method is usually efficient for small size greenhouses located in the moderate climates. These passive heating methods can be combined with the active heating system to reduce heating cost of large commercial greenhouses. The following section reviewed the potential heating energy saving in winter greenhouse with the passive mode of heating systems.

4.8.2.1 Water heat storage

The heat storage in greenhouse by using water as storage media can be achieved by placing the water-filled plastic bags and ground tubes in the greenhouse between two rows of plants, and water tanks/barrels can be placed either inside or outside of greenhouses. These systems act as solar collectors and heat storage media during daytime and release heat at night. Several researchers (Farah, 1987; Grafiadellis, 1987; Mavrogianopulos et al., 1993; Montero et al., 1987; Pacheco, 1987) have studied the thermal performance of water-filled polyethylene bag and ground tubes for greenhouse heating. These systems could maintain 2–10˚C higher inside air temperature depending on the volume of water used in the system and the size of greenhouses. The bag diameters ranged between 23-35 cm, containing 60–70 liters of water per meter of tube length, and the length of tubes ranged between 2-12 m (Sethi and Sharma, 2008). A layer of 2–3 cm thick insulating sheet made of polystyrene is recommended below the ground tubes to reduce the heat loss to the ground (Farah, 1987; Sallanbus et al., 1987). However, these water tubes could cover from 20–30% of the greenhouse floor surface which could not be used for crop growing.

Several researchers (Dutt, Rai, Tiwari, & Yadav, 1987; Gupta & Tiwari, 2002; Santamouris et al., 1994; Sethi, Lal, Gupta, & Hans, 2003; Sorensen, 1989) have studied the thermal performance of different type of water tanks which usually were placed on the side of the greenhouse along the north wall. These systems were able to maintain the indoor temperature 4-10˚C high than ambient temperature depending on the solar absorption capacity of tanks, volume of water, and size of greenhouses. The water storage tank can be painted black to improve the heating performance of greenhouses. The water heat storage tanks placing outside of greenhouses were usually combined either with the air-water heat exchanger (Grafiadellis, 1987; Levav and Zamir, 1987) or the solar flat plate collectors (Hazami et al., 2005; Kumari, Tiwari, & Sodha, 2003). Shallow water pond (SSP) is another technique of using water mass for heat storage, where water-filled plastic containers are placed inside of greenhouses. The water body can be insulated at the bottom and side with a transparent plastic cover. Different chemicals or salt can be used to increase the heat storage capacity of the water pond. Carnegie et al. (1983) reported about 77% of annual heating energy saving from the shallow solar pond ($1/5^{th}$ area of the greenhouse) in a commercial greenhouse. Al-Hussaini & Suen (1998) conducted an analytical study for using shallow solar ponds as a heating source for greenhouses under cold climates of the United Kingdom (51˚18N). About 30% of the greenhouse floor area was considered as a solar pond having a black bottom in

a double poly greenhouse. The result showed that the system saved a significant amount of greenhouse heating energy from March to October and 100% saving in summer between May-September. The water heat storage system is very convenient for the small size of greenhouses which located in the moderate climate, but these systems occupied a significant greenhouse floor area.

4.8.2.2 Rock bed heat storage

In the rock bed heat storage system, the hot air from greenhouses is circulated into to the storage medium through recirculating fans to store the heat from solar radiation, and release by reverse circulation process at night when the indoor temperature is below the optimum level. The storage area of rock-bed can be inside and outside near to the greenhouse at a depth 40-50 cm, and most commonly used rock bed material is gravel having 2–10 cm diameter (Sethi and Sharma, 2008). A large number of studies (Bouhdjar et al., 1996; Kavin & Kurtan, 1987; Kürklü, Bilgin, & Özkan, 2003; Öztürk & Başçetinçelik, 2003; Santamouris et al., 1994) have been conducted to evaluate the thermal performance of rock-bed heat storage as a passive mode of greenhouse heating. The previous studies show that rock bed heat storage systems satisfied 15-76% of annual heating needs in greenhouses. Based on the review study conducted by the Sethi & Sharma (2008), the heating energy potentials of different type of rock bed as heat storage system for greenhouse heating are listed in Table 4.2. Most of these studies were conducted for the small-scale greenhouses because these passive heating systems might not be feasible for the large-scale production. Because the initial costs for these systems could be very high, and the heat storage density of solids is usually less than water thereby large amounts of solids are needed than water (Öztürk and Başçetinçelik, 2003b).

Table 4.2: Summary of heating performance of the different passive heating system with the rock bed as heat storage material.

Description of Greenhouse	Description of rock-bed	Thermal performance	Reference
Glass covered greenhouse (176 m^2) located in the USA (34.83˚N, 77.3˚W)	15,700 kg of gravel	Indoor temperature 5˚C higher	(Huang et al., 1981)
Polyethylene covered greenhouse (2850 m^2) located in Canada (45.5˚N, 73.5˚W)	202,000 kg of gravel	40% of heating needs	(Bricault, 1982)
Polyethylene covered greenhouse (300 m^2) located in Cyprus (35.2˚N, 33.3˚E)	74,000 kg of gravel	76% of heating needs	(Fotiades, 1987)
Glass covered greenhouse (432 m^2) located in Prague (50.1˚N, 14.3˚E)	43,000 kg of gravel	Indoor temperature 4-6˚C higher	(Jelinkova, 1987)
Polyethylene covered greenhouse (100 m^2) located in Hungary (47.4˚N, 19.1˚E)	48,000 kg of brick	53% of heating needs	(Kavin & Kurtan,1987)
Double glass-covered greenhouse (161 m^2) located in Germany (50.5˚N, 7.1˚E)	14,000 kg of gravel	20% of heating needs	(Santamouris et al., 1994)
Polyethylene covered greenhouse (120 m^2) located in Turkey (37.1˚N, 35.2˚E)	64,480 kg of Volcanic	18.9% of heating needs	(Öztürk and Başçetinçelik, 2003b)

4.9 Use of alternative energy for greenhouse heating

The increased price of fossil fuels and the effect of using fossil fuel on the environment are encouraging greenhouse growers to consider alternative fuels for greenhouse heating. The possible alternate sources for greenhouse heating cloud be industrial waste heat, geothermal heat, and wood biomass. The following section includes the previous studies about the potential use of alternative fuels for greenhouse heating.

4.9.1 Industrial waste heat for greenhouse heating

The term “waste heat” refers to heat that is either lost through the flue stack of an industrial operation, or which is rejected from a power generation station to improve the thermodynamic efficiency of the cycle (Andrews and Pearce, 2011). A huge amount of heat generally in the form of flue gases or warm water is released from industrial and power plant processing systems, these

waste heat can be utilized for greenhouse heating. The use of low-temperature industrial wastewater (20-25ºC) heating system has been proved to be a good approach in terms of greenhouse energy conservation (Connellan, 1986; Malfa, G., Noto, G., Parrini, 1992; Qaisar et al., 2010; Vreugdenhil and Mittleider, 2009). The wastewater from a power plant was used for heating six commercial Velno type greenhouses (53,000 m^2) covered with single glass (Brendenbeck, 1992). The heating system could maintain the greenhouse temperature up to 22ºC even with the outside temperature of 14ºC. Pietzsch and Meyer (2008) studied the potential of using reject heat from the biogas power plants for heating a greenhouse in Freising, Germany. Results showed that the useable reject of 650 kW could heat the greenhouse size of 5279 m^2. However, the useable reject heat from biogas power plant could be fluctuated by large margin, which might complicate greenhouse heating system. Chinese et al. (2005) studied the technical and economic feasibility of using low-temperature waste heat for greenhouse heating, and heat was released from the chair manufacturing industrial plant located in an industrial district of North-Eastern Italy. The study found that the proposed renewable energy solution could lead to significant savings in comparison to traditional fossil fuel from the point of view of costs and environmental impact. The result showed that the system could save up to 20% of fuel oil to maintain the indoor temperature range between 14-16ºC. Andrews & Pearce (2011) studied the feasibility of using waste heat from a glass industry for greenhouse application, and the system was found more economical than a purely natural gas heating system for the selected experimental greenhouse. Thomas et al. (2017) studied the energy-saving potential of using waste heat from a sugar plant discharge hot water (average temperature 46˚C and average flow rate of 7571 m^3 per day) for heating a greenhouse (1.2 ha) located in Lovell, USA. The simulated results showed that the heating energy consumption could be reduced by 67% through utilization of waste heat and water to air heat pumps when compared to the variable air volume heating (VAV) system. A similar study reported that the amount of waste heat from the sugar plant would be sufficient to provide the annual heating demands in a 1.25 ha greenhouse and a water to air heat pump system utilizing waste heat could save about 74% of the total annual site energy for greenhouse heating (Denzer et al., 2017).

Also, the effective use of industrial flue gas heat for greenhouse heating could be an alternative to reduce the CO_2 emission from the industry. The Kiawana Industrial complex in Australia performed an energy assessment of their local industry park and found the potential mitigation of

CO_2 emission up to 7% (Van Beers and Biswas, 2008). Therefore, the use of industrial was heat for greenhouse heating would be beneficial for reducing the heating cost and mitigation of CO_2 emission. However, the biggest barrier for using the waste heat is the high investment costs to connect wasted heat to the greenhouse, and another main barrier is the unreliability of waste energy to support required energy for greenhouse year around because of different maintenance periods in the processes and industries (Manning et al., 1983). Therefore, a detailed feasibility study is required for decision making regarding the use of industrial waste heat for greenhouse heating.

4.9.2 Geothermal energy for greenhouse heating

The use of geothermal energy for greenhouse heating can be another option for minimizing the heating cost in winter greenhouses. Based on the review of 2005, about 7.5% of the global use of geothermal energy is used for crop production in greenhouses (Lund et al., 2005). The worldwide use of geothermal energy for greenhouse heating increased by 10% in installed capacity and 13% in annual energy use. Geothermally heated greenhouses can reduce production costs up to 35%, allow production in cold temperatures where commercial greenhouses production would not be feasible (Lund, 2010). Depending on the underground soil and water temperature, the geothermal energy can be used through different techniques. Hot underground water (>60ºC) can directly supply into greenhouse heating system with pump and return to the reservoir (Bartok, 2015). Adaro et al. (1999) used underground warm water (average 27˚C) for heating a 1000 m^2 greenhouse located at Argentina (33.2˚N, 64.3˚W), and indoor temperature was 3-4˚C higher than ambient temperature. Similarly, Ghosal & Tiwarin (2004) used geothermal warm water (28˚C) for heating of a double poly greenhouse, which incorporated with thermal curtain and blanket just over plants. The results show that indoor temperature of the air surrounding the plant was about 5-10˚C higher than ambient temperature. The heat exchanger between geothermal water and the greenhouse heating system can be installed for using the low-temperature geothermal water. A steel plate main heat exchanger was used between geothermal water and the greenhouse heating system for heating a large commercial greenhouse located in Greece (Bakos et al., 1999). The system could maintain an inside temperature of 20ºC when the outside temperature was 7ºC and the inside temperature of 15ºC when the outside temperature falls to 2ºC. Kondili and Kaldellis (2006) studied the heating performance a greenhouse (10,000 m^2) in Greece using the geothermal hot water of temperatures around 82˚C and yields a flow rate over 30 m^3/h. According to the results obtained the mean daily heating deficit during winter was about 5 MW h/day, and about 50% of

the available geothermal energy from the system could support the heating requirement in the greenhouse during the winter season. Sethi & Sharma (2007) studied the thermal performance of a greenhouse (24 m^2) which heated using the underground water (24-25˚C) from an irrigation well. The greenhouse air was circulated through the pipe (fully immersed in water) placed horizontally in the trench in the opposite direction (Figure 4.7). The air circulation system was connected to the heat exchanger, and the system was able to maintain the greenhouse room air temperature 7–9˚C above ambient during winter nights.

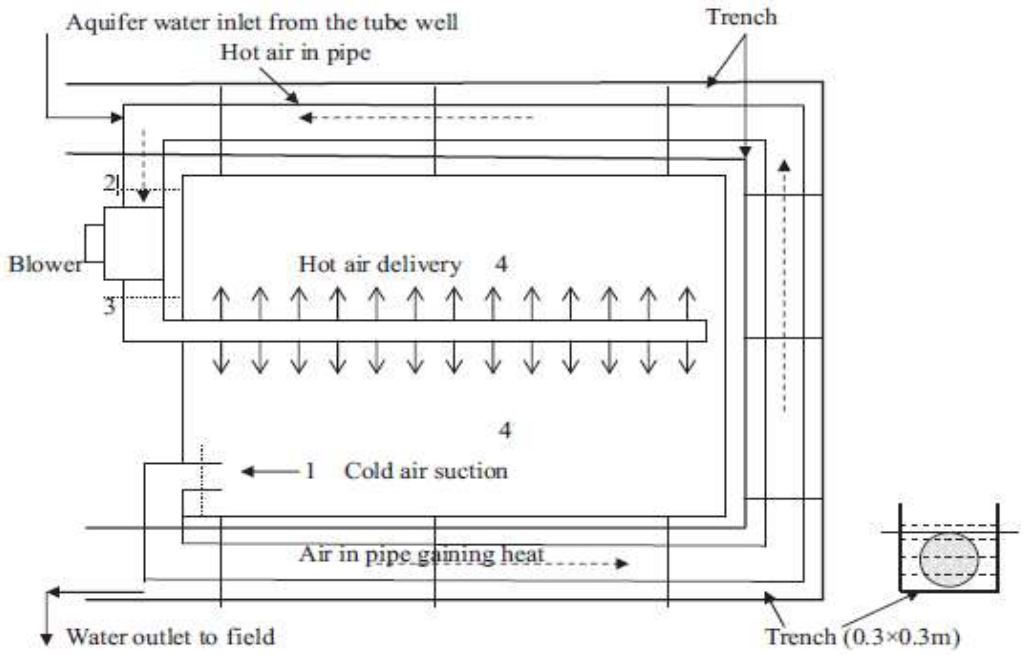

Figure 4.7: Top view of greenhouse geothermal heating system integrated with the irrigation well (Sethi and Sharma, 2007).

On the other hand, the geothermal energy can be used with an earth-to-air heat exchanger (EAHE), where indoor air circulated through underground pipes, and the air passed through the tubes warm up by high soil temperature. Similarly, a liquid such as propylene glycol or methyl alcohol can be circulated through the underground piping system (Bartok, 2015). A large number of studies (Balghouthi et al., 2005; Esen and Yuksel, 2013; Gauthier et al., 1997; Ghosal and Tiwari, 2006; Sharan et al., 2004; Tiwari et al., 2006) have been conducted to evaluate the potential of earth-to-air heat exchanger (EAHE) for greenhouse heating. Sethi & Sharma (2008) reviewed the energy-saving potential of a heating system with EAHE for different size of greenhouses (30-2500 m^2).

The diameter of underground pipes ranged between 0.1-.025 m with spacing between 0.4-0.8 m. The air velocity through the pipes cloud be between 4-11 m s^{-1}. These systems satisfied about 28-62% of greenhouse heating demand depending on the types of greenhouses and their locations. Ground-source or geothermal heat pumps (GSHPs) also used to transfer the underground heat into the greenhouses to provide heating. Several studies (Benli, 2011; D'Arpa et al., 2016; Hepbasli, 2011; Noorollahi et al., 2016; Ozgener and Hepbasli, 2005) have been conducted to study thermal performance of using GSHPs for greenhouse heating. Chai et al. (2012) evaluated the heating performance of the GSHP system for a greenhouse in northern China (39.4˚N). The results showed that the heating cost of the greenhouse with GSHP was lower than gas-fired heating system (GFH) by 11.4%, but were higher than coal-fired heating system (CFH) by 12.9%. Miller (2008) compared the geothermal greenhouse heating systems with the conventional ones (hot water boiler) to evaluate their economic aspects. Results indicated that the average energy costs per unit area of greenhouse floor would decrease if GSHP heating systems were utilized in greenhouses instead of using conventional ones. Benli (2013) compared the performance of horizontal and vertical GSHPs for greenhouse heating in Elazig, Turkey. The study concluded that in the vertical layout, the ground temperature was relatively stable, whereas in the horizontal layout, the ground temperature changed dramatically during a year. Furthermore, the coefficient of performances (COPs) was obtained to be in the range of 3.2-3.8 and 3.1-3.6 for vertical and horizontal GSHPs, respectively. Anifantis et al. (2017) studied the performance of a renewable energy system for heating a greenhouse (32 m^2) in Bari, Italy. The system consisted of GSHP and photovoltaic panels which connected to an electrolyser to produce hydrogen by electrolysis and then store it in a pressure tank (Figure 4.8). During the night, the hydrogen was converted into electricity and used for operation the GSHP to heat a tunnel greenhouse, and results showed that the overall system efficiency was about 11%.

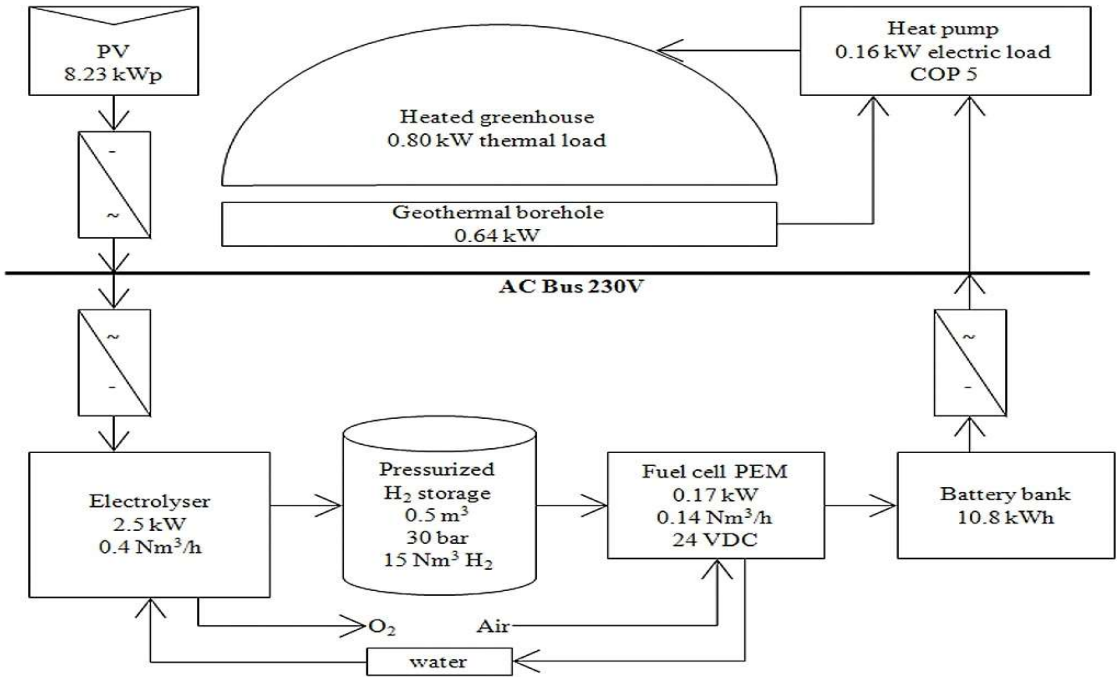

Figure 4.8: GSHP system connected with PV panel for heating the greenhouse (Anifantis et al., 2017).

The review of previous studies indicates the use of geothermal heat for greenhouse heating could be a potential energy saving option for the greenhouse industry. However, the use of geothermal energy for greenhouse heating is not very common for the large-scale production. The reasons could be the high initial costs, lack of adequate economically justified technologies, the complicated maintenance and exploitation, the environmental problems, and, most of all, the absence of governmental support and good organization (D'Arpa et al., 2016). Chiasson (2006) reported that the feasibility of heating greenhouses with geothermal energy is strongly dependent on the fuel cost and the installation costs. D'Arpa et al. (2016) studied the economic feasibility of using geothermal energy for greenhouse heating with GSHPs in southern Italy. The results indicated that the greenhouse heating with GSHPs is possible with a relatively short payback period as compared to the traditional air source heating systems. However, Noorollahi et al. (2016) found that the GSHP is not economical for supplying energy for greenhouses in Iran, as a gas burning heating system can do the same task with significantly lower costs. Therefore, the economic feasibility analysis is very important for using the geothermal energy in greenhouse heating for particular locations.

4.9.3 Wood biomass

The uncertainty of fossil fuel prices has forced greenhouses to consider alternative fuels, and wood biomass could be one of the options. The number of wood burning boilers installed in greenhouses in British Columbia, Canada, has been increasing since 2001 (Chau et al., 2009a). Hepbasli (2011) studied comparative investigation of various greenhouse heating options (solar assisted vertical ground-source heat pump, wood biomass boiler, and natural gas boiler) using exergy analysis method. Results showed that the most sustainable system becomes the wood biomass boiler among the cases studied. Chau et al. (2009) studied the techno-economic analysis of wood biomass boilers for a greenhouse (7.5 ha) in the Lower Mainland of British Columbia in Canada. The results showed that installing a wood biomass boiler (wood pellet or wood residue) to provide 40% of the annual demand is preferable than using the natural gas boiler to provide 100% heat. In another study, Chau et al. (2009b) reported that the wood pellet boiler operated greenhouse production could not be economically feasible when the annual wood pellets price increased by 20%, whereas installing a wood biomass boiler could be feasible when natural gas price increases more than 3% per year. McKenney et al. (2011) studied the economic feasibility of substitution the conventional heating system (fossil fuel) with the biomass operated the heating system for greenhouse heating in southern Ontario, Canada. Results showed that the biomass heating systems have payback periods of 10 to >22 years for substituting the heating oil systems and 18 to >22 years for replacing the natural gas operated heating systems. Similarly, other studies (Bibbiani et al., 2017; Bisaglia et al. (2011) also concluded that the replacement of the traditional heating system with the biomass boiler heating could be economical for greenhouse heating depending on the local price of wood biomass and fossil fuels (natural gas, electricity, heating oil).

Also, biomass heating system also has an economic benefit of CO_2 enrichment from exhaust gases over pure CO_2 (Chalabi et al., 2002). Conversely, CO_2 enrichment from the exhaust gas of biomass boilers is still challenging and expensive since wood biomass boilers generate a high volume of particulate matters (PM) and ash emissions than other fossil fuels. However, the recent technologies including wet scrubbers and other recent flue gas conditioning devices could be helpful to reduce costs and make this process more feasible (Bibbiani et al., 2017).

4.10 Energy saving potential of windbreaks

Wind speed greatly influences the heat loss from the greenhouses, so greenhouses should be in an area which is surrounded by the windbreak. The rate of heat loss from greenhouse become more than double when outdoor wind speed is about 7 m s^{-1} (Sanford, 2011). Therefore, the proper design and position of windbreaks around the greenhouse can reduce 5-10% of total annual heating energy requirement (Sanford, 2011; Sheard, 1977). Bartok (2001) has recommended the windbreaks should be on the north and northwest sides to reduce heat loss from greenhouses which caused by wind speed. Mistriotis et al. (2011) recommended plastic net cover windbreaks instead of traditional one which consisted of trees. However, the windbreaks should install at a certain distance, so that light entrance should not affect and do not accumulate snowdrifts against the greenhouses.

4.11 Conclusions

Several types of techniques have been applied for reducing the greenhouse heating requirement thereby reducing the heating cost. Based on the review of different heating options for reducing heating cost, the following conclusions can be made:

1. The heating energy saving potential of greenhouse shape depends on the location of greenhouse. And the east-west orientation of greenhouse is more energy-efficient for the winter greenhouse at high northern latitudes when the length-width ratio of greenhouses is greater than one.
2. Although the opaque north wall increases the need for supplemental lighting in greenhouses, but the overall reduction in energy consumption was found significant as compared to the uninsulated greenhouse. Similarly, the massive north wall could reduce the heating cost, but might not be appropriate for the large commercial greenhouses.
3. Each greenhouse covers influence the plant microclimates in unique ways; however, the use of newly developed greenhouse cover such as diffusive glass, IR barrier PE cover, and rigid plastic panels could save a significant of heating cost in greenhouses. And, about 20% of heating energy can be saved by using any energy screen at night in the winter greenhouses.
4. Insulating the greenhouse is recommended especially the perimeter and the side wall near the ground.

5. Depending on the location of greenhouses, temperature integration could save about 10-25% of greenhouse heating demand, and the supplemental lighting with HPS can contribute up to 30% of annual heating demand.
6. The hot water pipe heating system mostly used for the large commercial greenhouse, and the location of pipe near the ground is recommended to reduce the heat loss from a greenhouse. Infrared heating could be more energy-efficient for the small size of greenhouse, but there is a risk of burning the plant leaves. Most of the passive mode of heating systems such as water heat storage might not be efficient for large commercial greenhouses. However, these passive modes of heating can be combined with the active heating system to reduce greenhouse heating cost of large commercial greenhouses.
7. As the price of the fossil fuels is being increased, so the use of alternative energy such as industrial waste heat, geothermal energy, wood biomass could be a potential option to reduce the greenhouse heating cost. However, the detailed economic feasibility study is recommended for making the decision to replace the traditional heating systems with the renewable energy depending heating systems.

Although, many techniques are available for reducing the greenhouse heating energy cost in the winter greenhouses, but all the techniques cannot apply at a time. The energy saving option needs to select based on the types of greenhouses, location, and the resources available near the greenhouses.

Acknowledgement

The authors are highly thankful to the College of Graduate and Postdoctoral Studies (CGPS) at the University of Saskatchewan, as well as Innovation Saskatchewan for their financial support to this research.

CHAPTER 5

ENERGY EFFICIENT DESIGN OF GREENHOUSE FOR CANADIAN PRAIRIES USING A HEATING SIMULATION MODEL

(The manuscript presented in this chapter has been published in the International Journal of Energy Research, DOI: https://doi.org/10.1002/er.4019)

Overview

The energy-efficient design parameters for the conventional greenhouses were selected based on the research results presented in Chapter 4. In this chapter, we studied main greenhouse design parameters which impact could be different, or energy-saving potential could be significantly different depending on the location of greenhouses. The results presented in this chapter fulfill part of the second objective of this thesis (i.e., to analyze the heating energy saving potential of the selected design parameters of conventional greenhouses under the weather conditions of Saskatchewan). The outcomes from this study were used for the economic feasibility study of year-round vegetable production in a conceptually designed conventional greenhouse in high northern latitudes (Chapter 6). As the lead author of this manuscript, I conducted the research, analyzed the results, prepared the manuscript, incorporated co-authors comments, and addressed the reviewers' comments. The co-authors (Professor Huiqing Guo, and Professor Karen Tanino) have contributed to this manuscript through providing technical guidance to conduct the research and constructive review to improve the quality of research.

Abstract

Greenhouses in northern climates require a large amount of supplemental heating for growing crops in winter seasons, so energy efficient design of greenhouses based on local climate is important to minimize the heating demand. In this study, greenhouse design parameters including shape, orientation, the angle of the roof, and width of the span have been studied for the conceptual design of conventional greenhouses for Canadian Prairies using a heating simulation model. Five different shapes of greenhouses including even-span, uneven-span, modified arch, vinery, and quonset shape have been selected for the study. The simulation results proved that the uneven-span gable roof shape receives the highest solar radiation whereas the quonset shape receives the lowest solar radiation. However, the quonset shape greenhouse requires about 7.6% less annual heating as compared to the gable roof greenhouse, but the quonset would not be adopted as multi-span greenhouses. Therefore, the gable roof greenhouse is considered as energy efficient for the multi-span gutter connected greenhouses whereas quonset shape as a free-standing single span greenhouse. In high northern latitudes, the greenhouse with east-west orientation is more energy efficient from heating and cooling point of view when the length-width ratio of the greenhouse is more than one. The heating energy saving potential of the large span width in a single-span greenhouse is relatively higher as compared to the multi-span greenhouses.

5.1 Introduction

Greenhouses are very popular control environmental facilities for vegetable production in many parts of the world where outdoor climates are not favorable for growing crops. Greenhouses located in high northern latitudes such as Canada which operate year-round, need to supply a huge amount of supplemental heat for more than six months in a year. The heating cost in Canadian greenhouses is 15-20% of total greenhouse operational costs (Statistics Canada, 2008). Some studies also reported the heating energy requirement in a greenhouse located in the cold region represents up to 90-95% of the total energy demand for greenhouse production (Lristinsson, 2006). The high heating demand in northern greenhouses increases the production costs thereby increasing the market price of crops at the consumer level. Hence, several energy saving techniques such as energy efficient structural design, use of energy efficient coverings, use of thermal curtains, management of indoor microclimates, and use of renewable energy, have been practiced to reduce the heating costs in northern greenhouses. Several studies (Cakır and Sahin, 2015; Djevic and Dimitrijevic, 2009; El-Maghlany et al., 2015; Ghasemi et al., 2016; Gupta and Chandra, 2002; Kumari et al., 2007; Sethi, 2009; Singh and Tiwari, 2010; Tiwari and Gupta, 2002) have been performed to evaluate the energy-saving potential of greenhouses design parameters including the greenhouse shape and orientation under different climates. Some studies (Kumari et al., 2007; Sethi, 2009; Singh and Tiwari, 2010) reported the uneven-span gable roof shape as the most energy efficient greenhouse under different cold climate conditions in Indian. Conversely, Cakır and Sahin (2015) reported that the gothic arch shape as the optimum type in the studied region (40.3˚N) in Turkey. Previous studies (Ghasemi et al., 2016; Gupta and Chandra, 2002; Sethi, 2009; Stanciu et al., 2016) also reported that the east-west (E-W) oriented greenhouse as more energy efficient compared to the north-south (N-S) oriented one for high northern latitudes. Depending on the location of greenhouses, the heating energy saving potential in greenhouses with east-west orientation could be ranged between 2.0 and 28.0% (Gupta and Chandra, 2002; Stanciu et al., 2016; Tiwari and Gupta, 2002), and that of greenhouse shape ranging from 3 to 26% (Ghasemi et al., 2016; Singh and Tiwari, 2010; Tiwari and Gupta, 2002). The outcomes from previous studies indicate the energy-saving potential of some greenhouse design parameters varies significantly depending on the location of greenhouses, and the effect of these parameters is more significant in a greenhouse located at higher latitudes as compared to the lower latitudes (Kurata, 1993). However, very limited information is available regarding the energy efficient design of large

greenhouses suitable for the northern latitudes including Canadian Prairies. Chandra (1976) theoretically studied the thermal performance of greenhouse design parameters (orientation and shape) under the weather condition of Winnipeg (49˚N) in Canada; however the study was conducted only for the representative days of summer and winter season. The energy efficient design based on the simulation of one complete year is important as the energy saving potential from solar radiation varies significantly over the year. Also, the study was conducted for three different greenhouse shapes including even-span gable roof, gothic arch, and quonset shape. To our best knowledge, other design parameters such as angle of the roof and span width have been left out in the previous studies. Furthermore, most of the previous studies have been conducted for single-span greenhouses, the results may not be valid for multi-span greenhouses. Therefore, the energy efficient design of greenhouse parameters including shape, orientation, and span width for high northern latitudes to minimize annual heating requirement would be useful for researchers, manufacturers, and greenhouse growers.

The most effective and feasible approach to select design parameters is through simulation of greenhouse heating requirement. Depending on the application of models, a few mathematical models have been developed for predicting the microclimates of greenhouses. Some of the models (Chandra, 1976; Garzoli, 1985; Hill, 2006; Jolliet et al., 1991; Tunc et al., 1985) have been developed based on the steady-state heat balance of greenhouse for predicting the energy consumption in the greenhouse. However, the accuracy of prediction is limited because these models neglect some heat sources in greenhouses such as sensible heat used in plant transpiration, heat from supplemental lighting, and CO_2 generators, and also validity restricted to certain types of greenhouses. On the other hand, the complex dynamic models (Chou et al., 2004; Cooper and Fuller, 1983; De Zwart, 1996; Kindelan, 1980; Sengar and Kothari, 2008; Singh et al., 2006) are more precise for predicting the greenhouse microclimates. However, these complex dynamic models need many modifications to be applicable for various types of greenhouses, and also very complicated for hourly simulation for a long time such as a year. Also, most of the previous models need to input the solar radiation data for predicting the thermal environment of greenhouses. Ahamed et al. (2017b) developed and validated a quasi-steady model (GREENHEAT) with a solar radiation sub-model which considered most of the heat sources and sinks of greenhouses, and also can be applied for various types of greenhouses. This time-dependent thermal environment model

was used in this study to select the energy efficient design parameters of conventional greenhouses for Canadian Prairies.

The objective of this study is to select the energy efficient design parameters (shape, orientation, the angle of the roof, and width of span) of conventional style greenhouses for Canadian Prairies using the GREENHEAT greenhouse heating simulation model.

5.2 Materials and method

5.2.1 Introduction of the GREENHEAT model

The GREENHEAT model for simulation of the heating requirement was developed based on the lumped estimation of heat transfer parameters in the conventional greenhouses. The general heat balance equation of the model is as follows (Ahamed et al., 2017b):

$$Q_h = \text{Sources} - \text{Sinks} = \left(Q_s + Q_{sl} + Q_{co_2} + Q_m\right) - \left(Q_t + Q_i + Q_g + Q_p + Q_r + Q_e\right) \quad (5.1)$$

where Q_h is the supplemental heating requirement; Q_s is the net heat gain from solar radiation in the greenhouse; $Q_{sl,}$ Q_{CO_2}, and Q_m are the heat gain from supplemental lighting, CO_2 generator, and motor, respectively; Q_t is the heat transfer by conduction and convection, Q_i is the heat transfer caused by infiltration; Q_g is the heat transfer through greenhouse floor; Q_p is the heat transfer along the perimeter; Q_r is the heat transfer for exchange of long-wave radiation; and Q_e is the sensible heat used in the process of plant evapotranspiration.

GREENHEAT could estimate the hourly heating requirement of conventional greenhouse based input of indoor set-point parameters including temperature, relative humidity, air velocity, supplemental lighting, and CO_2 supply rate, physical and thermal properties of construction materials, leaf area index and characteristics length of the plant leaves, and hourly weather data including temperature, relative humidity, wind speed, and cloud cover. In GREENHEAT model, the solar energy through an inclined surface was modeled according to the isotropic diffuse model proposed by Liu and Jordan (Liu and Jordan, 1961), and the total solar insolation available in the greenhouse is the sum of solar radiation passed through different sections of greenhouse envelope.

5.2.2 Simulation of heating requirement

A double layer polyethylene covered single-span greenhouse (1000 m^2) located in Saskatoon (52.13˚N, 106.62˚W), Saskatchewan, Canada, was first considered for evaluating the heating energy saving potential of greenhouse roof shapes. The length, width, and ridge height of all five

each shape were 100 m, 10 m, and 6.5 m, respectively. Then a six-span greenhouse (length 100 m, width 10×6=60 m) with the selected energy efficient roof shape was also considered in other design parameters' evaluation. The hourly weather data (temperature, relative humidity, cloud cover, and wind speed) of Saskatoon for 2015 from the National Solar Radiation Database (NSRDB) were used for simulation of the greenhouse heating requirement. Tomato plants were considered to be grown in the study greenhouse, so the indoor set-point temperatures were set at 21˚C during the daytime and 18˚C during the night. The indoor relative humidity was assumed to be constant at 75% because most commercial greenhouses at high northern latitudes maintain the relative humidity at a set-point in heating season through different humidity control measures such as mechanical dehumidifier. The optimum photoperiod in greenhouses varies between 14 to 24 hours depending on the types of crops grown, and it is 14 hours for tomato. So, the supplemental lighting was considered to be turned on between 7 am to 10 pm when greenhouse solar radiation was lower than 250 W m^{-2} (Dorais, 2003). The CO_2 generator was operated only during the daytime. The thermal curtain was used at night. Other values used for heating simulation are presented in Table 5.1.

Table 5.1: Other input values used for heating simulation.

Parameters	Value
Air exchange rate per hour (ASABE, 2006)	1.0
Perimeter heats loss factor (ASHRAE, 2013)	0.85 (W m^{-1} K^{-1})
Angle of roof	26˚
Thermal conductivity of soil (ASHRAE, 2013)	1.4 (W m^{-1} K^{-1})
Number of layer in cover	2
Thermal conductivity cover (Professional Plastics, 2017)	0.33 (W m^{-1} K^{-1})
Emissivity of IR barrier poly cover (Sanford, 2011)	0.2
Transmissivity to solar radiation (Sanford, 2011)	0.75
Transmissivity to long-wave radiation (Sanford, 2011)	0.29
Average leaf area index of tomato (Castilla, 2013)	2.0
Characteristics length of tomato leaf (Rincón et al., 2012)	0.027 (m)
Emissivity coefficient of indoor components	0.9
Indoor air velocity (Castilla, 2013)	0.2 (m s^{-1})
Installed lighting wattage (Dorais, 2003)	100 (W m^{-2})
Number of recirculating fans	6
Rated power of motors	375 (W)
Motor efficiency	0.9
Motor load factor (ASHRAE, 2013)	1.0
Motor use factor (ASHRAE, 2013)	1.0
Net heating value of fuel (ASHRAE, 2013)	38 (MJ m^{-3} of gas)
Rate of CO_2 supply in greenhouse (Castilla, 2013)	4.5 (g m^{-2} hr^{-1})
CO_2 production rate (EIA, 2016)	2.7 (kg kg^{-1} of fuel)
Reflectivity of outdoor ground (ρ_r)	0.5

Five single-span greenhouses with different cross-section shapes including even-span gable roof, uneven-span gable roof, modified arch, vinery, and quonset are shown in Figure 5.1. Because of the complex geometry, the curved surface of the modified arch shape and the quonset shape were divided into three sections in solar radiation prediction. The details of each section of the greenhouse envelope with east-west (E-W) orientation are shown in Table 5.2. The energy efficient

shape of a greenhouse depends on allowing greatest solar heat gain and the least heat loss from the greenhouse. The availability of hourly solar radiation for each shape of greenhouse in east-west orientation was computed for the entire year.

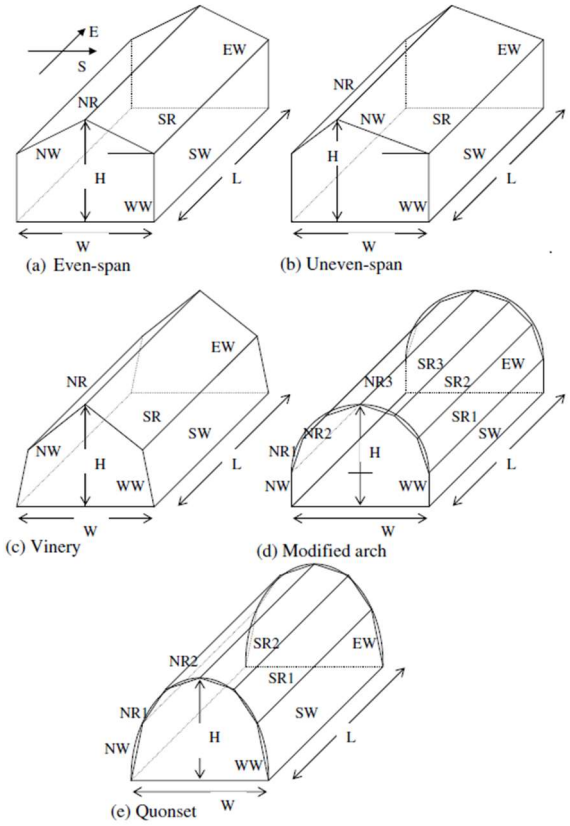

Figure 5.1: Cross-section views of different available shapes of conventional greenhouses (Sethi, 2009).

Table 5.2: Geometrical description of different sections of the greenhouses with east-west orientation.

Section of surfaces	Even-span	Uneven-span	Vinery	Modified arch	Quonset
South roof	A=559 m^2 β=26.6˚ γ=0˚	A=791 m^2 β=18.5˚ γ=0˚	A=523 m^2 β=35˚ γ=0˚	A=(189×3) m^2 β_1=75˚, β_2=45˚ β_3=15˚ γ=0˚	A=(286×2) m^2 β1= 57˚ β2= 35˚ γ=0˚
South wall	A=400 m^2 β=90˚ γ=0˚	A=400 m^2 β=90˚ γ=0˚	A=357 m^2 β=78.5˚ γ=0˚	A=400 m^2 β=90˚ γ=0˚	A=286 m^2 β=75˚ γ=0˚
North roof	A=559 m^2 β=153.4˚ γ=180˚	A=354 m^2 β=135˚ γ=180˚	A=523 m^2 β=145˚ γ=180˚	A= (189×3) m^2 β_1=105˚, β_2=135˚ β_3=165˚ γ=180˚	A=(286×2) m^2 β1=125˚ β2=145˚ γ=180˚
North wall	A=400 m^2 β=90˚ γ=180˚	A=400 m^2 β=90˚ γ=180˚	A=357 m^2 β=101.5˚ γ=180˚	A=400 m^2 β=90˚ γ=180˚	A=286 m^2 β=105˚ γ=180˚
East wall	A=52.5 m^2 β=90˚ γ=-90˚	A=52.5 m^2 β=90˚ γ=-90˚	A=45.3 m^2 β=90˚ γ=-90˚	A=57.5 m^2 β=90˚ γ=-90˚	A=43.3 m^2 β=90˚ γ=-90˚
West wall	A=52.5 m^2 β=90˚ γ=90˚	A=52.5 m^2 β=90˚ γ=90˚	A=45.3 m^2 β=90˚ γ=90˚	A=57.5 m^2 β=90˚ γ=90˚	A=43.3 m^2 β=90˚ γ=90˚
Total area	(2023 m^2)	(2050 m^2)	(1851 m^2)	(2049 m^2)	(1803 m^2)

*A= Area of surface, β = angle of surface, γ =surface azimuth

5.3 Results and discussion

5.3.1 Energy-efficient greenhouse shape

Figure 5.2 shows the variation of monthly average daily total solar insolation available into the single-span greenhouses with five different shapes. The highest solar radiation is received by the

uneven-span shape in all the months except November to January when modified arch shape receives the highest solar radiation, because of the largest south roof which receives maximum solar radiation as compared to the other roof types of greenhouses. On the other hand, it can be observed that the vinery shape and the quonset shape receive the lowest solar radiation because of the smaller exterior surface to receive the solar radiation as compared to the other greenhouse shapes with the same floor area. The total annual solar radiation in the uneven-span is about 8.4% higher than the even-span shape, whereas the modified arch shape, vinery shape, and quonset shape receive 0.7%, 5.8% and 7.1% less solar radiation than the even-span shape, respectively. A very similar trend of solar heat gain in different greenhouse shapes was reported from the studies conducted at high northern latitudes in India (Ghasemi et al., 2016; Sethi, 2009; Singh and Tiwari, 2010). Sethi (2009) reported that under cold climatic conditions (51˚N) of India, an uneven-span shape receives 11.3% more annual solar radiation compared to the even-span shape, and the modified arch shape receives 0.6% more radiation, whereas vinery and quonset shapes receive 9.4% and 11.6% less solar radiation, respectively when compared with the even-span shape.

Although the greenhouse dimensions including length, height, and width, are same for all selected shapes of greenhouses, the total solar radiation receives in greenhouses are different due to the difference in the ratio of the cover to the floor area (A_c/A_g) and also due to the difference in angle of incidence of solar radiation. As compared to the even-span shape, the uneven-span shape and the modified arch shape have 1.33% and 1.28% more A_c/A_g ratio while the vinery and the quonset shape have 10.9% and 8.5% less A_c/A_g ratio. Although the modified arch shape has a relatively higher A_c/A_g ratio as compared to the even-span but it receives lower solar radiation during spring and summer and fall seasons whereas higher solar radiation during the winter season. In the winter months from November to February, the modified arch shape receives highest solar radiation which is about 6.2% higher as compared the even-span shape, while the uneven-span shape receives about 5.7% higher solar radiation. Thus, the simulation results indicate that the shape of greenhouses has a considerable effect on the solar heat gain at high northern latitudes in winter when heating is needed.

In June, the modified arch shape receives about 1.8% less solar radiation as compared to the even-span shape, but the uneven-span receives about 9.7% higher solar radiation. The difference is caused by the difference in incidence angle because the high roof angle of modified arch shape

(especially near the gutter) might allow higher solar radiation when the solar altitude is relatively low and less solar radiation when the solar altitudes angle is relatively high.

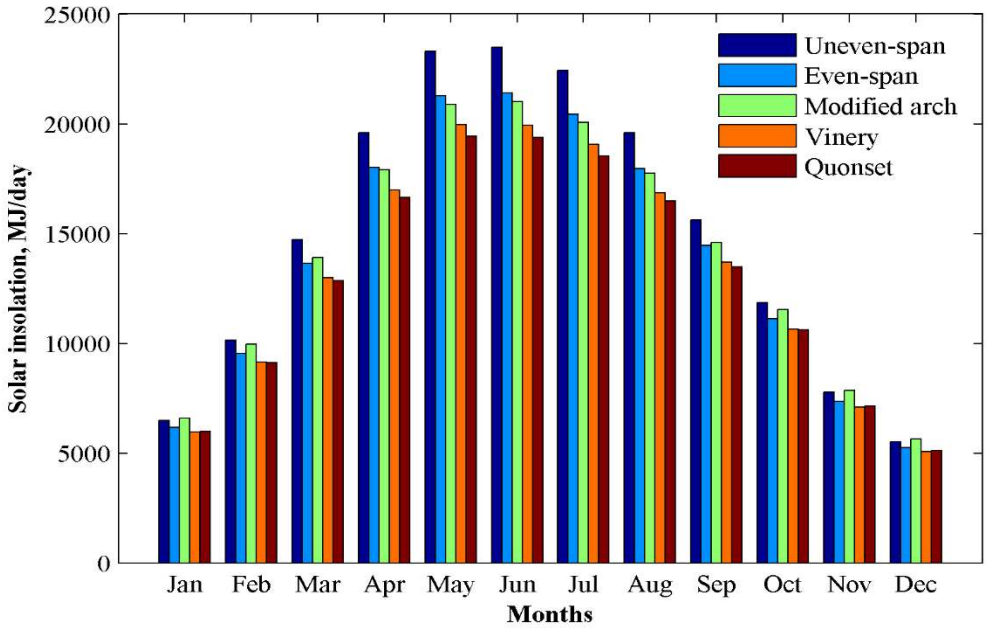

Figure 5.2: Annual variation of average daily total solar insolation into the greenhouses of different shapes with the east-west orientation.

Figure 5.3 shows the simulated annual total heating requirement in five different shapes of greenhouses with an east-west orientation. The modified arch shape requires the highest heating although it has a relatively smaller exterior envelope area than the uneven-span likely because it receives less solar radiation than the uneven-span gable roof shape. The even-span gable roof greenhouse requires about 1.0% less annual heating as compared to the modified arch shape, but no significant heating difference between the even-span and the uneven-span. Conversely, the even-span shape needs 5.9% and 7.6% higher heating as compared to the vinery shape and the quonset shape, respectively. Although the vinery and the quonset shape receive the least solar radiation but require the lowest heating because the northern greenhouses experience more heat loss per unit area of cover than the solar heat gain on the same area during the winter season. For the same floor area, the total exposed cover surface area in the vinery shape and quonset shape is 8.5% and 10.9% less as compared to the even-span, so less heat loss occurs as compared to the other shapes. Similarly, the modified arch shape receives greater solar radiation than the even-span

shape during heating period, but requires higher heating because the exposed area for the modified arch shape is about 1.3% higher.

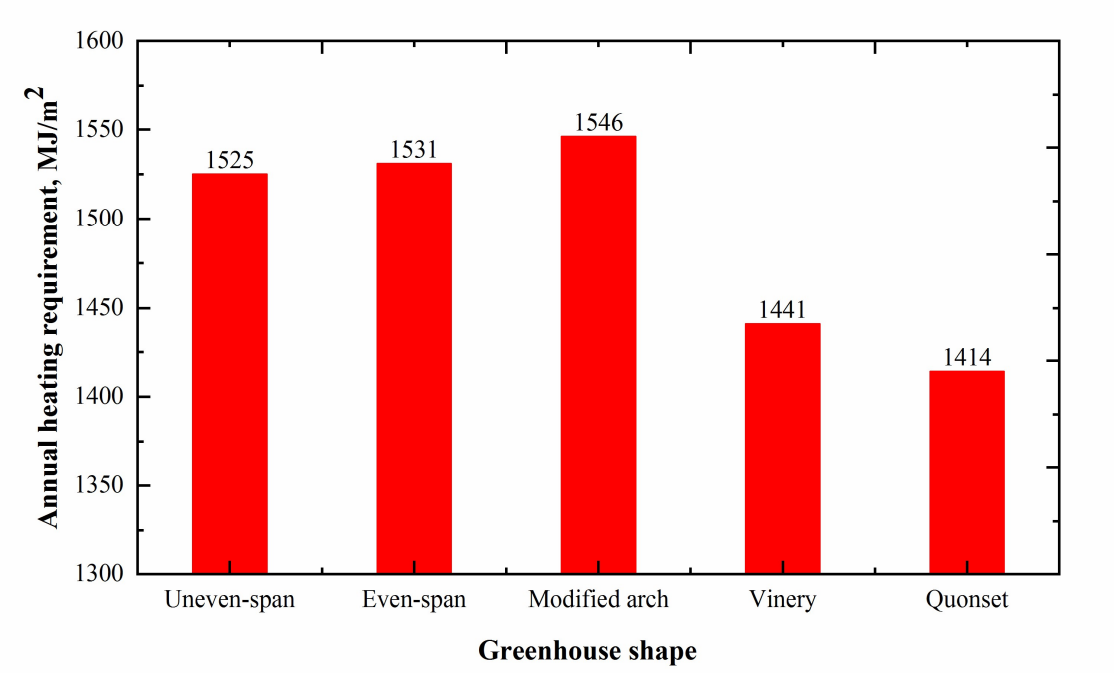

Figure 5.3: Predicted annual heating requirements in five different shapes of greenhouses with an east-west orientation.

The results indicate that the quonset shape is more energy efficient as compared to other types of greenhouses. However, the vinery and the quonset shape cannot be adopted as gutter connected multi-span greenhouses. Hence, the quonset shape is recommended for a single span greenhouse for northern latitudes, and the even-span gable roof shape in case of multi-span greenhouses as the uneven-span shape require high capital cost but having insignificant heating saving potential. The modified arch shape could be beneficial for the cooling purpose as less solar radiation gain in the summer season. However, the energy required for cooling in northern greenhouses is not very significant since the cooling in northern greenhouses is mostly provided by the natural ventilation which could be facilitated with roll-up sidewalls and roof vents or open roof designs (Sanford, 2011).

5.3.2 Energy efficient orientation

For the simulation with the north-south (N-S) orientation, the geometrical parameters (surface area, the angle of the surface, and surface azimuth) of the selected greenhouse shapes would be

changed based on the orientation of the surfaces. For this analysis, the energy efficient greenhouse orientation (E-W or N-S) was selected based on the availability of clear sky solar radiation because the heat loss from the greenhouse is not related to the orientation when the effect of wind direction is considered as negligible. Figure 5.4 shows the comparison of simulated average daily total solar radiation per unit floor area for each month in a single-span gable roof greenhouse with E-W and N-S orientation. The result indicates the E-W oriented greenhouse receives greater solar radiation during the cold season (October-March), but less solar radiation during the mild and warm seasons as compared to the N-S oriented greenhouse. Comparing with N-S orientation for a single span greenhouse, the E-W oriented greenhouse receives 51.8% more solar radiation in December but 20.1% less in June, thus need less heating in winter and less cooling in summer. A similar trend of solar gain in the single-span greenhouses with orientations also reported in other studies (Dragićević, 2011; Sethi, 2009), however, the intensity of solar gain could be significantly different depending on the location of greenhouses.

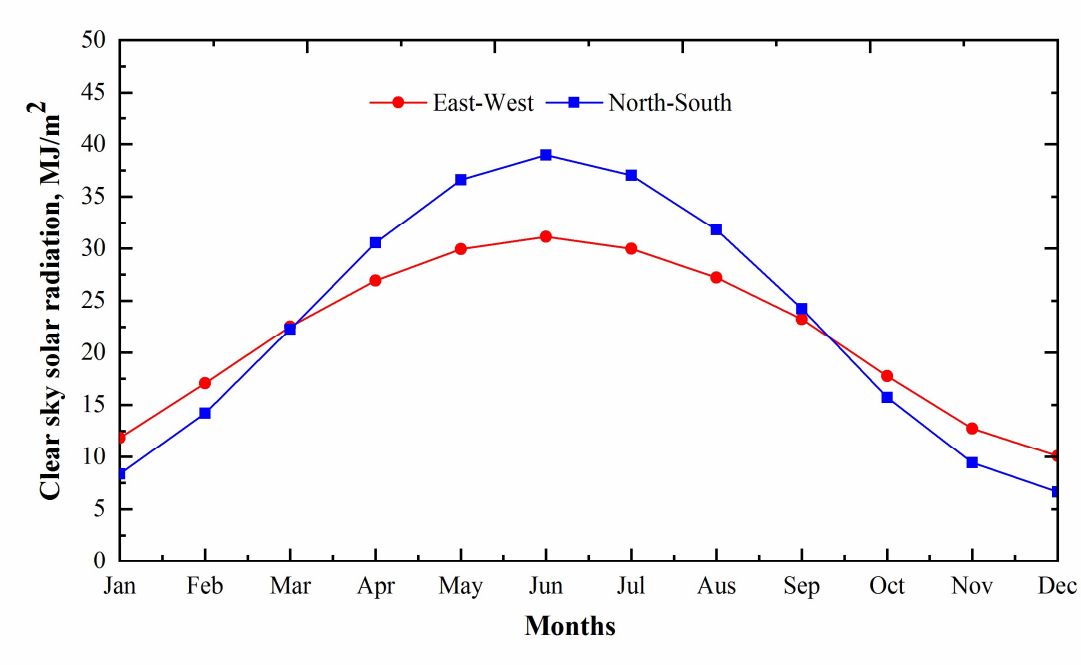

Figure 5.4: Annual variation in average daily solar radiation in a single-span greenhouse with E-W and N-S orientation.

Figure 5.5 shows the solar radiation availability in an E-W and N-S oriented six-span gable roof greenhouse. The simulated result indicates that the E-W oriented multi-span greenhouse receives 31.1% greater solar radiation in December, and 17.7% less in June than the N-S oriented one. The

high solar radiation gain during winter months with E-W orientation is because of the low altitude angle of the sun in northern latitudes thereby resulting in higher solar radiation in the longest southern section. The greenhouse with E-W orientation having a length-width ratio more than one has a greater southern section as compared to the N-S oriented one. Therefore, the solar radiation gain in northern greenhouses with E-W orientation will increase with the increase of greenhouse length-width ratio. The result also indicates that the E-W oriented multiple-span greenhouse receives about 35-40% less solar energy per square meter of floor area during the winter months (October-March) as compared with the single-span greenhouse, which is due to the difference in the ratio of the cover to the floor area (A_c/A_g). The ratio in the single-span and the multi-span greenhouse are 2.0 and 1.4, respectively. However, the multi-span greenhouses might require less heating per square meter in cold regions because of less exterior cover area per meter square of floor area.

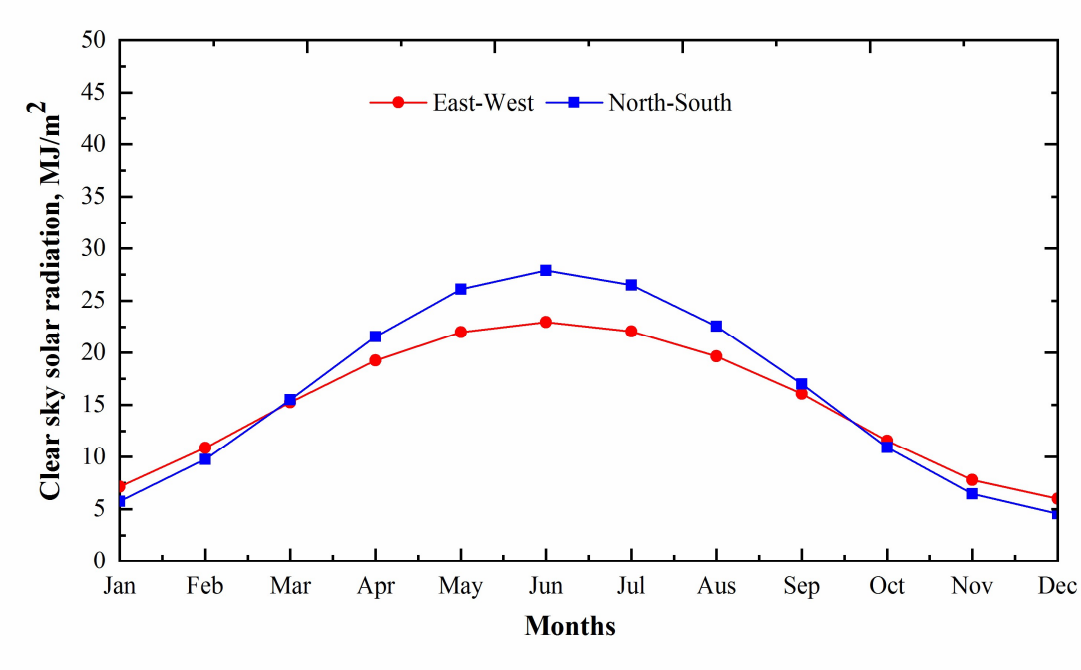

Figure 5.5: Annual variation in average daily solar radiation in a six-span greenhouse with E-W and N-S orientation.

Figure 5.6 shows the percentile increase or decrease of solar radiation in the E-W oriented greenhouse as compared to the N-S orientation for various length-width ratios of the greenhouse from 10 to 0.83. The results indicate the solar radiation gain in the multi-span greenhouse with E-W orientation reduces with the decrease of the length-width ratio in spring/fall and winter season,

but it is the opposite in summer. In December, the E-W oriented greenhouse with a length-width ratio of 0.83 and 10.0 could have solar radiation gain of 27.9% and 51.8% more than the N-S oriented one. In another word, the solar energy gain in the N-S oriented greenhouse with a length-width ratio of 10.0 is 52.2% more than that of 0.83; therefore length-width ratio cloud has a great impact on solar energy gain. From March to September, the E-W oriented greenhouse receives less solar energy than N-S oriented one (June 17.7% less); however, for the E-W oriented greenhouse, the length-width ratio has much less impact on solar radiation gain during this period of mild and warm seasons.

Therefore, in high latitude regions, the length-width ratio of the multi-span greenhouses needs to be high for greater solar gain to reduce the heating needs in winter season as well as reduce solar gain in summer to reduce the cooling needs.

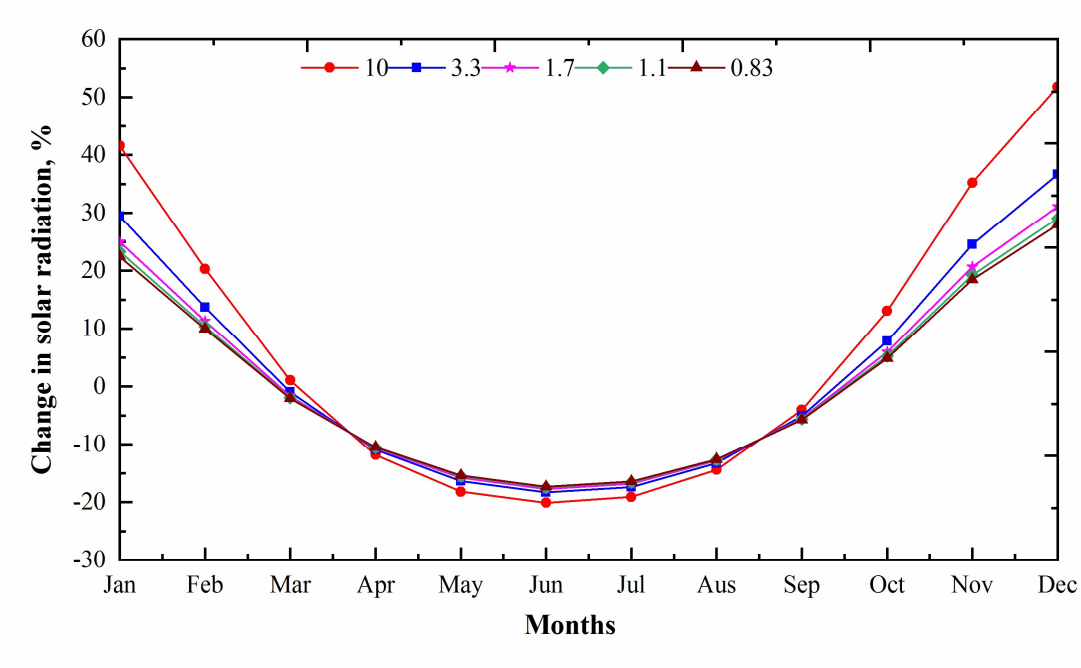

Figure 5.6. Percentile increase or decrease of solar radiation gain with the E-W orientation as compared to the N-S orientation for various length-width ratios of the multiple-span greenhouse.

5.3.3 Angle of roof and width of span

The availability of solar radiation and the heating requirement in the single-span gable greenhouse with the fixed span width of 10 m is simulated for various roof angles. Figure 5.7 shows the total heating requirement and the solar radiation gain per square meter of the greenhouse from

November-February. The result indicates that the solar radiation gains in the greenhouse increase linearly with the increase of roof angle because the cover surface area increases when the roof angle increases without changing the span width and the height of the sidewall. However, the increased roof angle also increases the heating demand in northern greenhouses during winter months because the heat loss per unit cover area is usually higher than the solar heat gain. Conversely, the low roof angle may affect the structural stability of cover because of the snow load in the winter season at northern latitudes, so it is recommended to keep the roof angle between 25-30˚ to allow snow to slide down.

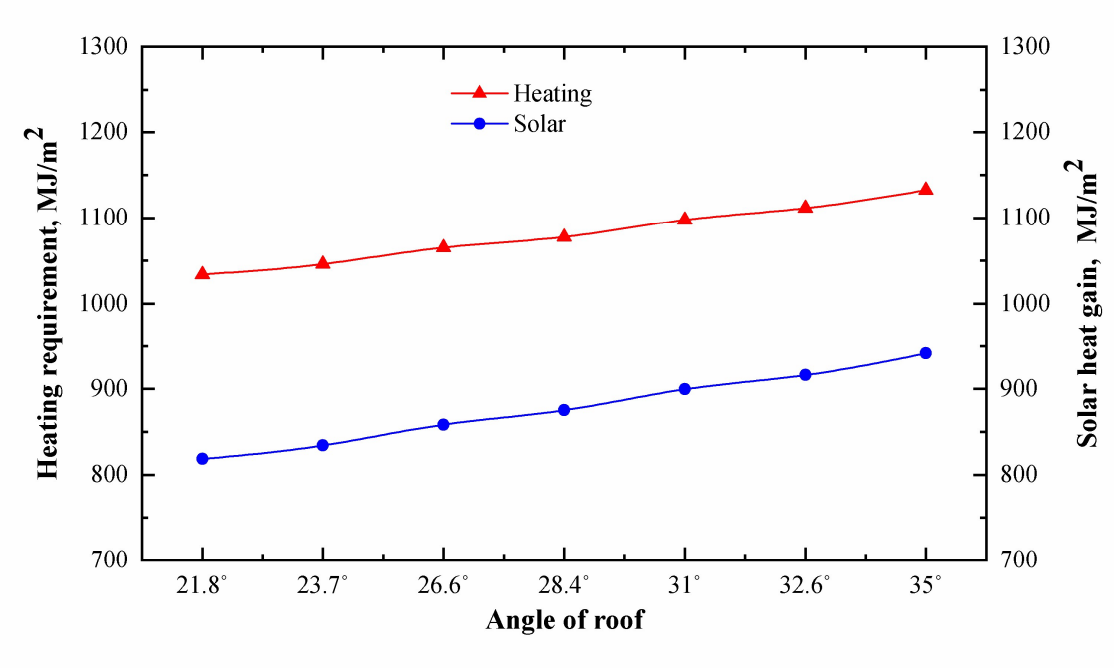

Figure 5.7: The heating requirement and the solar radiation gain with the various roof angle in the single-span greenhouse.

To find the impact of span width on the heating requirement, the angle of the greenhouse roof was selected at 26˚, the wall height is kept same but the ridge height would be different as several span widths 8 m, 10 m, 12 m, 14 m, and 16 m were selected for this analysis. Figure 5.8 and Figure 5.9 show the variation of solar heat gain per square meter of floor area in the single-span and the multi-span greenhouses with various span widths. The result indicates that the solar heat gain per square meter of floor area decreases with the increase of span width because the ratio (A_c/A_g) decrease for the increase of span width. In winter season from November to February, the solar energy gain of single span greenhouse with 8 m span is 30-35% higher than that of a 16 m span greenhouse;

however, the short span greenhouse appears to be disadvantageous during summer as it gains much higher solar energy (about 23.5% from June to August). The impact of span width on solar heat gain in the multi-span greenhouse is very small as compared to that of the single-span greenhouse (within 5-8% in winter, and 3-4% in summer) because the ratio (A_c/A) is small in the multi-span greenhouse.

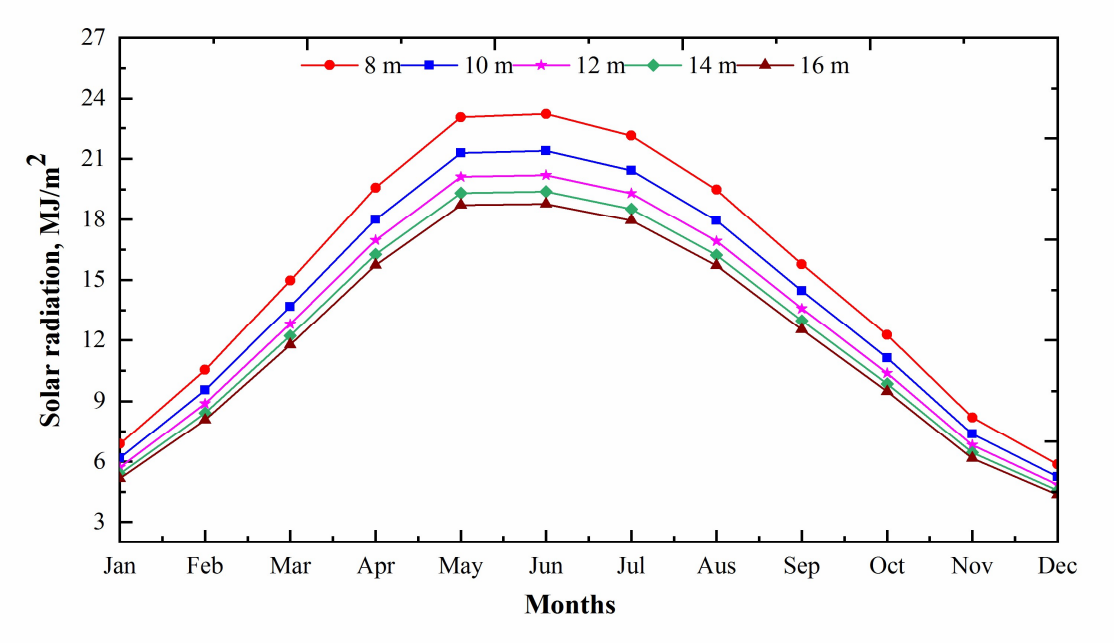

Figure 5.8: Average daily total solar heat gain per square meter of floor area in the selected single-span greenhouse for different span widths.

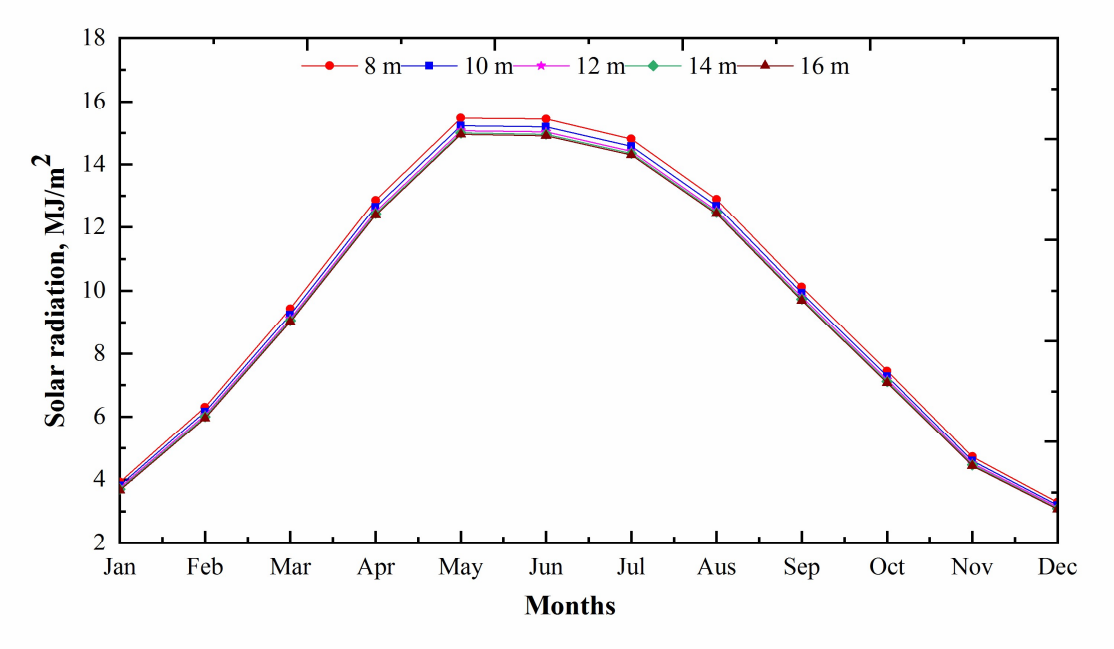

Figure 5.9: Average daily total solar heat gain per square meter of floor area in the selected multi-span (6 spans) greenhouse for different span widths.

Figure 5.10 shows the variation of the annual heating requirement in the single-span greenhouse and the multi-span greenhouse for different span widths. The result indicates the annual heating requirement per square meter of floor in the single-span greenhouse decreases 14.9% when the span width increase from 8 m to 16 m, because the A_c/A_g ratio decrease with the increase of span width such that the A_c/A_g ratio is 13.4% lower in the 16 m span greenhouse as compared to the greenhouse with 8 m span. Conversely, the increase of span width from 8 m to 16 m in the multi-span greenhouse causes a small reduction (3.5%) in annual heating requirement because the ratio (A_c/A_g) only slightly decrease (4.5%).

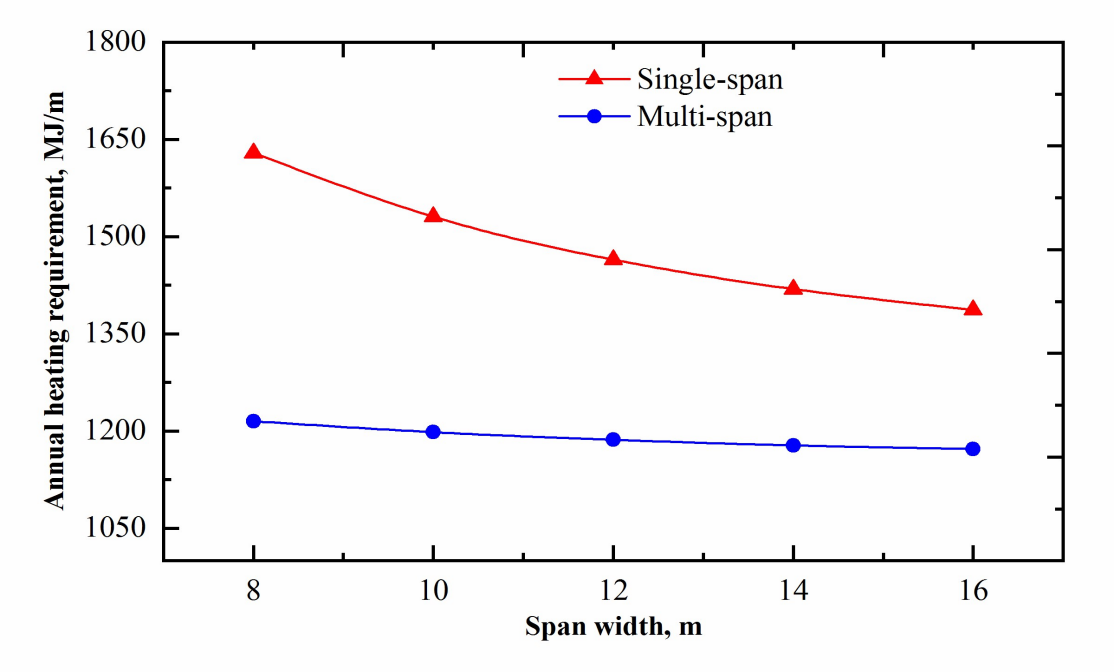

Figure 5.10: Annual heating requirement in the selected single-span and the multi-span greenhouse with various span widths.

5.4 Conclusions

The following conclusions can be drawn based on the theoretical analysis of solar radiation availability and the heating demand in northern greenhouses:

1. The uneven span gable roof greenhouse receives the highest solar radiation, but the heat loss is also high because of the large exterior surface thereby the heat loss per unit of the cover area exceeds the solar heat gain.
2. The gable roof greenhouses including even-span and uneven-span are found to be more energy efficient for the gutter connected multi-span greenhouses, and the quonset shape for the single span greenhouses.
3. Greenhouses in northern latitude need to be oriented in east-west, and also the length-width ratio needs to be greater than one for minimization of heating needs with an east-west orientation.
4. The angle of the roof could range between 25-30˚. The span width in single-span greenhouses needs to be wide as much as possible without compromising with the light transmittance to reduce heating needs. However, the impact of span width is negligible on the heating demand of multi-span greenhouses.

Based on the outcome of the study, it can be concluded that the east-west oriented multi-span gable roof greenhouse would be energy efficient for a large commercial greenhouse at high northern latitudes, whereas an east-west oriented (wider span) quonset shape would be energy efficient for the single-span greenhouse.

Acknowledgment

The authors are very thankful to the College of Graduate and Postdoctoral Studies (CGPS) at the University of Saskatchewan, as well as Innovation Saskatchewan for scholarship and financial support to this research.

CHAPTER 6

HEATING DEMAND AND ECONOMIC FEASIBILITY ANALYSIS FOR YEAR-ROUND VEGETABLE PRODUCTION IN CANADIAN PRAIRIES' GREENHOUSES

(The manuscript presented in this chapter was submitted to the Journal of Information Processing in Agriculture, submission no: IPA_2018_15)

Overview

Based on the results presented in Chapter 5, a conceptually designed conventional greenhouse was selected for studying the economic feasibility of year-round greenhouse production in northern Saskatchewan. The results presented in this chapter fulfill the third objective of this thesis (i.e., to conduct economic feasibility of year-round production in a conventional greenhouse). As the lead author of this manuscript, I conducted the research, analyzed the results, prepared the manuscript, and incorporated co-authors comments. The co-authors (Professor Huiqing Guo, and Professor Karen Tanino) have contributed to this manuscript through providing technical guidance to conduct the research and constructive review to improve the quality of research. Another co-author (Lisa Taylor) contributed to this manuscript by studying some required information about greenhouse vegetable production in Canadian greenhouses.

Abstract

Greenhouse vegetable production in Canadian Prairies is important for creating a sustainable regional food economy, especially in northern communities. This study included the estimation of heating demand for year-round production and evaluation of the economic feasibility of greenhouse vegetable production (tomato, cucumber, and pepper) in a conceptually designed greenhouse (0.6 ha) located in remote northern communities. The heating simulation was based on a greenhouse heating simulation model (GREENHEAT) developed by the authors recently. The simulation results showed that the annual heating requirement for the production of tomato, cucumber, and pepper are 1486, 1657, and 1754 MJ m^{-2}, respectively. The economic analysis indicates the net return (NR) from the production of tomato, cucumber, and pepper, are \$72.73/m^2, \$44.98/m^2 and \$47.4/m^2, respectively, based on the market price \$3.5/kg, \$2.7/kg, and \$8.0/kg, and yields of 55.0, 65.0, and 23.0 kg m^{-2}. The net present value (NPV) for the tomato, cucumber, and pepper production are \$ 22, \$12, and \$ 13 million, respectively, and the benefit-cost ratio (BCR) are 1.42, 1.23, and 1.22. The economic feasibility analysis indicates the year-round production of vegetables in a greenhouse at high northern latitudes would be economically profitable.

6.1 Introduction

Canadian greenhouse vegetable industry has been experiencing continuous growth over the last twenty years. The export of Canadian greenhouse vegetables has increased by 43% from $579 million in 2012 to a five-year high of $826 million in 2015 (Statistics Canada, 2015). However, about 96.0 % of the total greenhouse vegetable production area in Canada is from southern regions of Ontario, British Columbia, and Quebec. Greenhouses located in Canadian Prairies require a large amount of supplemental heat during the winter season, so the greenhouses are highly energy inefficient, and economically might not be profitable, especially in winter season from November-March. Depending on the type of greenhouse structure, crops, and location of greenhouses, the heating cost in Canadian greenhouses accounts for 10-35% of the total production costs (Spencer, 2009; Statistics Canada, 2008). The heating cost in a greenhouse varies depending on the type of vegetable grown in the greenhouses as different vegetables have different environment requirement including day and night set-point temperatures, supplemental lighting intensity, and CO_2 concentration, as well as plant evapotranspiration can significantly affect the heating requirement. Besides heating cost, other operational costs include the cost of labor, material input, humidity control, and marketing, as well as some capital investment, these costs also vary depending on the type of vegetable grown in the greenhouses. So far, most of the existing "Canadian Pararies greenhouses" are in operation for eight months of the year, closing in the coldest months; therefore, the accurate economic prediction is important for the year-round production of vegetables in Canadian Prairie's greenhouses. However, very limited information is available about the economic feasibility of greenhouse vegetable production in Canadian Prairies.

Using thermal models to predict heating requirement is an accurate, economical, and quick approach to acquire feasibility study results of greenhouses. Quite a few thermal models (Hill, 2006; Jolliet et al., 1991; V.P. Sethi and Sharma, 2007; Singh et al., 2006; Singh and Tiwari, 2010) have been developed for estimation of greenhouse heating requirements. However, these existing thermal models have neglected the heating contribution from environmental control systems whereas the environmental control systems contribute a significant amount of heat in northern greenhouses, and require complicated modification for the greenhouse with different configuration. Ahamed et al. (2017b) developed a time-dependent greenhouse thermal model (GREENHEAT) for simulation of the hourly heating requirement in conventional greenhouses considering all heat sources and sinks including environmental control systems and the most up-

to-date methods for heat transfer calculations. The model was validated using measured data from a commercial greenhouse and proved that it has a relatively good accuracy. It can be used as a scientific tool for predicting heating requirement of greenhouses. Hence, the objectives of this paper are to study the annual variation of heating demand for the production of major greenhouse vegetables (tomato, cucumber, and pepper), and assess the economic feasibility of year-round vegetable production in Canadian Prairie's greenhouses. A conceptually designed commercial greenhouse was used for this study, and the GREENHEAT model was used to simulate the heating requirement in the study greenhouse.

6.2 Materials and method

6.2.1 Description of the study greenhouse

A six-spans gable roof greenhouse with an east-west orientation (6,000 m^2) located in Saskatoon (52.13ºN, 106.62ºW), Saskatchewan, Canada was considered for this study. The physical dimensions and construction material of the greenhouse envelope were selected based on the study of the conceptual design of energy efficient conventional greenhouse for higher northern latitudes in Saskatchewan (Ahamed et al., 2018a). The greenhouse roof is covered with the air inflated double-layer polyethylene film, and the twin-wall polycarbonate (8 mm) enclosed the sidewall. The span width, the sidewall height, and the ridge height were 10 m, 4 m, and 6.5 m, respectively. The energy curtain was considered to be in operation during the night to reduce the heat loss through the transparent cover. The supplemental lighting system was considered in operation when solar radiation was less than 250 W m^{-2}. The CO_2 generator was in operation for the entire sunlight period, and the air-circulation system was considered to be effective for all the times.

6.2.2 Description of the heating model (GREENHEAT)

The greenhouse heating model developed by Ahamed et al. (2017b) was a time-dependent lumped estimation model. The general heat balance of the model is given as follows (Ahamed et al., 2017b):

$$Q_h = \text{Sources} - \text{Sinks} = \left(Q_s + Q_{sl} + Q_{co_2} + Q_m\right) - \left(Q_t + Q_i + Q_g + Q_p + Q_r + Q_e\right) \quad (6.1)$$

where Q_h is the heating requirement; Q_s is the net heat gain from solar radiation; Q_{sl}, Q_{CO_2}, and Q_m is the heat gain from supplemental lighting, CO_2 generators, and motors, respectively; Q_t is the heat transfer by conduction and convection; Q_i is the heat transfer caused by infiltration; Q_g is the

heat transfer through greenhouse floor; Q_p is the heat transfer along the perimeter; Q_r is the heat transfer by long-wave radiation; and Q_e is the heat used in the process of plant evapotranspiration.

The constant input parameters for simulation of heating requirements are listed in Table 6.1. The hourly weather data (temperature, relative humidity, wind speed, and cloud cover) in Saskatoon for 2015 from the National Solar Radiation Database (NSRDB) were used for estimation of hourly heating demand since the weather in remote Saskatchewan are not significantly different than Saskatoon.

Table 6.1: Constant input values for simulation of heating requirements in the study greenhouse.

Parameters	Value
Air exchange rate (ASABE, 2006)	1.0
Perimeter heat loss factor (Worley, 2009)	0.85 (W m^{-1} K^{-1})
Angle of roof	26˚
Thermal conductivity of soil (ASHRAE, 2013)	1.4 (W m^{-1} K^{-1})
Thermal conductivity of cover (Professional Plastics, 2017)	0.33 (W m^{-1} K^{-1})
Thermal conductivity of polycarbonate	0.2 (W m^{-1} K^{-1})
Emissivity of IR barrier poly cover (Sanford, 2011)	0.2
Emissivity of polycarbonate	0.65
Solar transmissivity of poly cover (Sanford, 2011)	0.75
Solar transmissivity of polycarbonate	0.78
Transmissivity of poly cover to infrared radiation (Sanford, 2011)	0.29
Transmissivity of polycarbonate to infrared radiation	0.03
Indoor air velocity (Castilla, 2013)	0.2 (m s^{-1})
Relative humidity	75(%)
Installed lighting wattage	50 (W m^{-2})
Number of recirculating fans	12
Rated power of motors	375 (W)
Net heating value of fuel (ASHRAE, 2013)	38 (MJ m^{-3} of gas)

Other input parameters include indoor set-point temperature, CO_2 supply rate, artificial photoperiod, characteristics length, and leaf area index which depend on the type of crop grown in greenhouses. The greenhouse vegetables including tomato, pepper, and cucumber, were selected

for the study since these three vegetables are mostly grown in Canadian greenhouses. For most vegetable crops, the 24 hours of optimum mean daytime temperature is ranged in 21-23˚C (Portree, 1996), and few degrees lower for night temperature (Elings et al., 2005b). In this study, the indoor set-point temperature was selected based on the optimum daytime temperature, and the night temperature was selected as low as possible without hampering the plant growth to minimize heat loss. Another major limiting factor for northern greenhouses is the low natural light, so the use of supplemental lighting is essential for the year-round production of high-quality vegetables in high latitude regions. The operation hours of supplemental lighting are usually different depending on the type of crops, e.g. lettuce could be benefited from 24 hr of photoperiod, but photoperiod more than 17 hr would be harmful to some crops such as tomato (Dorais, 2003). The supply rate of CO_2 is also different depending on the type of plants. The supply of CO_2 at the rate 4.5 g m^{-2} h^{-1} is recommended for most of the greenhouse vegetables to maintain the CO_2 concentration around 1000 ppm. However, the cucumber plant needs more CO_2 concentration compared to other greenhouse vegetables such as tomatoes and peppers, but should not exceed 1500 ppm concentration level (Castilla, 2013). The characteristic dimension or characteristic length of leaves is an important parameter for estimating the heat exchange in the process of plant evapotranspiration. However, the determination of plant leaf dimension is complicated because of complex geometry in plant leaves. Raunkiaer (1934) classified plant leaves in different categories based on the size and shape of plant leaves. Based on that classification, pepper leaves were considered in the macrophyll class, tomatoes in mesophyll class, and cucumbers in megaphylls class, respectively. The required input parameters for simulation of heating requirement that depend on the types of plants are listed in Table 6.2.

Table 6.2: Environmental control parameters' input values in heating requirement simulation.

Parameters	Tomato	Cucumber	Pepper	Ref.
Daytime temperature (˚C)	22	24	22	(Tesi, 2001)
Night time temperature (˚C)	16	20	18	(Tesi, 2001)
Leaf area index	3.0	3.5	5.0	(Castilla, 2013; Xiao et al., 2004)
CO_2 supply rate (g m^{-2} h^{-1})	4.5	6.0	4.5	(Castilla, 2013)
Characteristics length of leaf (m)	0.027	0.22	0.108	(Raunkiaer, 1934)
Photoperiod (hr)	14	18	16	(Dorais, 2003)

6.2.3 Economic analysis

6.2.3.1 Capital investment

The major capital costs in greenhouses include the building construction cost and the machinery and equipment costs. The machinery and equipment costs include the cost for heating system, irrigation system, lighting system, CO_2 supply system, air circulation/ventilation system, humidity control system, storage system, and other small machinery and tools. Greenhouse building construction cost in Canada ranged between $65-$85 per square meter depending on the types of greenhouses (Spencer, 2009). In this study, the capital investment for the greenhouse building was assumed to be $82 per square meter of floor area. However, the capital cost for the machinery and equipment are usually different depending on the types of crops grown in greenhouses. Alberta Agricultural and Rural Development Authority surveyed the required capital and variable costs in commercial greenhouses for the year of 2011 (Laate, 2013). Most of the capital costs were calculated based on the data from that study by considering 2% of average annual inflation of capital and variable costs (Chau et al., 2009a). Natural gas boilers operated heating system have been used in all of the surveyed greenhouses, and the capital cost for the heating system was considered to be same since the optimum temperature for tomato, cucumber, and pepper production range between 21-24˚C. The required capital cost for lighting and CO_2 supply system was considered based on the literature, because most of the surveyed greenhouses had no supplemental lighting facilities for vegetable production, and no valid data were reported regarding the capital cost of supplemental lighting and CO_2 supply system (Laate, 2013). The optimum

lighting in greenhouses depends on several factors such as daily light integral, crop species, lamp cost, electrical cost, and heating requirement. The capital cost for supplemental lighting in Canadian greenhouses is around \$50 m^{-2} when high-pressure sodium lamp (HPS) installed with 120 W m^{-2} wattage capacity (Dorais, 2003). However, the most common practice is to use 50 W m^{-2} by using HPS to provide useful PAR level of 10 W/m^2 (Urban, 1997). Thus, the capital cost for supplemental lighting was considered based on the installed wattage of the lighting system which is \$30/m^2. The capital cost for CO_2 generators was considered to be the same for all three selected vegetables because most greenhouse vegetables need to supply CO_2 at the rate of 4.5 g m^{-2} h^{-1} to maintain about 1000-ppm concentration in greenhouses (Van Berkel and Verveer, 1984). The capital cost for natural gas operated CO_2 supply system in Canadian greenhouses is around \$3.21/m^2 when supply rate is not greater than 5 g m^{-2} h^{-1} (Blom et al., 2002). The required capital costs in Canadian Prairies greenhouses for the production of tomato, cucumber, and pepper are listed in Table 6.3.

The annual depreciation of capital investments was calculated using the straight-line method of depreciation calculation based on 10% salvage value of the capital investment and reasonable economic life. Twenty years of economic life were considered for building, storage facilities, and HVAC system, and ten years for other machinery and equipment.

Table 6.3: Capital investment for growing tomato, cucumber, and pepper in Canadian Prairies' greenhouses.

Capital Investment ($CAD/m^2)	Tomato	Cucumber	Pepper
Building	82.00	82.00	82.00
Land	2.88	2.88	2.88
Machinery and equipment			
Warehouses / Storage facilities	3.00	1.44	5.78
Houses	4.82	6.20	2.98
Lighting	30.00	30.00	30.00
Heating system	42.78	42.78	42.78
Ventilation and RH control equipment	1.56	2.20	0.69
Benches	1.20	0.00	0.00
Irrigation system	2.00	1.10	1.54
Water Pumps / Sand Filters	0.48	0.25	0.78
CO_2 supply system	3.21	3.21	3.21
Storage / Mixing Tanks	1.75	0.30	4.55
Sterilizers, Fertilizer Injectors, and Sprayers	1.74	1.30	1.01
Carts and Dolleys	5.61	0.89	5.83
Small Tools / Hardware	1.21	1.40	2.31
Bobcats/forklifts	1.40	1.05	1.88
Trucks and Roto-Tillers	4.98	3.58	5.81
Total capital investment ($CAD/m^2)	190.62	180.58	194.03

6.2.3.2 Annual operating cost

The major variable costs in greenhouse vegetable production include labor cost, heating and lighting cost, CO_2 supply cost, marketing cost, fertilizer and chemical costs, repair and maintenance cost, material inputs, and other cash costs such as insurance. The heating cost was calculated based on the predicted annual heating requirements using the GREENHEAT model, the retail rate ($0.2886/m^3) of natural gas in Saskatchewan, and 90% efficiency of the heating system. Also, the operation costs for supplemental lighting and CO_2 supply were calculated based on the estimated annual operating hours of the lighting system and CO_2 supply system. The retail rate of

electricity ($0.114/kWh) in Saskatchewan, Canada, was used to calculate the operational cost of supplemental lighting in the greenhouse. Other variable costs including the cost of material inputs, labor costs, marketing costs, fertilizer and chemical costs, repair and maintenance costs, other cash costs of greenhouse production were collected from the survey study conducted for greenhouses in Alberta (Laate, 2013).

6.2.3.3 Gross return

The gross return from vegetable production was calculated based on the average annual production rate of tomato, cucumber, and pepper in commercial greenhouses, and the average market value of vegetables. Based on one cropping cycle, the annual yield of beefsteak tomato and bell peppers are around 55 kg m^{-2} and 23 kg m^{-2}, respectively (Alberta Agriculture and Rural Development, 2003). The cucumber yield rate is around 65 kg m^{-2} if three cropping cycles are practiced in commercial greenhouses (Badgery and James, 2010). The market prices of the selected vegetables could be very different depending on the location. Based on the sales data of the local Co-op grocery store at La Ronge, Saskatchewan, the local market prices of the vegetables were considered $3.5/kg for beefsteak tomato, 2.7/kg for large English cucumber, and $8.0/kg of bell pepper.

6.2.3.4 Benefit-cost analysis (BCA)

Different economic parameters such as the net return (NR), benefit-cost ratio (BCR), and net present value (NPV) are very important for the benefit-cost analysis of greenhouse vegetable production. The net return (NR) is calculated from the following general relation:

$$\text{NR} = \text{Total production value of vegetable } \left(\frac{\$}{\text{m}^2}\right) - \text{Total production costs } \left(\frac{\$}{\text{m}^2}\right) \qquad (6.2)$$

The net present value (NPV) and the benefit-cost ratio (BCR) are different decision-making criteria in benefit-cost analysis of any investment. However, sometimes conflicts may arise between NPV and BCR because greatest NPV and BCR do not always occur simultaneously in the investment (Zheng et al., 2009). Therefore, both NPV and BCR are important for decision-making about an investment and these two parameters can be calculated using following two relations (Zheng et al., 2009):

$$\text{NPV} = \sum_{\text{t}=0}^{\text{n}} \frac{\text{B}_\text{t} - C_t}{(1+\text{r})^\text{t}} \qquad (6.3)$$

$$BCR = \sum_{t=0}^{n} \frac{B_t}{(1+r)^t} / \sum_{t=0}^{n} \frac{C_t}{(1+r)^t} \quad (6.4)$$

where B_t and C_t are the gross benefit and cost in the t^{th} year; r is the discount rate (the required minimum annual rate of return of new investment); n is the expected project life, and t is the project timescale in years.

BCR and NPV were calculated based on the ten-year economic life of the greenhouse, and 10% discount rate. As the economic life of some capital investments is more than ten years, so the market value of these capital investments after ten years was calculated by subtracting the total ten years depreciated value from the initial capital investment.

Another new criteria is recommended by Gitman (1977) which is called the risk exposure-ratio (RE-Ratio), it measures the degree of exposure risk present in a given capital investment (Grafiadellis et al., 2000). The RE-Ratio can be used to explain the possible reduction in annual cash inflows that a project can allows for keeping the project acceptable (Grafiadellis, 1987). The RE-Ratio and the factor of present value ($F_{r,t}$) can be expressed as follows (Gitman, 1977):

$$RE - Ratio = (BCR - 1) \times \frac{1}{F_{r,t}} \quad (6.5)$$

$$F_{r,t} = \sum_{t=0}^{n} \frac{1}{(1+r)^t} \quad (6.5a)$$

6.2.3.5 Sensitivity Analysis

Sensitivity analysis gives an additional insight of the value of the investment, and an indicator to evaluate the effect of major variables on the derived outcomes (Grafiadellis et al., 2000). The enterprise value and cash flows in greenhouse production depend on several variables. The major variables including fuel price (natural gas), interest/discount rate, and product price were considered for analysis of the sensitivity of these two variables on the investment for greenhouse production in Canadian Prairies' region.

6.3 Results and discussion

6.3.1 Greenhouse heating requirement

The hourly heating requirement in the study greenhouse was simulated for year-round production of tomato, cucumber, and pepper. Figure 6.1 shows the monthly total heating requirements per

square meter of the greenhouse floor area. In general, the heating requirement for production of tomato is relatively lower compared to the production of cucumber and pepper production, the annual heating demand in the study greenhouse for year-round production of tomato, cucumber, and pepper are 1486, 1657, and 1754 MJ m^{-2}, respectively; i.e. cucumber and pepper heating demand is higher than tomato by 11.5% and 18.1%, respectively. This is mainly because the optimum temperature for cucumber and pepper plants is relatively low compared to the tomato. Also, the small value of leaf area index of tomato plants can be responsible for less evapotranspiration in the tomato greenhouse thereby the amount of heat used for evapotranspiration could be minimized. The optimum temperature for cucumber plants is relatively higher than the pepper plants but the heating requirement for the winter season (Nov-Feb) is slightly less than the heating requirement for pepper production since the pepper plants usually have a larger value of leaf area index. Therefore, greater heat could be used in the process of evapotranspiration. However, the heating requirement for pepper production is relatively higher in summer and spring season (March-October) since the evapotranspiration increase with the increase of solar radiation. The heating requirement for the coldest three months (December-February) are 58.4%, 57.0%, and 55.4% of the annual total heating requirements, for tomato, cucumber, and pepper, respectively; while the three summer months (June-August) heating are only about 2-5% of the annual requirement.

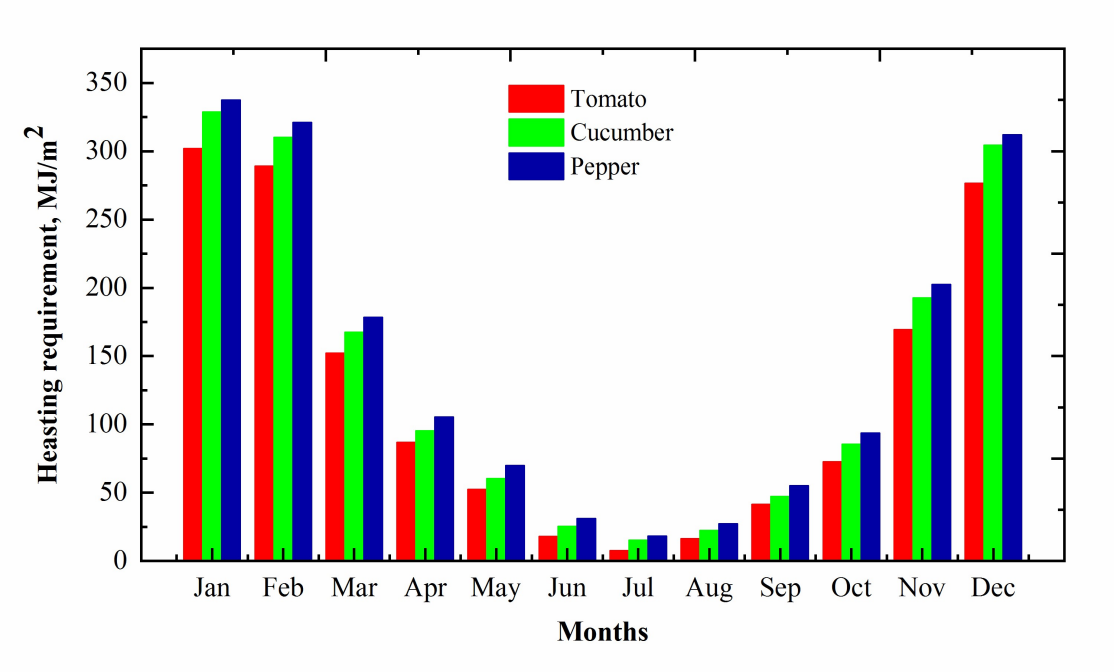

Figure 6.1: Monthly heating requirement of the greenhouse for the production of tomato, cucumber, and pepper.

6.3.2 Economic analysis

The major capital costs in Canadian greenhouses are building construction, heating system, supplemental lighting system, which are accounting about 80% of the total capital investment. The required total capital investment for tomato, cucumber, and pepper production are \$190.62/m^2, \$180.58/m^2, and \$194.03/m^2, respectively (Table 6.3). The calculated annual depreciation of capital investment and variable costs for the vegetable are given in Table 6.4. The annual depreciation of capital investments are similar for the production of tomato, cucumber, and pepper, because the major capital costs such as the cost of building construction, supplemental lighting, heating system, and CO_2 supply system, are not much different. The major operational costs include labor, heating and lighting, material input, and marketing. The material input cost include the cost of growing media, seed/cuttings, tray, boxes, and other packaging materials. In the study conducted by Laate (2013), the transportation cost including the expenses for trucks or other vehicles owned by the greenhouse owner were apportioned according to their use in greenhouse operation, personal and leisure driving. Other transportation cost such as freight charges paid to commercial or private carriers for hauling greenhouse produce or supplies were added to the marketing cost.

The analysis of greenhouse operation cost indicates the cost for labor is the largest operational cost for greenhouse production, which accounts for 31.6% of the total operational costs for tomato production, whereas 26.9% and 28.6%, respectively, for the production of cucumber and pepper. The marketing cost is the second largest operation cost (16.0%) for the production of tomato followed by the cost of heating (14.9%), material inputs cost (9.6%), and cost for lighting (7.9%). The material input costs for the production of cucumber and pepper are 14.6% and 14.0%, respectively, and the heating costs are 15.2% and 15.4%, respectively. The cucumber plants usually require longer photoperiod for optimum production, so the lighting cost in cucumber greenhouse is significantly greater than that of tomato and pepper.

The calculated annual depreciation of capital investment and variable costs for the production of tomato, cucumber, and peppers are shown in Table 6.4. The annual depreciation of capital investments is similar to the production of tomato, cucumber, and pepper, because the major capital investments sources such as the cost of building construction, supplemental lighting, heating system, and CO_2 supply system, are not significantly different. The major operational costs include the cost of labor, costs for heating and lighting, material input costs, and marketing cost. The material input costs include the cost of growing media, seed/cuttings, tray, boxes, and other packaging materials. In the study conducted by Laate (2013), the transportation costs including the expenses for trucks or other vehicles owned by the greenhouse owner were apportioned according to their use in greenhouse operation, personal and leisure driving. Other transportation costs such as freight charges paid to commercial or private carriers for hauling greenhouse produce or supplies were added to the marketing costs.

Table 6.4: Annual capital costs, variable costs, and net return (NR) for the production of tomato, cucumber, and pepper.

Parameters	Tomato	Cucumber	Pepper
Capital cost (CAD$/m^2.year)			
Building and equipment depreciation	9.46	8.59	9.81
Paid capital interest	1.63	2.90	2.93
Property and business tax	0.40	0.81	0.18
Variable cost (CAD$/m^2.year)			
Material costs	10.40	17.26	17.77
Labor costs	34.18	31.70	35.41
Marketing costs	17.37	14.65	17.37
Fertilizer and chemicals	7.27	5.90	7.27
Repair and maintenance	1.57	1.84	1.57
Other cash costs	4.91	4.41	5.73
Heating cost	16.12	17.85	19.03
Lighting cost	8.54	16.03	12.06
CO_2 supply cost	2.96	3.92	2.96
Others electrical costs	4.95	4.50	4.50
Total production costs ($CAD/m^2)	119.77	130.36	136.60
Total production value ($CAD/m^2)	192.50	175.00	184.00
Net return ($CAD/m^2)	72.73	44.98	47.40

As shown in Table 6.4, pepper production is the highest investment crop ($136.6/m^2) followed by cucumber ($130.36/m^2) and tomato ($119.77/m^2). The net return (NR) from tomato production is significantly higher ($72.73/m^2) as compared to the production of cucumber ($44.98/m^2) and pepper ($47.40/m^2). The NR value indicates that the production of tomato would give a greater return compared to cucumber and pepper because the major variable costs such as the cost of lighting and material input costs are higher for the production of cucumber and pepper.

Based on the market price and 10% of discount rate, the net present values (NPV) of greenhouse production for tomato, cucumber, and pepper are $ 21 million, $12 million, and $ 13 million, respectively, and the benefit-cost ratio (BCR) are 1.42, 1.23, and 1.22, respectively. The risk

exposure ratios (RE-ratio) are 6.84%, 3.68%, 3.58%, respectively, for the production of tomato, cucumber, and pepper. The RE-ratio indicates that the annual cash inflow from the production of tomato, cucumber, and pepper, can be reduced by 6.84%, 3.68%, 3.58%, respectively, and thereby the investments would still maintain the positive NPV.

6.3.2.1 Sensitivity analysis

Natural gas is commonly used to generate heat and CO_2 for commercial greenhouse production in Canada (Chau et al., 2009a). In 2010, about 79% of greenhouse growers used natural gas for heating greenhouses in Alberta (Laate, 2013). According to the SaskEnergy, the natural gas prices in Saskatchewan is fluctuated up to 50% over the last 15 years. The sensitivity of natural gas prices on NPV for the production of tomato, cucumber, and pepper, is shown in Figure 6.2. A 50% decrease in the natural gas price increases the NPV by 16.3%, 33.0%, and 32.2% respectively. Conversely, a 50% increase in the fuel price reduces the NPV by 16.1%, 32.7%, and 31.9%. The price of natural gas is fluctuated by a large margin and the heating cost usually the second largest operational cost of greenhouse production at northern latitudes. Hence, the sensitivity analysis indicates that the economic return from greenhouse production in Canadian Prairies can significantly affect by the fluctuation of heating fuel price.

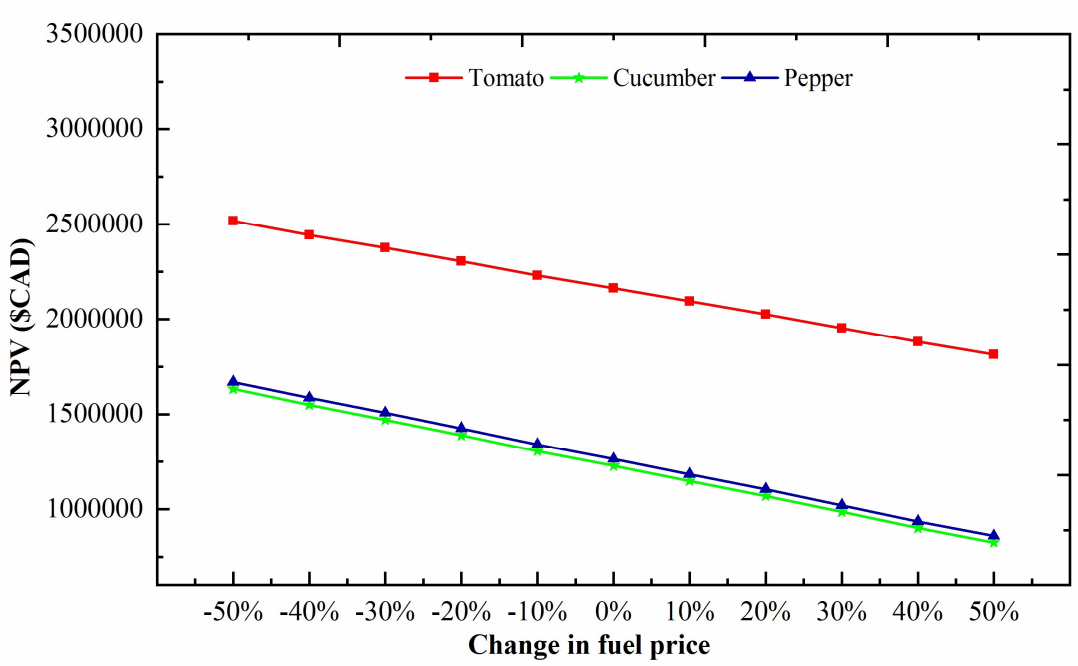

Figure 6.2: The effect of a change in heating fuel price on NPV for the production of tomato, cucumber, and pepper in the study greenhouse.

Figure 6.3 shows the sensitivity of discount rate on the NPV for the vegetable production. The sensitivity of discount rate and product price on the NPV are analyzed by changing the possible range of values. The discount rate decrease by 50% will result in the increase of NPV by 42.6%, 54.1%, and 55.1%, respectively, for the production of tomato, cucumber, and pepper, whereas 50% increase in discount rate will result in the reduction of NPV by 29.7%, 37.5%, and 38.2%, respectively. The discount rate reflects the macroeconomic conditions; producers cannot influence it; however, a larger change in discount rate could affect the outcome significantly.

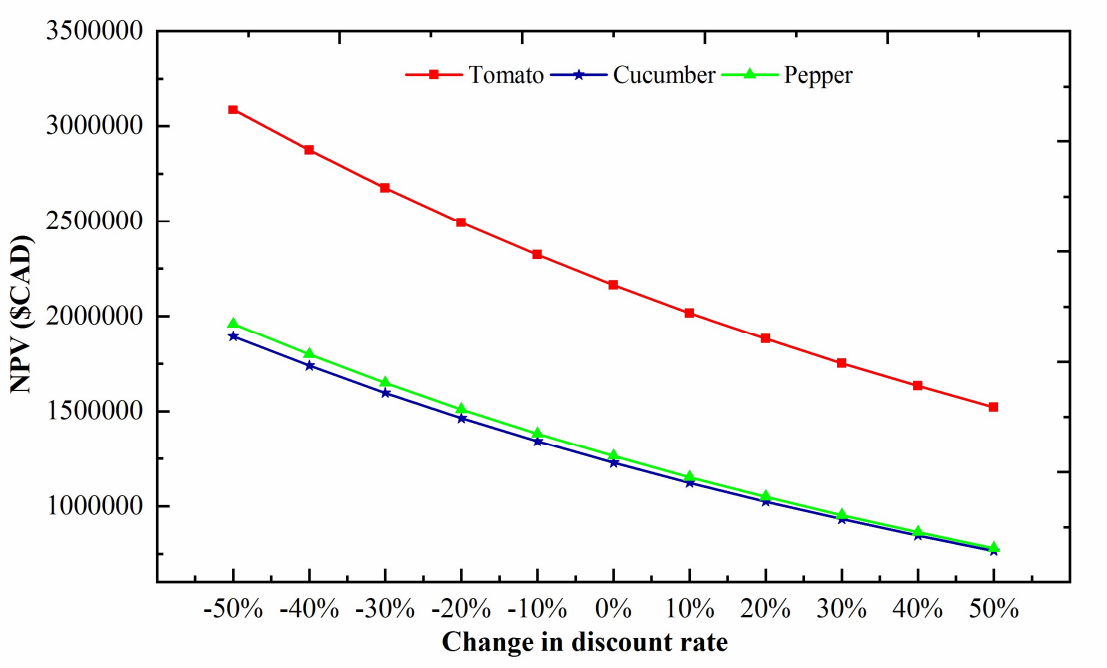

Figure 6.3: The effect of a change in discount rate on NPV for the production of tomato, cucumber, and pepper.

The sensitivity of product price on the NPV is shown in Figure 6.4. The product price has a perfect linear relation with NPV for the selected crops. For instance, a 10% decrease in tomato price causes the reduction of NPV by 32.2%, and 10% increase also increases the NPV by 32.8%. However, a 10% increase in the unit price of cucumber and pepper could cause a significantly larger change on NPV by 52.6% and 53.7%. The outcomes from sensitivity analysis indicate the product price is the crucial factor that can significantly affect the size of NPV.

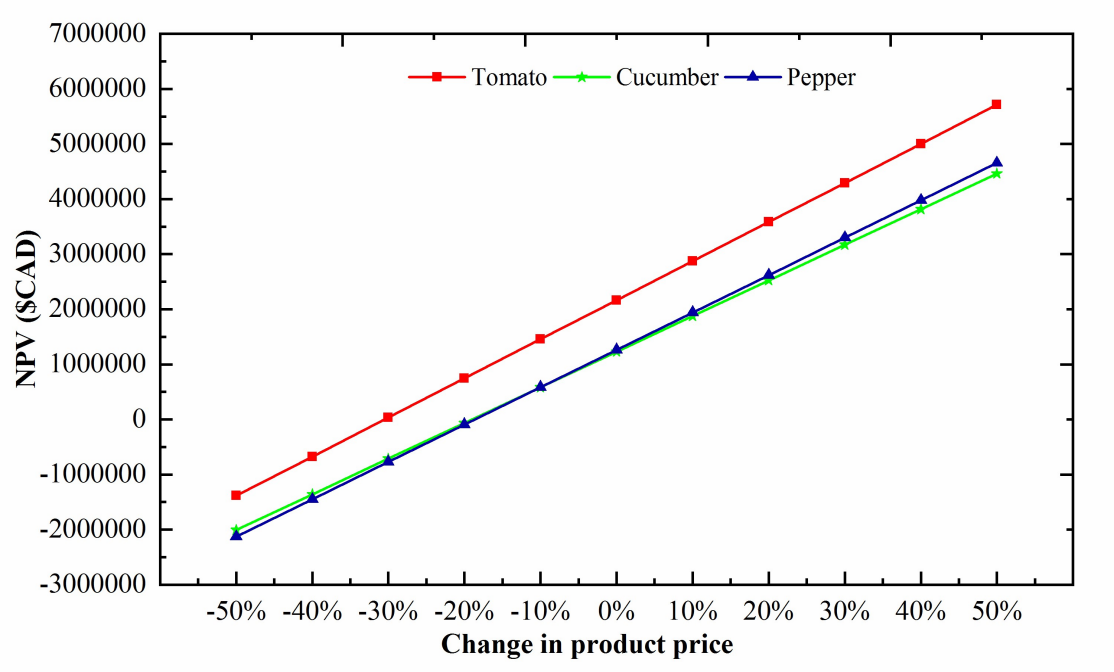

Figure 6.4: The effect of a change in product price on NPV for the production of tomato, cucumber, and pepper.

As the prices of vegetables in Canadian Prairies; especially northern Saskatchewan are extremely high and sometimes the vegetable price can double during extreme winter months (November-February). Therefore, the year-round production of vegetable in the greenhouses at higher northern latitudes can become economically feasible for greenhouse production as the unit price greatly affect the economic feasibility of greenhouse vegetable production. Consumers also would benefit from the quality of the local produce greenhouse products would exceed imported produce while providing local employment.

6.4 Conclusions

Based on the result of this study, the following conclusion can be drawn about the production of tomato, cucumber, and pepper in Saskatchewan greenhouses.

1. Supplemental lighting and the reduced night-time indoor temperature can significantly reduce the heating demand in Prairies greenhouses.
2. Heating is the second largest operational cost, accounting more than 15% of the total operational cost required in a Canadian Prairies greenhouses.
3. The production of tomato in the greenhouse could be more profitable than the production of cucumber and pepper. However, the RE-Ratio indicates that the investment in

greenhouse production for all three selected vegetables is stable from an economic point of view.

4. The sensitivity analysis indicates that the economic outcome from greenhouse production is very sensitive to the product price, and the product price at remote northern latitudes are relatively higher. So, the locally produce vegetable at remote northern latitudes would be economically profitable.

Acknowledgement

The authors are thankful to the College of Graduate and Postdoctoral Studies (CGPS) at the University of Saskatchewan, as well as the Innovation Saskatchewan for their financial support to this research.

CHAPTER 7

DEVELOPMENT OF A THERMAL MODEL FOR SIMULATION OF SUPPLEMENTAL HEATING REQUIREMENTS IN CHINESE-STYLE SOLAR GREENHOUSES

(The manuscript presented in this chapter was submitted to the Journal of Computer and Electronics in Agriculture, submission no: COMPAG_2018_106)

Overview

Building materials and indoor environmental control practice in a Chinese-style solar greenhouse (CSG) are significantly different than the conventional greenhouses. Therefore, the developed heating simulation model for the conventional greenhouses (Chapter 3) could not be used for simulation of the heating requirement in the CSGs. This chapter presents a heating simulation model CSGHEAT developed for CSG, which fulfills the third objective of this thesis (i.e., to develop a heating simulation model for the Chinese-style solar greenhouses). The developed model (CSGHEAT) was validated with the three days of experimental data from a commercial CSG in Winnipeg, Canada. CSGHEAT model was used to fulfill the fifth and sixth objectives (Chapter 8 and 9). As the lead author of this manuscript, I conducted the research, analyzed the results, prepared the manuscript, and incorporated co-authors comments. The co-authors (Professor Huiqing Guo, and Professor Karen Tanino) have contributed to this manuscript through providing technical guidance to conduct the research and constructive review to improve the quality of research.

Abstract

The simulation model CSGHEAT has been developed to estimate the hourly heating requirements in a Chinese-style solar greenhouse. The heating model was developed based on the heat balance of greenhouse air. With the set indoor temperatures, the surface temperatures of the floor and north wall were estimated by solving ordinary differential heat balance equations. The model is relatively easy to use because the model does not need to input measured data such as solar radiation like other models, and most of the heat sources and sinks in the Chinese-style solar greenhouse are included in the model. The model was validated with experimental data, and the predicted result was found to be in good agreement with the measured data. The mean difference between the measured and the estimated soil temperature is about 1.4˚C, and 1.8˚C for the north wall. The average percent error and relative root means square error (rRMSE) value for hourly heating prediction are 8.7%, and 11.5%, respectively. Therefore, the CSGHEAT model is considered to be sufficiently accurate and a reliable tool for researchers and others in the greenhouse industry to assist in designing and analyzing supplemental heating requirements in Chinese-style solar greenhouses.

Nomenclature

A_c, A_f, A_p	area of cover, floor, and plant, m^2
A_n, A_t	area of the non-transparent and transparent surface, m^2
C_p	specific heat capacity, J kg^{-1} K^{-1}
E_m	motor efficiency, %
F_c, F_{sk}	cover view factor and sky view factor, dimensionless
F_p	perimeter heat loss factor, W m^{-1} K^{-1}
F_{hc}, F_a	heat conversion factor and lighting allowance factor, dimensionless
F_{um}, F_{ul}	motor load factor and motor use factor, dimensionless
H_{cs}	depth of underground soil for constant temperature, m
h_a	air thermal conductance, W m^{-2} K^{-1}
h_i, h_o	convection coefficient for indoor and outdoor surface, W m^{-2} K^{-1}
I_b, I_d	direct beam radiation and diffuse radiation on horizontal surface, W m^{-2}
k_a, k_c, k_{cs}	thermal conductivity of air, cover, and soil, W m^{-1} K^{-1}
K	thermal conductivity of i^{th} section in composite wall, W m^{-1} K^{-1}
L_c, L_f	characteristics length of convective surfaces and plant leaves, m
L_v	latent heat of water vaporization, J kg^{-1}
MFR	carbon dioxide supply rate, kg m^{-2} hr^{-1}
M_T	moisture transfer rate, kg s^{-1}
N	day of the year, n=1, for 1^{st} January
N_c	number of layers in cover, dimensionless
N_r	number of re-circulation fans, dimensionless
NHV	net heating value of fuel, MJ kg^{-1}
P	perimeter of greenhouse, m
P_m	motor power rating, W
PR	production rate of CO_2 from fuel combustion, kg/kg fuel
Q	heat transfer rate, W
R_a, R_s	aerodynamic resistance and stomatal resistance, s m^{-1}
S	total solar radiation entering the greenhouse, W
T_c, T_i, T_o	cover temperature, indoor temperature, and outdoor temperature, K
T_{cs}, T_{sk}	underground constant soil temperature and sky temperature, K

T_R	turbidity factor, dimensionless
U_t, U_n	heat transfer coefficient for transparent and non-transparent surface, W m^{-1} K^{-1}
V	greenhouse volume, m^3
v_i, v_o	indoor airspeed and outdoor airspeed, m s^{-1}
W	installed power of lighting, W m^{-2}
w_{ps}	saturated humidity ratio of air at plant temperature, kg kg^{-1}
w_i	humidity ratio of air at indoor temperature, kg kg^{-1}

Greek letters

α	solar absorptivity, dimensionless
B	angle of inclined surface with horizontal, degrees
Γ	surface azimuth angle, degrees
ε_c, ε_i	emissivity of cover and indoor component, dimensionless
Θ	angle between two radiative surfaces, degrees
θ_z	zenith angle of the sun, degrees
θ_i	angle of incidence of surfaces, degrees
P	volumetric density, kg m^{-3}
ρ_r	reflectivity of outdoor ground, dimensionless
τ	solar transmissivity of cover, dimensionless
τ_l	transmissivity of cover to long-wave radiation, dimensionless

Subscripts

A	Air
nw	north wall
F	Floor

7.1 Introduction

A high amount of supplemental heat is needed during the long winter months for greenhouses located in northern latitudes. The heating cost in northern greenhouses such as Canada can be from 75 to 85% of the total operating cost, excluding costs associated with labor (Rorabaugh et al., 2002). Hence, reducing heating cost by improving greenhouse covering materials and optimizing greenhouse design has been an important research topic for cold regions. Chinese-style solar greenhouse (CSG), a mono-slope greenhouse, has great potential to serve as a model of an energy-efficient horticultural facility in northern latitudes because this type of greenhouse significantly reduce supplemental heating demands as compared to conventional greenhouses. It uses non-transparent north wall, north roof, ground, etc. to store excessive heat during the daytime and release the heat at night when heating is needed. CSGs have been used to produce warm season vegetables at latitudes of 40˚N in China with little or no supplemental heating during the winter season (Zhang et al., 2008). Beshada et al. (2006) studied the thermal performance of a CSG in Manitoba (49.9˚N) and reported the greenhouse could maintain an indoor temperature above 10˚C about 19% of the time when the outdoor temperature fluctuated between -29.2 and 4.5˚C; however, supplemental heating was required at up to 17.0 W m^{-2} for 19 h per day to maintain an indoor temperature of 10˚C in February. As the high heating cost is one of the crucial factors for determination of CSG feasibility in the cold region, accurate prediction on heating requirement is needed before the greenhouse growers can make decision on establishing such greenhouses. Hence, simulation of supplemental heating requirements in CSGs is essential for predicting heating needs in greenhouses at higher northern latitudes; furthermore, the heating simulation model can also be used to analyze heat gain and loss through each component of the CGS so the design of the CGSs can be improved to minimize heating loads.

A few thermal models (Du et al., 2012; Guo et al., 1994; Ma et al., 2010; Meng et al., 2009; Taki et al., 2016; Tong et al., 2009, 2008; Yu et al., 2016; Zhou et al., 2017; Zou et al., 2017) have been developed for simulation of microclimates in the CSGs. Most of these dynamic models (Ma et al., 2010; Meng et al., 2009; Taki et al., 2016; Zhou et al., 2017) have been developed for prediction of temperature variations of different interactive components in CSGs including indoor air, cover, plant, soil, north wall, and sidewalls. These types of dynamic models have a high degree of complexity with numerous parameters that have to be determined due to the difference of greenhouse locations, shape, orientation, cover materials, crop, and weather conditions (Chen et

al., 2015; Sethi et al., 2013), therefore, they are not readily available for use by other researchers and greenhouse industries. Computation fluid dynamics (CFD) is a powerful method to analyze the spatial and temporal distribution of temperature for various interactive components in greenhouses. Tong et al. (2009) have used CFD for simulation of time and space dependent temperature distributions in a CSG. However, CFD model is difficult for simulation of a large greenhouse due to long computation time; it could be very complicated for heating simulation over a long period such as a month or a year (Taki et al., 2016). It also needs specialty CFD skill, each model is for a specific greenhouse and cannot be easily applied to other greenhouses. Also, variety 'black box' methods have been used very recently for simulation of greenhouse thermal environment such as the artificial neural network (ANN), least squares support vector machine (LSSVM), convex bidirectional extreme learning machine (CB-ELM) (Yu et al., 2016; Zou et al., 2017). Yu et al. (2016) have developed the temperature prediction model based on the least squares support vector machine (LSSVM) model. Zou et al. (2017) present a novel temperature and humidity prediction model based on convex bidirectional extreme learning machine (CB-ELM). The black-box modeling methods need large amounts of data, otherwise, the model's reliability could be unacceptable (Chen et al., 2015). Several studies (Ahamed et al., 2017b; Du et al., 2012; Jolliet et al., 1991) indicate that the lumped estimation models based on the energy balance of greenhouse as a whole could be a simple and reliable tool for time-dependent simulation of the heating requirement in greenhouses. Du et al. (2012) developed a simulation heat transfer model to estimate heating demands in a CSG, however, this model did not consider heat addition from the north wall. This model also neglected the heat contributions from environmental control systems, including lighting and CO_2 generators, which are very important components for maintaining the optimum environment for plants in greenhouses at high northern latitudes. The previous studies (Du et al., 2012; Tong et al., 2009) did not consider the variation of solar radiation fraction available on the north wall and soil surface in the presence of plants in greenhouses. Also, most of the previous models (Du et al., 2012; Ma et al., 2010; Taki et al., 2016) either neglected the heat transfer from the canopy transpiration (Du et al., 2012) or used coefficients for estimation of evapotranspiration (Ma et al., 2010; Taki et al., 2016), but the canopy transpiration varies significantly depending on solar radiation available in greenhouses. Furthermore, most of the studies were conducted in China, and these models are not applicable for Canadian greenhouse practice because the greenhouses in China are basically passive greenhouses without automatic

control of temperature by heating and ventilation systems. This environment management method cannot be accepted by different regions especially western modern commercial greenhouses which require indoor temperature well controlled by environment control systems. Therefore, the existing lumped estimation models would result in high uncertainty if used in CSGs located at high northern latitudes. Besides, new materials for cover, insulation, heat storage, etc. have been developed continuously, and methods for estimating heat and moisture transfer in the greenhouses have been modified continuously, therefore, the thermal model should reflect these new technologies.

Conversely, the numerical models of buildings could not be used to accurately predict the energy requirement of greenhouses because the microclimate in greenhouses is affected by crop canopy and bare soil surface significantly. It also could be very complicated to integrate the environmental control systems of the greenhouse in building energy simulations models (Chen et al., 2015). Hence, the objective of the study was to develop a novel heating simulation model named "CSGHEAT" for estimation of time-dependent supplemental heat demand in Chinese-style solar greenhouses. It intended to include up-to-date greenhouse materials and energy saving technologies and heat source and sink models.

7.2 Principle of the model

Figure 7.1 shows the heat balance of a typical Chinese solar greenhouse during heating mode. The CSGHEAT model was designed to simulate heating requirements; therefore, the cooling load was not considered because the greenhouse's temperature is usually controlled by opening the vent near the ridge. Heat and mass transfer in the greenhouse is a complicated process, so thermal modeling to simulate greenhouse heating requirements can be complex. For this reason, the following assumptions are made for the development of the heating simulation model for the Chinese-style solar greenhouses:

1. The greenhouse is east-west oriented for receiving maximum benefit from solar radiation in heating season.
2. The solar radiation available on the floor and north wall is uniformly distributed and the shading influence of plants and greenhouse roof elements is neglected because the accurate distribution of solar radiation becomes complicated when developing the heating simulation model.

3. Heat storage in the sidewall (east and west) and north roof material is considered to be negligible since the sidewall consists of insulating and siding materials.
4. The fluctuation of indoor relative humidity is considered negligible since optimum humidity control is required for greenhouses at high northern latitudes.
5. Heat flow through the composite wall and greenhouse floor is one-dimensional.

Based on these assumptions, the heat balance of Chinese-style solar greenhouse can be given as follows:

$$Q_h = \text{Sources} - \text{Sinks} = (Q_s + Q_{s-i} + Q_{nw-i} + Q_{ec}) - (Q_{loss} + Q_i + Q_e) \quad (7.1)$$

where Q_h is the supplemental heat demand; Q_s is the net solar heat gain; $Q_{s\text{-}i}$ is the heat transfer between the ground and the indoor greenhouse components; $Q_{nw\text{-}i}$ is the heat transfer between the north wall and the indoor greenhouse components; Q_{ec} is the heat addition from environmental control systems including supplement lighting (Q_{sl}), carbon dioxide supply system (Q_{CO2}), and the air circulation system (Q_m); Q_{loss} is the transmission heat loss through the greenhouse envelope including conduction and convection loss (Q_t), perimeter loss (Q_p), and long-wave radiation loss (Q_r); Q_i is the heat transfer caused by air infiltration; and Q_e is the heat transfer in the process of plant evapotranspiration.

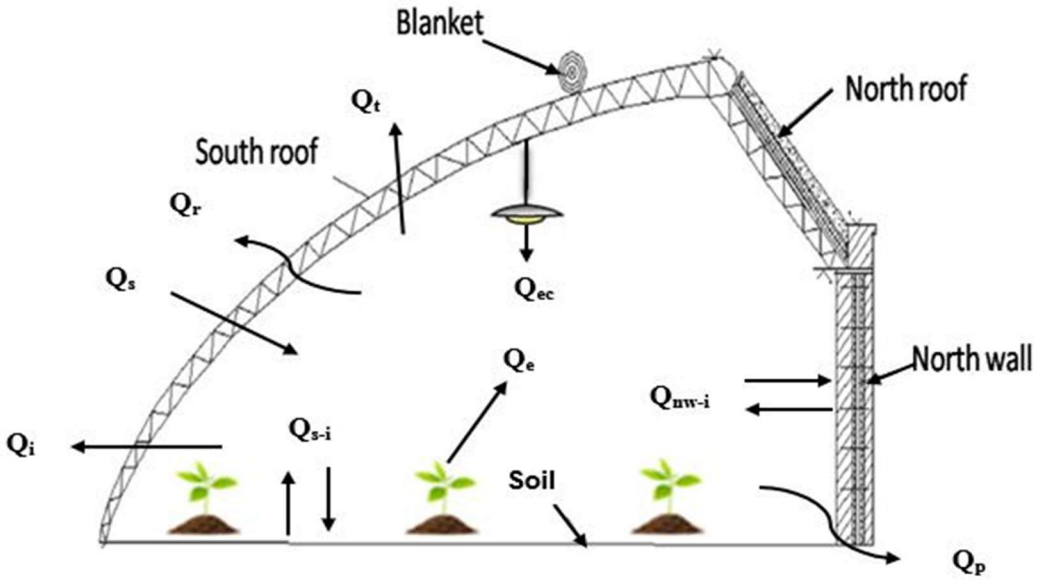

Figure 7.1: The heat balance in a Chinese solar greenhouse on a typical winter day.

7.2.1 Net solar heating gain

Solar radiation passing through the cover of the CSG can be grouped into a number of categories. A fraction of solar radiation is converted to sensible heat, which heats the interior greenhouse components (plant and air), while a fraction of solar radiation is absorbed by the north wall and floor. A very small fraction of solar radiation is also reflected back to the outside, and another small fraction (2-3%) is used in photosynthesis (Albright, 1990). The amount of solar radiation that directly contributes to increasing the greenhouse interior component temperature can be given by:

$$Q_s = S - \alpha_f S_f - \alpha_{nw} S_{nw} \quad (7.2)$$

Solar radiation through the inclined south roof is modeled according to the following equation (Liu and Jordan, 1963):

$$I_i = I_b \frac{\cos\theta_i}{\cos\theta_z} + [I_d \left(\frac{1+\cos\beta}{2}\right) + (I_b + I_d)\rho_r \left(\frac{1-\cos\beta}{2}\right)] \quad (7.3)$$

The shape of the south roof is an important factor for precise estimation of solar radiation in a Chinese-style solar greenhouse. Different shapes of the south roof have been used such as a straight south roof, two straight sections with one bend, and curved cross-section. The curved surface is the most popular shape recently for the south roof in Chinese solar greenhouses (Tong et al., 2013). With a curved roof, estimating the solar radiation is relatively complicated because the slope of the roof changes over the span length. The angle of the first section of the south roof near the ground needs to maintain an angle between 60˚ and 90˚, and the angle of the second section usually ranges between 20˚ to 30˚ depending on the location of the greenhouse (Zhang and Li, 1966). Therefore, the south roof of the greenhouse is separated into two sections to more accurately estimate the available solar radiation through the south roof. The total solar insolation available in the greenhouse through a transparent south roof can be estimated as follows:

$$S = \sum_i \tau_i A_i I_i \quad (7.4)$$

The hourly global solar radiation under actual sky conditions is modeled by using the solar radiation sub-model described by Ahamed et al. (2017b). In the solar radiation sub-model, the solar radiation is estimated using the Kasten-Czeplak (Kasten and Czeplak, 1980) model based on the cloud cover (Oktas) information, and the clear sky solar radiation is modeled using the turbidity factor model described in Tiwari (Tiwari, 2003).

7.2.2 Heat transfer between floor and indoor air

A fraction of incoming solar radiation in the greenhouse is absorbed by the floor, so the floor surface temperature does increase. Therefore, the heat would be exchanged between the greenhouse floor and the indoor air which can be calculated as follows:

$$Q_{f-i} = h_{f-i} A_f (T_f - T_i) \quad (7.5)$$

For heated horizontal soil surfaces facing upward, the convective heat transfer coefficient can be calculated as follows (Tiwari, 2003):

$$h_{f-i} = \left(\frac{k_a}{L_f}\right) 0.15(10^{10})^{0.33} \quad (7.6)$$

The heat balance of the greenhouse floor can be written as follows:

$$\rho_f C_{pf} V_f \frac{dT_f}{dt} = \alpha_f S_f - h_{f-i} A_f (T_f - T_i) - \frac{K_f}{H_{cs}} A_f (T_f - T_{cs}) \quad (7.7)$$

The above equation can be written in the following form:

$$\frac{dT_f}{dt} + \alpha T_f = B(t) \quad (7.8)$$

where,

$$\alpha = \frac{h_{f-i} A_f + \frac{K_f}{H_{cs}} A_f}{\rho_f C_{pf} V_f}$$

$$B(t) = \frac{\alpha_f S_f + h_{f-i} A_f T_i + \frac{K_f}{H_{cs}} A_f T_{cs}}{\rho_f C_{pf} V_f}$$

The analytical solution of the equation (8) can be written as follows:

$$T_f = \frac{B(t)}{\alpha}(1 - e^{-\alpha t}) + T_o e^{-\alpha t} \quad (7.9)$$

where T_o is the greenhouse floor temperature at t=0.

Estimating the solar radiation on the floor under the canopy is complicated because of several factors (e.g., the width of the greenhouse, solar altitude angle, type of crop, and growth stage of the plant), and each factor affects the solar radiation available on the floor. Several studies (Chen et al., 2014; Pieters and Deltour, 1997; Zhang et al., 2014) have used the Beer-Lambert law to estimate solar radiation under the plant canopy. The solar radiation available under the plant canopy can be calculated as follows using the canopy light extinction coefficient (Zhang et al., 2014):

$$S_f = F_f S \times e^{-K.LAI} \quad (7.10)$$

7.2.3 Heat transfer between north wall and indoor air

Heat transfer between the north wall and greenhouse air can be calculated as follows:

$$Q_{nw-} = h_{w-i} A_{nw} (T_{nw} - T_i) \quad (7.11)$$

For vertical hot surfaces under turbulent flow conditions, the indoor convective heat transfer coefficient can be calculated as follows (Tiwari, 2003):

$$h_{w-i} = \left(\frac{k_a}{L_w}\right) 0.1 \, (10^{11})^{0.33} \quad (7.12)$$

The north wall of Chinese-style solar greenhouses is usually made up of a layer of different materials such as insulation material, heat storage material, and sheathing material. The indoor sheathing material is usually very heat conductive and very thin, so the temperature difference between the heat storage material and the indoor sheathing material is assumed to be negligible. Therefore, the heat balance of the north wall can be written as follows:

$$\rho_{nw} C_{pnw} V_{nw} \frac{dT_{nw}}{dt} = \alpha_{nw} S_{nw} - h_{w-i} A_{nw} (T_{nw} - T_i) - U_{nw} A_{nw} (T_{nw} - T_o) \quad (7.13)$$

As with soil surface temperature, the change of the north wall surface temperature can be written in the following form:

$$\frac{dT_{nw}}{dt} + \alpha T_{nw} = B(t) \quad (7.14)$$

where,

$$\alpha = \frac{h_{w-i} A_{nw} + U_{nw} A_{nw}}{\rho_{nw} C_{pnw} V_{nw}}$$

$$B(t) = \frac{\alpha_{nw} S_{nw} + h_{w-i} A_{nw} T_i + U_{nw} A_{nw} T_o}{\rho_{nw} C_{pnw} V_{nw}}$$

The analytical solution of the equation (16) can be written as follows:

$$T_{nw} = \frac{B(t)}{\alpha}(1 - e^{-\alpha t}) + T_{no} e^{-\alpha t} \quad (7.15)$$

where T_{no} is the north wall surface temperature at t=0.

The interception of solar radiation on the north wall depends on several factors such as the projected length of the north roof, height of the plant being grown, the width of plant rows, and plant density. The solar radiation available on the north wall can be estimated as follows:

$$S_{nw} = (1 - \alpha_p) F_{nw} S \quad (7.16)$$

where α_p is a fraction of solar radiation intercepted by the plant for the north wall.

7.2.4 Solar fraction on the north wall and floor

The solar fraction on the north wall and floor can be defined as the ratio of solar radiation falling on the surface to the total solar radiation transmitted through the south roof of the greenhouse (Gupta and Tiwari, 2005a). A few theoretical studies (Gupta et al., 2012; Gupta and Tiwari, 2005a; Tiwari et al., 2003) have been carried out for calculating the solar fraction on the north wall of conventional greenhouses, but most of these studies have used the commercial Auto-CAD model without considering plants in greenhouses. In this model, the physical dimension and projection of sun rays are considered for estimating the solar fraction on the north wall and greenhouse floor. According to the physical dimension and projection of sun rays (Figure 2), the solar fraction for the north wall (F_{nw}) and greenhouse floor (F_f) can be expressed as follows:

$$F_{nw} = \frac{P}{P+W} = \frac{H}{H+W\tan\alpha} \tag{7.17}$$

$$F_f = \frac{W}{P+W} = \frac{W\tan\alpha}{H+W\tan\alpha} \tag{7.18}$$

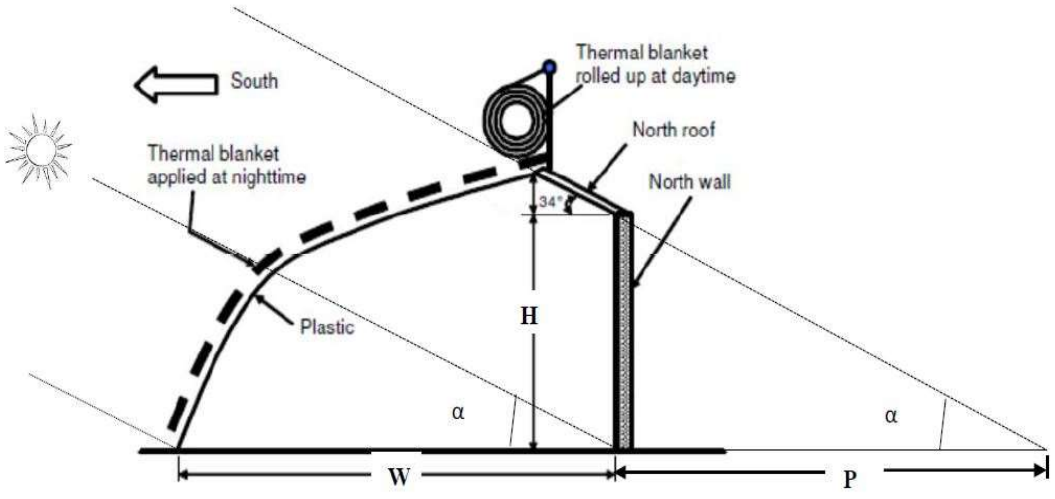

Figure 7.2: View of the projected length of sun rays entering a typical Chinese-style solar greenhouse (Beshada et al., 2006).

7.2.5 Heat gain from environmental control systems

A significant amount heat can be added to the greenhouse from environmental control systems, which may include supplemental lighting, air circulation fans, and carbon dioxide enrichment facilities; These can be estimated as follows (ASHRAE, 2013):

$$Q_{sl} = WF_{hc}F_a A_f \quad (7.19)$$

$$Q_{co_2} = 0.278 \times NHV \times MFR \times \frac{A_f}{PR} \quad (7.20)$$

$$Q_m = N_r \frac{P_m}{E_m} F_{um} F_{lm} \quad (7.21)$$

7.2.6 Heat loss through the greenhouse envelope

The transmission heat loss through the greenhouse envelope includes conduction and convection heat transfer, perimeter heat loss, and transfer of long-wave radiation loss. The heat loss through the greenhouse envelope can be given as follows (ASHRAE, 2013; Hill, 2006):

$$Q_{loss} = Q_t + Q_p + Q_r \quad (7.22)$$

$$Q_t = (A_c U_c + \sum A_w U_w) \times (T_i - T_o) \quad (7.23)$$

$$Q_p = F_p P (T_i - T_o) \quad (7.24)$$

$$Q_r = \left[\sigma \varepsilon_c A_c F_c \left(T_i^4 - T_c^4\right) + \sigma \varepsilon_i \tau_l A_f F_s \left(T_i^4 - T_{sk}^4\right)\right] \quad (7.25)$$

The combined conduction and convection heat transfer coefficient for the transparent south roof and the non-transparent composite wall (north roof, north wall, and sidewall) can be given as (Tiwari, 2003):

$$U_c = \left[\frac{1}{h_i} + \sum_i \frac{L_i}{K_i} + \sum_i \frac{1}{C_i} + \frac{1}{h_o}\right]^{-1} \quad (7.26)$$

$$U_w = \left[\frac{1}{h_i} + \sum_i \frac{L_i}{K_i} + \frac{1}{h_o}\right]^{-1} \quad (7.27)$$

The required values for estimating heat loss through the greenhouse envelope have been estimated according to the article by Ahamed et al. (2017b).

7.2.7 Heat loss caused by infiltration

The infiltration rate in Chinese-style solar greenhouses is comparatively low compared to the fully closed, gutter-connected greenhouses because CSGs have small operational windows and minimum joints in the envelope. A large number of studies have been conducted to estimate infiltration rates in conventional greenhouses, but very limited information is available for infiltration rates in Chinese-style solar greenhouses. Tong et al. (2008) developed a model using

the thermal balance method to estimate air exchange rates in CSGs, but the model is complicated to use as a sub-model. Jolliet et al. (1991) modified the building air leakage model to estimate greenhouse air leakage by placing the greenhouses in three groups (very airtight, airtight, and leaky). Therefore, the air exchange rate in CSGs can be estimated using the modified building model with minimum complexity (Jolliet et al., 1991):

$$Q_i = \rho_a Q C_{pa} (T_i - T_o) \quad (7.28)$$

$$Q = A_L \sqrt{C_w^2 v_w^2 + f_t^2 (T_i - T_o)} \quad (7.29)$$

$$A_L = A_c f_c \quad (7.30)$$

where Q is the air exchange rate in greenhouse ($m^3\ s^{-1}$); A_L is the effective air leakage area (m^2); C_w is the average wind pressure coefficient (0.22) and f_t is the temperature difference factor (0.16 ($m\ s^{-1}\ K^{-1/2}$); v_w is the wind velocity ($m\ s^{-1}$); f_c is the characterization of tightness of the cover to air infiltration (2.5×10^{-4} for very tight frames covered with rubber tape, 5×10^{-4} for tight covers without apparent holes, and $(10\text{-}20)\times10^{-4}$ for leaky covers with cracks or holes); with a thermal screen/blanket f_c is reduced by 25%.

7.2.8 Heat loss caused by evapotranspiration

Evapotranspiration in greenhouses includes the evaporation from the floor/growth media and transpiration from the plants, both of which are responsible for a significant amount heat loss from greenhouses. The estimation of evapotranspiration in greenhouses is very complicated, and most of the existing models (Stanghellini model, Takaura model, and Penman-Monteith ET model) are usually developed to estimate evapotranspiration from farmland. Most previous studies (Boulard and Wang, 2000; Fatnassi et al., 2004) that estimate greenhouse evapotranspiration consider only evapotranspiration from the plant because of the complexity of modeling soil evaporation. Therefore, the heat used by plants in the process of plant evapotranspiration and the rate of evapotranspiration in greenhouses can be estimated as follows (Nobel, 1974):

$$Q_e = M_T L_v \quad (7.31)$$

$$M_T = A_p \rho \left[\frac{w_{ps} - w_i}{(R_a + R_s)}\right] \quad (7.32)$$

The required values for moisture transfer rate have been estimated according to the method described by Ahamed et al. (2017b).

7.3 Model development and validation

7.3.1 CSGHEAT model development

The programming language Matlab was used to develop the "CSGHEAT" computer program for simulating the hourly heating requirements in Chinese-style solar greenhouses. The computer program can simulate the hourly heating requirements based on the input information of indoor microclimates (temperature, relative humidity, air velocity, lighting capacity) and plants, outdoor weather data (temperature, relative humidity, wind speed, cloud cover), and the physical and thermal properties of the greenhouse constructional material. The hourly supplemental heating requirement is the main output from the model, and a negative value of Q_h would indicate a need for heating and positive value indicate cooling need in the greenhouse. The model does not consider the cooling needs because greenhouse temperature is usually controlled with natural ventilation system. The model also simulates other parameters including solar radiation, floor temperature, and north wall temperature for prediction of heating requirement.

7.3.2 Description of the study greenhouse

The developed model was validated with experimental data collected from a commercial Chinese solar greenhouse located in Elie, Manitoba (49.9˚N, 97.75˚W). The model greenhouse (7 m wide and 30 m long) is east-west oriented, and tomato plants were transplanted for growing in the greenhouse, while they were still small. The single layer polyethylene cover (6 mils) encloses the curved south side of the greenhouse. For a curved surface, the angle near the ground is usually greater than the angle of the roof up to a certain height because a small angle near the ground is not suitable for effective use of floor space. The angle near the ground up to 1.0 m height was considered to be 60˚, 26˚ for the rest of the section of the south roof, and about 34˚ for the non-transparent north roof. The height of the greenhouse at the ridge was 3.5 m, and the height of the north wall was 2.1 m. The north wall (a wood stud wall) consisted of a complex layer of different materials; a 2-mm thick inside and outside sheathing of galvanized sheet steel, 152 mm of sand, 13 mm of plywood, and 152 mm of fiberglass insulation; a plastic vapor barrier film was placed between the sand and fiberglass insulation. The side-wall and the north roof of the greenhouse were also supported by wood studs, plywood (13 mm) on the outside, and insulated from the inside with 152 mm of fiberglass insulation which was cover by the plastic film from inside as vapor

barrier. A cotton thermal blanket (20 mm) was used to minimize nighttime heat loss through the transparent south roof.

7.3.3 Measurement method and simulation of study greenhouse

Three days (March 28-30, 2017) of experimental data were collected for validation of the model. The hourly weather data of the study location including air temperature, relative humidity, wind speed, and global solar radiation, were recorded every 10 minutes using a portable weather station positioned near the greenhouse. The data from the weather station were obtained by a data logger (CR1000, Campbell Scientific Inc., USA) and compiled with CR1000 programming software. To simulate the solar radiation, three days of cloud cover data from the national solar radiation database (NSRDB) were used. The natural ventilation system was used to control the daytime high indoor temperature through an opening vent near the ridge, and the night-time temperature was controlled by providing heat from a small, electric space heater. The thermostat of the heater was set to turn on when the temperature went below 12˚C, and would turn off when the temperature went above 18˚C. The indoor greenhouse climate was not well controlled, and the heating load was simulated based on the input of measured room temperature and relative humidity. The air temperature and relative humidity were measured with a temperature and relative humidity probe (CS500, Campbell Scientific Inc., USA), and inside solar radiation was monitored with a pyrometer (LI-200, LI-COR Inc. Lincoln, Nebraska, USA) placed horizontally at 0.5 m above the ground. The greenhouse floor and north wall temperature were measured using wire-type thermocouples. The supplemental heating energy consumption of the heater was measured using an AC sensor. All indoor data were recorded at 10 minute intervals using another data logger (CR10X, Campbell Scientific Inc., USA) and then compiled with CR10X programming software. The average hourly data was calculated based on the measured data recorded at 10 minute intervals.

The thermal environment of the greenhouse was simulated based on the input of the required measured data, which include the outdoor temperature, relative humidity, wind speed, and cloud cover, and the indoor temperature and relative humidity. The other input values included physical and thermal properties of the greenhouse materials, which are listed in Table 7.1. The heat contribution from environmental control systems was not considered for heating calculation

because the study greenhouse had no environmental control systems (lighting, CO_2 supply, air circulation) except a small, electric space heater.

Table 7.1: Constant parameters used for simulation of heating requirement.

Parameters	Value
South roof	
Emissivity of IR barrier poly cover (Hill, 2006)	0.2
Transmissivity to solar radiation (Sanford, 2011)	0.9
Transmissivity to long-wave radiation (Sanford, 2011)	0.29
Thermal conductivity of cover	0.33 (W m^{-1} K^{-1})
Thermal conductivity of night curtain (Beshada et al., 2006)	0.015 (W m^{-1} K^{-1})
North roof and side wall	
Thermal conductivity of plywood (ASHRAE, 2013)	0.12 (W m^{-1} K^{-1})
Thermal conductivity of fiberglass insulation (ASHRAE, 2013)	0.04 (W m^{-1} K^{-1})
North wall	
Thermal conductivity of steel sheet	16 (W m^{-1} K^{-1})
Absorptivity for solar radiation	0.9
Specific heat capacity of sand (Beshada et al., 2006)	920 (J kg^{-1} K^{-1})
Mass density of sand (Beshada et al., 2006)	2240 (kg m^{-3})
Soil characteristics	
Thermal conductivity (ASHRAE, 2013)	1.4 (W m^{-1} K^{-1})
Absorptivity for solar radiation (Du et al., 2012)	0.92
Mass density (Du et al., 2012)	1975 (kg m^{-3})
Specific heat capacity	1480 (J kg^{-1} K^{-1})
Soil temperature at greater depth (Florides and Kalogirou, 2004)	15 (˚C)
Depth for constant soil temperature (Florides and Kalogirou, 2004)	3.0 (m)
Air characteristics (Tiwari, 2003)	
Specific heat of air	1006 (J kg^{-1} K^{-1})
Air density	1.2 (kg m^{-3})
Thermal conductivity of air	0.026 (W m^{-1} K^{-1})
Plant characteristics	

Leaf area index	1.0
Characteristics length of leaf	0.01 (m)
Light extinction coefficient	0.64
Plant factor for solar radiation interception on the north wall	0.85
Emissivity of plant and indoor components	0.9
Other parameters	
Indoor air velocity	0.1 (m s^{-1})
Latent heat of water vaporization (ASHRAE, 2013)	2450 (kJ kg^{-1})
Outside albedo for diffuse radiation	0.5
Perimeter heats loss factor (Worley, 2009)	0.85 (W m^{-1} K^{-1})

7.3.4 Model performance evaluation

The model performance was evaluated in quantitative terms using the percent error, root mean square error (RMSE), and relative root means square error (rRMSE):

$$\text{Percent error} = \frac{(y_m - y_e)}{y_m} \times 100 \quad (7.33)$$

$$\text{RMSE} = \sqrt{\frac{\sum(y_m - y_e)^2}{n}} \quad (7.34)$$

$$\text{rRMSE} = \frac{100}{\acute{y}} \left(\sqrt{\frac{\sum(y_m - y_e)^2}{n}} \right) \quad (7.35)$$

where y_m is the measured data; y_e is the estimated data; n is the number of data points; and $\acute{y}$ is the mean value of measured data. Previous studies (Baptista, 2007; Vanthoor et al., 2011) indicate an rRMSE value of around 10% is reasonably acceptable for transient simulation from greenhouse climate models. Therefore, the rRMSE value around 10% or less is considered reasonably sufficient and accurate.

7.4 Results and discussion

7.4.1 Greenhouse indoor climate

Figure 7.3 shows the hourly variation of solar radiation in the greenhouse and the temperature profile of different components in the greenhouse. The greenhouse inside temperature varied from 15.5 to 35.3°C, while the outdoor temperature fluctuated between -1.6 and 11.4°C. Solar radiation contributed significantly to greenhouse indoor temperature fluctuations, and the average indoor

daytime temperature was 16.9˚C higher than the outside daytime temperature. The nighttime greenhouse temperature was mostly stable because an electric heater was turned on for heating the greenhouse. The indoor temperature, wall temperature, and soil temperature during the daytime mostly followed a similar trend of solar radiation in the greenhouse because the electric heater was turned off during the daytime. Sometimes the inside temperature fluctuated by a large amount, mostly at noon, which could be caused by the operation of the natural ventilation system in the greenhouse.

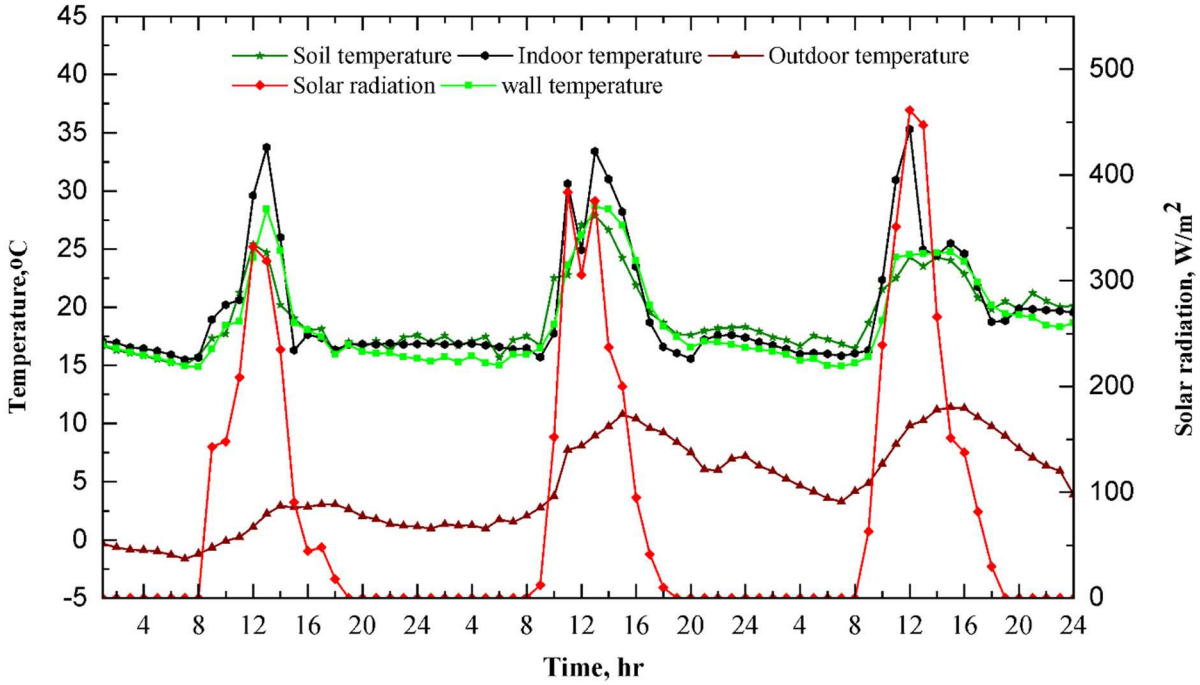

Figure 7.3: Hourly temperature variation of the soil surface, north wall surface, indoor and outdoor air, and solar radiation in the greenhouse on March 28-30, 2017.

7.4.2 Evaluation of the solar radiation sub-model

Figure 7.4 shows the comparison of the predicted and measured global solar radiation on the horizontal surface. The estimated global solar radiation is found to be relatively consistent with the measured data. The coefficient of determination (R^2), RMSE, and rRMSE value are 0.71, 68.34 W m^{-2}, and 30.54%, respectively, which indicates the estimation of solar radiation from the sub-model is reasonably accurate. The small difference over a couple of hours could be due to the difference in cloud cover data because the cloud data used in the simulation was for the City of Winnipeg, which is about 46 km away from the study area.

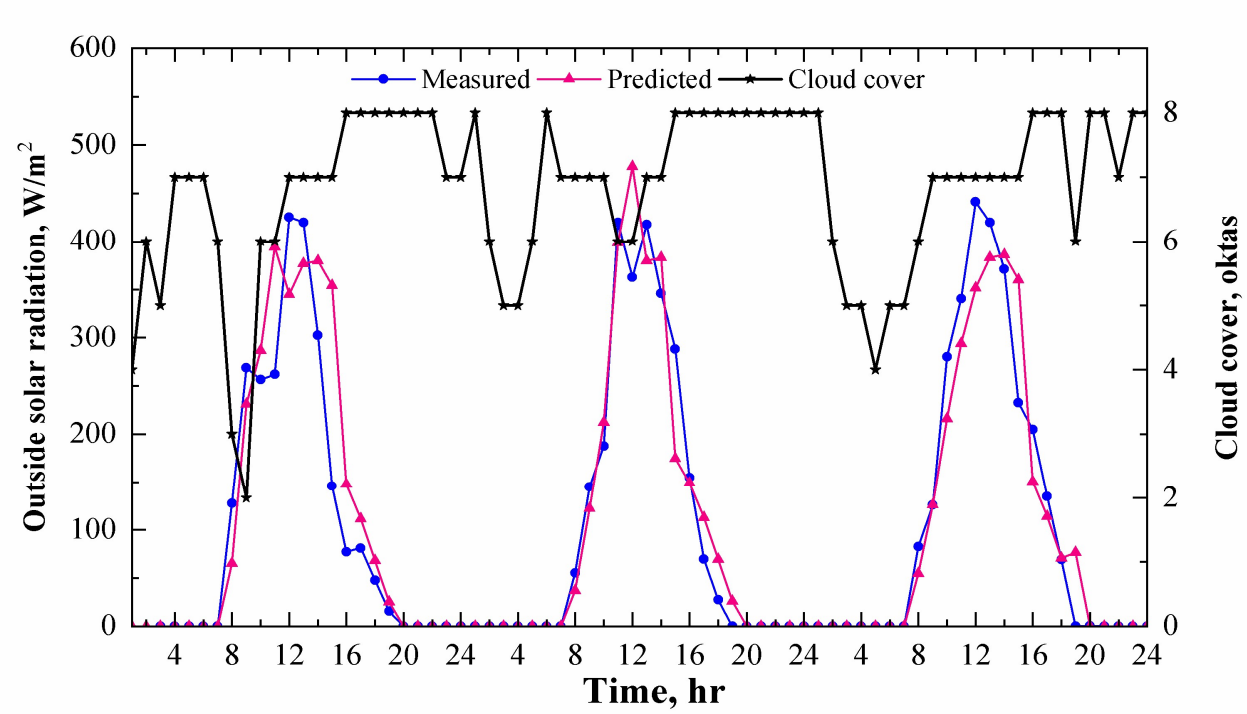

Figure 7.4: Comparison of measured and predicted global solar radiation on the horizontal surface on March 28-30, 2017.

7.4.3 Comparison of simulated and measured temperature of ground and north wall

Figure 7.5 shows the comparison between the simulated and the measured values of the soil temperature. The mean value and standard deviation of the difference between the measured and the predicted temperature were 1.4˚C and 1.2˚C, respectively, and the maximum difference was about 4.5˚C, which usually occurred around noon when the greenhouse temperature was adjusted through the operation of the natural ventilation system. The simulation was performed without considering the greenhouse air-exchange through the natural ventilation system. The predicted soil temperature on the third night was relatively high because a soil heating cable in the growing bed was operating; however, the heat gain from the cable heating system was not included in the simulation as the experimental setup could not record this additional heat source for the greenhouse. The statistical indicators including the R^2, RMSE, and rRMSE value are 0.68, 1.8˚C, and 9.35% respectively.

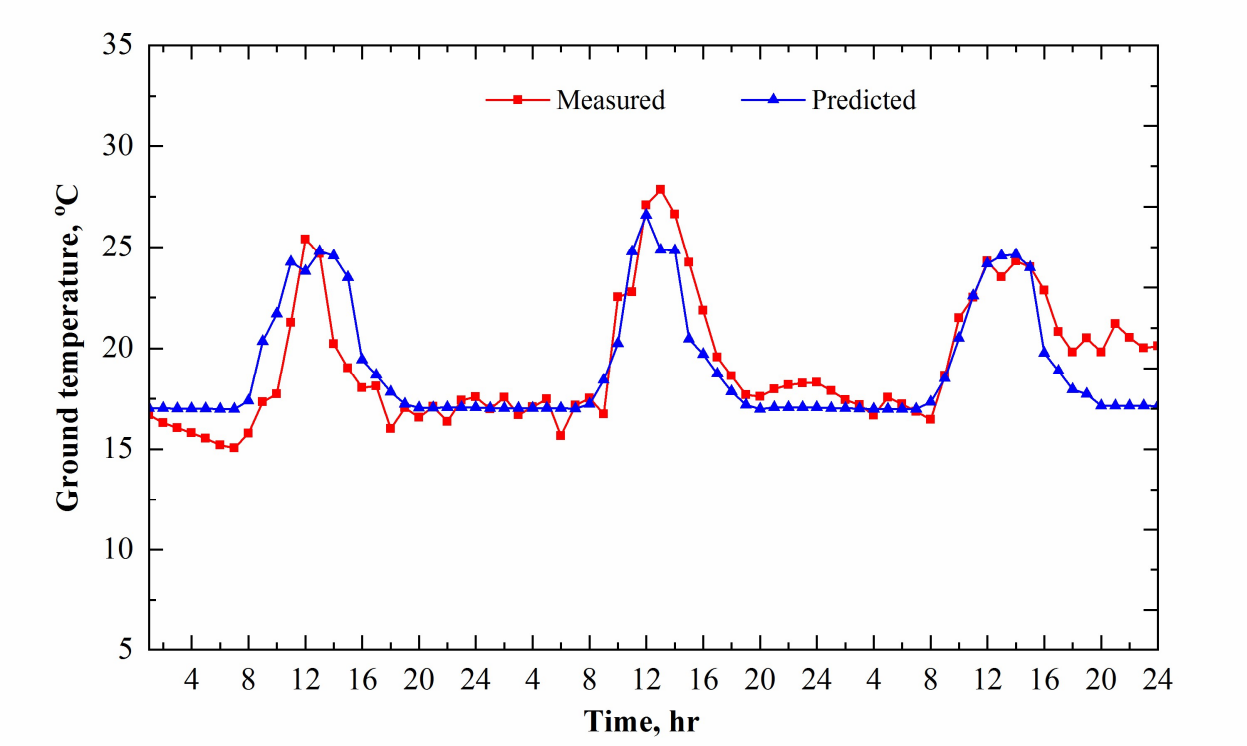

Figure 7.5: Comparison between the predicted and the measured ground temperature in the greenhouse on March 28-30, 2017.

Figure 7.6 shows the comparison between the simulated and the measured temperature of the north wall. The mean value and standard deviation of the difference between measured and predicted temperatures were found to be about 1.8˚C and 1.4˚C, respectively. Similarly, the maximum difference was about 6.5˚C around noon because of opening the vent for controlling high indoor temperatures. Also, the predicted temperature of the first two nights was higher than the measured value, but the higher measured temperature on the third night may have been caused by the additional heat gain in the greenhouse from the soil cable heating system. Based on the statistical analysis of results, the R^2, RMSE, and rRMSE value are 0.77, 2.2˚C, and 11.9%, respectively.

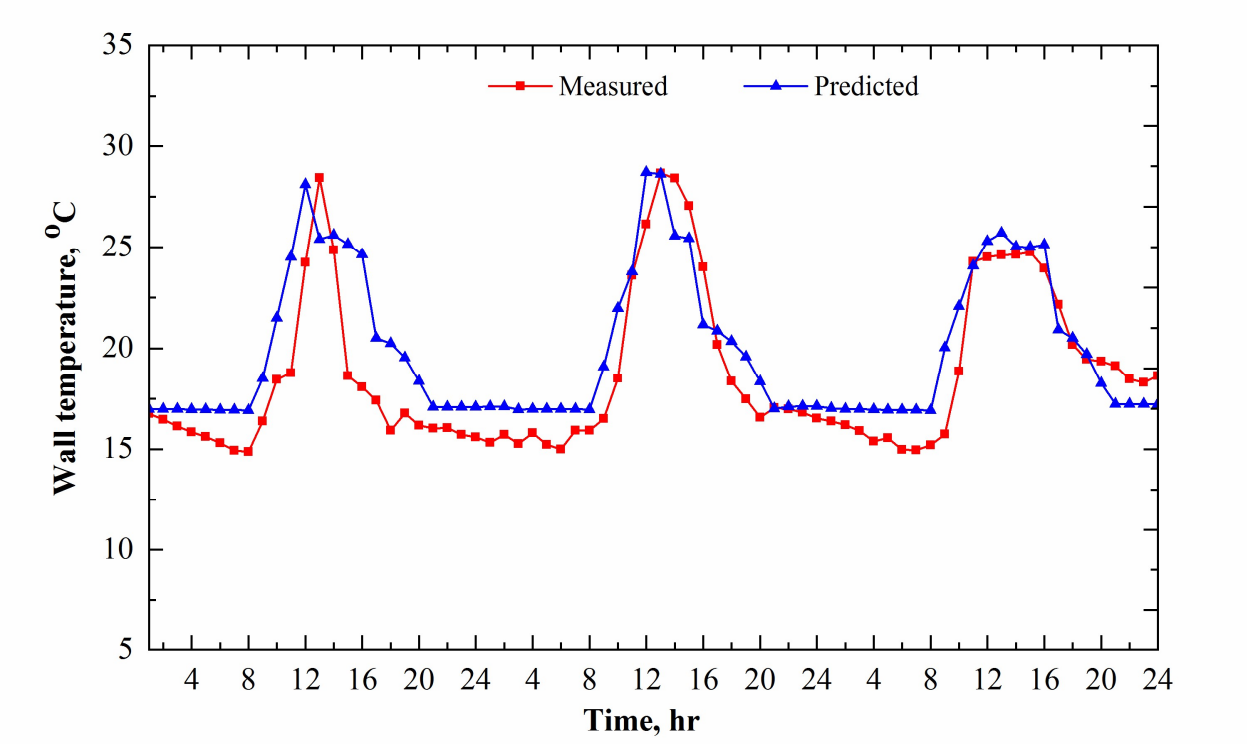

Figure 7.6: Comparison between the predicted and the measured temperature of the north wall on March 28-30, 2017.

The RMSE value for estimation of ground and north wall temperatures is relatively low compared to other studies from greenhouse climate models (Singh et al., 2006; Vanthoor et al., 2011). Also, the rRMSE value is about 10%, so it can be concluded the estimation of the surface temperature of the ground and north wall are reasonably accurate.

7.4.4 Validation for heating simulation

The greenhouse mostly required cooling during the daytime, and the daytime greenhouse temperature was controlled through a natural ventilation system by opening a vent near the ridge. The heating/cooling requirement for the daytime was not considered for validation of the model because no supplemental heating was provided during the daytime. Figure 7.7 shows the comparison of simulated hourly heating requirement with the measured heating requirement in the study greenhouse. The figure indicates that the simulated hourly heating requirement is not significantly different than the actual heating requirement in the greenhouse except during the night of March 30th. The difference on the third night could be due to the additional heat gain from the soil cable heating system located in the growing bed, which was not in operation in the first

two nights. The percent error in prediction varies from 0.2% to 24.9%, and the average error is around 8.7% when the data for the last night is excluded from the analysis. The rRMSE value is 11.5%, so it could be considered that the simulated heating requirement from the developed model would be consistent with the actual supplemental heating requirement in a Chinese-style solar greenhouse. It needs to point out that the experimental greenhouse ventilation was not welled controlled, contributing to the discrepancies of the model predictions and measured data. In the future, the model could be further validated when better field data are available.

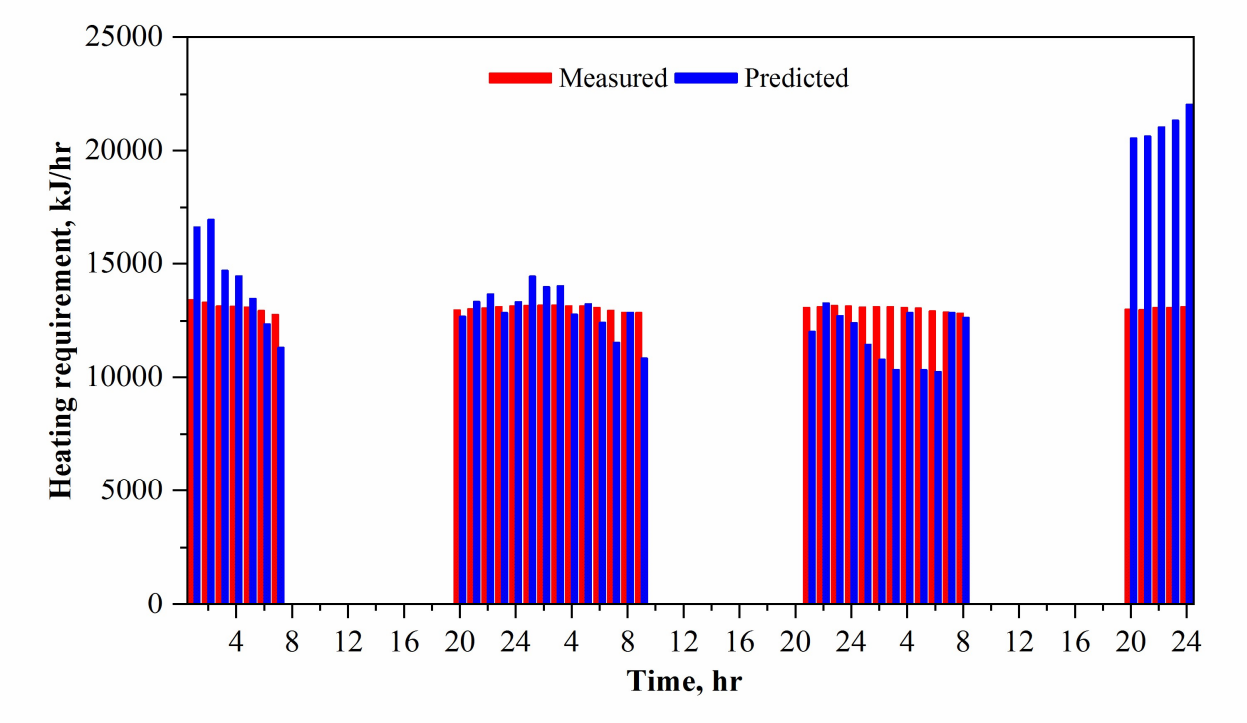

Figure 7.7: Comparison of measured and predicted heating requirement in the study greenhouse on March 28-30, 2017.

7.5 Conclusions

A time-dependent heating simulation model, "CSGHEAT," was developed for predicting the supplemental heating demand for Chinese-style solar greenhouses. It included up-to-date greenhouse materials and energy saving technologies and heat source and sink models. The simulation results show that the model can predict the hourly heating requirement of a CSG in good agreement with the experimental data. The model allows simulation of each heat source and sink in the greenhouse for short or long term, therefore, it can be used as a tool for assisting with the energy-efficient design of CSGs in any locations, and also predict additional heating

requirement for year-round production at high northern latitudes. The results also indicate that the Chinese-style greenhouses indoor temperature can be significantly higher than the outside temperature when solar radiation is available. Hence, Chinese-style solar greenhouse could be an alternative to conventional greenhouses for reducing heating cost in northern regions. The future work will focus on using the model to optimize the design parameters of the greenhouse.

Acknowledgement

The authors are very thankful to the College of Graduate and Postdoctoral Studies (CGPS) at the University of Saskatchewan, as well as Innovation Saskatchewan for their support and provision of research funding.

CHAPTER 8

SENSITIVITY ANALYSIS OF CSGHEAT MODEL FOR ESTIMATION OF HEATING ENERGY CONSUMPTION IN A CHINESE-STYLE SOLAR GREENHOUSE

(The manuscript presented in this chapter was submitted to the Journal of Computer and Electronics in Agriculture, submission no: COMPAG_2018_316)

Overview

A sensitivity analysis could be a useful tool for evaluation of model performance to the different values of input parameters and default parameters used for modeling. This chapter includes the sensitivity of the heating requirement predicted by the CSGHEAT model (Chapter 7). The results presented in this chapter fulfill the fifth objective of this thesis (i.e., to analyze the sensitivity of the CSGHEAT model on heating requirement). In this manuscript, we used the one-parameter-at-a-time (OAT) approach of sensitivity analysis. As the lead author of this manuscript, I conducted the research and prepared the manuscript for submission to the journal. The co-authors (Professor Huiqing Guo, and Professor Karen Tanino) have contributed to this manuscript through providing technical guidance to conduct the research and constructive review to improve the quality of research.

Abstract

The sensitivity of a heating simulation model (CSGHEAT) was performed for estimation of the time-dependent heating requirement in a Chinese-style solar greenhouse in cold region. Results showed that the constant value of air thermal conductance was the main default parameter of the model that significantly affected the model output. The results also indicated the heating requirement is highly sensitive to the greenhouse design parameters including the thermal properties of cover, thermal blanket, and greenhouse perimeter. The thermal blanket is the most important design parameter for the Chinese-style solar greenhouse, and the heating requirement could be increased between 32-41% during the coldest three months (January, February, and December) for changing the thermal conductivity from 0.01 to 0.05 $Wm^{-1} K^{-1}$. Increasing daytime indoor set-point temperature from 19 to 23˚C would increase the heating demand between 13-20%, whereas the heating demand could be increased by 9-18% for increasing the night-time temperature from 16 to 20˚C. Results also indicate the heating demand could be reduced up to 20% during the coldest period for increasing the indoor relative humidity from 70 to 90%. The results from this study could be useful for providing advice on energy saving management of greenhouse operations and for designing the energy-efficient Chinese-style solar greenhouses in cold regions.

8.1 Introduction

Chinese-style Solar Greenhouses (CSGs) have become popular to grow vegetables without any auxiliary heating or with minimum heating depending on the locations of greenhouses. CSGs are mostly used in China and are also being adopted by many countries including Canada. The adaptation of the CSGs beyond China might require some modification in design and environmental control systems. In northern China, mostly no auxiliary heating is supplied to the greenhouse, but supplemental heating might be required for extending the growing period in relatively high northern latitudes. The heating requirement in a typical CSG located in Saskatoon (52.13˚N) could be about 50% less as compared to a typical gutter connected commercial greenhouse (Ahamed et al., 2016). However, a substantial amount of supplemental heating is still required for year-round production at high northern latitudes.

A few thermal models (Guo et al., 1994; Ma et al., 2010; Meng et al., 2009) have been developed to simulate the microclimate of the CSGs. However, almost all of the models are developed for simulation of temperature variation in different components in the CSGs. Ahamed et al. (2018b) developed and validated a time-dependent heating simulation model (CSGHEAT) for estimation of the heating requirement in the CSGs. Greenhouse thermal models are usually developed based on some assumptions and approximation of different heat transfer parameters. It is very important to analyze the effect of these parameters on the model output with a different value before the developed model is incorporated into a practical application. Also, the variation of some user-defined input variables about greenhouse design and indoor environmental control systems could greatly affect the model output. As some variables have a higher impact than others on heating needs, the identification of highly sensitive variables is important from both a technical and economic perspective and should be handled with utmost care (Lam and Hui, 1996). Sensitivity analysis would identify the most influential parameters on the greenhouse heating demand.

The objective of this study was to conduct a sensitivity analysis of a recently developed heating simulation model (CSGHEAT) for estimation of the heating energy requirement in a CSG at high northern latitudes. The results could be helpful to understand the degrees of sensitivity of the model to various influential parameters, and also to better understand energy-efficient design principles and operating strategies of environmental control systems used in cold regions.

8.2 Materials and methods

8.2.1 Heating simulation model (CSGHEAT)

The CSGHEAT model was developed for simulation of time-dependent heating requirements in the CSGs, and the cooling load was not considered because the greenhouse temperature is usually controlled by opening the vent near the ridge. The general heat balance equation of the developed model is given by (Ahamed et al., 2018b):

$$Q_h = \text{Sources} - \text{Sinks} = (Q_s + Q_{s-i} + Q_{nw-i} + Q_{ec}) - (Q_{loss} + Q_i + Q_e) \quad (8.1)$$

where Q_h is the supplemental heat demand; Q_s is the net solar heat gain; $Q_{s\text{-}i}$ is the heat transfer between the ground and the indoor greenhouse components; $Q_{nw\text{-}i}$ is the heat transfer between the north wall and the indoor greenhouse components; Q_{ec} is the heat addition from environmental control systems including supplement lighting (Q_{sl}), carbon dioxide supply system (Q_{CO2}), and air circulation system (Q_m); Q_{loss} is the transmission heat loss through the greenhouse envelope including conduction and convection loss (Q_t), perimeter loss (Q_p), and long-wave radiation loss (Q_r); Q_i is the heat transfer caused by air infiltration; Q_r is the heat transfer caused by exchanging of long-wave radiation through the transparent cover; and Q_e is the heat transfer in the process of plant evapotranspiration.

CSGHEAT simulates the hourly heating requirement based on the input information of indoor microclimates (temperature, relative humidity, air velocity, lighting capacity), plants, weather data (temperature, relative humidity, wind speed, cloud cover), and the physical and thermal properties of greenhouse building materials. The hourly supplemental heating requirement (Q_h) is the main output from the model.

8.2.2 Sensitivity analysis

Sensitivity analysis is a general concept used for energy simulations. There are many ways of conducting sensitivity analysis, which can be categorized into two basic approaches as local sensitivity method and global sensitivity method (Tian, 2013). Local sensitivity analysis method is based on a one-parameter-at-a-time (OAT) approach. The evaluation of output variability is based on the change of one parameter between certain ranges while the other parameters are maintained at a constant level. This method is a very effective way of comparing the relative importance of various parameters on the model output (Ioannou and Itard, 2015). Conversely, the global sensitivity analysis method is more reliable than the local sensitivity analysis but more

complicated and with high computational demand, because all inputs are varied simultaneously over the entire input space, allowing observation of the effect on the output of all individual inputs and also interactions between inputs. The local sensitivity analysis has been extensively used for building energy analysis because this method is straightforward to explain the effect on individual input parameters on the output (Tian, 2013). The sensitivity coefficient is often used for sensitivity study in the field of mathematics and control engineering (Lam and Hui, 1996). Among different forms of sensitivity coefficients for building energy simulation studies, the following form is the most suitable for multiple sets of data (Lam and Hui, 1996):

$$\text{Sensitivity coeffcient} = \frac{\Delta OP/OP_{base}}{\Delta IP/IP_{base}} \quad (8.2)$$

where OP_{base} and IP_{base} are the base output and input; ΔOP and ΔIP are the variations of output and input, respectively. A high sensitivity coefficient would indicate that the model output is highly impacted by the input value; therefore the value must be chosen very carefully (Yang et al., 2016). The maximum heating in Canadian Prairies greenhouses is required during the coldest three months (December, January, and February), so the sensitivity analysis was conducted for these three months.

The important parameters of CSGHEAT model were categorized into two main groups including the default parameters for model development and input parameters for heating simulation. The input parameters for heating simulation were further separated into three groups such as the greenhouse design parameters, crops related parameters, and indoor environmental control parameters. The sensitivities of these parameters on the model output (heating requirement) were studied with the OAT approach of sensitivity analysis.

8.2.3 Base case model and weather data

The choice of base case model is very important for the local sensitivity analysis methods because all subsequent calculations and analyses are based on the comparison with it. The base case of simulation was selected based on optimum or standard practices for greenhouse operation in cold regions. So, it is expected that the base case can represent a typical CSG at high northern latitudes. A double layer air-inflated polyethylene covered CSG (60 m × 10 m area) with east-west orientation located in Saskatoon, Canada, was considered for this study. The angle of curved shape south roof near the ground was set at 60˚ (up to 1 m height), 26˚ for the rest of the section of the

south roof, and 34˚ for the non-transparent north roof. The height of the greenhouse at the ridge was 4.5 m, and the height of the north wall was 3.0 m. The north wall (wood stud wall) consisted of multi-layer of different materials: a 2 mm thick inside and outside sheathing of galvanized sheet steel, 152 mm of sand, 19 mm of plywood, and 65 mm of extruded polystyrene insulation. The side-wall and the north roof of the greenhouse were made by plywood (19 mm) and insulated by extruded polystyrene insulation (65 mm). The plastic film vapor barrier resisted diffusion of moisture through the walls and north roof. A cotton made thermal blanket (20 mm) was considered to reduce the night time heat loss through the transparent south roof. For the study, tomato plants were considered to be grown in the greenhouse, so the daytime indoor set-point temperature was set at 21˚C and 18˚C for the night. The relative humidity was assumed to be constant at 80% during the entire simulation period. Depending on the types of crops, the supplemental lighting is usually turned off when solar radiation reaches below 240-300 W m^{-2} (Dorais, 2003), and about 14 h of photoperiod was recommended for optimum growth of tomato in greenhouses (Demers et al., 1998). Therefore, it was considered that the supplemental lighting to be supplied when solar radiation in the greenhouse was reduced to 250 W m^{-2}, and the artificial lighting was turned off between 10 PM-7 AM to maintain the 14 h of optimum photoperiod. The CO_2 generator was considered to be operating only for the daytime, the thermal blanket was used at night, and the air recirculation system was in operation all the time for 24 h a day. A brief description of the greenhouse base case is given in Table 8.1.

Table 8.1: Base case value for constant parameters used for simulation of the heating requirement.

Parameters	Value
South roof	
Emissivity of IR barrier poly cover (Hill, 2006)	0.2
Transmissivity to solar radiation (Sanford, 2011)	0.78
Transmissivity to long-wave radiation (Sanford, 2011)	0.2
Thermal conductivity of cover (6 mils)	0.33 (W m^{-1} K^{-1})
Thermal conductivity of night curtain (20 mm) (Beshada et al., 2006)	0.03 (W m^{-1} K^{-1})
North roof and side wall (ASHRAE, 2013)	
Thermal conductivity of plywood (19 mm)	0.12 (W m^{-1} K^{-1})
Thermal conductivity of polystyrene insulation (65 mm)	0.033 (W m^{-1} K^{-1})
North wall (Beshada et al., 2006)	
Thermal conductivity of steel sheet (2 mm)	16 (W m^{-1} K^{-1})
Absorptivity for solar radiation	0.9
Heat capacity of sand	920 (J kg^{-1} K^{-1})
Mass density of sand	2240 (kg m^{-3})
Soil characteristics	
Thermal conductivity (ASHRAE, 2013)	1.4 (W m^{-1} K^{-1})
Absorptivity for solar radiation	0.8
Soil temperature at greater depth (Hanova and Dowlatabadi, 2007)	10 (˚C)
Mass density (Du et al., 2012)	1975 (kg m^{-3})
Specific heat capacity	1480 (J kg^{-1} K^{-1})
Depth for constant soil temperature (Florides and Kalogirou, 2004)	3.0 (m)
Air characteristics (Tiwari, 2003)	
Specific heat of air	1006 (J kg^{-1} K^{-1})
Air density	1.2 (kg m^{-3})
Thermal conductivity of air	0.026 (W m^{-1} K^{-1})
Plant characteristics (Rincón et al., 2012)	
Leaf area index	2.0
Characteristics length of leaf	0.027 (m)

Light extinction coefficient	0.64
Emissivity of plant and indoor components	0.9
Other parameters	
Indoor air velocity (Castilla, 2013)	0.1 (m s^{-1})
Latent heat of water vaporization	2450 (kJ kg^{-1})
Outside albedo for diffuse radiation	0.5
Perimeter heats loss factor (Worley, 2009)	0.85 (W m^{-1} K^{-1})
Installed lighting wattage	20 (W m^{-2})
Heat conversion factor (Castilla, 2013)	0.75
Lighting allowance factor (ASHRAE, 2013)	1.2
Number of recirculating fans	2
Rated power of motors	300 (W)
Motor efficiency	0.9
Motor load factor (ASHRAE, 2013)	1.0
Motor use factor (ASHRAE, 2013)	1.0
Net heating value of fuel (ASHRAE, 2013)	38 (MJ m^{-3} of gas)
Rate of CO_2 supply in greenhouse (Castilla, 2013)	4.5 (g m^{-2} h^{-1})
CO_2 production rate (EIA, 2016)	2.7 (kg / kg of fuel)

Apart from the building descriptions, the hourly weather data of Saskatoon (52.13˚N, 106.62˚W) including temperature, relative humidity, wind speed, and cloud cover data of 2015 from the National Solar Radiation Database (NSRDB) were used for simulation of the heating requirement.

8.3 Results and discussion

8.3.1 Sensitivity of CSGHEAT model to default parameters

The thermal model was developed based on some assumptions to reduce the complexity of the model. The sensitivity of the model to some important parameters with default values in the model related to the assumptions in model development was conducted to evaluate their significance on the model output. These parameters include air thermal conductance of double-layer cover, greenhouse floor parameters, and characteristic length of convective surfaces.

8.3.1.1 Air thermal conductance of air spaces in a double-layer cover

The model estimates the heat transfer coefficient (conduction and convection) of multi-layer greenhouse covers by considering a constant value of 3.85 W m^{-2} K^{-1} for the air thermal conductance across the air gap in the inflated plastic films. According to the ASHRAE fundamental (2013), the air thermal conductance of airspace (13-90 mm) in the inclined surface is ranged between 2.0-6.5 W m^{-2} K^{-1}; therefore, the sensitivity of airspace thermal conductance was conducted for the value range between 2.0-6.0 W m^{-2} K^{-1}. Figure 8.1 shows the sensitivity of different values of air thermal conductance on the heating requirement predicted by the model. The result indicates the predicted heating requirement is sensitive to the value of air thermal conductance. The sensitivity coefficient decreased with the increase of air thermal conductance since the air thermal conductance is inversely correlated with the model output. The result also indicates that the model is more sensitive to the low air thermal conductance than the high value. The heating demand increased by about 18% for increasing the value of from 2.2 to 5.4 W m^{-2} K^{-1}. As compared to the base case (3.85 W m^{-2} K^{-1}), the heating requirement decreased up to 12% for decreasing the value to 2.2 W m^{-2} K^{-1} and increased up to 7.5% for using 5.4 W m^{-2} K^{-1}. However, the greenhouse covers with low-emissivity (0.2-0.5) are mostly used in commercial greenhouse production, and the air thermal conductance of the airspace ranges between 3.5-5.2 W m^{-2} K^{-1} for the surface emissivity ranges between 0.2-0.5 (ASHRAE, 2013). Hence, the assumption of constant air thermal conductance value at 3.85 W m^{-2} K^{-1} is reasonably acceptable as the transient simulation of air thermal conductance is very complicated.

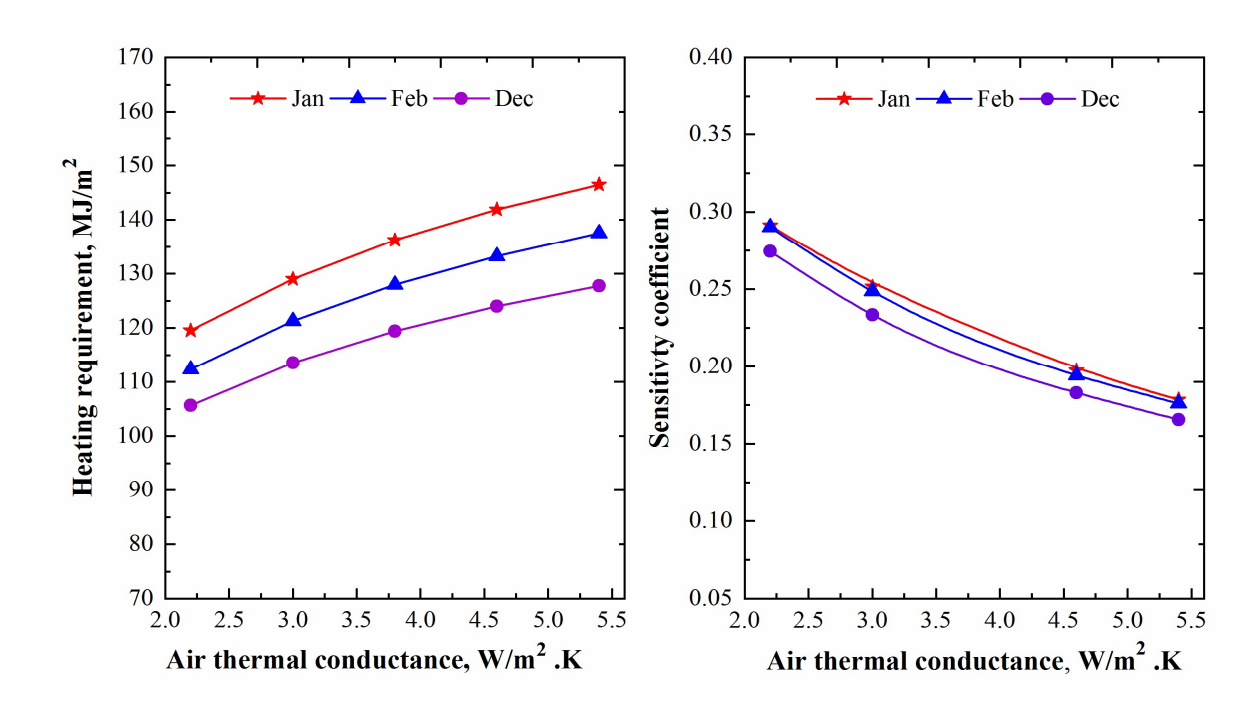

Figure 8.1: The sensitivity of air thermal conductance of air gap in the double layer cover.

8.3.1.2 Greenhouse floor parameters

Greenhouse floor parameters including the underground soil temperature, depth of soil for negligible temperature fluctuation, and thickness of top soil layer, were considered for sensitivity analysis. The underground soil temperatures are affected by meteorological factors including incoming solar radiation, snow cover, air temperature, precipitation, and thermal properties of soils. Depending on the locations, the annual fluctuation of underground soil temperature after a certain depth (3-10 m) could be relatively constant (Florides and Kalogirou, 2004; Hanova and Dowlatabadi, 2007). The underground soil temperatures in Canada (45˚N) below 3 m could be ranged between 7-15˚C, so the sensitivity of underground soil temperature was conducted for the range between 6-14˚C. In CSGHEAT model, the greenhouse floor surface temperature was estimated by solving the heat balance of the greenhouse top-soil layer, and the temperature up to the depth of 10 cm was considered to be uniform. So, the sensitivity of the thickness of topsoil layer from 4 to 16 cm was considered for the analysis.

Figure 8.2 shows the model sensitivity to greenhouse floor parameters. The result indicates the heating requirement decreased by less than 1.0% for increasing the underground soil temperature from 6 to 14˚C. Similarly, a negligible change in heating demand was found for changing the depth

of underground soil for constant temperature from 2 to 4 m, and the heating demand changed by about 3.5% for changing the thickness of the top-soil layer from 0.04 to 0.16 m. The heating requirement increased by less than 1% for increasing the value from 0.1 to 0.16 m, but heating demand decreased by about 2.5% for decreasing from 0.1 to 0.04 m. The sensitivity coefficient is mostly stable for changing the input value of underground soil temperature and depth of soil for constant temperature; however, the thickness of topsoil layer need to be chosen with utmost care especially for the thickness less than 0.1 m. The value of sensitivity coefficient for the underground temperature and depth of underground soil is relatively high in December; this could be due to the large number of hours of low set-point temperature (18˚C) at night. Therefore, the relative change of heating requirement could be higher in December as compared to the value in January and February. However, the high value of the coefficient for the thickness of the top-soil layer was found in February, because the greenhouse soil surface temperature could be significantly different depending on the availability of solar radiation in greenhouses which could be almost double in February as compared to the solar radiation in January and December. The overall sensitivity coefficient is very low for all three parameters, so the default value used for the floor parameters in the model could be reasonably acceptable.

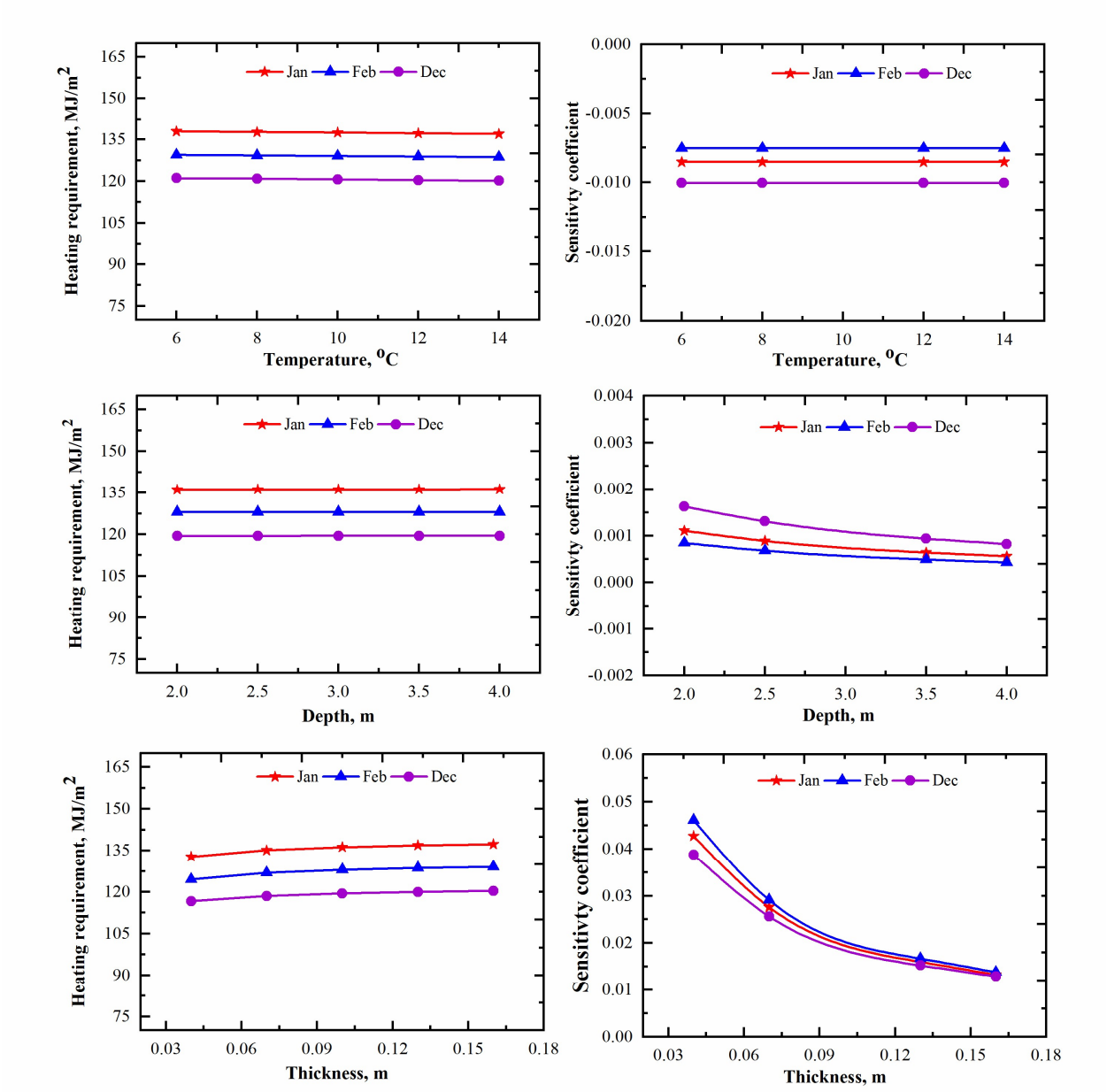

Figure 8.2: The sensitivity of underground soil temperature, depth of soil for negligible temperature fluctuation, and thickness of topsoil layer.

8.3.1.3 Characteristic length of convective surface

The characteristic length of any heat transfer body depends on the geometry of the surface. In the model, the height of the vertical surface and the ratio of the surface area and perimeter (A/P) for horizontal surfaces such as south roof were considered as the characteristic length for estimating the convection heat transfer coefficient. The highest heat transfer in the Chinese-style solar greenhouse usually occurs through the north wall and south roof, so the characteristic lengths of

these two surfaces were considered for the sensitivity analysis. In the study greenhouse, the height of the north wall was 3 m, and the sensitivity analysis was conducted for the range between 2.4-3.6 m. The characteristic length of the south roof (ratio of the surface area and the greenhouse perimeter) was about 4.3 m, so the sensitivity analysis was performed for the range between 3.7-4.9 m. Figure 8.3 shows the change of heating requirement with the different values of characteristic lengths of the north wall and south roof. The heating demand increased by about 3.0% for increasing the characteristic length of north wall from 2.4 to 3.6 m. The heating requirement changed by less than 1% for changing the characteristic length of the south roof from 3.7 to 4.9 m. The low sensitivity coefficient also indicates that the reasonable change in characteristic length has a negligible effect on the model output. The monthly difference in sensitivity coefficients also could be due to the difference of the number of hours of the set point temperature for the daytime and night-time.

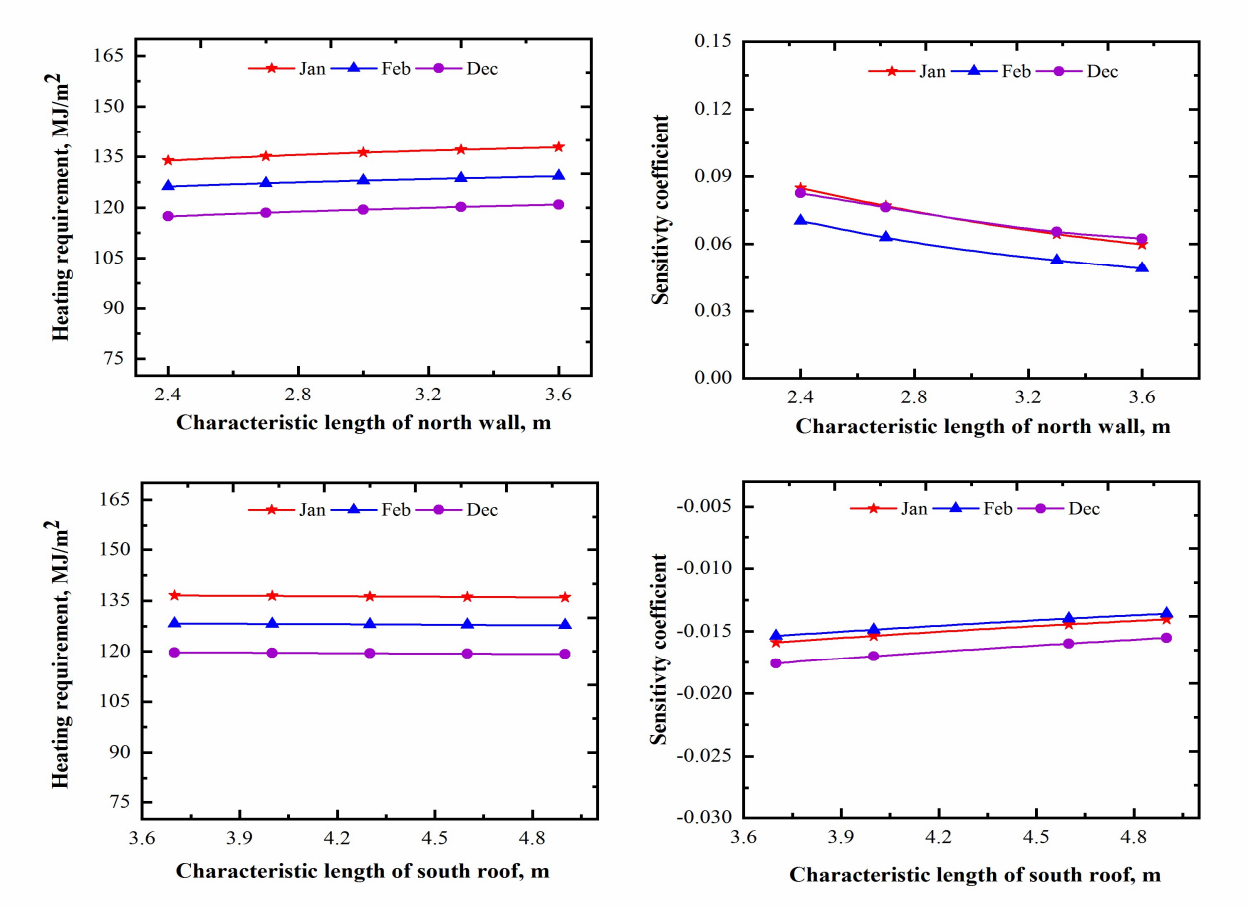

Figure 8.3: The sensitivity of characteristic length of the north wall and the south roof.

8.3.2 Sensitivity of greenhouse building materials

The thermal properties of the north wall and the south roof are more sensitive than other parts of greenhouse envelope because the heat transfer from the CSGs mostly occurs through these two parts due to their large area exposed to the outside. Also, the greenhouse perimeter is an important design parameter as the ratio of perimeter and floor area in CSGs is relatively greater than that of conventional greenhouses because they are narrow and long.

8.3.2.1 Greenhouse cover and thermal blanket

The thermal properties of transparent greenhouse cover including solar transmissivity, transmissivity to long-wave radiation, and emissivity, were considered for the sensitivity study. Depending on the types of covers, the solar transmissivity varies between 70-90%, and the transmissivity to the long-wave radiation varies between 3-50% (Sanford, 2011). The emissivity of the greenhouse covers can be as low as for 0.2 for the polyethylene film to as high as 0.9 for the traditional glass (Aldrich and Bartok, 1994). However, the emissivity of newly developed polyethylene is relatively low, and the sensitivity of emissivity coefficient of greenhouse cover was conducted for the range between 0.01-0.4. Figure 8.4 shows the model output is sensitive to all three parameters. The heating requirement decreased by about 8.5% for increasing the solar transmissivity from 66 to 90%. As compared to the base case, the heating increased by about 5.0% for decreasing the transmissivity from 78 to 66%, and about 4.0% decreased by increasing the value from 78 to 90%. Conversely, the heating requirement could be reduced up to 36% by using the cover has a low transmissivity to the long-wave radiation (0.02) as compared to the cover with high transmissivity (0.4) to the long-wave radiation. Similarly, the heating requirement increased up to 29% for increasing the emissivity coefficient from 0.02 to 0.4. The sensitivity analysis indicates thermal properties greenhouse cover including solar transmissivity, transmissivity to long-wave radiation, and emissivity have a great impact on the greenhouse heating requirement. Therefore, the selection of suitable greenhouse cover is very important to reduce the greenhouse heating requirement.

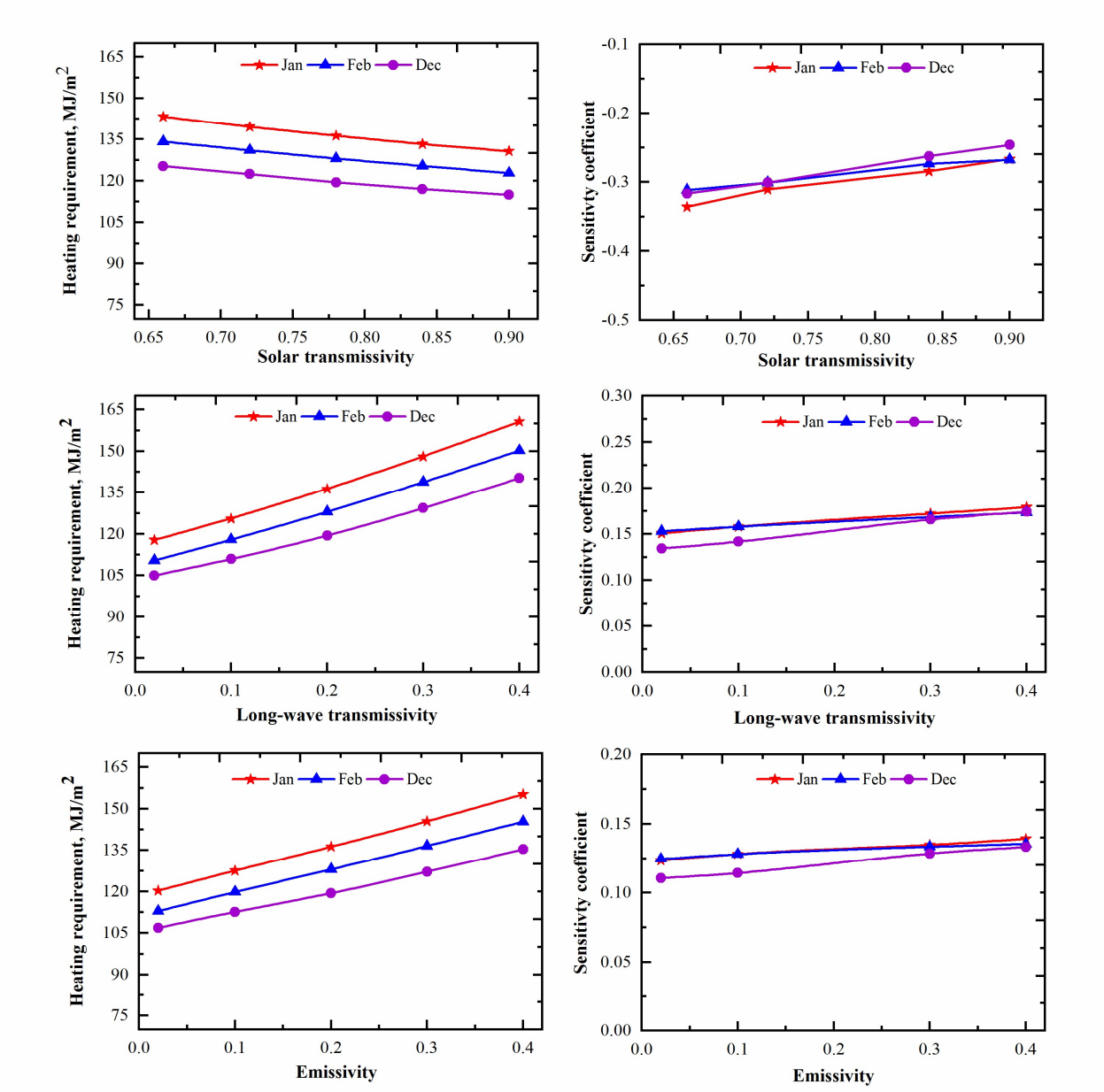

Figure 8.4: The sensitivity of solar transmissivity, transmissivity to the long-wave radiation, and emissivity coefficient of greenhouse double layered poly cover.

The thermal resistance of the south roof blanket is a very important parameter in the CSGs; the sensitivity analysis was also conducted for thermal conductance between 0.01-0.05 W m^{-1} K^{-1}. Figure 8.5 shows that the heating requirement is very sensitive to the thermal conductivity of the blanket. The heating requirement increased between 32-41% for changing the thermal conductivity from 0.01 to 0.05 Wm^{-1} K^{-1}. Therefore, the selection of high thermal resistance material for a thermal blanket is very important for reducing heating demand for the winter season. The value of

sensitivity coefficient also changed significantly for changing the value of thermal conductivity since the thermal conductivity has an inverse relation with the heating requirement. The result also indicates that the sensitivity coefficients are relatively high in December, it could be due to the difference of the day-length thereby the operational hours of the thermal blanket are relatively high in December. So, the sensitivity coefficient is relatively higher since the relative change of heating requirement would be higher in December.

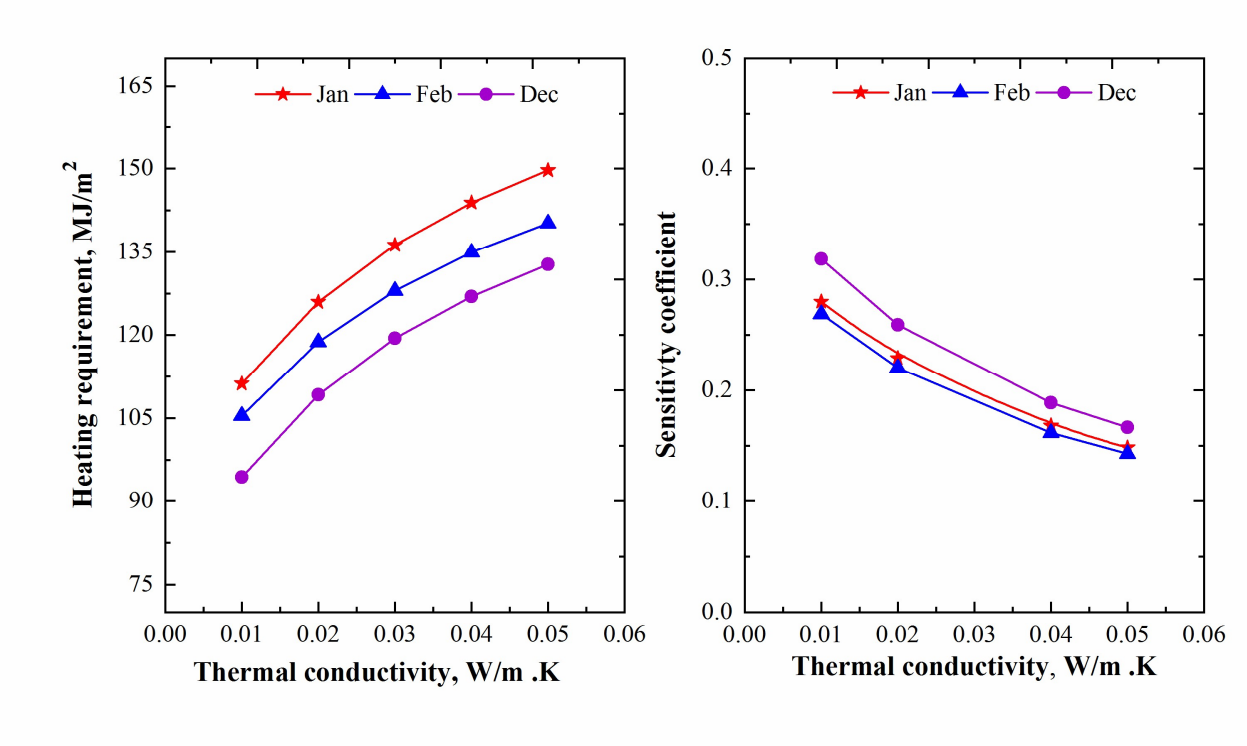

Figure 8.5: The sensitivity of the thermal blanket on the heating requirement.

8.3.2.2 North wall

The important parameters of the north wall include thermal conductivity of insulation material and solar absorptivity of the north wall. Figure 8.6 shows the sensitivity of thermal conductivity of the insulation material and the solar absorptivity of the north wall. The base case value of thermal conductivity and solar absorptivity were considered 0.033 W m^{-1} K^{-1} and 0.9, respectively. The result indicates heating demand increased by about 7.5% with the increase of the thermal conductivity of insulation material from 0.011 to 0.055 W m^{-1} K^{-1}. And, the heating requirement decreased by about 1.5% for increasing the solar absorptivity of the north wall from 0.8 to 0.99.

The sensitivity analysis indicates the solar absorptivity has a very small effect on the heating requirement during the coldest winter months.

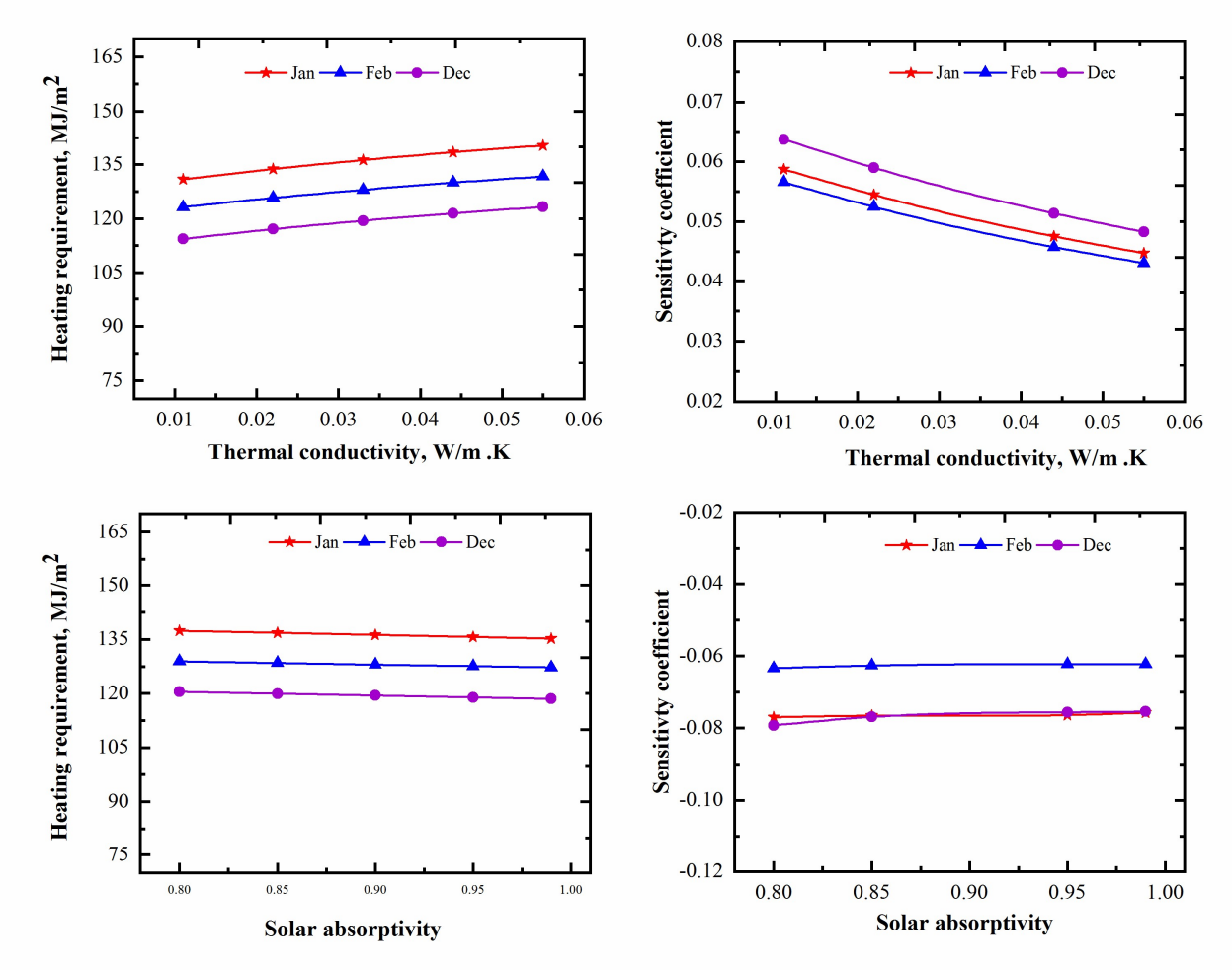

Figure 8.6: The sensitivity of the thermal conductivity of insulation material and solar absorptivity of the north wall.

8.3.2.3 Greenhouse perimeter

Heat loss along the greenhouse perimeter depends on the type of insulation used along the perimeter. Depending on the type of insulation, the perimeter heat loss factor in greenhouses could be ranged between 0.5-1.1 W m^{-1} K^{-1} (Worley, 2009). The sensitivity of the model to perimeter heat loss factor was conducted for the range between 0.45-1.25 W m^{-1} K^{-1}, and Figure 8.7 shows the results. The heating demand increased by about 12% for increasing the heat loss factor value from 0.45 to 1.25 W m^{-1} K^{-1}. The sensitivity coefficient is stable for changing the perimeter heat loss factor which indicates the perimeter heat loss factor has a linear relation to the model output.

The result indicates good insulation along the perimeter could reduce a significant amount heating demand in the CSGs.

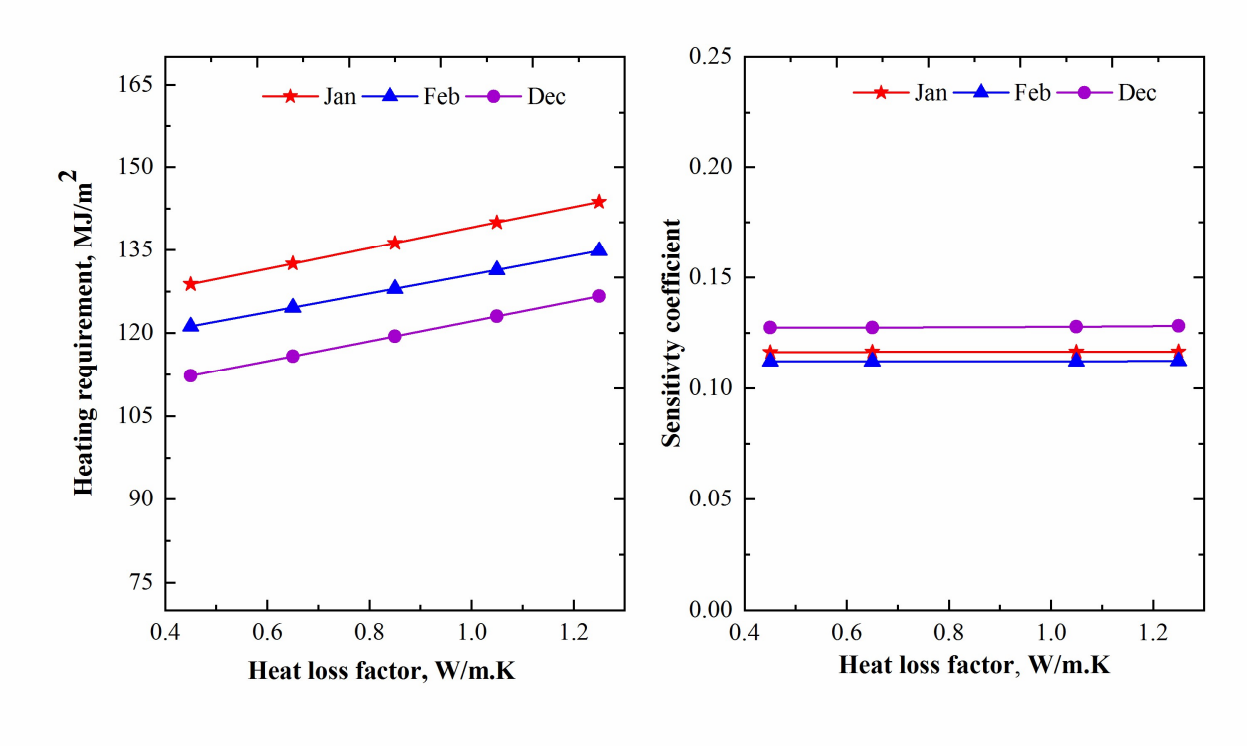

Figure 8.7: The sensitivity of the perimeter heat loss factor on the heating requirement.

8.3.3 Sensitivity of crop parameters

The crop parameters including the leaf area index (LAI) and canopy light extinction coefficient were considered for the sensitivity study. For sensitivity analysis, LAI was considered from 1.0 to 3.0, and the light extinction coefficient was considered between 0.5-0.76. Figure 8.8 shows the heating requirement increased with the increase of leaf area index since the plant transpiration rate increase with the increase of leaf area index. The heating requirement increased between 16-20% for changing the LAI from 1.0 to 3.0. As compared to the base case (2.0), the heating requirement decreased between 6-8% for the input value of 1.0 and increased between 8-10% for the input value of 3.0. However, the heating demand changed by a small amount (about 2.0%) for changing values of the light extinction coefficient from 0.5 to 0.76. Also, the small value of sensitivity coefficient indicates the canopy light extinction coefficient has a relatively low impact on the model output.

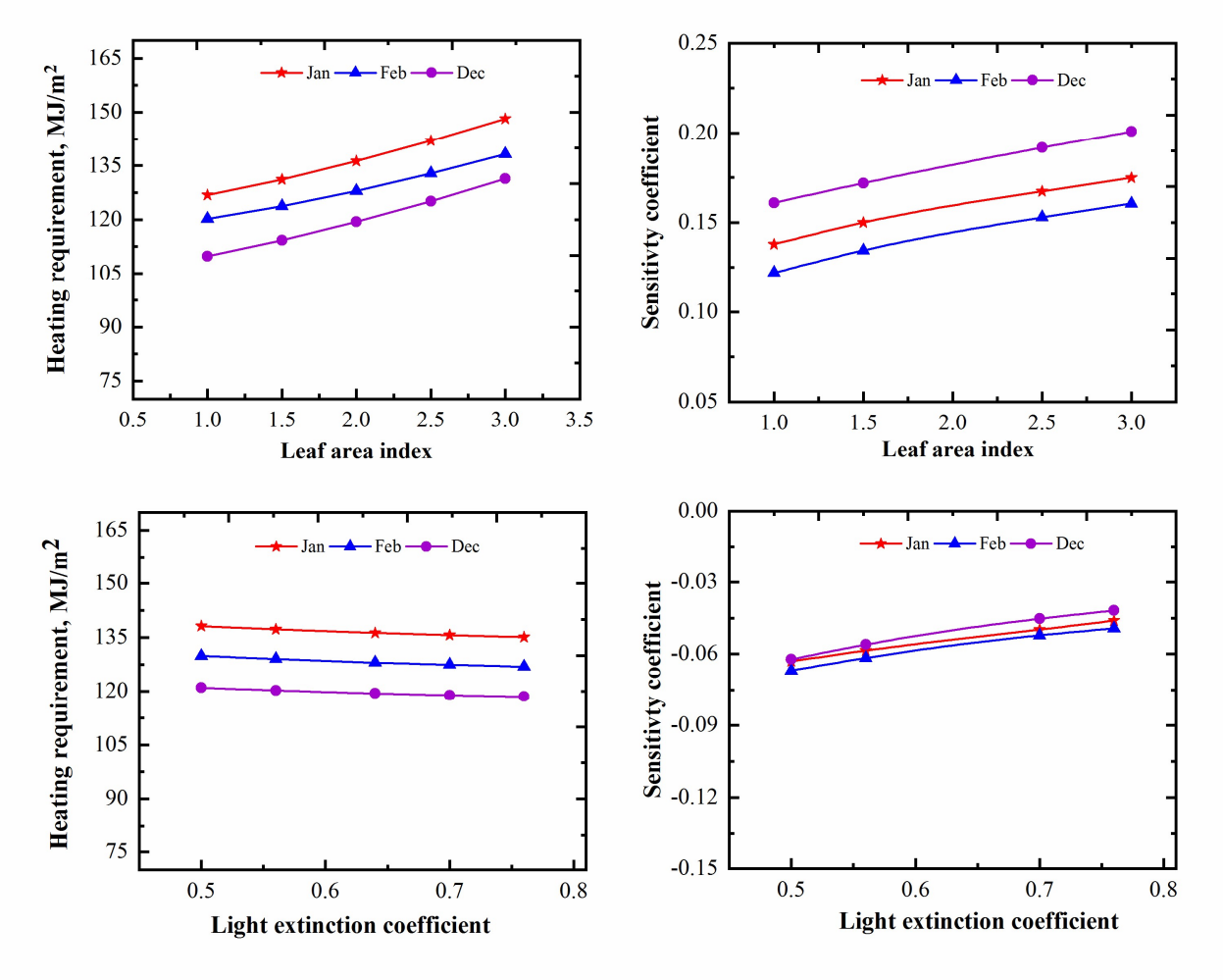

Figure 8.8: The sensitivity of the leaf area index and the canopy light extinction coefficient.

8.3.4 Sensitivity of indoor climatic parameters

The indoor environment parameters including set-point temperature, relative humidity (RH), air velocity, supplemental lighting, and CO_2 supply rate, were considered for the sensitivity study. The optimum daytime temperature for tomato should be maintained between 21-27˚C and 16-18˚C for the night (Buschermohle and Grandle, 2002). The sensitivity of indoor temperatures on the heating requirement was evaluated by selecting the daytime temperature between 19-23˚C, and the night-time temperature between 16-20˚C, and the result is shown in Figure 8.9. The result indicates the change of daytime set-point temperature from 19 to 23˚C increased the heating demand by 13-20%, whereas the heating demand increased by 9-18% for increasing the night-time temperature from 16 to 20˚C.

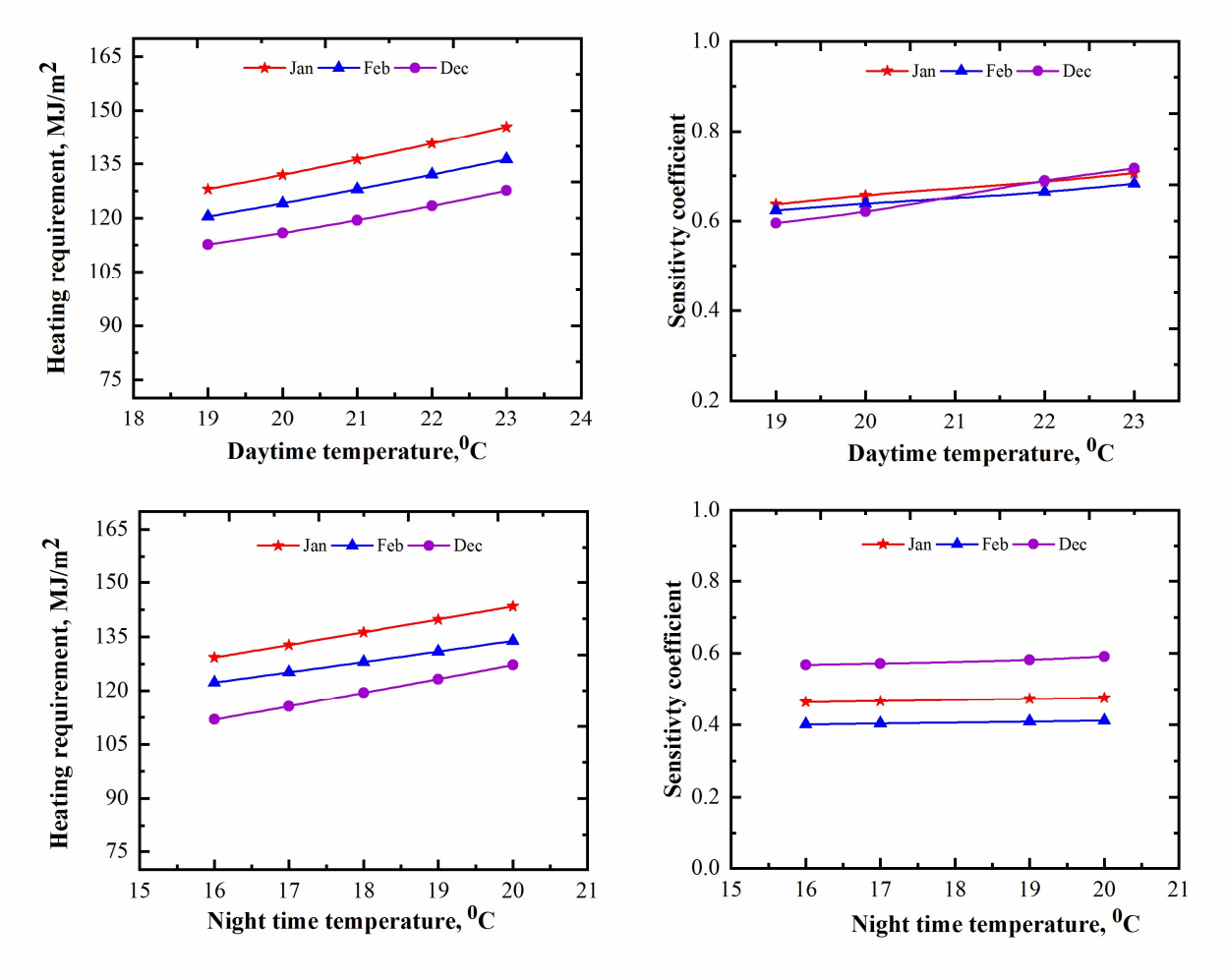

Figure 8.9: The sensitivity of the indoor set-point temperature (daytime and night-time).

The relative humidity of 60-75% could be optimal for pollination, fruit set, and development of most greenhouse crops (Bakker, 1991; Snyder, 1992). However, the relative humidity in the fully closed greenhouses could be 90-100% during the winter season when the ventilation is low, and the sensitivity of the indoor relative humidity was conducted between 70-90%. The indoor air velocity more than 1.0 ms^{-1} around the leaf restricts the plant growth (ASABE, 2006), and some authors recommended that air velocity in greenhouses should be about 0.2-0.7 ms^{-1} (Castilla, 2013; Hanan, 1998b). For the sensitivity analysis, the indoor air velocity was chosen between 0.2-0.6 m s^{-1}. Figure 8.10 shows the sensitivity of the heating requirement with the change of the indoor relative humidity and air velocity. The heating demand decreased with the increase of indoor relative humidity as the high relative humidity slows down the plant evapotranspiration rate in the greenhouse, so the heat used in plant transpiration could be reduced. The heating demand reduced

up to 18-20% for increasing the indoor relative humidity from 70 to 90%. However, the relative humidity over 85% could provide a favorable environment for fungal pathogens and plant disease because the water transfer through the stomata is slowly lost to the air (Wollaeger, 2015). Therefore, maintaining high relative humidity in the greenhouse could reduce heating demand but would increase the fungal disease in greenhouses. The high RH also would result in condensation on cover and plants, leading to plant disease, so high RH must be prevented. The indoor air velocity has a relatively low impact on the heating requirement because in CSGHEAT model, the change of indoor air velocity is only related to the heat lost by plant transpiration. The impact of indoor air velocity on heat loss through the building envelope and on condensation formation on the south cover was not considered. The increased air velocity enhances the heating demand because the high air velocity reduces the leaf aerodynamic resistance to the transpiration. So, the heating demand increased by about 6.0% for increasing the air velocity from 0.2 to 0.6 m s^{-1}.

For the conventional greenhouses, the recommended illumination level for vegetable production ranges between 10-24 W m^{-2} PAR (Hanan, 1998b). The high-pressure sodium (HPS) lamp of the installed power of 50 W m^{-2} can provide useful PAR (Photosynthetically active radiation) level of 10 W m^{-2} (Urban, 1997). However, CSGs typically use no supplemental lighting in northern China (James, 2013), but the supplemental lighting might require for offsetting the seasonally limited solar radiation in northern climates (Gomez and Mitchell, 2013). Therefore, the installed power of supplemental lighting between 10-30 W m^{-2} was considered for the sensitivity analysis. The recommended CO_2 concentration in greenhouses varies with crop species, light intensity (PAR), leaf temperature, stage of crop development, as well as economic reasons such as the price of CO_2 and benefit of its use (Castilla, 2013). The CO_2 concentration of 1000 ppm is usually considered a suitable benchmark for most greenhouse vegetables (Hanan, 1998b). The CO_2 supply rate of 4.5 gm^{-2} h^{-1} is recommended for maintaining the concentration level of 1,000 ppm (Van Berkel and Verveer, 1984). Hence, the sensitivity of CO_2 supply rate range between 3.9-5.1 gm^{-2} h^{-1} was considered for the study. Figure 8.11 shows the sensitivity of the heating requirement to the installed power of supplemental lighting and the CO_2 supply rate. The heating demand decreased significantly with the increase of installed power of supplemental lighting, but not very high for changing the supply rate of CO_2. The sensitivity coefficient of the supplemental lighting and the CO_2 supply rate is relatively stable for the change around the base case. The result indicates the heating demand decreased by 6-10% for changing the lighting power from 10 to 30 W m^{-2}, and a

relatively small change (2.5%) of heating demand was found for the change of CO_2 supply rate from 3.9 to 5.1 gm^{-2} h^{-1}. The result shows that the supplemental lighting from HPS and the CO_2 generation from fossil fuel combustion could reduce the heating requirement, but greenhouse growers need to make the decision based on the capital and operation costs for these systems and also plants response to these systems. The sensitivity coefficient is mostly stable which also indicates these parameters has a linear relation with the model output.

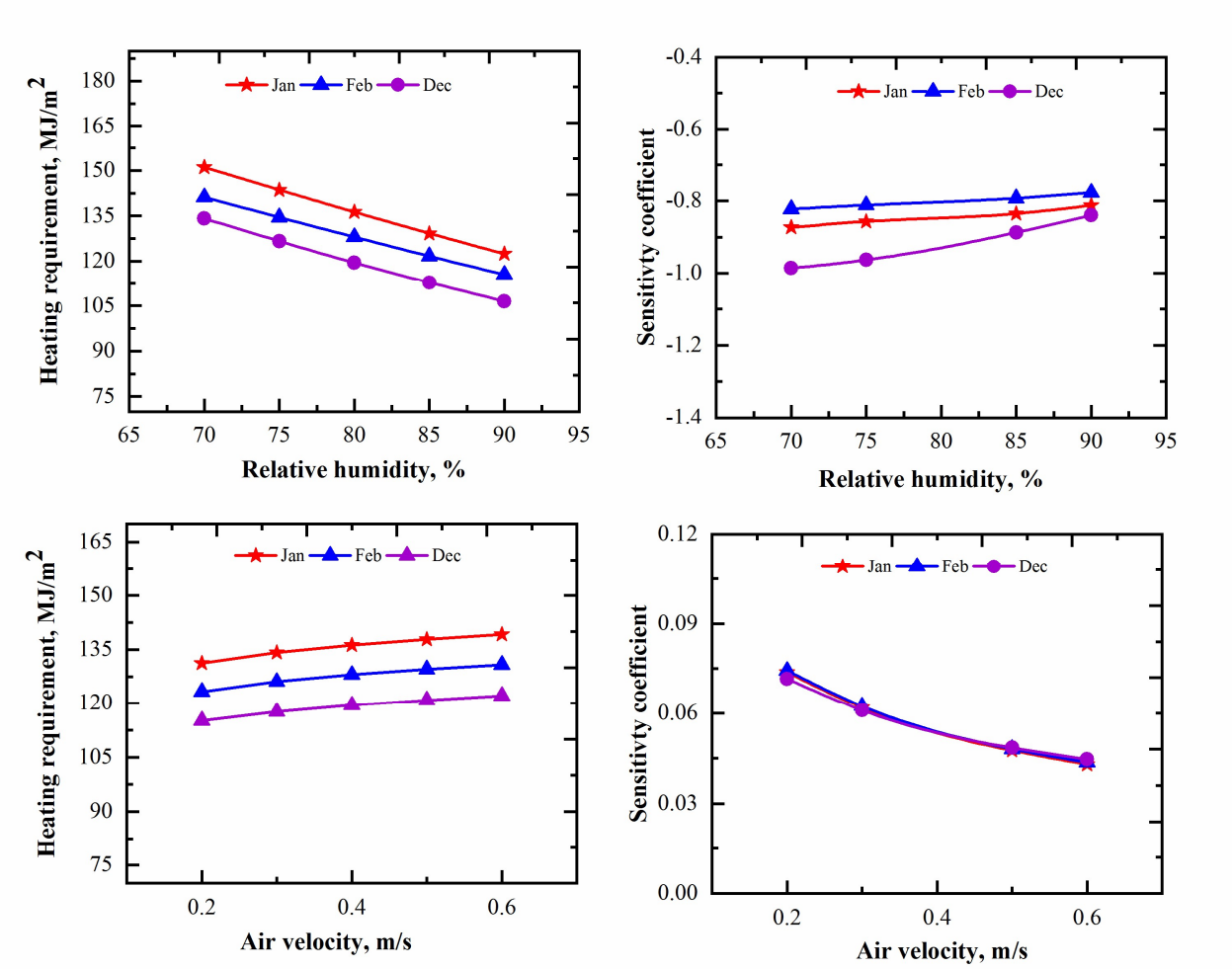

Figure 8.10. The sensitivity of the indoor relative humidity and the air velocity on the heating requirement.

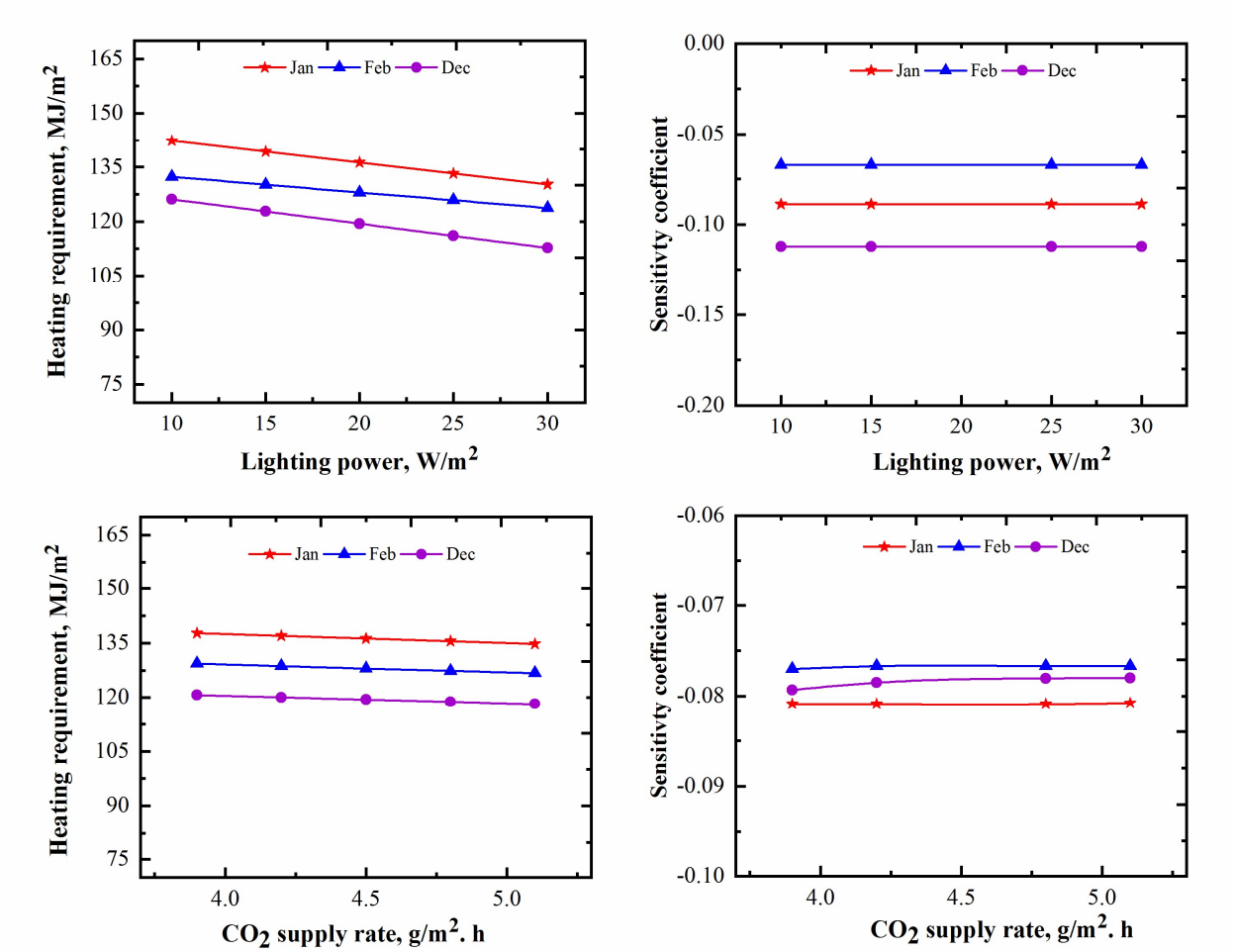

Figure 8.11: The sensitivity of the installed power of supplemental lighting and the CO_2 supply rate on the heating requirement.

8.3.5 Summarizing discussion of sensitivity analysis

The sensitivity analysis of greenhouse thermal simulation models is an essential component for the evaluation exercise of any model before using the model for engineering purposes including the design of appropriate heating systems, estimation of heating requirements, and energy-efficient design of envelope and environmental control systems in greenhouses. The sensitivity analysis indicates most of the default parameters used for model development are not very sensitive to the heating requirement except the air thermal conductance of the double-layered greenhouse cover. The sensitivity of greenhouse structural design parameters including the thermal properties greenhouse cover and thermal blanket, thermal properties of the materials used in the north wall, and perimeter heat loss factors would be useful for the understanding of the energy-efficient design

of the CSGs at higher northern latitudes. The results indicate that the thermal properties of the transparent cover and the thermal blanket are the most important design parameters for making the CSG more energy-efficient under cold climates. The plant characteristic especially the input of leaf area index (LAI) has a significant effect on the heating requirement, so the input value of LAI should be chosen with utmost care for simulation of the heating requirement. The indoor environment parameters including set-point temperature and RH in CSGs are usually not very well controlled like a modern conventional commercial greenhouse in Canada. The sensitivity analysis indicates the automatic control of indoor environmental parameters especially indoor temperature and RH could make the greenhouse more energy-efficient under very cold climates.

8.4 Conclusions and recommendations

In this study, the sensitivity of the heating simulation model (CSGHEAT) was conducted to evaluate the performance of the model for different values of the selected default parameters and also the sensitivity of design parameters and environmental control parameters on the heating requirement. The results indicate that the value used for default parameters in model development is reasonably acceptable. The sensitivity analysis also indicates the design parameters including the thermal properties of cover, thermal blanket, and parameter insulation are the most important structural design parameters to reduce the heating requirement in the CSGs. The heating requirement could be increased up to 41% for changing the thermal conductivity of the blanket from 0.01 to 0.05 Wm^{-1} K^{-1}, and the heating demand could be reduced up to 36% by using the cover with a low transmissivity (0.02) to the long-wave radiation as compared cover with high transmissivity (0.4). Also, the environmental parameters including indoor set-point temperature and relative humidity have a high impact on the greenhouse heating requirement. The heating demand could be reduced by about 20% for increasing the RH from 70 to 90%. However, the greenhouse RH above 90% could enhance the fungal disease in greenhouses.

Based on the sensitivity analysis, it could be concluded the predicted heating requirement from the model could be reasonably acceptable. The results from the sensitivity analysis of design parameters and environment control parameters would be useful for design and operation of the CSGs at high northern latitudes.

Acknowledgement

The authors are highly thankful to the College of Graduate and Postdoctoral Studies (CGPS) at the University of Saskatchewan, and the Innovation Saskatchewan for their financial support to the research.

CHAPTER 9

MODELING OF HEATING DEMAND IN THE CHINESE-STYLE SOLAR GREENHOUSE USING TRANSIENT BUILDING ENERGY SIMULATION MODEL TRNSYS

(The manuscript presented in this chapter is ready for submission to the Journal)

Overview

Building simulation tools (TRNSYS and EnergyPlus) were used in a couple of studies for simulation of greenhouse thermal environment. This chapter includes the comparative performance of CSGHEAT model and TRNSYS software for simulation of the heating requirement in a typical Chinese-style solar greenhouse. The results presented in this chapter fulfill the sixth objective of this thesis (i.e., to compare the performance of CSGHEAT model with building simulation software "TRANSYS). This manuscript also reported the major challenges and limitations of TRNSYS for simulation of greenhouse microclimates. As the lead author of this manuscript, I conducted the research and prepared the manuscript for submission to the journal. The co-authors (Professor Huiqing Guo, and Professor Karen Tanino) have contributed to this manuscript through providing technical guidance to conduct the research and constructive review to improve the quality of research.

Abstract

Building simulation program TRNSYS is user-friendly and widely used for transient simulation of thermal systems of commercial and residential buildings. A few researchers have attempted using TRNSYS for simulation of greenhouse microclimates. In this study, the performance of TRNSYS for simulation of transient heating requirement in a Chinese-style solar greenhouse was compared with a greenhouse heating simulation model CSGHEAT. The major limitations of using TRNSYS in greenhouses were identified. The results showed that the difference in the heating simulation was less than 5.0% when some specific features of greenhouse operation such thermal blanket and plants were excluded in the simulation. However, the difference was larger when the operation of thermal blanket and plants were considered in simulation. Also, the use of TRNSYS for greenhouse modeling requires very sophisticated knowledge on TRNSYS. Thus, the building simulation tool (TRNSYS) is not suitable and practical for modeling of the actual greenhouse thermal environment, in which a high error in the simulation could occur.

9.1 Introduction

Energy use in the agricultural industry is relatively small as compared to the total energy use in many countries such as only 8.1% of total energy use in the Netherland represents the agricultural sectors (Vadiee and Martin, 2013). However, for increased yield and controlled growth under very cold climates, the greenhouse industry is one of the most energy demanding sectors in the agricultural industry (Vadiee, 2011). Heating costs for greenhouse production in northern regions could be more than 75% of thermal energy consumption in agriculture (Schepens et al., 1987). Different energy saving techniques have been used to reduce the heating requirement in the conventional greenhouses, but the heating energy still represents 70-80% of the total energy consumption in a typical conventional-style greenhouses in northern latitudes (Sanford, 2011). Conversely, the Chinese-style Solar Greenhouses (CSGs) are used to grow vegetables in northern China without additional heating during the coldest three months (monthly average temperature falls below -10˚C) of the year (Tong et al., 2013). As shown in Figure 9.1, CSG is characterized by a thick wall at the north, east and west sides and a transparent south facing curved roof (de Zwart, 2016). CSGs are mostly used for growing winter horticultural crops in China, and also being adopted by many countries including Japan, Korea, Russia, and Canada.

Several thermal models (Du et al., 2012; Guo et al., 1994; Ma et al., 2010; Meng et al., 2009; Tong et al., 2008) have been developed for simulation of indoor microclimate and analysis of energy management in CSGs. Tong et al. (2008) used Computational Fluids Dynamics (CFD) model for simulation of temperature variations in different sections of a greenhouse in Shenyang, China. Deiana et al. (2014) investigated the influence of different building materials on the indoor temperature of the same CSG in Shenyang using dynamic building energy simulation program EnergyPlus. Yu et al. (2016) developed a temperature prediction model based on the least squares support vector machine (LSSVM) model. Most of the previous studies focused on the simulation of indoor microclimate including the fluctuation of temperature and relative humidity in the greenhouse. However, a significant amount of auxiliary heating is required for year-round production at higher northern latitudes including Canadian Prairies (Beshada et al., 2006). Ahamed et al. (2018b) developed and validated a thermal model CSGHEAT for simulation of supplemental heating demand of the Chinese-style solar greenhouses. Also, different types of building energy simulation programs such as TRNSYS, EnergyPlus, and RETScreen have been used for simulation of greenhouse microclimates. TRNSYS is a versatile energy simulation tool for simple or complex

systems as well as complete energy analysis of single or multi-zone buildings. It is widely used to evaluate energy load of commercial and residential buildings by many researchers (Al-ajmi and Hanby, 2008; Rahman et al., 2010; Tzivanidis et al., 2011). Greenhouses also consist of a dynamic heat and mass transfer process like commercial and residential buildings. However, the heat and mass transfer process involved in greenhouses is very different because of the use of many different techniques for maintaining the optimum indoor microclimates, and the process of plant photosynthesis and transpiration, which significantly affect the heat and mass transfer process in greenhouses. A few studies (Ha et al., 2015; Henshaw, 2016; Semple et al., 2017, 2016; Vadiee and Martin, 2013) used TRNSYS for simulation of microclimate and energy load of different types of conventional greenhouses, while little has been done on CSGs. Most of the previous studies for greenhouse energy simulation using TRNSYS have been performed for different types of conventional greenhouses. Therefore, the objective of the study is to model the heating requirement in a typical CSG using TRNSYS, compare the performance of TRNSYS model with a greenhouse heating simulation model (CSGHEAT), and analyze the major challenges of using TRNSYS for modeling of greenhouse microclimate.

9.2 Materials and method

9.2.1 Description CSG model using TRNSYS

A heating simulation model for the CSG was developed using transient system simulation software program TRNSYS (Solar Energy Laboratory, 2014a). TRNSYS simulation model consists of many components including weather data component, solar radiation component, a multizone building component, and control systems. A schematic layout of the developed model is presented in Figure 9.2. The weather data component TYPE 15-5 (Canadian weather for energy calculation) was used to input the typical meteorological year (TMY) data of Saskatoon (52.13˚N, 106.62˚W), Canada (Government of Canada, 2017). The global solar radiation incident on the south roof is calculated for each time step by internal modules based on the location, orientation, and geometry of the greenhouse.

A typical Chinese-style solar greenhouse is shown in Figure 9.1. The greenhouse had a floor area of 210 m^2 (30 m × 7 m), 3.5 m height at the ridge. The south roof of the greenhouse was considered to be glass-covered, and all the other three walls and north roof were non-transparent. The referenced greenhouse was modeled by a multi-zone subroutine component TYPE 56, which is

normally coupled to a weather data file for simulation of building heating and cooling loads. The information about the greenhouse including physical and thermal properties was defined by utilizing the TRNSYS sub-program called TRNBuild. The detailed description of the materials used for modeling of walls, roofs, and floor are listed in Table 9.1.

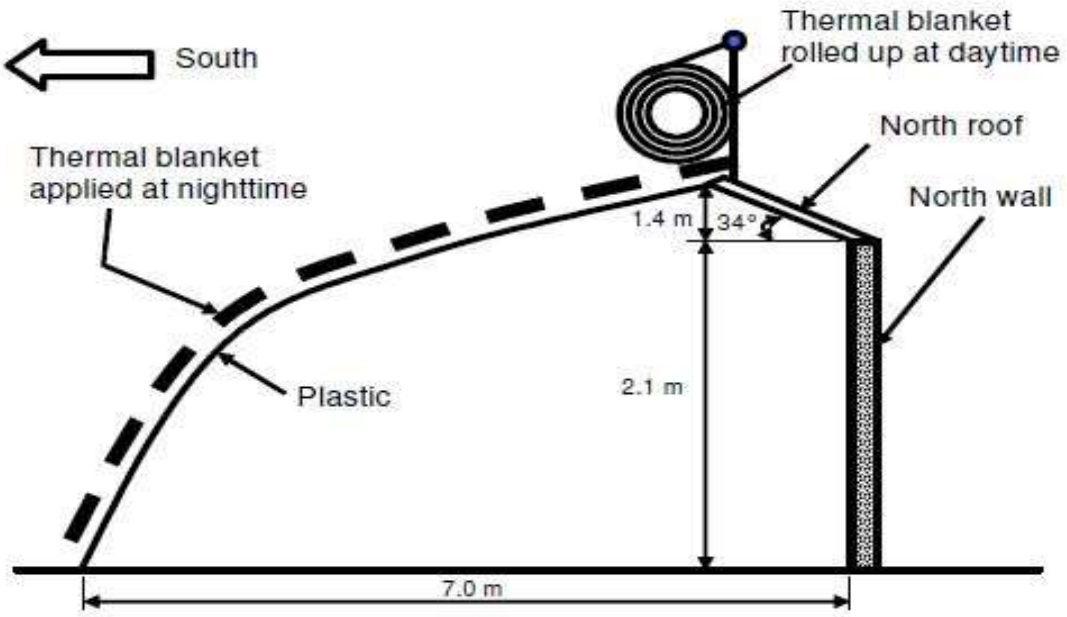

Figure 9.1: Side view of a typical Chinese-style solar greenhouse (Beshada et al., 2006).

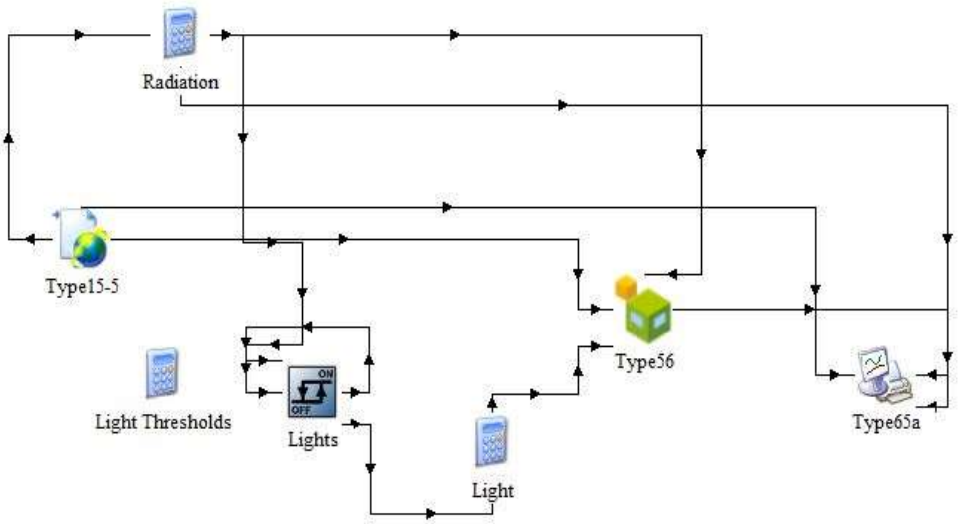

Figure 9.2: Components of TRNSYS heating simulation model of the Chinese-style solar greenhouse.

It was assumed that the south roof covered by 98% of the window for the daytime, which is considered to be only single layered glass cover material, and the heat transfer coefficient was assumed 5.68 W m^{-2} K^{-1}. The heat transfer coefficient would not be constant as it is calculated by the TYPE 56 component at each time step based on the outside climate parameters and interior conditions (Solar Energy Laboratory, 2014b). The thermal blanket of the CSG is usually operated based on the availability of solar radiation, but TRNSYS has limitation to model the operation of the thermal blanket, so the thermal blanket was considered as external shading device which covered the south roof only for the night time, and the additional thermal resistance was assumed to be 0.37 h.m^2 K kJ^{-1}. The operation of the thermal blanket was modeled based on a schedule type manager of TRNBuild.

Table 9.1: Physical and thermal properties of building materials used in modeling of the CSG using TRNSYS.

Surfaces	Materials	Thermal Properties
South roof	Single layer glass (0.04 m)	U = 5.86 W m^{-2}.K g-value = 0.85 Convection coefficient = 11 kJ h^{-1} m^{-2} K^{-1} (inside), 64 kJ h^{-1} m^{-2} K^{-1} (outside)
North roof and end walls	Plywood (0.013 m), extruded polystyrene insulation (0.065 m), and plastic sheet (from outside to inside).	U= 0.25 W m^{-2}.K Longwave emission coefficient = 0.9 Convection coefficient = 11 kJ h^{-1} m^{-2} K^{-1} (inside), 64 kJ h^{-1} m^{-2} K^{-1} (outside)
North wall	Galvanized steel (0.002 m), sand (0.152 m), extruded polystyrene insulation (0.065 m), plywood (0.013 m), and steel (0.002 m) (from outside to inside).	U= 0.23 W m^{-2}.K Solar absorptance = 0.8 Longwave emission coefficient = 0.9 Convection coefficient = 11 kJ h^{-1} m^{-2} K^{-1} (inside), 64 kJ h^{-1} m^{-2} K^{-1} (outside)
Floor	Plaster/Clay (0.1 m)	U= 2.61 W m^{-2}.K Solar absorptance = 0.8 Longwave emission coefficient = 0.9 Convection coefficient = 4.5 kJ h^{-1} m^{-2} K^{-1}

The sensible energy flux of the air node of inside air can be described as follows (Solar Energy Laboratory, 2014b) :

$$Q_{sens,i} = Q_{surf,i} + Q_{inf,i} + Q_{ven,i} + Q_{g,c,i} + Q_{cplg,i} + Q_{solair,i} \quad (9.1)$$

where, $Q_{sens,i}$ is the sensible energy flux of the zone; $Q_{surf,i}$ is the convective gain from surfaces; $Q_{inf,i}$ is the infiltration gain; $Q_{ven,i}$ is the ventilation gain; $Q_{g,c,i}$ is the internal convective gain (people, equipment, illumination, radiators, etc.); $Q_{cplg,i}$ is the gain from coupling air flow from adjacent zones; and $Q_{solair,i}$ is the fraction of solar radiation entering an air node through external windows.

The thermal capacitance of the zone needs to be simulated in the presence of plants. The crop density in the greenhouse could be significantly different from planting time to the maturity level. However, considering the change of thermal capacitance throughout the year was not possible, so a constant crop density of 6.0 kg m^{-2} was considered and thermal properties of crops were assumed to be similar as water (Semple et al., 2017).

The latent energy flux of the air node can be given as (Solar Energy Laboratory, 2014b):

$$Q_{lat,i} = h_v[m_{inf,i}(w_a - w_{req,i}) + m_{ven,i}(w_{vent} - w_{req,i}) + W_{g,i} + \sum_{i-j}^{surfaces} m_{cplg}(w_j - w_i) - M_{eff}\left(\frac{w_{req,i} - w_{i,t-\Delta t}}{\Delta t}\right)] \quad (9.2)$$

where, $Q_{lat,i}$ is the latent energy flux of the zone (kJ h^{-1}); h_v is latent heat of water vaporization (kJ kg^{-1}); m is the air mass flow rate (kg m^{-3}); w is the humidity ratio (kg_{water}/kg_{air}); $W_{g,i}$ is the internal humidity gain (kg_{water} h^{-1}); M_{eff} is the effective moisture capacitance of zone (kg); Δt is the length of time step, (subscripts, a = ambient, vent = ventilation, inf = infiltration, req = required, cplg = coupling).

Evapotranspiration (ET) including evaporation and transpiration in greenhouses plays a significant role in the energy balance of greenhouse microclimates. Evaporation and transpiration occur simultaneously, and it is very complicated to distinguish between these two processes; therefore, they are always combined as evapotranspiration. The moisture production through evaporation and transpiration in greenhouses depends on several factors including solar radiation, vapor pressure deficit, air velocity, types of plants, and inter-cultural practices used in greenhouses. Among these factors, the solar radiation has a strong correlation with the moisture production in greenhouses, and evaporation from the growing media is very small compared to crop transpiration during daytime (Katsoulas and Kittas, 2011). However, it is not possible to model the actual transient scenario of moisture production in greenhouses using TRNSYS. Therefore, evapotranspiration in greenhouses was modeled by adding an internal humidity gain with a schedule type manager.

9.2.2 CSGHEAT model

CSGHEAT model was developed based on the heat balance of the greenhouse air (Ahamed et al., 2018b). The general heat balance equation of the developed model is given by:

$$Q_h = \text{Sources} - \text{Sinks} = (Q_s + Q_{s-i} + Q_{nw-i} + Q_{ec}) - (Q_{loss} + Q_i + Q_e) \quad (9.3)$$

where Q_h is the supplemental heating demand; Q_s is the net solar heat gain; Q_{s-i} is the heat transfer between the ground and the indoor greenhouse components; Q_{nw-i} is the heat transfer between the north wall and the indoor greenhouse components; Q_{ec} is the heat addition from environmental control systems including supplement lighting (Q_{sl}), carbon dioxide supply system (Q_{CO2}), and air circulation system (Q_m); Q_{loss} is the transmission heat loss through greenhouse envelope including conduction and convection loss (Q_t), perimeter loss (Q_p), and long-wave radiation loss (Q_r); Q_i is

the heat transfer caused by air exchange through infiltration as no active ventilation usually provide during heating mode; Q_r is the heat transfer caused by exchanging of long-wave radiation through the transparent cover; and Q_e is the heat transfer in the process of plant evapotranspiration.

CSGHEAT model could simulate the hourly heating requirement in a CSG based on the input information of indoor microclimates (temperature, relative humidity, air velocity, and lighting capacity) and plants, and weather data (temperature, relative humidity, wind speed, cloud cover), and the physical and thermal properties of the greenhouse building materials. As like TRNSYS model, a similar physical and thermal properties of building materials and typical meteorological year data of Saskatoon were used for heating simulation with CSGHEAT.

9.2.3 Simulation of heating requirement

The study greenhouse was located in Saskatoon (49.9˚N, 97.75˚W). The heating set-point temperatures for the day and night were considered as 21°C and 18°C, respectively, and the optimum relative humidity was considered at 80%. The cooling mode was set at 23˚C of indoor temperature, and dehumidification mode was considered to be effective at 81% of indoor RH. The indoor air velocity was assumed at 0.1 m s^{-1} and the infiltration rate was considered at 0.5 air changes per hour (ACH) (Castilla, 2013; Xu et al., 2013). CSG usually closed all vents during the heating mode, so only infiltration was considered but no active ventilation was considered for heating simulation. The supplemental lighting was considered at 30 W m^{-2}, which would be turned on when solar radiation would reach below 250 W m^{-2}, and the lighting was considered to be turned off from 10:00 pm to 6:00 am, thereby 16 h of photoperiod was maintained in the greenhouse. The CO_2 supply to the greenhouse could contribute to the heating of the greenhouse when CO_2 is produced by combustion of fossil fuel, quite often natural gas. The heat gain from the CO_2 generator was simulated based on the CO_2 supply rate 4.5 g m^{-2} h^{-1} and the CO_2 production rate 2.7 kg per kg of fuel, and the net heating value of natural gas was considered at 38.0 MJ m^{-3} of gas (ASHRAE, 2013; Castilla, 2013). The CO_2 generator was considered in operation for daytime from 6:00 am to 7:00 pm for TRNSYS, whereas the schedule for the CO_2 generator in CSGHEAT is based on the availability of solar radiation. The air circulation system was considered in operation for the entire simulation period. The greenhouse simulation was performed over one-year period beginning 1st hour of the year with one hour of equal time-step.

9.3 Results and discussion

The monthly average ambient air temperature and monthly average solar radiation on a horizontal surface are shown in Figure 9.3. Typical meteorological year data set represents the typical conditions based on ten years of data from 1998 to 2013. The analysis of dataset indicates that the lowest monthly lowest average temperature (-15.5˚C) in Saskatoon was recorded in January, whereas the lowest monthly average solar radiation (36 W m^{-2}) occurred in December. The highest monthly average temperature (18.6˚C) was found in July, but the maximum monthly average solar radiation (260 W m^{-2}) was recorded in June.

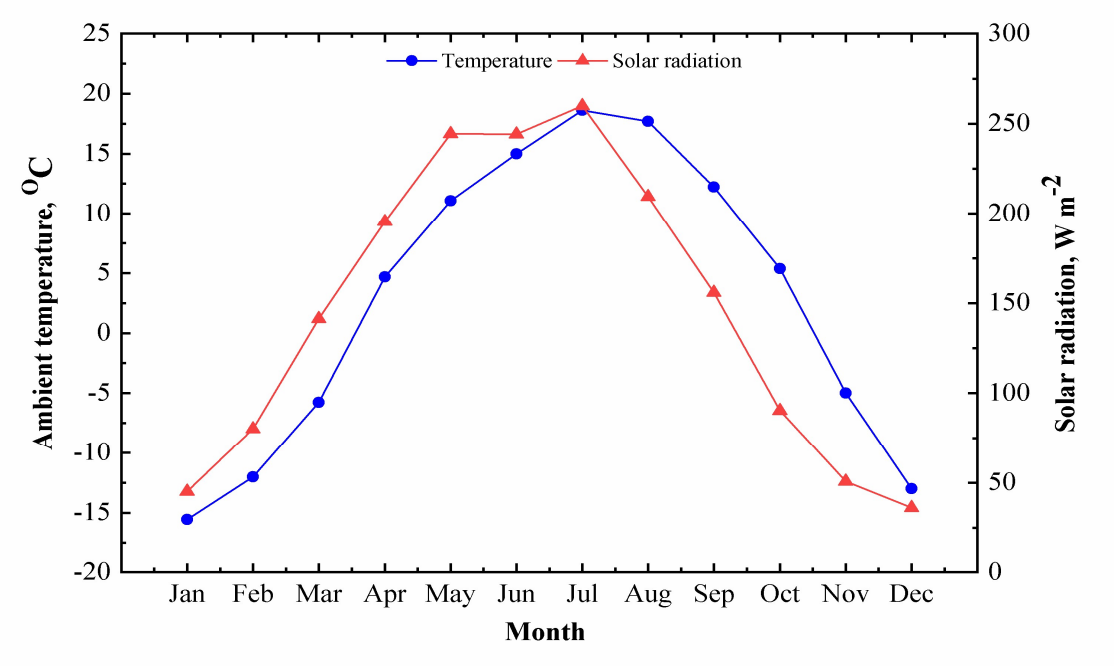

Figure 9.3: Monthly average ambient temperature and solar radiation on the horizontal surface in Saskatoon.

9.3.1 Comparative performance of TRNSYS and CSGHEAT model

Similar physical and thermal properties of greenhouse envelopes and operating conditions were considered for simulation except for the operating schedule of environmental control systems such as the schedule of the CO_2 supply system and the thermal blanket. In CSGHEAT, the schedule for environmental control systems is based on the availability of solar radiation instead of the schedule type manager used in the TRNSYS model. Different scenarios were considered to compare the

performance of these two selected models for estimation of the heating requirement in the study greenhouse.

Figure 9.4 shows the comparison of the simulated monthly average daily total heating requirement in the study greenhouse from TRNSYS and CSGHEAT. The heating requirement was simulated without considering the effect of thermal blanket and evapotranspiration in the greenhouse as TRNSYS has limitation to model the actual scenario of these two aspects of greenhouse operation. The annual total heating requirement from the TRNSYS and CSGHEAT model is 1489 W m^{-2} and 1516 W m^{-2}, respectively. The simulated heating requirement from the CSGHEAT is usually higher than the heating demand from the TRNSYS model. If the results for the summer months (June, July, and August) were excluded from the analysis because of low heating requirement, then the maximum difference in the heating simulation is found in October (15.1%), and 5.03% is the average difference.

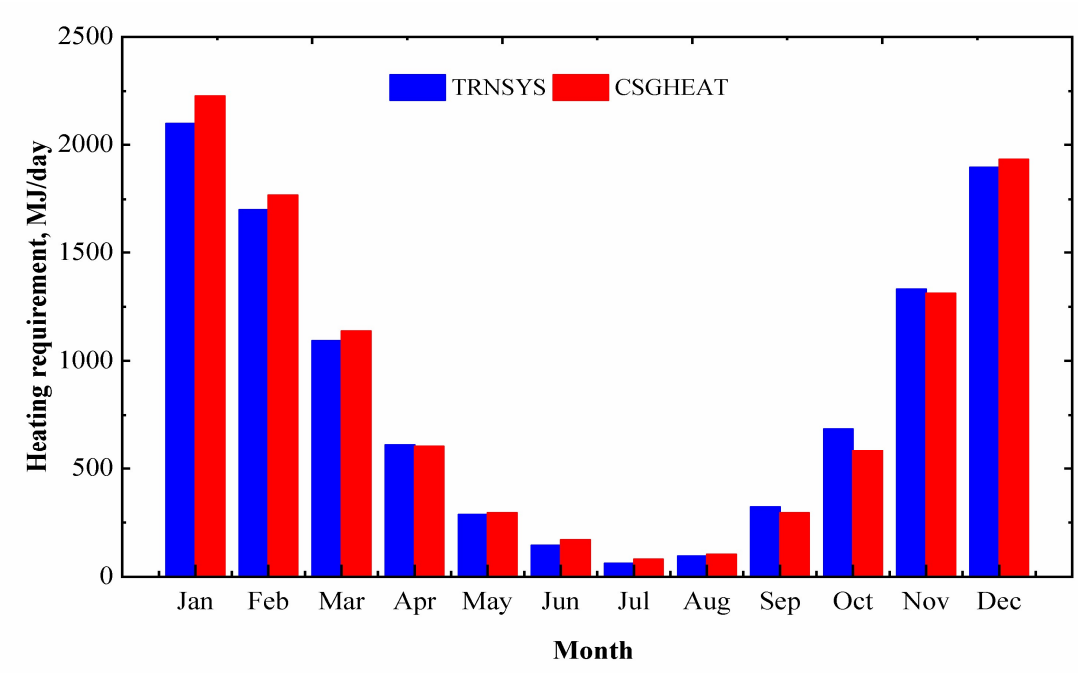

Figure 9.4: Monthly average daily heating requirement in the study greenhouse as predicted by TRNSYS and CSGHEAT without thermal blanket and plants.

Thermal screens/blankets are usually used in greenhouses to reduce the radiative and conductive heat loss at night. For a commercial building, the shading feature is opposite to the deployment logic of night covers for greenhouses. This shading feature for the building is designed to close the shades when the total radiation on the window exceeds a certain value, and open them when the radiation is less than another (lower) value. Therefore, a schedule was created to open and close the thermal blanket of the CSG, such that the south roof was insulated with the thermal blanket from 6:00 pm to 7:00 am, and open otherwise. However, the actual operation of thermal blanket could not be modeled using schedule type manager as TRNBuild has limitation to set up the actual scenario. Figure 9.5 showed a comparison of the simulated heating requirement from these models when the thermal blanket was considered for greenhouse operation. The simulated result from the CSGHEAT indicates the use of thermal blanket could reduce the annual heating requirement by 60%, whereas about 61.5% based on the simulated result from the TRNSYS model. In general, the simulated heating requirement from the CSGHEAT model during the coldest four months is found lower than the value from the TRNSYS model since the CSGHEAT considers the operation of thermal blanket based on the availability of solar radiation. For the winter months (December-February), the solar radiation is usually available at around 9:00 am, but in TRNSYS model the thermal blanket was considered to open after 7:00 am. Conversely, the opposite trend was found for the rest of the period since the thermal blanket in TRANSYS model was in operation for a couple of hours after sunrise. The results indicate a significant error can be caused in heating simulation if the operation schedule of thermal blanket does not represent the actual scenario of the CSG.

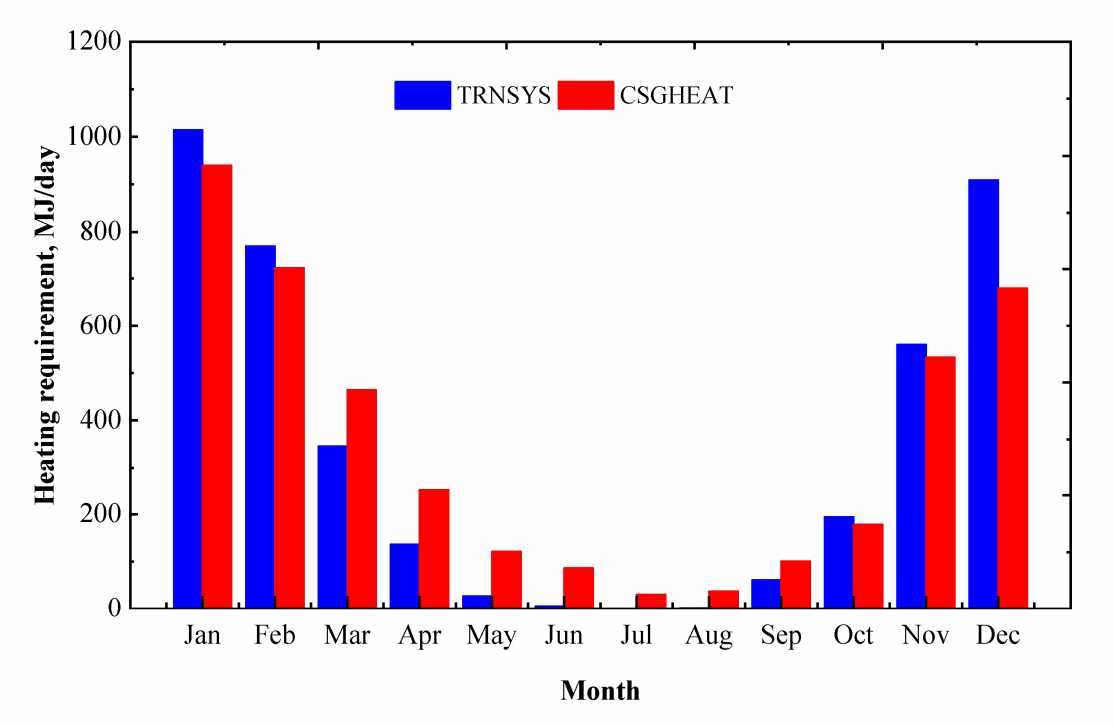

Figure 9.5: Monthly average daily heating requirement in the reference greenhouse as predicted by TRNSYS and CSGHEAT with consideration of the thermal blanket.

Another challenge in greenhouse energy simulation is the model of moisture production in greenhouses. Most of the previous studies for greenhouse simulation with TRNSYS (Ha et al., 2015; Henshaw, 2016; Vadiee and Martin, 2013) did not consider the plants in the greenhouses. Semple et al. (2017) modeled the moisture production rate by using a constant internal humidity gain in the greenhouse that does not represent actual moisture production rate in greenhouses. Plant transpiration in greenhouses depends on the aerodynamic and stomatal resistance, and the stomatal resistance mainly depends on solar radiation. The aerodynamic resistance depends on the indoor air velocity, but the air velocity is relatively low in the greenhouse without forced ventilation. Therefore, the transpiration at night is very small as compared to that during the daytime. In this study, the internal humidity gain in the greenhouse for the daytime was assumed at 21.5 grams of water/hour/m^2 whereas about 3.6 grams of water/hour/m^2 for the night time, and these values are close to the average value of moisture production rate estimated in CSGHEAT model for the winter months.

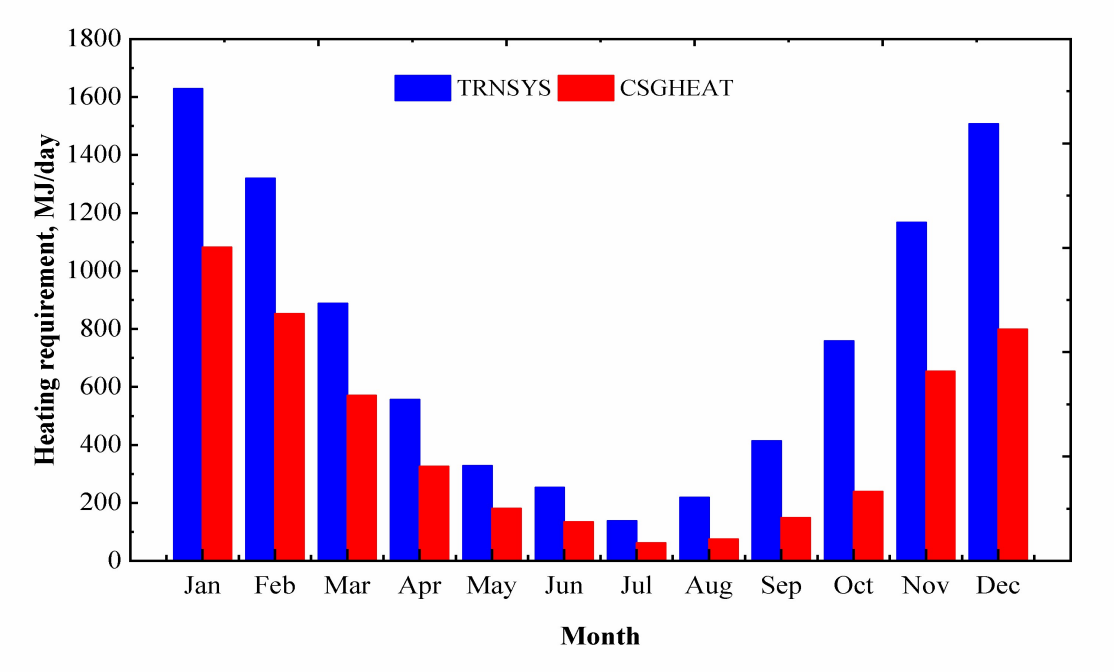

Figure 9.6: Monthly average daily heating requirement in the study greenhouse as predicted by TRNSYS and CSGHEAT with consideration of thermal blanket and evapotranspiration.

Figure 9.6 shows the simulated monthly average daily heating requirement in the greenhouse when thermal blanket and evapotranspiration were considered. The simulated monthly average daily heating requirements from the TRNSYS model are about 33-68% higher than the estimated heating requirement from the CSGHEAT model. This high difference in simulation was caused by the difference in moisture production rate because the TRNSYS model simulated the heat used for evaporation from the input value of constant internal moisture gain; however, the moisture production rate in the greenhouse mostly depends on the availability of solar radiation in greenhouses.

9.3.2 Sensitivity analysis

The sensitivity analysis was carried out to determine the relative impact of changing some parameters in TRNSYS model. The selected parameters for sensitivity analysis were identified based on the difference of some major parameters between TRNSYS and CSGHEAT. The transient change of evapotranspiration rate and infiltration rate in greenhouses is complicated to model using TRNSYS; however, the time-dependent value of these parameters is estimated in the CSGHEAT model. Therefore, the internal moisture gain and infiltration rate were considered for

the sensitivity analysis. The sensitivity analysis was performed for the coldest three months (January, February, and December) of the year.

The sensitivity coefficient is widely used for sensitivity studies in the field of mathematics and control engineering (Lam and Hui, 1996). Among different forms of sensitivity coefficients for building energy simulation, the following form is most suitable for multiple sets of data (Lam and Hui, 1996).

$$\text{Sensitivty coeffcient} = \frac{\Delta OP/OP_{base}}{\Delta IP/IP_{base}} \quad (9.4)$$

Where OP_{base} and IP_{base} are the base output and input, respectively; ΔOP and ΔIP are the variations of output and input, respectively. A high sensitivity coefficient would indicate that the model is more sensitive to the parameter and its value must be chosen very carefully (Yang et al., 2016).

Figure 9.7 shows the change of heating demand relative to the base-case condition of simulation in TRNSYS model. The result indicates the heating requirement was changed significantly for different input values of internal moisture gain and infiltration rate. The heating requirement increased up to 20.5% for increasing moisture gain from 4.5 to 5.5 kg h^{-1} (22.2% increase), whereas about 9% increase for increased infiltration rate from 0.5 to 0.8 ACH (60% increase). For the whole simulated range of 3.5 to 5.5 kg h^{-1}, the heating increased up to 53%; while 0.2 to 0.75 ACH, heating increased up to 20%. Similarly, the high values of sensitivity coefficient (SC) indicate that the internal moisture gain and ACH have high impact on the heating requirement, so a small change in input value would cause a large change in the heating requirement. Comparing these two parameters, the SC of moisture gain is much higher than that of the ACH, indicating the moisture gain has high impact on the heating requirement than the ACH. Therefore, the simulation of greenhouse heating requirement with TRNSYS could give a high error since it could not represent the actual scenario of moisture gain and infiltration rate in greenhouses.

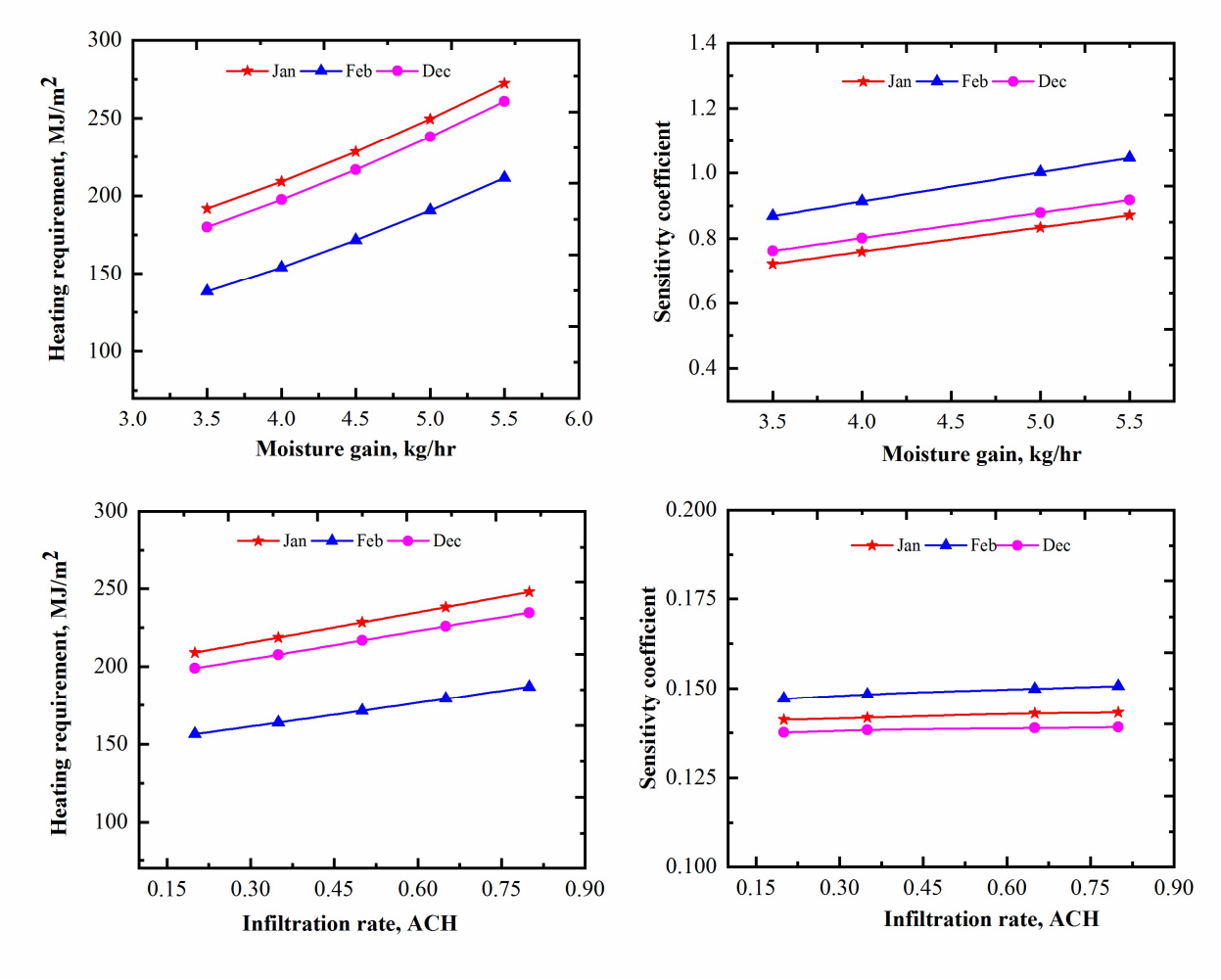

Figure 9.7: Sensitivity of the change of moisture gain and infiltration rate on the heating requirement.

9.4 Conclusions

TRNSYS simulation program is accurate, user-friendly, and widely used for transient simulation of thermal system of the commercial and residential buildings; however, the greenhouse physical parameters, transient moisture production rate, and indoor environmental control systems are quite different than usual buildings. The heating simulation results from this study indicate the difference between these two models is not significant when some specific features in greenhouses are excluded, which are unrealistic circumstances for a greenhouse in production. There are major challenges of using TRNSYS model for simulation of greenhouse heating requirements as summarized below.

1. The result indicates TRNSYS has limitation to model the actual scenario of operation of the thermal blanket, thereby, a significant error may occur in simulation of the heating requirement in greenhouses.
2. The heat used in the process of evapotranspiration is one of the major contributors to the greenhouse energy balance. The moisture production rate through evapotranspiration mainly depends on solar radiation. In TRNSYS, the energy used for evapotranspiration have to be calculated by adding an internal humidity gain, where the moisture production rate either need to input as constant or need to schedule based on data from the literature. It is difficult to simulate the year-round situation by using a schedule based on calculated evapotranspiration rate based on the actual greenhouse conditions.
3. The sensitivity analysis indicates that assumption of constant internal moisture gain, and the constant infiltration rate also can cause a significant error in heating prediction. Further, heating requirement is more sensitive to the internal moisture gain than the ACH.
4. Above all, the use of TRNSYS for greenhouse modeling needs very sophisticated knowledge about TRNSYS because most design features in greenhouses are very different than the usual building shell, the heat and moisture sources are constantly changing, ventilation rate changes greatly and is difficult to estimate as a mixed mechanical and natural ventilation is used.

Based on the results from this study, it can be concluded that the building simulation tools such as TRNSYS need very complicated modification for simulation of greenhouse thermal environment. Also, some actual scenario of greenhouse could not be represented in TRNBuid. Hence, the building simulation tool TRNSYS is not suitable for simulation of greenhouse thermal environments.

Acknowledgement

The authors are highly thankful to the College of Graduate and Postdoctoral Studies (CGPS) at the University of Saskatchewan, and the Innovation Saskatchewan for their support to provide the fund for the research.

CHAPTER 10

CONCLUDING REMARKS

10.1 Contributions

In this thesis, two mathematical models have been developed to simulate the time-dependent heating requirement in the conventional and Chinese-style solar greenhouses. The study also includes various energy saving measures in greenhouses located at high northern latitudes. The major contributions of the study are as follows:

1. This study developed a quasi-steady state thermal model and the computer program based on the developed model (GREENHEAT) using MATLAB for simulation of the heating requirement in the conventional greenhouses. GREENHEAT was developed by considering most of the heat sources and sinks in greenhouses including evapotranspiration, the heating contribution of environmental control systems including supplemental lighting, CO_2 generator, and air-circulation system, which were mostly not considered in previous studies.
2. A critical review of different heating energy saving technologies was conducted for the conventional greenhouses under cold climates. Some of the design parameters in greenhouses could be significantly different depending on the location. GREENHEAT model was used for evaluating the heating energy saving potential of greenhouse design parameters including shape, orientation, and width of span under the weather conditions of Saskatchewan. Furthermore, the study of the economic feasibility of year-round vegetable production in the conventional commercial greenhouses in northern Saskatchewan.
3. A Chinese-style solar greenhouse is significantly different than the convention greenhouse; therefore, another thermal model (CSGHEAT) was developed for simulation of the time-dependent heating requirement in the Chinese-style solar greenhouses. The sensitivity analysis was conducted to evaluate the sensitivity of CSGHEAT model for simulation of the heating requirement in a typical CSG under Canadian weather conditions. The study

4. also includes the impact of different building materials and indoor environmental control parameters on the heating requirement.
5. This study set up TRNSYS model for simulating heating requirement of the Chinese-style solar greenhouses and revealed major limitations of using building simulation tools for modeling of greenhouse thermal environment.

The results presented in this thesis also provide the detailed analysis of different heat sources and sinks in the conventional and Chinese-style solar greenhouse under cold climates. The outcomes from this study would be useful for researchers, greenhouse growers, and industry for their study and decision making about the greenhouse production in high northern latitudes. A summary of the major conclusions of each chapter which collectively address the overall thesis objectives is provided in the following section.

10.2 Summary and conclusions

The simulation of the time-dependent heating requirement in greenhouses is essential for design and optimization, and feasibility studies of greenhouse production under a particular weather condition. The estimation of time-dependent solar radiation is the important factor in the greenhouse heating simulation model. In Chapter 2, the cloud cover based solar radiation model (Kasten-Czeplak model) model has been evaluated to estimate global solar radiation on the horizontal surfaces based on the input of cloud cover data (Oktas). The results show the estimated hourly global solar radiation from the model with the locally fitted coefficients are consistent with the dataset from the NSRDB in four different locations in Western Canada.

Chapter 3 presents the development of GREENHEAT model including the detailed principle of GREENHEAT model, the analysis of various heat sources and sinks in the conventional greenhouses, and validation of the model. GREENHEAT model was developed based on the lumped estimation of heat sources and sinks in the conventional greenhouses, and the programming language MATLAB was used for computer simulation. The results show that the estimated heating requirement from GREENHEAT model is consistent (average error less than 5%) with the actual heating data from a commercial greenhouse located in Saskatoon, Canada. The results also indicate that environmental control systems including supplemental lighting, CO_2 generators, and air circulation system, have significant contributions to the greenhouse heating

requirement; however, the heating contributions from these sources were ignored in most of the previous studies.

In Chapter 4, a comprehensive review of different energy saving measures for the conventional greenhouses was performed. Previous studies show that a large number of techniques have been implemented to reduce the greenhouse heating energy cost, but the suitable energy saving techniques need to be selected based on the types of greenhouses, location, and the resources available near the greenhouses. Some features of energy-efficient greenhouse design could be different depending on the location of greenhouses. So, the parameters for studying the energy-efficient design of greenhouse for cold regions were only selected for those whose energy saving potential could be significantly different depending on the location of greenhouses.

Chapter 5 presents the selection of energy-efficient design parameters (shape, orientation, the angle of the roof, and width of span) of a large conventional greenhouse for Canadian Prairies using GREENHEAT model. The simulation results showed that the uneven span gable roof greenhouse received the highest solar radiation, but the highest heating requirement was found for the modified arch shape of greenhouses. The results indicate the gable roof greenhouses including even-span and uneven-span could be more energy-efficient for the gutter connected multi-span greenhouses, and the quonset shape for the single span greenhouses. The potential change of solar gain with east-west orientation is relatively low when the length-width ratio of greenhouses is greater than one. Also, the heating energy saving potential of the large span in a single-span greenhouse is relatively high as compared to the multi-span greenhouse.

Most of the commercial greenhouses in Canadian Prairies are usually shut-down the operation during the coldest period (December-February) in winter season due to high heating cost. Also, the heating demand could be significantly different depending on the types of crops grown in greenhouses. Using GREENHEAT model, the variation of heating demands for year-round production of different vegetables (Tomato, Cucumber, and Pepper) under Canadian Prairies weather conditions, and the economic feasibility of vegetable production in a conceptually designed greenhouse located in Saskatchewan were predicted and included in Chapter 6. The economic feasibility analysis indicates the year-round production of vegetables in a greenhouse at higher northern latitudes of Canadian Prairies could be economically profitable; however, the tomato could be more profitable than the production of cucumber and pepper.

Chinese-style solar greenhouses (CSGs) have been proved as an energy-efficient horticultural facility for crop production at high northern latitudes. So, the adaptation of the CSG could be the alternate option to reduce the heating cost for greenhouse production in cold regions. A model for simulation of the heating requirement in the CSG is essential for feasibility study in cold regions. The development of CSGHEAT model for estimation of supplemental heating demand in the Chinese-style solar greenhouses is described in Chapter 7. CSGHEAT model can simulate the hourly heating requirement in CSGs based on the input of physical and thermal properties of building materials and indoor environmental control parameters. The model was validated against three days of experimental data from a commercial CSG in Winnipeg, Canada, and the results showed that the model could predict the hourly heating requirement of a greenhouse in good agreement (8.7% average error in prediction) with the experimental data. The developed model would be a very useful tool for assisting with the energy-efficient design of CSGs in particular locations, and also to analyze additional heating requirement under very cold climates.

Chapter 8 includes the sensitivity study of different default parameters of CSGHEAT model and some input parameters on the heating requirements. The results showed that the default values used in the model could be reasonably acceptable since the heating requirement is not very sensitive to these parameters. The sensitivity study also indicated that the design parameters including the thermal properties of cover, thermal blanket, and perimeter insulation are the most important design parameters which are need to select with utmost care to reduce the heating energy consumption in the CSGs. The greenhouse heating requirement also found very sensitive to the small change of indoor environmental parameters such as indoor set-point temperature and relative humidity, so the optimum control of these parameters are important for making the CSGs more energy efficient.

In Chapter 9, the building transient simulation program TRNSYS was used to simulate the supplemental heating requirement of a CSG located in Saskatoon, Canada, and the performance of TRNSYS model was compared with CSGHEAT model to identify the major challenges and limitations of the building simulation tools for simulation of greenhouse microclimates. The results showed that modeling of greenhouse thermal environment using TRNSYS could have high error in heating estimation as the actual scenarios of some specific greenhouse features such as the dynamic change of moisture production, the actual scenario for the operation of thermal blanket and environmental control parameters, could not be represented correctly in TRNSYS software.

Based on the results presented in this thesis, it can be concluded that the developed models (GEEENHEAT and CSGHEAT) would be useful tools to simulate the time-dependent heating requirement in the conventional and Chinese-style solar greenhouses. Also, the overall the results of this thesis provide important insights about energy-efficient design of both conventional and CSG greenhouses and economic feasibility of greenhouse production in cold regions. The models would be beneficial to researchers, engineers, governments and greenhouse growers with their decision-making regarding energy-efficient design and feasibility analysis of greenhouse production in high northern latitudes.

10.3 Future works

The current study could be advanced for commercial application of the developed models for the greenhouse industry. Some potential avenues are discussed below:

1. CSGHEAT model could be used to optimize the design parameters of CSG to make the greenhouse more energy efficient based on the local climate condition at higher northern latitudes.
2. Developed models need to be improved like other commercial software for the wide-spread use of these models for simulation of heating requirement.
3. The model also could be improved to estimate the ventilation and cooling need in greenhouses.
4. CSGHEAT model was validated against the three days of experimental data from a commercial greenhouse where environmental control parameters were not well controlled. So, the validation of CSHHEAT model against the data of entire one-year from a well-controlled greenhouse would be useful for evaluating the performance of CSGHEAT model.

Appendix A

A.1 MATLAB Code for computer program of conventional greenhouse

Main model

```
clear all
close all
clc
%------------------------------Input--------------------------%
%-----------------------Input for Location--------------------%
LATD=52.09;
LON=-106.82;
LST=-90
%-------------------------Input got greenhouse---------------%
L=43.29;                % Length of span
W=6.4;                  % Width of span
NS=4;                   % Number of span
H=5.3;                  % Height up to the ridge
HS=3.65;                % Gutter height
%--------------------------Roof--------------------------------%
SRA=26;                 % Angle of south roof
SRA1=0;
SRA2=0;
ASR=155.86*NS;          % Area of south roof
ASR1=0*NS;
ASR2=0*NS;
NRAA=26;                % Angle of north roof
NRA=180-NRAA;
NRA1=180-SRA1;
NRA2=180-SRA2;
ANR=155.86*NS;          % Area of north roof
ANR1=0*NS;
ANR2=0*NS;
TSR=0.75;               % Solar transmissivity of roof
emr=0.2;                % Emissivity of roof
TLR=0.29;               % Transmissivity to the long-wave radiation
NPR=2;                  % Number of layer in roof
KR=0.33;                % Thermal conductivity of roof cover
LR=0.00152;             % Thickness of the roof cover
%-------------------------South Wall--------------------------%
HTSW=2.0;               % Height of transparent wall
HNSW=1.65;              % Height of non-transparent wall
HTASW=0;                % Height of angular wall

SWA=90;                 % Angle of wall
ASW=79.22;              % Area of transparent wall
```

```
ASW1=79.22;           % Area of non-transparent wall
ASW2=0.0;            % Area of angular wall
TSW=0.78;            % Transmissivity of wall
emsw=0.65;           % Emissivity of transparent  wall
TLSW=0.03;           % Transmissivity to the long-wave radiation
NPSW=2;              % Number of layer in transparent cover
KSW=0.2;             % Thermal conductivity of cover
LSW=0.008;           % Thickness of cover
KSWI=0.03;           % Thermal conductivity of insulation
KSWS=0.12;           % Thermal conductivity of siding material
LSWI=0.065;          % Thickness of insulation
LSWS=0.019;          % Thickness of siding material
%-----------------------North Wall-----------------------------%
HTNW=0;              % Height of transparent wall
HNNW=3.65;           % Height of non-transparent wall
HTANW=0;             % Height of angular wall
NWA=180-SWA;         % Angle of wall
ANW=L*HTNW;          % Area of transparent wall
ANW1=L*HNNW;         % Area of non-transparent wall
ANW2=L*HTANW;        % Area of angular wall
TNW=0.78;            %Solar transmissivity of wall cover
emnw=0.65;           %Emissivity of wall cover
TLNW=0.03;           %Long-wave transmissivity
NPNW=2;              %Number of layer
KNW=0.2;             %Thermal conductivity
LNW=0.008;           %Thickness
KNWI=0.03;           %Thermal conductivity of insulation
KNWS=0.12;           %Thermal conductivity of siding material
LNWI=0.065;          %Thickness of insulation
LNWS=0.019;          %Thickness of siding material
%---------------------------East wall-------------------------%
HTEW=1.2;            %Height of Transparent wall
HNEW=2.43;           %Height of non-transparent wall
EWA=90;              %Angle of wall
AEW=(W*HTEW+0.5*W*(H-HS))*NS; %Area of transparent wall
AEW1=(W*HNEW)*NS;    % Area of non-transparent wall
TEW=0.78;            % Solar transmissivity
emew=0.65;           % Emissivity
TLEW=0.03;           %Long-wave transmissivity
KEW=0.2;             %Thermal conductivity
LEW=0.008;           %Thickness of cover
NPEW=2;              % Number of layer
KEWI=0.03;          % Thermal conductivity of insulation material
KEWS=0.12;          % Thermal conductivity of siding material
LEWI=0.065;         % Thickness of insulation material
LEWS=0.019;         % Thickness of siding material
%---------------------West wall-----------------------------%
```

```
HTWW=1.2;           %Height of transparent wall
HNWW=2.43;          %Height of non-transparent wall
WWA=90;             %Angle of wall
AWW=(W*HTWW+0.5*W*(H-HS))*NS; %Area of transparent wall
AWW1=(W*HNWW)*NS;    % Area of non-transparent wall
TWW=0.78;            % Solar transmissivity
emww=0.65;           % Emissivity of wall
TLWW=0.03;           %Long-wave transmissivity
KWW=0.2;             %Thermal conductivity
LWW=0.008;           %Thickness of cover
NPWW=2;              % Number of layer
KWWI=0.03;          % Thermal conductivity of insulation material
KWWS=0.12;          % Thermal conductivity of siding material
LWWI=0.065;         % Thickness of insulation material
LWWS=0.019;         % Thickness of siding material

%----Environmental Control parameters and others input--------%
N=1.0;              %Infiltration rate (ACH)
T_id=21;            % Day time set point temperature
T_in=18;            % Night time set point temperature
RH=0.75;            % Indoor relative humidity
Vi=0.2;             % Indoor air velocity
IW=100;             % Install lighting wattage
Turn_off=22;        % lighting turn off time
Turn_on=7;          % Lighting turn on time
Pw=375;             %Motor power rating
Em=0.9;             % motor efficiency
MLF=1.0;            %Motor load factor
MUF=1.0;            % Motor use factor
NF=8;               %Number of fan
MNHV=38;            %Heating value of fuel
MFR=4.5;            %CO2 flow rate
F=0.85;             %Perimeter heat loss
Lf=0.027;           % Characteristics length of leaf
LA=2.0;             %Leaf area index
% ---------------------Outdoor weather-----------------------%
T_o=xlsread('TMY_saskatoon.xlsx','sheet1','E12:E8771');
RH_o=xlsread('TMY_saskatoon.xlsx','sheet1','G12:G8771');
V_o=xlsread('TMY_saskatoon.xlsx','sheet1','J12:J8771');
CCF=xlsread('TMY_saskatoon.xlsx','sheet1','M12:M8771');
GHI=xlsread('TMY_saskatoon.xlsx','sheet1','N12:N8771');

%------------------------Internal Calculation----------------%
WG=W*NS;          % Total Width of greenhouse
A=L*WG;           % Total Area of greenhouse
V=A*HS+0.5*W*(H-HS)*L*NS;        %Volume of greenhouse
P=2*(L+WG);                      %Perimeter of the greenhouse
```

```
ha=3.8;          %Thermal air conductance of air spaces
CLr=ASR/(2*(L+sqrt((W/2).^2+(H-HS).^2)));
Fsk=1.0;                              %Sky view factor
Fsr=(1+cosd(SRA))/2;                  %Cover view factor
TAR=(ASR+ASR1+ASR2+ANR+ANR1+ANR2);
CLnw=HTSW;            %Characteristics length
CLnwn=HNSW;           %Characteristics length
Fnw=(1+cosd(NWA))/2; %view factor

CLew=HTEW;            %Characteristics length
CLewn=HNEW;           %Characteristics length
Few=(1+cosd(EWA))/2; % view factor
CLww=HTWW;            %Characteristics length
CLwwn=HNWW;           %Characteristics length
Fww=(1+cosd(WWA))/2; % view factor
CLsw=HTSW;
CLswn=HNSW;
Fsw=(1+cosd(SWA))/2; %view factor

curtain_on=0;
curtain_off=1;

IWZ=0;                %Lighting power for no lighting
QV=(N*V)/3600;
F_sa=1.2;             % light allowance factor
F_hc=0.75;            % heat conversion factor
Pwn=375;
NFR=ceil(NF);
PR=2.70;                        %KG of CO2/kg of fuel.
C=0.2778;                       % conversion factor

Rs=220*(Lf.^0.2/Vi.^0.8);       % Stomatal resistance
emis=0.9;                       % emissivity of indoor plant
Ap=L*WG*LA;                     % surface area of plant
LV=2450000;                     % Latent heat of water

ad=1.2;                          %Air density
Cpa=1005.0;                      %Specific heat of air
K2=0.0243;                       %Thermal conductivity
visco=1.725*10^-5;               % Viscosity of air kg/ms
vc=3.67*10^-3;                   %Volumetric expansion coefficient
Pr=(visco*Cpa)/K2;               % Prandatl number
K=1.4;                           %Thermal conductivity
SH=3;                            % Depth
Ts=20;                           %Underground soil temperature
BC=5.6*10^-8;                    %Stefen-Boltzman constant
```

```
%--------------------Time dependent calculation---------------%
Counter1=1;
for n=1:365;
    M=n*24;
    T_O((1:24),n)=T_o(Counter1:M);
    RH_O((1:24),n)=RH_o(Counter1:M);
    V_O((1:24),n)=V_o(Counter1:M);
    CCF_1((1:24),n)=CCF(Counter1:M);
    GHI_1((1:24),n)=GHI(Counter1:M);
    Counter1=M+1;
End

ST=solarradyear(LATD,LON,LST,SRA,SRA1,SRA2,TSR,SWA,TSW,NRA,NRA1,
NRA2,NWA,TNW,EWA,TEW,WWA,TWW,ASR,ASR1,ASR2,ANR,ANR1,ANR2,ASW,ANW
,AEW,AWW,CCF_1);
SRActual=outsidesolar(LATD,LON,LST,CCF_1);
SR=SRActual;
ast=reshape(SR,8760,1);
SumSR=sum(SR)';
SumGHI=sum(GHI_1)';

for n=1:365
    for t=1:24
      if ST(t,n)<=0
        Ti(t,n)=T_in;
        else
        Ti(t,n)=T_id;
      end
    end
end

for n=1:365;
    for t=1:24
    STT(t,n)=ST(t,n)*0.75;
    Ra(t,n)=200*(1+(1/(exp(0.05*(TSR*SRActual(t,n)-50)))));
    T_s(t,n)=Ts;
    if V_O(t,n)<=1
       V_O(t,n)=1;
       else
        V_O(t,n)=V_O(t,n);
       end
TD(t,n)=(RH_O(t,n)/100).^0.125*(112+0.9*(T_O(t,n)))+0.1*(T_O(t,n
))-112;  %Dew point temperature C
ec_sky(t,n)=0.787+0.764*log((TD(t,n)+273.16)/273); % Clear sky
emissivity
e_sky(t,n)=(1+0.0224*(CCF_1(t,n))-
0.0035*(CCF_1(t,n))^.2+0.00028*(CCF_1(t,n)).^3)*ec_sky(t,n);
```

```
e_sky(e_sky>1)=0.9;
Tsk(t,n)=(T_O(t,n)+273.16)*e_sky(t,n).^0.25;
T_c(t,n)=(2/3)*T_O(t,n)+(1/3)*Ti(t,n);       %Cover temperature
T_ck(t,n)=T_c(t,n)+273.16;
vt(t,n)=abs(Ti(t,n)-T_c(t,n));

     if vt(t,n)<=1;
             vt(t,n)=1.0;
             else
             vt(t,n)=vt(t,n);
     end
%----------------------Roof-----------------------------------%
Grr(t,n)=(9.8*vc*CLr.^3*vt(t,n))/(visco).^2;  %grashof number
Rayr(t,n)=Grr(t,n)*Pr;
hir(t,n)=(K2/CLr)*0.1*(Rayr(t,n)).^0.33;
Rexr(t,n)=(ad*V_O(t,n)*CLr)/visco; % Reynold number
h_Or(t,n)=((K2/CLr)*0.037*(Rexr(t,n)).^0.8*Pr.^0.33);
Ur(t,n)=1/(1/hir(t,n)+NPR*(LR/KR)+(NPR-1)*1/ha+1/h_Or(t,n));
q_TR(t,n)=(Ur(t,n)*TAR*(Ti(t,n)-T_O(t,n)))*3.6;
%----------------------South wall-----------------------------%
Grsw(t,n)=(9.8*vc*CLsw.^3*vt(t,n))/(visco).^2;  %grashof number
Raysw(t,n)=Grsw(t,n)*Pr;
hisw(t,n)=(K2/CLsw)*0.1*(Raysw(t,n)).^0.33;
Rexsw(t,n)=(ad*V_O(t,n)*CLsw)/visco; % Reynold number
h_Osw(t,n)=((K2/CLsw)*0.037*(Rexsw(t,n)).^0.8*Pr.^0.33);
Usw(t,n)=1/(1/hisw(t,n)+NPSW*(LSW/KSW)+(NPSW-
1)*1/ha+1/h_Osw(t,n));
q_TSW(t,n)=(Usw(t,n)*ASW*(Ti(t,n)-T_O(t,n)))*3.6;
q_rsw1(t,n)=(BC*emsw*ASW*Fsw*((Ti(t,n)+273.16).^4-
T_ck(t,n).^4));
q_rasw1(t,n)=(BC*emsw*ASW2*Fsw*((Ti(t,n)+273.16).^4-
T_ck(t,n).^4));
q_RSW(t,n)=(q_rsw1(t,n)+q_rasw1(t,n))*3.6;
Rexswn(t,n)=(ad*V_O(t,n)*CLswn)/visco; % Reynold number
h_Oswn(t,n)=((K2/CLswn)*0.037*(Rexswn(t,n)).^0.8*Pr.^0.33);
hiswn(t,n)=(K2/CLswn)*0.1*(10.^11).^0.33;
Uswn(t,n)=((1/hiswn(t,n))+(LSWI/KSWI)+(LSWS/KSWS)+(1/h_Oswn(t,n)
))^-1;
q_TSWN(t,n)=(Uswn(t,n)*ASW1*(Ti(t,n)-T_O(t,n)))*3.6;
%-------------North wall-------------------------------------%
Grnw(t,n)=(9.8*vc*CLnw.^3*vt(t,n))/(visco).^2;  %grashof number
Raynw(t,n)=Grnw(t,n)*Pr;
hinw(t,n)=(K2/CLnw)*0.1*(Raynw(t,n)).^0.33;
Rexnw(t,n)=(ad*V_O(t,n)*CLnw)/visco; % Reynold number
h_Onw(t,n)=((K2/CLnw)*0.037*(Rexnw(t,n)).^0.8*Pr.^0.33);
Unw(t,n)=1/(1/hinw(t,n)+NPNW*(LNW/KNW)+(NPNW-
1)*1/ha+1/h_Onw(t,n));
```

```
q_TNW(t,n)=(Unw(t,n)*ANW*(Ti(t,n)-T_O(t,n)))*3.6;
q_rnw1(t,n)=(BC*emnw*ANW*Fnw*((Ti(t,n)+273.16).^4-
T_ck(t,n).^4));
q_ranw1(t,n)=(BC*emnw*ANW2*Fnw*((Ti(t,n)+273.16).^4-
T_ck(t,n).^4));
q_RNW(t,n)=(q_rnw1(t,n)+q_ranw1(t,n))*3.6;
Rexnwn(t,n)=(ad*V_O(t,n)*CLnwn)/visco; % Reynold number
h_Onwn(t,n)=((K2/CLnwn)*0.037*(Rexnwn(t,n)).^0.8*Pr.^0.33);
hinwn(t,n)=(K2/CLnwn)*0.1*(10.^11).^0.33;
Unwn(t,n)=((1/hinwn(t,n))+(LNWI/KNWI)+(LNWS/KNWS)+(1/h_Onwn(t,n)
))^-1;
q_TNWN(t,n)=(Unwn(t,n)*ANW1*(Ti(t,n)-T_O(t,n)))*3.6;
  %----------------------East wal-----------------------------%
Grew(t,n)=(9.8*vc*CLew.^3*vt(t,n))/(visco).^2;  %grashof number
Rayew(t,n)=Grew(t,n)*Pr;
hiew(t,n)=(K2/CLew)*0.1*(Rayew(t,n)).^0.33;
Rexew(t,n)=(ad*V_O(t,n)*CLew)/visco; % Reynold number
h_Oew(t,n)=((K2/CLew)*0.037*(Rexew(t,n)).^0.8*Pr.^0.33);
Uew(t,n)=1/(1/hiew(t,n)+NPEW*(LEW/KEW)+(NPEW-
1)*1/ha+1/h_Oew(t,n));
q_TEW(t,n)=(Uew(t,n)*AEW*(Ti(t,n)-T_O(t,n)))*3.6;
q_rew1(t,n)=(BC*emew*AEW*Few*((Ti(t,n)+273.16).^4-
T_ck(t,n).^4));
q_REW(t,n)=(q_rew1(t,n))*3.6;
Rexewn(t,n)=(ad*V_O(t,n)*CLewn)/visco; % Reynold number
h_Oewn(t,n)=((K2/CLewn)*0.037*(Rexewn(t,n)).^0.8*Pr.^0.33);
hiewn(t,n)=(K2/CLewn)*0.1*(10.^11).^0.33;
Uewn(t,n)=((1/hiewn(t,n))+(LEWI/KEWI)+(LEWS/KEWS)+(1/h_Oewn(t,n)
))^-1;
q_TEWN(t,n)=(Uewn(t,n)*AEW1*(Ti(t,n)-T_O(t,n)))*3.6;
%----------------------West wall-----------------------------%
Grww(t,n)=(9.8*vc*CLww.^3*vt(t,n))/(visco).^2;  %grashof number
Rayww(t,n)=Grww(t,n)*Pr;
hiww(t,n)=(K2/CLww)*0.1*(Rayww(t,n)).^0.33;
Rexww(t,n)=(ad*V_O(t,n)*CLww)/visco; % Reynold number
h_Oww(t,n)=((K2/CLww)*0.037*(Rexww(t,n)).^0.8*Pr.^0.33);
Uww(t,n)=1/(1/hiww(t,n)+NPWW*(LWW/KWW)+(NPWW-
1)*1/ha+1/h_Oww(t,n));
q_TWW(t,n)=(Uww(t,n)*AWW*(Ti(t,n)-T_O(t,n)))*3.6;
q_rww1(t,n)=(BC*emww*AWW*Fww*((Ti(t,n)+273.16).^4-
T_ck(t,n).^4));
q_RWW(t,n)=(q_rww1(t,n))*3.6;
Rexwwn(t,n)=(ad*V_O(t,n)*CLwwn)/visco; % Reynold number
h_Owwn(t,n)=((K2/CLwwn)*0.037*(Rexwwn(t,n)).^0.8*Pr.^0.33);
hiwwn(t,n)=(K2/CLwwn)*0.1*(10.^11).^0.33;
Uwwn(t,n)=((1/hiwwn(t,n))+(LWWI/KWWI)+(LWWS/KWWS)+(1/h_Owwn(t,n)
))^-1;
```

```
q_TWWN(t,n)=(Uwwn(t,n)*AWW1*(Ti(t,n)-T_O(t,n)))*3.6;
%-----------Total transmission loss--------------------------%
q_T(t,n)=q_TR(t,n)+q_TSW(t,n)+q_TSWN(t,n)+q_TNW(t,n)+q_TNWN(t,n)
+q_TEW(t,n)+q_TEWN(t,n)+q_TWW(t,n)+q_TWWN(t,n);
q_W(t,n)=q_RSW(t,n)+q_RNW(t,n)+q_REW(t,n)+q_RWW(t,n);
%-----Ventilation, Perimeter, and soil conduction heat loss----%
q_I(t,n)=(ad*QV*Cpa*(Ti(t,n)-T_O(t,n)))*3.6;
q_P(t,n)=F*P*(Ti(t,n)-T_O(t,n))*3.6;
q_CS(t,n)=(K/SH)*A*(Ti(t,n)-T_s(t,n))*3.6;
%------------Transpiration heat loss--------------------------%
Re(t,n)=Ra(t,n)+Rs;
pws(t,n)=(exp(-5.80002206e3/(Ti(t,n)+273)+1.3914993-48.640239e-
3*(Ti(t,n)+273)+41.764768e-6*(Ti(t,n)+273)^2-14.452093e-
9*(Ti(t,n)+273)^3+6.5459673*log(Ti(t,n)+273)))/1000;
pw(t,n)=pws(t,n)*RH;          % Actual partial vapor pressure
w(t,n)=(0.62198*pw(t,n))/(101.325-pw(t,n));
ws(t,n)=(0.62198*pws(t,n))/(101.325-pws(t,n));
Mt(t,n)=(Ap*ad*(ws(t,n)-w(t,n)))/Re(t,n);
q_RE(t,n)=(Mt(t,n)*LV)*3.6;
%----------------------Operation of Supplemental Lighting------%
if STT(t,n)<=0
curtain(t,n)=curtain_on;
q_rc(t,n)=(BC*emis*TLR*A*Fsk*curtain(t,n)*((Ti(t,n)+273.16).^4-
Tsk(t,n).^4));
q_rc1(t,n)=(BC*emr*TAR*Fsr*curtain(t,n)*((Ti(t,n)+273.16).^4-
T_ck(t,n).^4));
q_RR(t,n)=(q_rc(t,n)+q_rc1(t,n))*3.6;
%------------Total radiation loss-----------------------------%
q_R(t,n)=q_RR(t,n)+q_W(t,n);
%--------------------Motors and CO2---------------------------%
NHV(t,n)=0;
q_co2(t,n)=3.6*((C*NHV(t,n)*MFR*A)/PR);
q_m(t,n)=NFR*(Pwn/Em)*MLF*MUF*3.6;
else
curtain(t,n)=curtain_off;
q_rc(t,n)=(BC*emis*TLR*A*Fsk*curtain(t,n)*((Ti(t,n)+273.16).^4-
Tsk(t,n).^4));
q_rc1(t,n)=(BC*emr*TAR*Fsr*curtain(t,n)*((Ti(t,n)+273.16).^4-
T_ck(t,n).^4));
q_RR(t,n)=(q_rc(t,n)+q_rc1(t,n))*3.6;
%----------------------Total radiation loss-------------------%
q_R(t,n)=q_RR(t,n)+q_W(t,n);
%--------------------Motors and CO2---------------------------%
NHV(t,n)=MNHV;
q_co2(t,n)=3.6*((C*NHV(t,n)*MFR*A)/PR);
q_m(t,n)=NFR*(Pw/Em)*MLF*MUF*3.6;
end
```

```
      STSL(t,n)=ST(t,n)/A;
      if STSL(t,n)<250
            SW(t,n)=IW;
            q_sl(t,n)=SW(t,n)*A*F_hc*F_sa*3.6;
      else
            SW(t,n)=IWZ;
            q_sl(t,n)=SW(t,n)*A*F_hc*F_sa*3.6;
      end

      if t>=Turn_off
          q_sll(t,n)=0;
      elseif t<=Turn_on
          q_sll(t,n)=0;
      else
          q_sll(t,n)=q_sl(t,n);
      end

     %-------------Heat balance equation----------------------%
     q=q_T+q_R+q_CS+q_P+q_RE+q_I;
     q_gain=q_co2+q_m+STT+q_sll;
     q_heat=q-q_gain;
     q_trsum=sum(q_T.*(q_T>0))';
     q_rsum=sum(q_R.*(q_R>0))';
     q_cssum=sum(q_CS.*(q_CS>0))';
     q_psum=sum(q_P.*(q_P>0))';
     q_ssum=sum(q_cssum+q_psum,2);
     q_resum=sum(q_RE)';
     q_isum=sum(q_I.*(q_I>0))';
      q_slsum=sum(q_sll)';
     q_co2sum=sum(q_co2)';
     q_msum=sum(q_m)';
     q_solarsum=sum(STT)';
     q_heatsum=sum(q_heat.*(q_heat>0))';
     end
end

for i=1:365;
     if i==1;
         Q_T=q_heat(:,i);
     else
         Q_T=[Q_T;q_heat(:,i)];
     end
end

Q=(Q_T);
```

```
tt=[1:365*24];
HH=tt';
figure
hold on
plot(HH,Q/1000,'r','linewidth',0.1);
plot([1,8760],[1500,1500],'k');
plot([1,8760],[0,0],'b');
plot([8760,8760],[-1500,1500],'k');
set(gca, 'Fontname','Times new roman')
xlim([1 8760]);
xlabel('Time,hr','fontweight','bold')
ylabel('Energy Requirement,MJ/hr','fontweight','bold')
set(gca,'YTickLabel', num2str(get(gca,'YTick')','%d'
```

Solar Radiation Sub-Model

```
functionST=solarradyear(LATD,LON,LST,SRA,SRA1,SRA2,TSR,SWA,TSW,N
RA,NRA1,NRA2,NWA,TNW,EWA,TEW,WWA,TWW,ASR,ASR1,ASR2,ANR,ANR1,ANR2
,ASW,ANW,AEW,AWW,CCF_1);

SC=1368;              %Solar constant

SASR=0;
SASW=0;
SANR=180;
SANW=180;
SAER=-90;
SAEW=-90;
SAWR=90;
SAWW=90;
pg=0.5;               %reflectivity of the ground
%-------------- --------------Loop over year----------------%
for n=1:365;
    B(1,n)=(n-1)*(360/365);
    IO(1,n)= SC*(1+0.033*cosd(360*(n-3)/365));
    ET(1,n)= 229.2*(0.000075+0.001868*cosd(B(1,n))-
0.032077*sind(B(1,n))-.014615*cosd(2*B(1,n))-
0.04089*sind(2*B(1,n)));
DA(1,n)=23.45*sind(360*(n+284)/365);

    if n<=31 && n>=1
        TR(1,n)=2.2;
    elseif n>=32 && n<=59
        TR(1,n)=2.2;
    elseif n>=60 && n<=90
        TR(1,n)=2.5;
    elseif n>=91 && n<=120
```

```
        TR(1,n)=2.9;
    elseif n>=121 && n<=151
        TR(1,n)=3.2;
    elseif n>=152 && n<=181
        TR(1,n)=3.4;
    elseif n>=182 && n<=212
        TR(1,n)=3.5;
    elseif n>=213 && n<=243
        TR(1,n)=3.3;
    elseif n>=244 && n<=273
        TR(1,n)=2.9;
    elseif n>=274 && n<=304
        TR(1,n)=2.6;
    elseif n>=305 && n<=334
        TR(1,n)=2.3;
    else
        TR(1,n)=2.2;
    End

%-----------------Daily loop-----------------------------%
for h=1:24
  p=24*(n-1)+h;
  tttt(1,p)=p;
  AST(h,n)=h+(ET(1,n)/60)+(LON-LST)/15;    HA(h,n)=15*(AST(h,n)-
12);
coz(h,n)=sind(LATD)*sind(DA(1,n))+cosd(LATD)*cosd(DA(1,n))*cosd(
HA(h,n));%Zemith angle
 ZAD(h,n)=acosd(coz(h,n)); % Zenith angle in degree
 coisr(h,n)=sind(DA(1,n))*sind(LATD)*cosd(SRA)-
sind(DA(1,n))*cosd(LATD)*sind(SRA)*cosd(SASR)+cosd(DA(1,n))*cosd
(LATD)*cosd(SRA)*cosd(HA(h,n))+cosd(DA(1,n))*sind(LATD)*sind(SRA
)*cosd(SASR)*cosd(HA(h,n))+cosd(DA(1,n))*sind(SRA)*sind(SASR)*si
nd(HA(h,n));

coisr1(h,n)=sind(DA(1,n))*sind(LATD)*cosd(SRA1)-
sind(DA(1,n))*cosd(LATD)*sind(SRA1)*cosd(SASR)+cosd(DA(1,n))*cos
d(LATD)*cosd(SRA1)*cosd(HA(h,n))+cosd(DA(1,n))*sind(LATD)*sind(S
RA1)*cosd(SASR)*cosd(HA(h,n))+cosd(DA(1,n))*sind(SRA1)*sind(SASR
)*sind(HA(h,n));

 coisr2(h,n)=sind(DA(1,n))*sind(LATD)*cosd(SRA2)-
sind(DA(1,n))*cosd(LATD)*sind(SRA2)*cosd(SASR)+cosd(DA(1,n))*cos
d(LATD)*cosd(SRA2)*cosd(HA(h,n))+cosd(DA(1,n))*sind(LATD)*sind(S
RA2)*cosd(SASR)*cosd(HA(h,n))+cosd(DA(1,n))*sind(SRA2)*sind(SASR
)*sind(HA(h,n));
```

```
 coinr(h,n)=sind(DA(1,n))*sind(LATD)*cosd(NRA)-
sind(DA(1,n))*cosd(LATD)*sind(NRA)*cosd(SANR)+cosd(DA(1,n))*cosd
(LATD)*cosd(NRA)*cosd(HA(h,n))+cosd(DA(1,n))*sind(LATD)*sind(NRA
)*cosd(SANR)*cosd(HA(h,n))+cosd(DA(1,n))*sind(NRA)*sind(SANR)*si
nd(HA(h,n));

coinr1(h,n)=sind(DA(1,n))*sind(LATD)*cosd(NRA1)-
sind(DA(1,n))*cosd(LATD)*sind(NRA1)*cosd(SANR)+cosd(DA(1,n))*cos
d(LATD)*cosd(NRA1)*cosd(HA(h,n))+cosd(DA(1,n))*sind(LATD)*sind(N
RA1)*cosd(SANR)*cosd(HA(h,n))+cosd(DA(1,n))*sind(NRA1)*sind(SANR
)*sind(HA(h,n));

coinr2(h,n)=sind(DA(1,n))*sind(LATD)*cosd(NRA2)-
sind(DA(1,n))*cosd(LATD)*sind(NRA2)*cosd(SANR)+cosd(DA(1,n))*cos
d(LATD)*cosd(NRA2)*cosd(HA(h,n))+cosd(DA(1,n))*sind(LATD)*sind(N
RA2)*cosd(SANR)*cosd(HA(h,n))+cosd(DA(1,n))*sind(NRA2)*sind(SANR
)*sind(HA(h,n));

coisw(h,n)=sind(DA(1,n))*sind(LATD)*cosd(SWA)-
sind(DA(1,n))*cosd(LATD)*sind(SWA)*cosd(SASW)+cosd(DA(1,n))*cosd
(LATD)*cosd(SWA)*cosd(HA(h,n))+cosd(DA(1,n))*sind(LATD)*sind(SWA
)*cosd(SASW)*cosd(HA(h,n))+cosd(DA(1,n))*sind(SWA)*sind(SASW)*si
nd(HA(h,n));

coinw(h,n)=sind(DA(1,n))*sind(LATD)*cosd(NWA)-
sind(DA(1,n))*cosd(LATD)*sind(NWA)*cosd(SANW)+cosd(DA(1,n))*cosd
(LATD)*cosd(NWA)*cosd(HA(h,n))+cosd(DA(1,n))*sind(LATD)*sind(NWA
)*cosd(SANW)*cosd(HA(h,n))+cosd(DA(1,n))*sind(NWA)*sind(SANW)*si
nd(HA(h,n));

coiew(h,n)=sind(DA(1,n))*sind(LATD)*cosd(EWA)-
sind(DA(1,n))*cosd(LATD)*sind(EWA)*cosd(SAEW)+cosd(DA(1,n))*cosd
(LATD)*cosd(EWA)*cosd(HA(h,n))+cosd(DA(1,n))*sind(LATD)*sind(EWA
)*cosd(SAEW)*cosd(HA(h,n))+cosd(DA(1,n))*sind(EWA)*sind(SAEW)*si
nd(HA(h,n));

coiww(h,n)=sind(DA(1,n))*sind(LATD)*cosd(WWA)-
sind(DA(1,n))*cosd(LATD)*sind(WWA)*cosd(SAWW)+cosd(DA(1,n))*cosd
(LATD)*cosd(WWA)*cosd(HA(h,n))+cosd(DA(1,n))*sind(LATD)*sind(WWA
)*cosd(SAWW)*cosd(HA(h,n))+cosd(DA(1,n))*sind(WWA)*sind(SAWW)*si
nd(HA(h,n));

 RBSR(h,n)=coisr(h,n)/coz(h,n);
 RBSR1(h,n)=coisr1(h,n)/coz(h,n);
 RBSR2(h,n)=coisr2(h,n)/coz(h,n);
 RBSW(h,n)=coisw(h,n)/coz(h,n);
 RBNR(h,n)=coinr(h,n)/coz(h,n);
```

```
 RBNR1(h,n)=coinr1(h,n)/coz(h,n);
 RBNR2(h,n)=coinr2(h,n)/coz(h,n);
 RBNW(h,n)=coinw(h,n)/coz(h,n);
  RBEW(h,n)=coiew(h,n)/coz(h,n);
  RBWW(h,n)=coiww(h,n)/coz(h,n);
  ab(h,n)=90-ZAD(h,n);
  abc(h,n)=(0.9+9.4*sind(ab(h,n)));
  abcd(h,n)=-TR(1,n)/abc(h,n);
    std(h,n)=exp(abcd(h,n));
    IN(h,n)=IO(1,n)*std(h,n);
    IN(IN>1360)=0;
    IN(IN<0)=0;          % kick out negative values
    IB(h,n)=IN(h,n)*coz(h,n);
    IB(IB<0)=0;          % kick out negative values
    ID(h,n)=(1/3)*(IO(1,n)-IN(h,n))*coz(h,n);
    ID(ID<0)=0;         % kick out negative values

    SR(h,n)=(IB(h,n)+ID(h,n));
    SRActual(h,n)=SR(h,n)*(1-0.66*(CCF_1(h,n)/8)^0.63);
    IDActual(h,n)=SRActual(h,n)*(0.3+0.7*(CCF_1(h,n)/8)^2);
    IBActual(h,n)=SRActual(h,n)-IDActual(h,n);

    IBSR(h,n)=IBActual(h,n)*RBSR(h,n);
    IBSR(IBSR<0)=0;
    IBSR1(h,n)=IBActual(h,n)*RBSR1(h,n);
    IBSR1(IBSR1<0)=0;
    IBSR2(h,n)=IBActual(h,n)*RBSR2(h,n);
    IBSR2(IBSR2<0)=0;
    IBSW(h,n)=IBActual(h,n)*RBSW(h,n);
    IBSW(IBSW<0)=0;
    IBNR(h,n)=IBActual(h,n)*RBNR(h,n);
    IBNR(IBNR<0)=0;
    IBNR1(h,n)=IBActual(h,n)*RBNR1(h,n);
    IBNR1(IBNR1<0)=0;
    IBNR2(h,n)=IB(h,n)*RBNR2(h,n);
    IBNR2(IBNR2<0)=0;
    IBNW(h,n)=IBActual(h,n)*RBNW(h,n);
    IBNW(IBNW<0)=0;
    IBEW(h,n)=IBActual(h,n)*RBEW(h,n);
    IBEW(IBEW<0)=0;
    IBWW(h,n)=IBActual(h,n)*RBWW(h,n);
    IBWW(IBWW<0)=0;

SRSR(h,n)=(IBSR(h,n)+IDActual(h,n)*((1+cosd(SRA))/2)+pg*SRActual
(h,n)*((1-cosd(SRA))/2))*ASR*TSR*3.6;
```

```
SRSR1(h,n)=(IBSR1(h,n)+IDActual(h,n)*((1+cosd(SRA1))/2)+pg*SRAct
ual(h,n)*((1-cosd(SRA1))/2))*ASR1*TSR*3.6;

SRSR2(h,n)=(IBSR2(h,n)+IDActual(h,n)*((1+cosd(SRA2))/2)+pg*SRAct
ual(h,n)*((1-cosd(SRA2))/2))*ASR2*TSR*3.6;

SRSW(h,n)=(IBSW(h,n)+IDActual(h,n)*((1+cosd(SWA))/2)+pg*SRActual
(h,n)*((1-cosd(SWA))/2))*ASW*TSW*3.6;

SRNR(h,n)=(IBNR(h,n)+IDActual(h,n)*((1+cosd(NRA))/2)+pg*SRActual
(h,n)*((1-cosd(NRA))/2))*ANR*TSR*3.6;

SRNR1(h,n)=(IBNR1(h,n)+IDActual(h,n)*((1+cosd(NRA1))/2)+pg*SRAct
ual(h,n)*((1-cosd(NRA1))/2))*ANR1*TSR*3.6;

SRNR2(h,n)=(IBNR2(h,n)+IDActual(h,n)*((1+cosd(NRA2))/2)+pg*SRAct
ual(h,n)*((1-cosd(NRA2))/2))*ANR2*TSR*3.6;

SRNW(h,n)=(IBNW(h,n)+IDActual(h,n)*((1+cosd(NWA))/2)+pg*SRActual
(h,n)*((1-cosd(NWA))/2))*ANW*TNW*3.6;

SREW(h,n)=(IBEW(h,n)+IDActual(h,n)*((1+cosd(EWA))/2)+pg*SRActual
(h,n)*((1-cosd(EWA))/2))*AEW*TEW*3.6;

SRWW(h,n)=(IBWW(h,n)+IDActual(h,n)*((1+cosd(WWA))/2)+pg*SRActual
(h,n)*((1-cosd(WWA))/2))*AWW*TWW*3.6;

ST(h,n)=SRSR(h,n)+SRSR1(h,n)+SRSR2(h,n)+SRSW(h,n)+SRNR(h,n)+SRNR
1(h,n)+SRNR2(h,n)+SRNW(h,n)+SREW(h,n)+SRWW(h,n);
STT=(sum(ST))';
end
end
```

Outside solar radiation on horizontal surface

```
function SRActual=outsidesolar(LATD,LON,LST,CCF_1)
SC=1368;
pg=0.5;
%---------------------------Loop over year---------------------%

for n=1:365;
    B(1,n)=(n-1)*(360/365);
    IO(1,n)= SC*(1+0.033*cosd(360*(n-3)/365));
    ET(1,n)= 229.2*(0.000075+0.001868*cosd(B(1,n))-
0.032077*sind(B(1,n))-.014615*cosd(2*B(1,n))-
0.04089*sind(2*B(1,n)));
    DA(1,n)=23.45*sind(360*(n+284)/365);
```

```
     if n<=31 && n>=1
        TR(1,n)=2.2;
    elseif n>=32 && n<=59
        TR(1,n)=2.2;
    elseif n>=60 && n<=90
        TR(1,n)=2.5;
    elseif n>=91 && n<=120
        TR(1,n)=2.9;
    elseif n>=121 && n<=151
        TR(1,n)=3.2;
    elseif n>=152 && n<=181
        TR(1,n)=3.4;
    elseif n>=182 && n<=212
        TR(1,n)=3.5;
    elseif n>=213 && n<=243
        TR(1,n)=3.3;
    elseif n>=244 && n<=273
        TR(1,n)=2.9;
    elseif n>=274 && n<=304
        TR(1,n)=2.6;
    elseif n>=305 && n<=334
        TR(1,n)=2.3;
    else
        TR(1,n)=2.2;
    end
%-----------------------------Daily loop----------------------%
for h=1:24
   p=24*(n-1)+h;
   tttt(1,p)=p;
   AST(h,n)=h+(ET(1,n)/60)+(LON-LST)/15;
   HA(h,n)=15*(AST(h,n)-12);

coz(h,n)=sind(LATD)*sind(DA(1,n))+cosd(LATD)*cosd(DA(1,n))*cosd(
HA(h,n));%Zemith angle
    ZAD(h,n)=acosd(coz(h,n)); % Zenith angle in degree
    ab(h,n)=90-ZAD(h,n);
    abc(h,n)=(0.9+9.4*sind(ab(h,n)));
    abcd(h,n)=-TR(1,n)/abc(h,n); % Problem in this section
    std(h,n)=exp(abcd(h,n));
    IN(h,n)=IO(1,n)*std(h,n);
    IN(IN>1360)=0;
    IN(IN<5)=0;  % kick out negative values
    IB(h,n)=IN(h,n)*coz(h,n);
    IB(IB<0)=0;  % kick out negative values
    ID(h,n)=(1/3)*(IO(1,n)-IN(h,n))*coz(h,n);
    ID(ID<0)=0;  % kick out negative values
    SR(h,n)=IB(h,n)+ID(h,n);
```

```
    SRActual(h,n)=SR(h,n)*(1-0.66*(CCF_1(h,n)/8)^0.63);
end
end
```

A.2 MATLAB Code for computer program of Chinese-style solar greenhouse

Main model

```
clear all
close all
clc
%-------------------------Input-----------------------------%
LATD=52.09;
LON=-106.82;
LST=-90;
LFA=0.66;       %Local factor for solar radiation model
LFB=0.63;       %Local factor for solar radiation model
L=30;           %Length of span
W=7.0;          %Width of span
Hs=1.4;         %Height from wall to ridge
HS=2.1;         %Height of north wall
H=Hs+HS;        %Height at ridge
A=L*W;          %Total Area of greenhouse
V=A*HS;         %Volume of greenhouse
P=2*(L+W);      %Perimeter of the greenhouse
%--------------- South Roof and south wall-----------------%
SRA=26;          % Angle of inclined south wall
SRA1=60;
SRA2=0;
ASR=180;          %Total area of south roof %%%%%%%%%%%%%%%%%
ASR1=35;
ASR2=0;
TAR=(ASR+ASR1+ASR2); %Area of the roof cover
TSR=0.85;
TLR=0.03;
emc=0.3;           %Emissivity of the cover
SWA=90;
ASW=0;             %Transparent vertical south wall
ASW1=0;            %Non-transparent vertical south wall
TSW=0.85;
%-------------------North roof and wall---------------------%
NRA=34;
WNR=((H-HS)/sind(NRA)); %Slope length of north roof
ANR=L*WNR;              %Area of north roof
ANW=L*HS;               %Non-transparent north wall
%--------------------------Side wall--------------------------%
AEW=26.75;              %Non-transparent east wall
AWW=AEW;                %Non-transparent west wall
TASW=AEW+AWW+ASW1;
%-----------------------Cover thermal properties-------------%
NPR=1;                   %Single layer or multilayer in roof
K1=0.5;                  %Thermal conductivity of cover
K2=0.026;                %Thermal conductivity of air
```

```
L1=0.04;                %Thickness of cover
ha=3.8;                 %Air thermal conductance
Kn=0.015;               %Thermal conductivity of night curtain
Ln=0.02;                %Thickness of night curtain
%----------------------North wall thermal properties-----------%
Knw=0.2;              %Thermal conductivity of north-wall material
Knis=16.0;            %Indoor sheathing material
Kns=16;               %Outside sheathing material
Kni=0.033;            %Insulation material
Kns1=0.1;             %Plywood
Lnw=0.152;            %Thickness of north-wall material
Lns1=0.013;           %Siding material (Plywood)
Lns=0.002;            %Inside sheathing material
Lni=0.065;            %Insulation material
anw=0.9;              %Solar absorptivity
Cpw=920;              %Heat capacity of heat storage material
adw=2240;             % Mass density of heat storing material
%----------------------North roof-----------------------------%
Knr=0.33;           %Thermal conductivity vapor barrier
Knrs=0.1;           %Siding material (plywood)
Knri=0.033;         %Insulation material
Lnr=0.00015;        %Thickness of north-roof vapor barrier
Lnrs=0.013;         %Siding material (plywood)
Lnri=0.065;         %Insulation material
%----------------------Sidewall-------------------------------%
Ksw=0.33;           %Thermal conductivity of vapor barrier
Ksws=0.1;           % Siding material (plywood)
Kswi=0.033;         %Insulation material
Lsw=0.00015;        % Thickness of north-roof vapor barrier
Lsws=0.013;         %Siding material (plywood)
Lswi=0.065;         %Insulation material
%--------------------Set point-------------------------------%
T_id=21;            %Day time set point temperature
T_in=18;            %Night time set point temperature
RH=0.8;             %Indoor relative humidity
Vi=0.1;             %Indoor air velocity
%-----------------Lighting, CO2 and air circulation-----------%
IW=30;              %Install light wattage
IWZ=0;
F_sa=1.0;           %Light allowance factor
F_hc=0.75;          %Heat conversion factor

Pw=300;             %Power rating of motor
Pwn=300;            %Night time
Em=0.9;             %Motor efficiency
MLF=1.0;            %Motor load factor
MUF=1.0;            %Motor use factor
```

```
NF=2;              %Number of fan for air recirculation
NFR=ceil(NF);

NHV=38;            %Heating value of fuel
MFR=4.5;           %CO2 flow rate
MFRN=0;            %Night time C02 supply rate
PR=2.70;           %KG of CO2/kg of fuel.
C=0.2778;          %Conversion factor
%-----------------Others input parameters---------------%
F=0.5;             %Perimeter heat loss coefficient
emis=0.9;          %Emissivity of indoor plant and air
ad=1.2;            %Air density
Cpa=1005.0;        %Specific heat of air
CF=0.00025;        %Cover factor
CFn=CF-CF*0.25;
WF=0.22;           %Wind factor
TF=0.16;           %Temperature factor
Fsr=1.0;           %View factor betn south roof and sky
Fgsr=(1+cosd(SRA))/2;
BC=5.6*10^-8;       %Stefen-Boltzman constant
visco=1.725*10^-5; %Viscosity of air kg/ms
Pr=(visco*Cpa)/K2; %Prandatl number
vc=3.67*10^-3;     %Volumetric expansion coefficient
CLr=TAR/P;         %Characteristics length of surface
CLsw=HS;
CLnw=HS;
CLnr=WNR;
CLf=(A/P);
LV=2450000;        %Latent heat of water vaporization
Mw=adw*(HS*Lnw*L);
Ms=ads*(A*dxs);
%----------------Soil and Plant   information-------------%
K=1.4;              %Thermal conductivity of soil
as=0.8;             %Solar absorptivity
Cps=900;
ads=1300;
dxs=0.1;
Tcs=20;
Zs=3.0;              %Depth of constant soil temperature

Lf=0.027;            %Characteristics length of leaf
SIP=0.7;             %Solar interception by plant on north wall
Rs=220*(Lf.^0.2/Vi.^0.8); %Stomatal resistance of plant leaf
LAI=2.0;             %Leaf area index of   plants
Ap=A*LAI;            %Surface area of plant
LEC=0.64;            %Light extinction coefficient of plant
% ------------------input value of simulation-----------------%
```

```
T_o=xlsread('TMY_saskatoon.xlsx','sheet1','E12:E8771'); %
Outside temperature
RH_o=xlsread('TMY_saskatoon.xlsx','sheet1','G12:G8771');%
Outside temperature
V_o=xlsread('TMY_saskatoon.xlsx','sheet1','J12:J8771'); %Outside
air velocity
CCF=xlsread('TMY_saskatoon.xlsx','sheet1','M12:M8771'); %Cloud
cover

curtain_on=0;
curtain_off=1;
%-------------------Numerical calculation--------------------%
h=waitbar(0,'Initializing waitbar');
Counter1=1;
for n=1:365;
    M=n*24;
    T_O((1:24),n)=T_o(Counter1:M);
    RH_O((1:24),n)=RH_o(Counter1:M);
    V_O((1:24),n)=V_o(Counter1:M);
    CCF_1((1:24),n)=CCF(Counter1:M);
    GHI_1((1:24),n)=GHI(Counter1:M);
    Counter1=M+1;
end
[ST,SRActual]=solarradyear(LATD,LON,LST,LFA,LFB,SRA,SRA1,SRA2,TS
R,SWA,TSW,ASW,ASR,ASR1,ASR2,CCF_1);
AA=altitudeangle(LATD,LON,LST);
ast=reshape(SRActual,8760,1);
SumSR=sum(SRActual)';
SumGHI=sum(GHI_1)';
Effective=1.0;
%----------------SOIL AND WALL TEMPERASTURE---------------%
for n=1:365;
    Teo=18;
    Tew=18;
    for t=1:24
       if V_O(t,n)<=1.0
       V_O(t,n)=1.0;
       else
        V_O(t,n)=V_O(t,n);
       end
    T_s(t,n)=Tcs;
    %-----------------North Wall-----------------------%
    Renw(t,n)=(ad*V_O(t,n)*CLnw)/visco; % Reynold number
    h_onw(t,n)=((K2/CLnw)*0.037*(Renw(t,n)).^0.8*Pr.^0.33);
    hinw(t,n)=(K2/CLnw)*0.1*(10.^11).^0.33;
    Unw(t,n)=1/((Lni/Kni)+(Lns1/Kns1)+(Lns/Kns)+(1/h_onw(t,n)));
    %------------------soil---------------------------------%
```

```
    hsi(t,n)=(K2/CLf)*0.15*(10.^10).^0.33;

    if ST(t,n)<=0
        Ti(t,n)=T_in;
        else
        Ti(t,n)=T_id;
    end


FSR(t,n)=(W*tand(AA(t,n)))/(HS+W*tand(AA(t,n)));
STg(t,n)=FSR(t,n)*ST(t,n)*exp(-LEC*LAI);
PPs(t,n)=((as*STg(t,n))+(hsi(t,n)*Ti(t,n)*A)+((K/Zs)*A*T_s(t,n))
)/(Cps*Ms);
AAAs(t,n)=((hsi(t,n)*A)+((K/Zs)*A))/(Cps*Ms);
QQs(t,n)=PPs(t,n)/AAAs(t,n);

for i=1:3600
    Bts(i,t,n)=QQs(t,n);
    Ts(i,t,n)=Bts(i,t,n)*(1-exp(-AAAs(t,n)*i))+Teo*exp(-
AAAs(t,n)*i);
     Teo=Ts(t,n);
end
Tsst=Ts(3600,:);
%-------------------------Wall-----------------------------%
FSN(t,n)=SIP*(HS)/(HS+W*tand(AA(t,n)));
STw(t,n)=FSN(t,n)*ST(t,n);
AAA(t,n)=((hinw(t,n)*ANW)+(Unw(t,n)*ANW))/(Cpw*Mw);

PP(t,n)=(anw*STw(t,n)+hinw(t,n)*Ti(t,n)*ANW+Unw(t,n)*T_O(t,n)*AN
W)/(Cpw*Mw);
QQ(t,n)=PP(t,n)/AAA(t,n);

for i=1:3600
    Btw(i,t,n)=QQ(t,n);
    Tw(i,t,n)=Btw(i,t,n)*(1-exp(-AAA(t,n)*i))+Tew*exp(-
AAA(t,n)*i);
    Tew=Tw(t,n);
end
    Twt=Tw(3600,:);
    End
End

Counter1=1;
for nw=1:365;
M=nw*24;
T_sst((1:24),nw)=Tsst(Counter1:M);
T_wt((1:24),nw)=Twt(Counter1:M);
```

```
Counter1=M+1;
end

for n=1:365;
for t=1:24
Ra(t,n)=200*(1+(1/(exp(0.05*(TSR*0.9*SRActual(t,n)-50)))));
%---------------------Sidewall-------------------------%
Resw(t,n)=(ad*V_O(t,n)*CLsw)/visco; % Reynold number
hisw(t,n)=(K2/CLsw)*0.1*(10.^11).^0.33;
h_osw(t,n)=((K2/CLsw)*0.037*(Resw(t,n)).^0.8*Pr.^0.33);
Usw(t,n)=1/((1/hisw(t,n))+(Lsw/Ksw)+(Lswi/Kswi)+(Lsws/Ksws)+(1/h
_osw(t,n)));
%-----------------------North Roof-------------------------%
Renr(t,n)=(ad*V_O(t,n)*CLnr)/visco; % Reynold number
hinr(t,n)=(K2/CLnr)*0.1*(10.^11).^0.33;
h_onr(t,n)=((K2/CLnr)*0.037*(Renr(t,n)).^0.8*Pr.^0.33);
Unr(t,n)=1/((1/hinr(t,n))+(Lnr/Knr)+(Lnri/Knri)+(Lnrs/Knrs)+(1/h
_onr(t,n)));
%-----------------------Cover temperature-------------------%
T_c(t,n)=T_O(t,n)+1/8*(Ti(t,n)-T_O(t,n));
T_ck(t,n)=T_c(t,n)+273.16;
vt(t,n)=abs(Ti(t,n)-T_c(t,n));

if vt(t,n)<=1;
             vt(t,n)=1.0;
             else
             vt(t,n)=vt(t,n);
end
%-------------------------south Roof-------------------------%
Rer(t,n)=(ad*V_O(t,n)*CLr)/visco;
Grr(t,n)=(9.8*vc*CLr.^3*vt(t,n))/(visco).^2;
Rayr(t,n)=Grr(t,n)*Pr;
hir(t,n)=(K2/CLr)*0.15*(Rayr(t,n)).^0.33;
h_or(t,n)=((K2/CLr)*0.037*(Rer(t,n)).^0.8*Pr.^0.33);
%------------------Sky temperature---------------------------%
TD(t,n)=(RH_O(t,n)/100).^0.125*(112+0.9*(T_O(t,n)))+0.1*(T_O(t,n
))-112; %Dew point temperature C
ec_sky(t,n)=0.787+0.764*log((TD(t,n)+273.16)/273); % Clear sky
emissivity
e_sky(t,n)=(1+0.0224*(CCF_1(t,n))-
0.0035*(CCF_1(t,n))^.2+0.00028*(CCF_1(t,n)).^3)*ec_sky(t,n);
e_sky(e_sky>1)=0.9;
Tsk(t,n)=(T_O(t,n)+273.16)*e_sky(t,n).^0.25;
%----------------------Perimeter heat loss-------------------%
q_p(t,n)=F*P*(Ti(t,n)-T_O(t,n))*3.6; %
%--------------------Transpiration heat loss-----------------%
 Re(t,n)=Ra(t,n)+Rs;
```

```
 pws(t,n)=(exp(-5.80002206e3/(Ti(t,n)+273)+1.3914993-48.640239e-
3*(Ti(t,n)+273)+41.764768e-6*(Ti(t,n)+273)^2-14.452093e-
9*(Ti(t,n)+273)^3+6.5459673*log(Ti(t,n)+273)))/1000;
 pw(t,n)=pws(t,n)*RH;
 w(t,n)=(0.62198*pw(t,n))/(101.325-pw(t,n));
 ws(t,n)=(0.62198*pws(t,n))/(101.325-pws(t,n));
 Mt(t,n)=(Ap*ad*(ws(t,n)-w(t,n)))/Re(t,n);
 q_re(t,n)=(Mt(t,n)*LV)*3.6;
%--------------------Heat gain/loss from soil and wall-------%
 q_soil(t,n)=(hsi(t,n)*A*(T_sst(t,n)-Ti(t,n)))*3.6;
 q_wall(t,n)=(hinw(t,n)*ANW*(T_wt(t,n)-Ti(t,n)))*3.6;
 q_solar(t,n)=Effective*(ST(t,n)-STg(t,n)-STw(t,n));

if ST(t,n)<=0
R(t,n)=(1/hir(t,n)+(Ln/Kn)+NPR*(L1/K1)+(NPR-
1)*(1/ha)+1/h_or(t,n));
Ur(t,n)=1/R(t,n);
q_tr(t,n)=(Ur(t,n)*TAR*(Ti(t,n)-T_O(t,n))+Unr(t,n)*ANR*(Ti(t,n)-
T_O(t,n))+Usw(t,n)*TASW*(Ti(t,n)-T_O(t,n)))*3.6;
%---------------------------Infiltration----------------------%
Al(t,n)=TAR*CFn;
AE(t,n)=Al(t,n)*sqrt(WF.^2*(V_O(t,n)).^2+TF.^2*abs(Ti(t,n)-
T_O(t,n)));
AEE(t,n)=(AE(t,n)*3600)/V;
q_vi(t,n)=(ad*AE(t,n)*Cpa*(Ti(t,n)-T_O(t,n)))*3.6;
%-----------------------Long-wave radiation-------------------%
curtain(t,n)=curtain_on;
q_rc(t,n)=(BC*emis*TLR*A*Fsr*curtain(t,n)*((Ti(t,n)+273.16).^4-
Tsk(t,n).^4));
q_rc1(t,n)=(BC*emc*TAR*Fgsr*curtain(t,n)*((Ti(t,n)+273.16).^4-
T_ck(t,n).^4));
q_r(t,n)=(q_rc(t,n)+q_rc1(t,n))*3.6;
q_co2(t,n)=3.6*((C*NHV*MFRN*A)/PR);
q_m(t,n)=NFR*(Pwn/Em)*MLF*MUF*3.6;
else
%-------------------------south Roof-------------------------%
R(t,n)=(1/hir(t,n)+NPR*(L1/K1)+(NPR-1)*(1/ha)+1/h_or(t,n));
Ur(t,n)=1/R(t,n);
q_tr(t,n)=(Ur(t,n)*TAR*(Ti(t,n)-T_O(t,n))+Unr(t,n)*ANR*(Ti(t,n)-
T_O(t,n))+Usw(t,n)*TASW*(Ti(t,n)-T_O(t,n)))*3.6;
%---------------------Infiltration-------------------------%
Al(t,n)=TAR*CF;
AE(t,n)=Al(t,n)*sqrt(WF.^2*(V_O(t,n)).^2+TF.^2*abs(Ti(t,n)-
T_O(t,n)));
AEE(t,n)=(AE(t,n)*3600)/V;
q_vi(t,n)=(ad*AE(t,n)*Cpa*(Ti(t,n)-T_O(t,n)))*3.6;
%---------------------Long-wave radiation-------------------%
```

```
curtain(t,n)=curtain_off;
q_rc(t,n)=(BC*emis*TLR*A*Fsr*curtain(t,n)*((Ti(t,n)+273.16).^4-
Tsk(t,n).^4));
q_rc1(t,n)=(BC*emc*TAR*Fgsr*curtain(t,n)*((Ti(t,n)+273.16).^4-
T_ck(t,n).^4));
q_r(t,n)=(q_rc(t,n)+q_rc1(t,n))*3.6;
%--------------------Heat gain from motor and CO2-------------%
q_co2(t,n)=3.6*((C*NHV*MFR*A)/PR);
q_m(t,n)=NFR*(Pw/Em)*MLF*MUF*3.6;
%---------------------Supplemental lighting option------------%
STSL(t,n)=ST(t,n)/A;
     if STSL(t,n)<250
           SW(t,n)=IW;
           q_sl(t,n)=SW(t,n)*A*F_hc*F_sa*3.6;
     else
           SW(t,n)=IWZ;
           q_sl(t,n)=SW(t,n)*A*F_hc*F_sa*3.6;
     end
     if t>=22
         q_sll(t,n)=0;
     elseif t<=7
         q_sll(t,n)=0;

     else
         q_sll(t,n)=q_sl(t,n);
     end

 q=q_tr+q_r+q_p+q_vi+q_re-q_soil-q_wall-q_solar-q_co2-q_sll-q_m;

    q_trsum=sum(q_tr.*(q_tr>0))'; % only sum the positive value
    q_rsum=sum(q_r.*(q_r>0))';
    q_psum=sum(q_p.*(q_p>0))';
    q_resum=sum(q_re)';
    q_visum=sum(q_vi.*(q_vi>0))';
    q_solarsum=sum(q_solar.*(q_solar>0))';
    q_soilsum=sum(q_soil.*(q_soil>0))';
    q_wallsum=sum(q_wall.*(q_wall>0))
    q_slsum=sum(q_sl)';
    q_co2sum=sum(q_co2)';
    q_msum=sum(q_m)';
    q_heatsum=sum(q.*(q>0))';
    end
end


for i=1:365;
    if i==1;
```

```
        Q_T=q(:,i);
        AEE_T=AEE(:,i);
    else
        Q_T=[Q_T;q(:,i)];
        AEE_T=[AEE_T;AEE(:,i)];
    end
     waitbar(0.5,h,'Halfway there...')
end
Q=(Q_T);
tt=[1:365*24];
HH=tt;
plot(HH,Q/1000,'r','linewidth',0.1);
xlabel('Time,hr','fontweight','bold')
ylabel('Energy Requirement,MJ/hr','fontweight','bold')
close(h)
```

Solar radiation sub-model

```
function
[ST,SRActual]=solarradyear(LATD,LON,LST,LFA,LFB,SRA,SRA1,SRA2,TS
R,SWA,TSW,ASW,ASR,ASR1,ASR2,CCF_1)
SC=1368;            %Solar constant (W/m^2)
SASR=0;
SASW=0;
pg=0.5;             %reflectivity of the ground
%--------------Loop over year-------------------------------%
for n=1:365;
B(1,n)=(n-1)*(360/365);
IO(1,n)= SC*(1+0.033*cosd(360*(n-3)/365));       %    ET(1,n)=
229.2*(0.000075+0.001868*cosd(B(1,n))-0.032077*sind(B(1,n))-
.014615*cosd(2*B(1,n))-0.04089*sind(2*B(1,n)));
DA(1,n)=23.45*sind(360*(n+284)/365);
    if n<=31 && n>=1
        TR(1,n)=2.2;
    elseif n>=32 && n<=59
        TR(1,n)=2.2;
    elseif n>=60 && n<=90
        TR(1,n)=2.5;
    elseif n>=91 && n<=120
        TR(1,n)=2.9;
    elseif n>=121 && n<=151
        TR(1,n)=3.2;
    elseif n>=152 && n<=181
        TR(1,n)=3.4;
    elseif n>=182 && n<=212
        TR(1,n)=3.5;
    elseif n>=213 && n<=243
```

```
        TR(1,n)=3.3;
    elseif n>=244 && n<=273
        TR(1,n)=2.9;
    elseif n>=274 && n<=304
        TR(1,n)=2.6;
    elseif n>=305 && n<=334
        TR(1,n)=2.3;
    else
        TR(1,n)=2.2;
    end
%------------------------Daily loop--------------------------%
for h=1:24
    p=24*(n-1)+h;
    tttt(1,p)=p;
    AST(h,n)=h+(ET(1,n)/60)+(LON-LST)/15;
    HA(h,n)=15*(AST(h,n)-12);
coz(h,n)=sind(LATD)*sind(DA(1,n))+cosd(LATD)*cosd(DA(1,n))*cosd(
HA(h,n));
ZAD(h,n)=acosd(coz(h,n)); % Zenith angle in degree
coisr(h,n)=sind(DA(1,n))*sind(LATD)*cosd(SRA)-
sind(DA(1,n))*cosd(LATD)*sind(SRA)*cosd(SASR)+cosd(DA(1,n))*cosd
(LATD)*cosd(SRA)*cosd(HA(h,n))+cosd(DA(1,n))*sind(LATD)*sind(SRA
)*cosd(SASR)*cosd(HA(h,n))+cosd(DA(1,n))*sind(SRA)*sind(SASR)*si
nd(HA(h,n));

coisr1(h,n)=sind(DA(1,n))*sind(LATD)*cosd(SRA1)-
sind(DA(1,n))*cosd(LATD)*sind(SRA1)*cosd(SASR)+cosd(DA(1,n))*cos
d(LATD)*cosd(SRA1)*cosd(HA(h,n))+cosd(DA(1,n))*sind(LATD)*sind(S
RA1)*cosd(SASR)*cosd(HA(h,n))+cosd(DA(1,n))*sind(SRA1)*sind(SASR
)*sind(HA(h,n));

coisr2(h,n)=sind(DA(1,n))*sind(LATD)*cosd(SRA2)-
sind(DA(1,n))*cosd(LATD)*sind(SRA2)*cosd(SASR)+cosd(DA(1,n))*cos
d(LATD)*cosd(SRA2)*cosd(HA(h,n))+cosd(DA(1,n))*sind(LATD)*sind(S
RA2)*cosd(SASR)*cosd(HA(h,n))+cosd(DA(1,n))*sind(SRA2)*sind(SASR
)*sind(HA(h,n));

coisw(h,n)=sind(DA(1,n))*sind(LATD)*cosd(SWA)-
sind(DA(1,n))*cosd(LATD)*sind(SWA)*cosd(SASW)+cosd(DA(1,n))*cosd
(LATD)*cosd(SWA)*cosd(HA(h,n))+cosd(DA(1,n))*sind(LATD)*sind(SWA
)*cosd(SASW)*cosd(HA(h,n))+cosd(DA(1,n))*sind(SWA)*sind(SASW)*si
nd(HA(h,n));
    RBSR(h,n)=coisr(h,n)/coz(h,n);
    RBSR1(h,n)=coisr1(h,n)/coz(h,n);
    RBSR2(h,n)=coisr2(h,n)/coz(h,n);
    RBSW(h,n)=coisw(h,n)/coz(h,n);
    ab(h,n)=90-ZAD(h,n);
```

```
    abc(h,n)=(0.9+9.4*sind(ab(h,n)));
    abcd(h,n)=-TR(1,n)/abc(h,n); % Problem in this section
    std(h,n)=exp(abcd(h,n));
    IN(h,n)=IO(1,n)*std(h,n);
    IN(IN>1360)=0;
    IN(IN<1)=0;
    IN(IN<0)=0;  % kick out negative values
    IB(h,n)=IN(h,n)*coz(h,n);
    IB(IB<0)=0;  % kick out negative values
    ID(h,n)=(1/3)*(IO(1,n)-IN(h,n))*coz(h,n);
    ID(ID<0)=0;  % kick out negative values
    SR(h,n)=IB(h,n)+ID(h,n);
    SRActual(h,n)=SR(h,n)*(1-LFA*(CCF_1(h,n)/8)^LFB);
    IDActual(h,n)=SRActual(h,n)*(0.3+0.7*(CCF_1(h,n)/8)^2);
    IBActual(h,n)=SRActual(h,n)-IDActual(h,n);
    IBSR(h,n)=IBActual(h,n)*RBSR(h,n);
    IBSR(IBSR<0)=0;
    IBSR1(h,n)=IBActual(h,n)*RBSR1(h,n);
    IBSR1(IBSR1<0)=0;
    IBSR2(h,n)=IBActual(h,n)*RBSR2(h,n);
    IBSR2(IBSR2<0)=0;
    IBSW(h,n)=IBActual(h,n)*RBSW(h,n);
    IBSW(IBSW<0)=0;

TotalBeam(h,n)=IBSR(h,n)*(ASR*TSR*3.6)+IBSR1(h,n)*(ASR1*TSR*3.6)
+IBSR2(h,n)*(ASR2*TSR*3.6)+IBSW(h,n)*(ASW*TSW*3.6);
    % Diffused
    IDSR(h,n)=IDActual(h,n)*((1+cosd(SRA))/2);
    IFSR(h,n)=pg*SRActual(h,n)*((1-cosd(SRA))/2);
    IDSR1(h,n)=IDActual(h,n)*((1+cosd(SRA1))/2);
    IFSR1(h,n)=pg*SRActual(h,n)*((1-cosd(SRA1))/2);
    IDSR2(h,n)=IDActual(h,n)*((1+cosd(SRA2))/2);
    IFSR2(h,n)=pg*SRActual(h,n)*((1-cosd(SRA2))/2);
    IDSW(h,n)=IDActual(h,n)*((1+cosd(SWA))/2);
    IFSW(h,n)=pg*SRActual(h,n)*((1-cosd(SWA))/2);

TotalDiffuse(h,n)=(IDSR(h,n)+IFSR(h,n))*(ASR*TSR*3.6)+(IDSR1(h,n
)+IFSR1(h,n))*(ASR1*TSR*3.6)+(IDSR2(h,n)+IFSR2(h,n))*(ASR2*TSR*3
.6)+(IDSW(h,n)+IFSW(h,n))*(ASW*TSW*3.6);
    %%%%%%%%%%%%%%%%%%%%
    ST(h,n)=TotalBeam(h,n)+TotalDiffuse(h,n);
end
end
```

Appendix B

B.1 Copyright Permissions

Appendix B includes the copyright permissions for the published and unpublished manuscripts presented in this thesis. For manuscripts that form part of a thesis, the College of Graduate and Postdoctoral Studies (CGPS) requires a written request from:

- the publisher (copyright holder) for previously published manuscripts, and
- the co-author(s) for unpublished manuscripts.

The permissions for using the published manuscripts in this thesis are presented in Sections B.1, B.2, and B.3, and the permission for using the unpublished manuscripts are presented in Section B.4.

B.1.1 Permission for manuscript used in Chapter 2

3/2/2018 Rightslink® by Copyright Clearance Center

Copyright Clearance Center RightsLink®

Home | Account Info | Help

Taylor & Francis
Taylor & Francis Group

Title:	Evaluation of a cloud cover based model for estimation of hourly global solar radiation in Western Canada
Author:	Md Shamim Ahamed, Huiqing Guo, Karen Tanino
Publication:	International Journal of Sustainable Energy
Publisher:	Taylor & Francis
Date:	Mar 1, 2018

Rights managed by Taylor & Francis

Logged in as:
Md Shamim Ahamed
University of Saskachewan
Account #:
3001249291
LOGOUT

Thesis/Dissertation Reuse Request

Taylor & Francis is pleased to offer reuses of its content for a thesis or dissertation free of charge contingent on resubmission of permission request if work is published.

BACK | CLOSE WINDOW

Copyright © 2018 Copyright Clearance Center, Inc. All Rights Reserved. Privacy statement. Terms and Conditions.
Comments? We would like to hear from you. E-mail us at customercare@copyright.com

B.1.2 Permission for manuscript used in Chapter 2

Dear Mr. Ahamed,

As an Elsevier journal author, you retain the right to include the article in a thesis or dissertation (provided that this is not to be published commercially) whether in full or in part, subject to proper acknowledgment; see https://www.elsevier.com/about/our-business/policies/copyright/personal-use for more information. As this is a retained right, no written permission from Elsevier is necessary.

If I may be of further assistance, please let me know.

Best of luck with your thesis and best regards,

Laura

Laura Stingelin

Permissions Helpdesk Associate

ELSEVIER | Global E-Operations Books

+1 215-239-3867 office

l.stingelin@elsevier.com

Contact the Permissions Helpdesk

+1 800-523-4069 x3808 | permissionshelpdesk@elsevier.com

B.1.3 Permission for manuscript used in Chapter 5

This Agreement between University of Saskatchewan - Md Shamim Ahamed ("You") and John Wiley and Sons ("John Wiley and Sons") consists of your license details and the terms and conditions provided by John Wiley and Sons and Copyright Clearance Center.

License Number	4287240899968
License date	Feb 13, 2018
Licensed Content Publisher	John Wiley and Sons
Licensed Content Publication	International Journal of Energy Research
Licensed Content Title	Energy-efficient design of greenhouse for Canadian Prairies using a heating simulation model
Licensed Content Author	Md Shamim Ahamed,Huiqing Guo,Karen Tanino
Licensed Content Date	Feb 13, 2018
Licensed Content Pages	1
Type of use	Dissertation/Thesis
Requestor type	Author of this Wiley article
Format	Print and electronic
Portion	Full article
Will you be translating?	No
Title of your thesis / dissertation	THERMAL ENVIRONMENT MODELING AND OPTIMIZATION OF GREENHOUSE IN COLD REGIONS
Expected completion date	Mar 2018
Expected size (number of pages)	238
Requestor Location	University of Saskatchewan 1004-107 Cumberland Ave S Saskatoon, SK s7n2r6. Canada Attn: University of Saskatchewan
Publisher Tax ID	EU826007151
Total	0.00 CAD

B.1.4 Permission for manuscript used in Chapter 4, 6-8

The manuscript used in Chapter 4, 6-8 are unpublished, and thus copyright permissions are obtained from the coauthors of the papers (Huiqing Guo, Lisa Taylor, and Karen Tanino) as follows.

Copyright Permission Request Form

The manuscripts presented in Chapter 4, 6-8 would be published as chapter of my Ph.D. thesis, and to be submitted to the College of Engineering at the University of Saskatchewan. The authors contributing in the completion of this manuscript are Md Shamim Ahamed, Huiqing Guo, and Karen Tanino.

I am requesting permission to use the materials described in aforementioned manuscripts in my Ph.D. thesis. Please indicate agreement by signing below.

Sincerely,
Md Shamim Ahamed
March, 2018

Permission granted by: Professor Huiqing Guo
Signature:
Date:

Copyright Permission Request Form

The manuscripts presented in Chapter 4, 6-8 would be published as chapter of my Ph.D. thesis, and to be submitted to the College of Engineering at the University of Saskatchewan. The authors contributing in the completion of this manuscript are Md Shamim Ahamed, Huiqing Guo, and Karen Tanino.

I am requesting permission to use the materials described in aforementioned manuscripts in my Ph.D. thesis. Please indicate agreement by signing below.

Sincerely,

Md Shamim Ahamed

March, 2018

Permission granted by: Professor Karen Tanino

Signature:

Date:

Copyright Permission Request Form

I am preparing the manuscript titled "Heating demand and economic feasibility analysis for year-round vegetable production in Canadian Prairies' greenhouses" to be published as the sixth chapter of my Ph.D. thesis, and to be submitted to the College of Engineering at the University of Saskatchewan. The authors contributing in the completion of this manuscript are Md Shamim Ahamed, Huiqing Guo, Lisa Taylor, and Karen Tanino.

I am requesting permission to use the materials described in aforementioned manuscript in my Ph.D. thesis and any subsequent editions that may be prepared at the University of Saskatchewan. Please indicate agreement by signing below.

Sincerely,
Md Shamim Ahamed
March, 2018

Permission granted by: Lisa Taylor
Signature:
Date:

References

Abak, K., Bascetincelik, A., Baytorun, N., Altuntas, Ö., Öztürk, H.H., 1993. Influence of double plastic cover and thermal screens on greenhouse temperature, yield and quality of tomato, in: In II Symposium on Protected Cultivation of Solanacea in Mild Winter Climates 366. pp. 149–155.

Aberkani, K., Gosselin, A., Vineberg, S., Dorais, M., 2006. Effects of insulating foams between double polythylene films on light transmission, growth and productivity of greenhouse tomato plants grown under supplemental lighting, in: Acta Horticulturae. pp. 449–454.

Aberkani, K., Hao, X., Halleux, D. De, Papadopoulos, A.P., Dorais, M., Vineberg, S., Gosselin, A., 2011. Energy saving achieved by retractable liquid foam between double polyethylene films covering greenhouses. Trans. ASABE 54, 275–284.

Adaro, J.A., Galimberti, P.D., Lema, A.I., Fasulo, A., Barral, J.R., 1999. Geothermal contribution to greenhouse heating. Appl. Energy 64, 241–249. doi:10.1016/S0306-2619(99)00049-5

Ahamed, M.S., Guo, H., Tanino, K., 2018a. Energy efficient design of greenhouse for Canadian prairies using heating simulation model. Int. J. Energy Res. 1–10.

Ahamed, M.S., Guo, H., Tanino, K., 2018b. Development of a thermal model for simulation of supplemental heating requirements in Chinese-style solar greenhouses. Manuscr. Submitt. Publ.

Ahamed, M.S., Guo, H., Tanino, K., 2017a. Evaluation of Cloud Cover Based Model for Simulation of Hourly Global Solar Radiation in Western Canada, in: CSBE/SCGAB 2017 Annual Conference. Canadian Society of Bioengineering, Canad Inns Polo Park, Winnipeg, MB, 6-10 August,2017., pp. 1–15.

Ahamed, M.S., Guo, H., Tanino, K., 2017b. A quasi-steady state model for predicting the heating requirements of conventional greenhouses in cold regions. Inf. Process. Agric. 1–13. doi:10.1016/j.inpa.2017.12.003

Ahamed, M.S., Guo, H., Tanino, K.K., 2016. Modeling of heating requirement in Chinese Solar Greenhouse, in: 2016 American Society of Agricultural and Biological Engineers Annual International Meeting, ASABE 2016. doi:10.13031/aim.20162455669

Al-ajmi, F.F., Hanby, V.I., 2008. Simulation of energy consumption for Kuwaiti domestic buildings. Energy Build. 40, 1101–1109. doi:10.1016/j.enbuild.2007.10.010

Al-Helal, I.M., Abdel-Ghany, A.M., 2011. Energy partition and conversion of solar and thermal radiation into sensible and latent heat in a greenhouse under arid conditions. Energy Build. 43, 1740–1747. doi:10.1016/j.enbuild.2011.03.017

Al-Hussaini, H., Suen, K.O., 1998. Using shallow solar ponds as a heating source for greenhouses in cold climates. Energy Convers. Manag. 39, 1369–1376.

Al-Mostafa, Z.A., Maghrabi, A.H., Al-Shehri, S.M., 2012. Assessment of sunshine based global radiation models using data measured in Riyadh, Saudi Arabia. J. Energy Inst. 85, 114–121.

doi:10.1179/174396711X13116932752038

Alberta Agriculture and Rural Development, 2003. Commercial Greenhouse Tomato Production: Introduction [WWW Document]. URL http://www1.agric.gov.ab.ca/$Department/deptdocs.nsf/all/opp7556 (accessed 7.12.17).

Albright, L.D., 1990. Environment control for animals and plants. American Society of Agricultural Engineers, Michigan, USA.

Aldrich, R.A., Bartok, J.W., 1994. Greenhouse Enginering. In: Hill (eds).Dynamic modeling of tree growth and energy use in a nursery greenhouse using Matlab and Simulink., 3rd Editio. ed.

Andersson, N.E., 2010. Properties of thermal screens used for energy saving in greenhouses, in: In International Conference on Agricultural Engineering-AgEng 2010: Towards Environmental Technologies. Clermont-Ferrand, France.

Andersson, N.E., Nielsen, O.F., 2000. Energy Consumption , Light Distribution and Plant Growth in Greenhouse partly insulated with non-transparent Material. Gartenbauwissenschaft 65, 190–194.

Andrews, R., Pearce, J.M., 2011. Environmental and economic assessment of a greenhouse waste heat exchange. J. Clean. Prod. 19, 1446–1454. doi:10.1016/j.jclepro.2011.04.016

Anifantis, A.S., Colantoni, A., Pascuzzi, S., 2017. Thermal energy assessment of a small scale photovoltaic, hydrogen and geothermal stand-alone system for greenhouse heating. Renew. Energy 103, 115–127. doi:10.1016/j.renene.2016.11.031

ASABE, 2006. Heating, ventilating, and cooling greenhouse. ASABE standards., 53rd ed. ASABE, St. Joseph Charter Township, Michigan, USA.

ASHRAE, 2013. ASHRAE Handbook of Fundamentals, SI Edition. ed. American Society of Heating Ventilation Refrigeration and Air-conditioning Engineers, Atlanta, USA.

Avissar, R., Mahrer, Y., 1982. Verification study of a numerical greenhouse microclimate model. Trans. ASAE 25, 1711–1720.

Badescu, V., 2002. A new kind of cloudy sky model to compute instantaneous values of diffuse and global solar irradiance. Theor. Appl. Climatol. 72, 127–136. doi:10.1007/s007040200017

Badescu, V., 1999. Correlations to estimate monthly mean daily solar global irradiation: Application to Romania. Energy 24, 883–893. doi:10.1016/S0360-5442(99)00027-4

Badescu, V., Dumitrescu, A., 2016. CMSAF products Cloud Fraction Coverage and Cloud Type used for solar global irradiance estimation. Meteorol. Atmos. Phys. 128, 525–535. doi:10.1007/s00703-015-0424-y

Badescu, V., Dumitrescu, A., 2014a. Simple models to compute solar global irradiance from the CMSAF product Cloud Fractional Coverage. Renew. Energy 66, 118–131. doi:10.1016/j.renene.2013.11.068

Badescu, V., Dumitrescu, A., 2014b. New types of simple non-linear models to compute solar global irradiance from cloud cover amount. J. Atmos. Solar-Terrestrial Phys. 117, 54–70. doi:10.1016/j.jastp.2014.05.010

Badgery, P.J., James, L., 2010. Commercial Greenhouse Cucumber Production. Industry & Investment NSW.

Bailey, A., Critten, D.L., 1982. Greenhouse solar collection with a heat storage system. In: Sethi & Sharma (eds). Survey and evaluation of heating technologies for worldwide agricultural greenhouse applications. Sol. Energy 82, 832–859.

Bailey, B.J., 1985. Wind dependent control of greenhouse temperature, in: Symposium Greenhouse Climate and Its Control 174. pp. 381–386.

Bailey, B.J., 1981. The reduction of thermal radiation in glasshouses by thermal screens. J. Agric. Eng. Res. 26, 215–224. doi:10.1016/0021-8634(81)90106-2

Bailey, B.J., Winspear, K., 1975. Reducing the heat requirement of a glasshouse. In: Chandra (eds) Predicting the effects of greenhouse orientation and insulation on energy conservation. Unpubl. Masters thesis, Dep. Agric. Eng. Univ. Manitoba.

Baille, A., 1993. Artificial light source for crop production. In: Castilla (eds): Greenhouse Technology and Mangement.

Bakirci, K., 2008. Correlations for Estimation of Solar Radiation on Horizontal Surfaces. J. Energy Eng. 134, 130–134.

Bakker, J.C., 2006. Energy saving greenhouses. Chron. Hortivulturae 49, 19–23.

Bakker, J.C., 1995. Greenhouse climate control-an integrated approach. Wageningen Academic Pub, Wegeningen, The Netherland.

Bakker, J.C., 1991. Analysis of Humidity Effects on Growth and Production of Glasshouse Fruit Vegetables. Wageningen University, The Netherland.

Bakos, G.C., Fidanidis, D., Tsagas, N.F., 1999. Greenhouse heating using geothermal energy 28, 759–765.

Balghouthi, M., Kooli, S., Farhat, A., Daghari, H., Belghith, A., 2005. Experimental investigation of thermal and moisture behaviors of wet and dry soils with buried capillary heating system. Sol. Energy 79, 669–681. doi:10.1016/j.solener.2005.06.011

Banboul, T., Banbouserale, J., 1987. Heating of greenhouse with solar energy. In: Sethi, & Sharma (eds). Survey and evaluation of heating technologies for worldwide agricultural greenhouse applications. Sol. Energy 82, 832–859.

Baptista, F.J., 2007. Modelling the climate in unheated tomato greenhouses and predicting Botrytis cinerea infection. Evora University.

Barr, A.G., McGinn, S.M., Cheng, S.B., 1996. A comparison of methods to estimate daily global solar irradiation from other climatic variables on the Canadian prairies. Sol. Energy 56, 213–

224. doi:10.1016/0038-092X(95)00100-6

Bartok, J.W., 2015. Geothermal Heat for Greenhouses [WWW Document]. URL http://ipm.uconn.edu/documents/raw2/html/660.php?aid=660 (accessed 6.28.17).

Bartok, J.W., 2001. Energy conservation for commercial greenhouses. Natural Resource, Agriculture, and Engineering Service, USA.

Bartzanas, T., Tchamitchian, M., Kittas, C., 2005. Influence of the Heating Method on Greenhouse Microclimate and Energy Consumption. Biosyst. Eng. 91, 487–499. doi:10.1016/j.biosystemseng.2005.04.012

Benli, H., 2013. A performance comparison between a horizontal source and a vertical source heat pump systems for a greenhouse heating in the mild climate Elazığ, Turkey. Appl. Therm. Eng. 50, 197–206. doi:10.1016/j.applthermaleng.2012.06.005

Benli, H., 2011. Energetic performance analysis of a ground-source heat pump system with latent heat storage for a greenhouse heating. Energy Convers. Manag. 52, 581–589. doi:10.1016/j.enconman.2010.07.033

Bennett, I., 1969. Correlation of daily insolation with daily total sky cover, opaque sky cover and percentage of possible sunshine. Sol. Energy 12, 391–393.

Berroug, F., Lakhal, E.K., El Omari, M., Faraji, M., El Qarnia, H., 2011. Thermal performance of a greenhouse with a phase change material north wall. Energy Build. 43, 3027–3035. doi:10.1016/j.enbuild.2011.07.020

Beshada, E., Zhang, Q., Boris, R., 2006. Winter performance of a solar energy greenhouse in southern Manitoba. Can. Biosyst. Eng. 48, 1–8.

Bibbiani, C., Campiotti, C.A., Schettini, E., Vox, G., 2017. A sustainable energy for greenhouses heating in Italy: Wood biomass. Acta Hortic. 1170, 523–530. doi:10.17660/ActaHortic.2017.1170.65

Bisaglia, C., Romano, E., Cutini, M., Nucci, F., 2011. Conversion of a high-demanding thermal-energy level greenhouse from conventional oil heating system to wood-based renewable sources heating system for tropical plants production in mediterranean conditions, in: Acta Horticulturae. pp. 421–428.

Black, J.N., 1956. The distribution of solar radiation over the Earth's surface. Arch. für Meteorol. Geophys. und Bioklimatologie 7, 165–189. doi:10.1007/BF02243320

Bland, A., Khzouz, M., Statheros, T., Gkanas, E.I., 2017. PCMs for Residential Building Applications: A Short Review Focused on Disadvantages and Proposals for Future Development. Buildings 7, 78. doi:10.3390/buildings7030078

Blom, T.J., Ingratta, F.J., Hughes, J., 1981. Greenhouses. In: Kavga et al. (eds). Investigation of the potential of long wave radiation heating to reduce energy consumption for greenhouse heating. In International Symposium on High Technology for Greenhouse System Management.

Blom, T.J., Straver, W.A., Ingratta, F.J., Khosla, S., Brown, W., 2002. Carbon dioxide in greenhouses. Ontario. Ministry of Agriculture and Food [WWW Document]. URL http://www.omafra.gov.on.ca/english/crops/facts/00-077.htm (accessed 7.12.17).

Boodley, J.W., 1998. The commercial greenhouse, 2nd ed. Delmar Publishers.

Borhan, M.S., 2007. Effects of temperature integration regimes with low pre-night temperatures on energy consumption, microclimate, and fruit yield in early greenhouse tomato production, in: International Symposium on High Technology for Greenhouse System Management: Greensys2007 801. pp. 473–478.

Bot, G.P.A., 1983. Greenhouse climate: from physical processes to a dynamic model. University of Wageningen.

Bouadila, S., Lazaar, M., Skouri, S., Kooli, S., Farhat, A., 2014. Assessment of the greenhouse climate with a new packed-bed solar air heater at night, in Tunisia. Renew. Sustain. Energy Rev. 35, 31–41. doi:10.1016/j.rser.2014.03.051

Bouhdjar, A., Belhamel, M., Belkhiri, F.E., Boulbina, A., 1996. Performance of sensible heat storage in a rockbed used in a tunnel greenhouse. Renew. Energy 9, 724–728.

Boulard, T., Baille, A., Gall, F.L., 1991. Study of various methods of cooling on climate and tomato transpiration in greenhouse. Agronomie 11, 259–274.

Boulard, T., Wang, S., 2000. Greenhouse crop transpiration simulation from external climate conditions. Agric. For. Meteorol. 100, 25–34. doi:10.1016/S0168-1923(99)00082-9

Brault, D., Gueymard, C., Boily, R., Gosselin, A., 1989. Contribution of HPS lighting to the heating requirements of a greenhouse, in: American Society of Agricultural Engineers Conference. ASABE, Michigan, p. 4039.

Brendenbeck, H., 1992. The use of waste heat from a power plant for greenhouse heating in commercial application in Germany. In: Sethi and Sharma (eds). Survey and evaluation of heating technologies for worldwide agricultural greenhouse applications. Sol. Energy 82, 832–859.

Breuer, J.J.G., Short, T.H., 1985. Greenhouse energy demands comparisons for the Netherlands and Ohio, USA. Acta Hortic. 174, 145–153.

Bricault, M., 1982. Use of heat surplus from a greenhouse for soil heating. In: Sethi and Sharma (eds). Survey and evaluation of heating technologies for worldwide agricultural greenhouse applications. Sol. Energy 82, 832–859.

Brinsfield, R., Yaramanoglu, M., Wheaton, F., 1984. Ground level solar radiation prediction model including cloud cover effects. Sol. Energy 33, 493–499.

Buschermohle, M.J., Grandle, G.F., 2002. Controlling the environment in greenhouses used for tomato production. Agricultural Extension Service, The University of Tennessee.

Cakır, U., Sahin, E., 2015. Using solar greenhouses in cold climates and evaluating optimum type

according to sizing, position and location: A case study. Comput. Electron. Agric. 117, 245–257. doi:10.1016/j.compag.2015.08.005

Campen, J.B., Bot, G.P.A., De Zwart, H.F., 2003. Dehumidification of Greenhouses at Northern Latitudes. Biosyst. Eng. 86, 487–493. doi:10.1016/j.biosystemseng.2003.08.008

Caouette, P., Gauthier, L., Casault, B., Marquis, A., 1990. Temperature and radiation distribution in an infrared-heated greenhouse with a polyethylene cover. Can. Agric. Eng. 32, 111–116.

Carnegie, E.J., Niles, P.W., Walter, V.R., 1983. Shallow solar ponds to heat greenhouses, in: III International Symposium on Energy in Protected Cultivation 148. pp. 791–798.

Castilla, N., 2013. Greenhouse Technology and Management, 2nd ed. Cabi, Oxfordshire, UK.

Cemek, B., Demir, Y., Uzun, S., Ceyhan, V., 2006. The effects of different greenhouse covering materials on energy requirement, growth and yield of aubergine. Energy 31, 1444–1452. doi:10.1016/j.energy.2005.08.004

Chai, L., Ma, C., Ni, J.-Q., 2012. Performance evaluation of ground source heat pump system for greenhouse heating in northern China. Biosyst. Eng. 111, 107–117. doi:10.1016/j.biosystemseng.2011.11.002

Chalabi, Z.S., Biro, A., Bailey, B.J., Aikman, D.P., Cockshull, K.E., 2002. Optimal control strategies for carbon dioxide enrichment in greenhouse tomato crops, part II: Using the exhaust gases of natural gas fired boilers. Biosyst. Eng. 81, 323–332. doi:10.1006/bioe.2001.0020

Challa, H., Heuvelink, E., Meeteren, U., 1995. Crop growth and development. In: Spanomitsios (eds). SE—Structure and Environment: Temperature Control and Energy Conservation in a Plastic Greenhouse. J. Agric. Eng. Res. 80, 251–259.

Chandra, P., 1976. Predicting the effects of greenhouse orientation and insulation on energy conservation. Masters thesis, University of Manitoba.

Chandra, P., Albright, L.D., 1981. Analytical determination of the effect on greenhouse heating requirements of using night curtains. Trans Am. Soc. Agric Eng 23, 994–1000.

Chau, J., Sowlati, T., Sokhansanj, S., Preto, F., Melin, S., Bi, X., 2009a. Techno-economic analysis of wood biomass boilers for the greenhouse industry. Appl. Energy 86, 364–371. doi:10.1016/j.apenergy.2008.05.010

Chau, J., Sowlati, T., Sokhansanj, S., Preto, F., Melin, S., Bi, X., 2009b. Economic sensitivity of wood biomass utilization for greenhouse heating application. Appl. Energy 86, 616–621. doi:10.1016/j.apenergy.2008.11.005

Chen, J., Yang, J., Zhao, J., Xu, F., Shen, Z., Zhang, L., 2015. Energy demand forecasting of the greenhouses using nonlinear models based on model optimized prediction method. Neurocomputing 174, 1087–1100. doi:10.1016/j.neucom.2015.09.105

Chen, T.W., Nguyen, T.M.N., Kahlen, K., Stutzel, H., 2014. Quantification of the effects of

architectural traits on dry mass production and light interception of tomato canopy under different temperature regimes using a dynamic functional-structural plant model. J. Exp. Bot. 65, 6399–6410. doi:10.1093/jxb/eru356

Chiapale, J.P., Kittas, C., 1981. Estimation regionale des besoins de chauffage des serres. Acta Hortic. 115, 493–503.

Chiasson, A., 2006. Greenhouse heating with geothermal heat pump systems. 2006 ASABE Annu. Int. Meet. Portland, … 300, 2–5.

Chinese, D., Meneghetti, A., Nardin, G., 2005. Waste-to-energy based greenhouse heating : exploring viability conditions through optimisation models. Renew. Energy 30, 1573–1586. doi:10.1016/j.renene.2004.11.008

Chou, S.K., Chua, K.J., Ho, J.C., Ooi, C.L., 2004. On the study of an energy-efficient greenhouse for heating, cooling and dehumidification applications. Appl. Energy 77, 355–373. doi:10.1016/S0306-2619(03)00157-0

Clark, G., Allen, C., 1978. The estimation of atmospheric radiation for clear and cloudy skies., in: Proc. 2nd Nat. Passive Solar Conf. Philadelphia, uSA, p. 676.

Connellan, G., 1986. Solar greenhouse using liquid collectors. In: Sethi and Sharma (eds). Survey and evaluation of heating technologies for worldwide agricultural greenhouse applications. Sol. Energy 82, 832859.

Cooper, P.I., Fuller, R.J., 1983. A transient model of the interaction between crop, environment and greenhouse structure for predicting crop yield and energy consumption. J. Agric. Eng. Res. 28, 401–417.

Coulon G., Wacquant, C., 1984. Greenhouse climate management. In: Gupta & Chandra (eds). Effect of greenhouse design parameters on conservation of energy for greenhouse environmental control. Energy 27, 777–794.

Cui, Q., Wang, J., 2002. Temperature and energy-saving effects of applying the mobile double layers thermal screen in a greenhouse. Transcations Chinese Soc. Agric. Eng. 18, 111–114.

Cutforth, H.W., Judiesch, D., 2007. Long-term changes to incoming solar energy on the Canadian Prairie. Agric. For. Meteorol. 145, 167–175. doi:10.1016/j.agrformet.2007.04.011

D'Arpa, S., Colangelo, G., Starace, G., Petrosillo, I., Bruno, D.E., Uricchio, V., Zurlini, G., 2016. Heating requirements in greenhouse farming in southern Italy: evaluation of ground-source heat pump utilization compared to traditional heating systems. Energy Effic. 9, 1065–1085. doi:10.1007/s12053-015-9410-y

Dawson, J.R., Winspear, K.W., 1976. The reduction of glasshouse heat losses by internal blinds. J. Agric. Eng. Res. 21, 431–438. doi:10.1016/0021-8634(76)90062-7

De Jong, R., Stewart, D.W., 1993. Estimating global solar radiation from common meteorological observations in western Canada. Can. J. Plant Sci. 73, 509–518. doi:10.4141/cjps93-068

de Zwart, H.F., 2016. Chinese–Dutch cooperation on the Chinese Solar Greenhouse experiment in Shouguang. No. 1399. Wageningen UR Greenhouse Horticulture.

De Zwart, H.F., 2014. Energy conserving dehumidification of greenhouses. Acta Hortic. doi:10.17660/ActaHortic.2014.1037.21

De Zwart, H.F., 1996. Analyzing energy-saving options in greenhouse cultivation using a simulation model. PhD Thesis, University of Wageningen.

Deiana, A., Torino, P., To, I.T.T., 2014. Energy performance optimization of typical Chinese solar greenhouses by means of dynamic simulation, in: Interanational Conference of Agricultural Engineering. Zurich, pp. 6–10.

Delwich, S.R., Willits, D.H., 1984. The effect of condensation on the heat transfer through polyethylene films. Trans. ASAE 5, 1476–1482.

Demers, D.A., Dorais, M., Wien, C.H., Gosselin, A., 1998. Effects of supplemental light duration on greenhouse tomato (Lycopersicon esculentum Mill.) plants and fruit yields. Sci. Hortic. (Amsterdam). 74, 295–306.

Denzer, A., Wang, L., Thomas, Y., McMorrow, G., 2017. Greenhouse Design with Waste Heat: Principles and Practices, in: AEI 2017. pp. 440–455.

Dieleman, J.A.., Hemming, S., 2009. Energy saving: from engineering to crop management, in: International Symposium on High Technology for Greenhouse Systems: GreenSys2009 893. pp. 65–75.

Djevic, M., Dimitrijevic, A., 2009. Energy consumption for different greenhouse constructions. Energy 34, 1325–1331. doi:10.1016/j.energy.2009.03.008

Dorais, M., 2003. The use of supplemental lighting for vegetable crop production: light intensity, crop response, nutrition, crop management, cultural practices, in: Canadian Greenhouse Conference. Toronto, Canada, pp. 1–8.

Dragićević, S.M., 2011. Determining the optimum orientation of a greenhouse on the basis of the total solar radiation availability. Therm. Sci. 15, 215–221. doi:10.2298/TSCI100220057D

Du, J., Bansal, P., Huang, B., 2012. Simulation model of a greenhouse with a heat-pipe heating system. Appl. Energy 93, 268–276. doi:10.1016/j.apenergy.2011.12.069

Duffie, J., Beckman, W., 2006. Solar engineering of thermal process, 3rd ed. Wiley-Interscience Publication, New Jersey, USA.

Duncan, G.A., Walker, J.N., Turner, L.W., 1979. Energy for greenhouses Part 1: Energy Conservation. University of Kentucky, College of Agriculture, Department of Agricultural Engineering.

Dutt, D.K., Rai, S.N., Tiwari, G.N., Yadav, Y.P., 1987. Transient analysis of a winter greenhouse. Energy Convers. Manag. Manag. 27, 141–147.

Eggers, H., 1975. Investigations on the microclimate under plastic film covers. In: Papadakis et al.

(eds). Review Paper (SE—Structures and Environment): Radiometric and thermal properties of, and testing methods. J. Agric. Eng. Res. 77, 7–38.

EIA, 2016. How much carbon dioxide is produced when different fuels are burned? [WWW Document]. URL https://www.eia.gov/tools/faqs/faq.cfm?id=73&t=11. (accessed 12.29.16).

El-Maghlany, W.M., Teamah, M.A., Tanaka, H., 2015. Optimum design and orientation of the greenhouses for maximum capture of solar energy in North Tropical Region. Energy Convers. Manag. 105, 1096–1104. doi:10.1016/j.enconman.2015.08.066

El-Metwally, M., 2004. Simple new methods to estimate global solar radiation based on meteorological data in Egypt. Atmos. Res. 69, 217–239. doi:10.1016/j.atmosres.2003.09.002

Elings, A., Kempkes, F.L.K., Kaarsemaker, R.C., Ruijs, M.N.A., van de Braak, N.J., Dueck, T.A., 2005a. The energy balance and energy saving measures in greenhouse tomato cultivation. ISHS Acta Hortic. 691, 67–74. doi:10.17660/ActaHortic.2005.691.5

Elings, A., Kempkes, F.L.K., Kaarsemaker, R.C., Ruijs, M.N.A., Van de Braak, N.J., Dueck, T.A., 2005b. The energy balance and energy-saving measures in greenhouse tomato cultivation, in: International Conference on Sustainable Greenhouse Systems-Greensys. pp. 67–74.

Elwell, D.L., Short, T.H., Fynn, R.P., 1984. A double-plastic greenhouse with a polystyrene energy screen and floor heating for winter tomato production. Acta Hortic. 148, 461–466.

Enshayan, K., 1984. Performance of a pellet insulation system for greenhouses. The Ohio State University.

Esen, M., Yuksel, T., 2013. Experimental evaluation of using various renewable energy sources for heating a greenhouse. Energy Build. 65, 340–351. doi:10.1016/j.enbuild.2013.06.018

Fabrizio, E., 2012. Energy reduction measures in agricultural greenhouses heating: Envelope, systems and solar energy collection. Energy Build. 53, 57–63. doi:10.1016/j.enbuild.2012.07.003

Facchini, U., Marelli, G., Canzi, L., 1983. Solar (heated) greenhouses with low energy consumption. Colt. Protette 12, 31–35.

Farah, J., 1987. Utilization of solar energy in greenhouse. In: Sethi & Sharma (eds). Survey and evaluation of heating technologies for worldwide agricultural greenhouse applications. Sol. Energy 82, 832–859.

Fatnassi, H., Boulard, T., Lagier, J., 2004. Simple indirect estimation of ventilation and crop transpiration rates in a greenhouse. Biosyst. Eng. 88, 467–478. doi:10.1016/j.biosystemseng.2004.05.003

Feuilloley, P., Issanchou, G., Jacques, J.C., Guillaume, S., Mekikdijan, C., F., M.J., 1994. Effects of condensation on plastic "lms used for greenhouses. In: Papadakis et al. (eds). Review Paper (SE—Structures and Environment): Radiometric and thermal properties of, and testing methods for, greenhouse covering. J. Agric. Eng. Res. 77, 7–38.

Fisher, P., Donnelly, C., Faust, J., 2001. Evaluating supplemental light for your greenhouse. Ohio Flor. Assoc. Bull. 6.

Fitz-Rodríguez, E., Kubota, C., Giacomelli, G.A., Tignor, M.E., Wilson, S.B., McMahon, M., 2010. Dynamic modeling and simulation of greenhouse environments under several scenarios: A web-based application. Comput. Electron. Agric. 70, 105–116. doi:10.1016/j.compag.2009.09.010

Florides, G., Kalogirou, S., 2004. Measurements of ground temperature at various depths, in: Proceedings of the 3rd International Conference on Sustainable Energy Technologies. Nottingham, UK, pp. 1–6.

Fotiades, I., 1987. Use of solar energy for heating of greenhouses. In: Sethi and Sharma (eds). Survey and evaluation of heating technologies for worldwide agricultural greenhouse applications. Sol. Energy 82, 832–859.

Francois, J., 1987. Use of solar energy for heating of greenhouses in mild winter climates. In: Sethi, & Sharma (eds). Survey and evaluation of heating technologies for worldwide agricultural greenhouse applications. Sol. Energy 82, 832–859.

Fuller, R.J., Sites, R., Blackwell, J., 1984. A thermal screen system for greenhouse energy conservation. In: Gupta & Chandra (eds). Effect of greenhouse design parameters on conservation of energy for greenhouse environmental control. Energy 27, 777–794.

Gao, Z., 2012. Dehumidification of greenhouses in cold regions. MS thesis. Saskatoon,Canada, University of Saskatchewan.

Garzoli, K., 1986. The Australian Greenhouse Handbook. In: Spanomitsios (eds). SE—Structure and Environment: Temperature Control and Energy Conservation in a Plastic Greenhouse. J. Agric. Eng. Res. 80, 251–259.

Garzoli, K., 1985. A simple greenhouse climate model, in: Symposium Greenhouse Climate and Its Control. pp. 393–400.

Garzoli, K. V, Blackwell, J., 1987. An Analysis of the Nocturnal Heat Loss from a Double Skin Plastic Greenhouse. J. Agric. Eng. Res. 36, 75–85.

Garzoli, K. V, Blackwell, J., 1981. An Analysis of the Nocturnal Skin Plastic Heat Loss from a Single Greenhouse. J. Agric. Eng. Res. 203–214.

Gauthier, C., Lacroix, M., Bernier, H., 1997. Numerical simulation of soil heat exchanger-storage systems for greenhouses. Sol. Energy 60, 333–346.

Ghasemi, H.M., Ajabshirchi, Y., Ranjbar, S.F., Matloobi, M., 2016. Solar energy conservation in greenhouse: Thermal analysis and experimental validation. Renew. Energy 96, 509–519. doi:10.1016/j.renene.2016.04.079

Ghosal, M.K., Tiwari, G.N., 2006. Modeling and parametric studies for thermal performance of an earth to air heat exchanger integrated with a greenhouse. Energy Convers. Manag. 47, 1779–1798. doi:10.1016/j.enconman.2005.10.001

Ghosal, M.K., Tiwari, G.N., 2004. Mathematical modeling for greenhouse heating by using thermal curtain and geothermal energy. Sol. Energy 76, 603–613. doi:10.1016/j.solener.2003.12.004

Ghosal, M.K., Tiwari, G.N., Das, D.K., Pandey, K.P., 2005. Modeling and comparative thermal performance of ground air collector and earth air heat exchanger for heating of greenhouse. Energy Build. 37, 613–621. doi:10.1016/j.enbuild.2004.09.004

Gilli, C., Kempkes, F., Munoz, P., Montero, J.I., Giuffrida, F., Baptista, F.J., Stepowska, A., Stanghellini, C., 2017. Potential of different energy saving strategies in heated greenhouse, in: Acta Horticulturae. pp. 467–474. doi:10.17660/ActaHortic.2017.1164.61

Gitman, L.J., 1977. Capturing risk exposure in the evaluation of capital budgeting projects. Eng. Econ. 22, 261–276.

Goebertus, T.M., 1988. The twofold effect of an aluminum screen: a temperature increase in winter and a temperature decrease in summer. Eng. Econ. Asp. Energy Sav. Prot. Cultiv. 245, 470–475.

Gomez, C., Mitchell, C.A., 2013. Supplemental lighting for greenhouse-grown tomatoes:Intercanopy LED towers vs. overhead HPS lamps, in: International Symposium on New Technologies for Environment Control, Energy-Saving and Crop Production in Greenhouse and Plant 1037. pp. 855–862.

Government of Canada, 2017. Engineering Climate Datasets-Canadian Weather Year for Energy Calculation (CWEC) [WWW Document]. URL http://climate.weather.gc.ca/prods_servs/engineering_e.html (accessed 7.20.08).

Grafiadellis, I., Mattas, K., Maloupa, E., Tzouramani, I., Galanopoulos, K., 2000. An economic analysis of soilless culture in gerbera production. HortScience 35, 300–303.

Grafiadellis, M., 1987. Development of a passive solar system for heating greenhouses. In: Sethi & Sharma (eds). Survey and evaluation of heating technologies for worldwide agricultural greenhouse applications. Sol. Energy 82, 832–859.

Groh, J.E., 1977. Liquid foam-greenhouse insulation and shading techniques. In: Aberkani et al. (eds): Energy saving achieved by retractable liquid foam between double polyethylene films covering greenhouses. Trans Am. Soc. Agric. Eng. 54, 275–284.

Gueymard, C., 2000. Prediction and Performance Assessment of Mean Hourly Global Radiation. Sol. Energy 68, 285–303. doi:10.1016/S0038-092X(99)00070-5

Guo, H., Li, Z., Zhang, Z., 1994. The dynamic simulation of temperature inside a sunlight greenhouse. J. Shenyang Agric. Univ. 438–443.

Gupta, A., Tiwari, G.N., 2002. Computer model and its validation for prediction of storage effect of water mass in a greenhouse : a transient analysis. Energy Convers. Manag. Manag. 43, 2625–2640.

Gupta, M.J., Chandra, P., 2002. Effect of greenhouse design parameters on conservation of energy

for greenhouse environmental control. Energy 27, 777–794. doi:10.1016/S0360-5442(02)00030-0

Gupta, R., Tiwari, G.N., 2005a. Modeling of energy distribution inside greenhouse using concept of solar fraction with and without reflecting surface on north wall. Build. Environ. 40, 63–71. doi:10.1016/j.buildenv.2004.03.014

Gupta, R., Tiwari, G.N., 2005b. Thermal modellina of a greenhouse having a north wall using periodic analysis and its experimental validation. Int. J. Ambient Energy 26, 115–128. doi:10.1080/01430750.2005.9674981

Gupta, R., Tiwari, G.N., Kumar, A., Gupta, Y., 2012. Calculation of total solar fraction for different orientation of greenhouse using 3D-shadow analysis in Auto-CAD. Energy Build. 47, 27–34. doi:10.1016/j.enbuild.2011.11.010

Ha, T., Lee, I.-B., Kwon, K.-S., Hong, S.-W., 2015. Computation and field experiment validation of greenhouse energy load using building energy simulation model. Int. J. Agric. Biol. Eng. 8, 116–127. doi:10.3965/j.ijabe.20150806.2037

Han, J., Gao, Z., Guo, H., Brad, R., Waterer, D., 2015. Comparison of Greenhouse Dehumidification Strategies. Appl. Eng. Agric. 31, 133–142. doi:10.13031/aea.31.10723

Hanan, J.J., 1998a. Greenhouses: advanced technology for protected horticulture.

Hanan, J.J., 1998b. Greenhouses: advanced technology for protected horticulture. In: Castilla (eds).Greenhouse Technology and Management.2nd Edition.Cabi.

Hanova, J., Dowlatabadi, H., 2007. Strategic GHG reduction through the use of ground source heat pump technology. Environ. Res. Lett. 2. doi:10.1088/1748-9326/2/4/044001

Hao, X., Zhang, L., Borhan, M.S., Khosla, S., 2011. Effects of temperature integration regimes with low pre-night temperatures on energy consumption, microclimate, and fruit yield in early greenhouse tomato production, in: International Symposium on High Technology for Greenhouse Systems: GreenSys2009. pp. 815–820.

Hao, X., Zheng, J., Little, C., 2015. Dynamic temperature integration with temperature drop to improve early fruit yield and energy efficiency in greenhouse cucumber production. Acta Hortic. 1107, 127–132. doi:10.17660/ActaHortic.2015.1107.17

Harnett, R.F., Sims, T.V., Bowman, G.E., 1979. Comparison of greenhouse types and their orientation. Exp. Hortic. 31, 59–66.

Hazami, M., Kooli, S., Lazaar, M., Farhat, A., 2005. Performance of a solar storage collector. Desalination 183, 167–172. doi:10.1016/j.desal.2005.03.033

Heartz, T.K., Lewis, A.J., 1982. Reflective wall reduces energy consumption. Am. Veg. Grow. 30, 22+4.

Hemming, S., Balendonck, J., Dieleman, J.A., De Gelder, A., Kempkes, F.L.K., Swinkels, G.L.A.M., De Visser, P.H.B., De Zwart, H.F., 2017. Innovations in greenhouse systems -

Energy conservation by system design, sensors and decision support systems, in: Acta Horticulturae. pp. 1–15. doi:10.17660/ActaHortic.2017.1170.1

Hemming, S., Kempkes, F.L.K., Janse, J., 2012. New greenhouse concept with high insulating double glass and new climate control strategies - Modelling and first results from a cucumber experiment, in: Acta Horticulturae. pp. 231–240.

Hemming, S., Kempkes, F.L.K., Mohammadkhani, V., 2011. New glass coatings for high insulating greenhouses without light losses - Energy saving, crop production and economic potentials, in: Acta Horticulturae. pp. 217–226.

Henshaw, P., 2016. Modelling changes to an unheated greenhouse in the Canadian subarctic to lengthen the growing season. Sustain. Energy Technol. Assessments. doi:10.1016/j.seta.2016.12.004

Hepbasli, A., 2011. A comparative investigation of various greenhouse heating options using exergy analysis method. Appl. Energy 88, 4411–4423. doi:10.1016/j.apenergy.2011.05.022

Heuvelink, E., 1989. Infuence of day and night temperature on the growth of young tomato plants. Sci. Hortic. (Amsterdam). 38, 11–22.

Hill, J.M., 2006. Dynamic modeling of tree growth and energy use in a nursery greenhouse using Matlab and Simulink. Masters thesis, New York, Cornell University.

Holman, J.P., 2010. Heat Transfer, 10th Editi. ed. Mc-GrawHill Higher education.

Hottel, H.C., 1976. A simple model for estimating the transmittance of direct solar radiation through clear atmospheres. Sol. Energy 18, 129–134.

Huang, B.K., Ozisik, M.N., Toksoy, M., 1981. Development of greenhouse solar drying for farm crops and processed products. In: Sethi and Sharma (eds). Survey and evaluation of heating technologies for worldwide agricultural greenhouse applications. Sol. Energy 82, 832–859.

Hubbard, K.G., 1994. Spatial variability of daily weather variables in the high plains of the USA. Agric. For. Meteorol. 68, 29–41. doi:10.1016/0168-1923(94)90067-1

Ioannou, A., Itard, L.C.M., 2015. Energy performance and comfort in residential buildings: Sensitivity for building parameters and occupancy. Energy Build. 92, 216–233. doi:10.1016/j.enbuild.2015.01.055

Iqbal, M., 1983. An introduction to solar radiation. Academic Press, Toronto, Canada.

Jain, D., Tiwari, G.N., 2003. Modeling and optimal design of ground air collector for heating in controlled environment greenhouse. Energy Convers. Manag. 44, 1357–1372. doi:10.1016/S0196-8904(02)00118-8

James, K., 2013. Chinese design for passive solar greenhouse [WWW Document]. URL http://spinfarming.com/tips/chinese-design-for-passive-solar-greenhouse/ (accessed 7.6.17).

Jelinkova, H., 1987. Utilization of solar energy in greenhouse. In: Sethi and Sharma (eds). Survey and evaluation of heating technologies for worldwide agricultural greenhouse applications.

Sol. Energy 82, 832–859.

Jeong, D.I., St-Hilaire, A., Gratton, Y., Bélanger, C., Saad, C., 2016. Simulation and Regionalization of Daily Global Solar Radiation: A Case Study in Quebec, Canada. Atmosphere-Ocean 54, 117–130. doi:10.1080/07055900.2016.1151766

Jolliet, O., Bourgeois, M., Danloy, L., Gay, J.B., Mantilleri, S., Moncousin, C., 1984. Test of a greenhouse using low-temperature heating. Greenhouse Construction and Covering Materials. Acta Hortic. 170, 219–226.

Jolliet, O., Danloy, L., Gay, J.B., Munday, G.L., Reist, A., 1991. HORTICERN : an improved static model for predicting the energy consumption of a greenhouse. Agric. For. Meteorol. 55, 265–294.

Kahimba, F.C., Bullock, P.R., Sri Ranjan, R., Cutforth, H.W., 2009. Evaluation of the SolarCalc model for simulating hourly and daily incoming solar radiation in the Northern Great Plains of Canada. Can. Biosyst. Eng. 51, 1–18.

Kasten, F., Czeplak, G., 1980. Solar and terrestrial radiation dependent on the amount and type of cloud. Sol. Energy 24, 177–189. doi:10.1016/0038-092X(80)90391-6

Katsoulas, N., Kittas, C., 2011. Greenhouse Crop Transpiration Modelling, in: Dr. Giacomo Gerosa (Ed.), Evapotranspiration - From Measurements to Agricultural and Environmental Applications. InTech Europe, Rijeka, Croatia.

Kavga, A., Pantelakis, S., Panidis, T., Bontozoglou, V., 2007. Investigation of the potential of long wave radiation heating to reduce energy consumption for greenhouse heating., in: International Symposium on High Technology for Greenhouse System Management. pp. 741–748.

Kavin, J., Kurtan, S., 1987. Utilization of solar energy in greenhouse. In: Sethi and Sharma (eds). Survey and evaluation of heating technologies for worldwide agricultural greenhouse applications. Sol. Energy 82, 832–859.

Kempkes, F.L.K., Janse, J., Hemming, S., 2014. Greenhouse concept with high insulating double glass with coatings and new climate control strategies; From design to results from tomato experiments. Acta Hortic. 1037, 83–92. doi:10.17660/ActaHortic.2014.1037.6

Kim, K.H., Baltazar, J.C., Haberl, J.S., 2014. Evaluation of meteorological base models for estimating hourly global solar radiation in Texas. Energy Procedia 57, 1189–1198. doi:10.1016/j.egypro.2014.10.106

Kindelan, M., 1980. Dynamic modeling of greenhouse environment. Trans Am. Soc. Agric. Biol. Eng. 1232–1239.

Kittas, C., 1994. Determination of the overall heat transfer coefficient of a greenhouse cover. Agric. For. Meteorol. 69, 201–221.

Kondili, E., Kaldellis, J.K., 2006. Optimal design of geothermal-solar greenhouses for the minimisation of fossil fuel consumption. Appl. Therm. Eng. 26, 905–915.

doi:10.1016/j.applthermaleng.2005.09.015

Körner, O., Challa, H., 2004. Temperature integration and process-based humidity control in chrysanthemum. Comput. Electron. Agric. 43, 1–21. doi:10.1016/j.compag.2003.08.003

Körner, O., Challa, H., 2003a. Design for an improved temperature integration concept in greenhouse cultivation. Comput. Electron. Agric. 39, 39–59. doi:10.1016/S0168-1699(03)00006-1

Körner, O., Challa, H., 2003b. Process-based humidity control regime for greenhouse crops. Comput. Electron. Agric. 39, 173–192. doi:10.1016/S0168-1699(03)00079-6

Körner, O., Van Straten, G., 2008. Decision support for dynamic greenhouse climate control strategies. Comput. Electron. Agric. 60, 18–30. doi:10.1016/j.compag.2007.05.005

Kristinsson, J., 2006. The Energy-producing Greenhouse, in: PLEA2006. pp. 6–8.

Kumari, N., Tiwari, G.N., Sodha, M.S., 2007. Performance Evaluation of Greenhouse having Passive or Active Heating in Different Climatic Zones of India, in: Agricultural Engineering International: The CIGR Ejournal. pp. 1–19.

Kumari, N., Tiwari, G.N., Sodha, M.S., 2003. Modelling of a greenhouse solar collector for thermal heating. Int. J. Ambient Energy 27.3, 125–136. doi:10.1080/01430750.2006.9675012

Kurata, K., 1993. Effects of greenhouse orientation and latitude on direct solar radiation transmissivity. Trans Am. Soc. Agric. Biol. Eng. 2, 8.

Kürklü, A., Bilgin, S., Özkan, B., 2003. A study on the solar energy storing rock-bed to heat a polyethylene tunnel type greenhouse. Renew. Energy 28, 683–697.

Kurpaska, S., Slipek, Z., 2000. Optimization of greenhouse substrate heating. J. Agric. Eng. Res. 76, 129–139.

Laate, E.A., 2013. The economics of production and marketing of greenhouse crops in Alberta. Economics Unit, Economics and Competitiveness Division, Alberta Agriculture, Food and Rural Development.

Lam, J.C., Hui, S.C.M., 1996. Sensitivity analysis of energy performance of office buildings. Build. Environ. 31, 27–39. doi:10.1016/0360-1323(95)00031-3

Lam, J.C., Li, D.H.W., 1998. Correlation analysis of solar radiation and cloud cover. Int. J. Ambient Energy 19, 187–198. doi:10.1080/01430750.1998.9675305

Langhans, R.W., Wolfe, M., Albright, L.D., 1985. Use of average night temperatures for plant growth for potential energy savings. Acta Hortic. 115, 31–36.

Langton, F.A., Hamer, P.J.C., 2003. Energy efficient production of high quality ornamental species.

Langton, F.A., Horridge, J.S., 2006. The effects of averaging sub- and supra-optimal temperatures on the flowering of Chrysanthemum morifolium. J. Hortic. Sci. Biotechnol. 81, 335–340.

Latimer, J.G., 2009. Dealing with the High Cost of Energy for Greenhouse Operations. Publication 430-101, Virginia Cooperative Extension, USA.

Lee, C.S., Costola, D., Swinkels, G.L.A.M., Hensen, J.L.M., 2012. On the Use of Building Energy Simulation Programs in the Performance Assessment of Agricultural Greenhouses, in: Proceedings of the 1st Asia Conference of the International Building Performance Simulation Association. Shanghai, China, pp. 1–8.

Levav, N., Zamir, N., 1987. Utilization of solar energy in greenhouse. In: Sethi & Sharma (eds). Survey and evaluation of heating technologies for worldwide agricultural greenhouse applications. Sol. Energy 82, 832–859.

Liu, B., Jordan, R.C., 1961. Daily insolation on surfaces tilted towards equator. ASHRAE Trans. 3, 53.

Liu, B.Y., Jordan, R.C., 1963. The long-term average performance of flat-plate solar-energy collectors: with design data for the US, its outlying possessions and Canada. Sol. Energy 7, 53–74.

Loutzenhiser, P.G., Manz, H., Felsmann, C., Strachan, P.A., Frank, T., Maxwell, G.M., 2007. Empirical validation of models to compute solar irradiance on inclined surfaces for building energy simulation. Sol. Energy 81, 254–267. doi:10.1016/j.solener.2006.03.009

Lristinsson, J., 2006. The energy-producing greenhouse, in: 23rd Conference on Passive and Low Energy Architecture. Geneva, Switzerland.

Lund, J.W., 2010. Direct utilization of geothermal energy. Energies 3, 1443–1471. doi:10.3390/en3081443

Lund, J.W., Freeston, D.H., Boyd, T.L., 2005. Direct application of geothermal energy : 2005 Worldwide review ☙ 34, 691–727. doi:10.1016/j.geothermics.2005.09.003

Ma, C.W., Han, J.J., Li, R., 2010. Research and development of software for thermal environmental simulation and prediction in solar greenhouse. North. Hortic. 15, 69–75.

Malfa, G., Noto, G., Parrini, F., 1992. Greenhouse heating with waste water in mild winter climatic conditions. Acta Hortic. 287, 39–46.

Malquori, L., Pellegrini, P., Tesi, R., 1993. Determination of solar energy transmitted by different greenhouse geometries. Colt. Protette 22, 81–85.

Manning, T.O., Buganski II, M.B., Mears, D.R., 1983. Engineering performance of a 1.1 hectare waste-heated greenhouse, in: III International Symposium on Energy in Protected Cultivation. p. 148 (pp. 209-218).

Martin, W., Robert, K., Ron, E., 1997. Hydrology water quantity and quality control. John Wiley & Sons, New York, USA.

Matuszko, D., 2012. Influence of the extent and general of cloud cover on solar radiation intensity. Int. J. Climatol. 31, 2403–2414.

Mavrogianopulos, G.N., Choustoulakis, P., Kyritsis, S., 1993. Tomato production in heated and unheated greenhouses. In: Teitel et al. (eds). A comparison between pipe and air heating methods for greenhouses. J. Agric. Eng. Res. 72, 259–273.

McKenney, D.W., Yemshanov, D., Fraleigh, S., Allen, D., Preto, F., 2011. An economic assessment of the use of short-rotation coppice woody biomass to heat greenhouses in southern Canada. Biomass and Bioenergy 35, 374–384. doi:10.1016/j.biombioe.2010.08.055

Meng, L., Yang, Q., Bot, G.P., Wang, N., 2009. Visual simulation model for thermal environment in Chinese solar greenhouse. Trans. Chinese Soc. Agric. Eng. 25, 164–170.

Miller, W.B., Albright, L.D., Langhans, R.W., 1985. Plant growth under averaged day/night temperatures, in: Symposium Greenhouse Climate and Its Control 174. pp. 313–320.

Mistriotis, A., Giannoulis, A., Briassoulis, D., 2011. Numerical estimation of wind loads on a greenhouse protected by a net-covered windbreak analysed as an integrated system, in: International Symposium on Advanced Technologies and Management Towards Sustainable Greenhouse Ecosystems. pp. 169–176.

Montero, M., Marfa, M., Serrano, T., Anton, S., 1987. Use of solar energy for heating of greenhouses. In. Sethi & Sharma (eds). Survey and evaluation of heating technologies for worldwide agricultural greenhouse applications. Sol. Energy 82, 832–859.

Morris, L.G., 1964. The heating and ventilation of greenhouses, National Institute of Agricultural Engineering. Silsoe, Bedfordahire.

Morris, L.G., 1956. Some aspects of the control of plant environment. J. Agric. Eng. Res. 1, 156–166.

Mpelkas, C.C., 1981. Greenhouse supplemental lighting for roses with high pressure sodium lamps, in: II International Symposium on Artificial Light in Horticulture 128. pp. 85–98.

Muneer, T., Gul, M.S., 2000. Evaluation of sunshine and cloud cover based models for generating solar radiation data. Energy Convers. Manag. 41, 461–482. doi:10.1016/S0196-8904(99)00108-9

Näslund, M., Schüssler, H.K., Ljungberg, A.S.A., 2002. Gas based infrared radiant heating in greenhouses.Aspects of energy use and plant development.

Nayak, S., Tiwari, G.N., 2008. Energy and exergy analysis of photovoltaic/thermal integrated with a solar greenhouse. Energy Build. 40, 2015–2021. doi:10.1016/j.enbuild.2008.05.007

Nederhoff, E., Houter, B., 2007. Improving energy efficiency in greenhouse vegetable production. Wellington, NZ.

Nelson, P. V., 1985. Greenhouse operation and management, 6th ed. Prentice Hall.

Nobel, P.S., 1974. Introduction to biophysical plant physiology. W. H. freeman and Company, San Fransisco, USA.

Noorollahi, Y., Bigdelou, P., Pourfayaz, F., Yousefi, H., 2016. Numerical modeling and economic

analysis of a ground source heat pump for supplying energy for a greenhouse in Alborz province, Iran. J. Clean. Prod. 131, 145–154. doi:10.1016/j.jclepro.2016.05.059

Orsini, A., Tomasi, C., Calzolari, F., Nardino, M., Cacciari, A., Georgiadis, T., 2002. Cloud cover classification through simultaneous ground-based measurements of solar and infrared radiation. Atmos. Res. 61, 251–275.

Ozgener, O., Hepbasli, A., 2005. Experimental performance analysis of a solar assisted ground-source heat pump greenhouse heating system. Energy Build. 37, 101–110. doi:10.1016/j.enbuild.2004.06.003

Öztürk, H.H., Başçetinçelik, A., 2003a. Effect of thermal screens on the microclimate and overall heat loss coefficient in plastic tunnel greenhouses. Turkish J. Agric. For. 86, 231–245. doi:10.1016/S1537-5110(03)00134-X

Öztürk, H.H., Başçetinçelik, A., 2003b. Energy and exergy efficiency of a packed-bed heat storage unit for greenhouse heating. Biosyst. Eng. 86, 231–245.

Pacheco, M., 1987. Passive system for heating greenhouses. In: Sethi & Sharma (eds). Survey and evaluation of heating technologies for worldwide agricultural greenhouse applications. Sol. Energy 82, 832–859.

Papadakis, G., Briassoulis, D., Scarascia Mugnozza, G., Vox, G., Feuilloley, P., Stoffers, J.A., 2000. Review Paper (SE—Structures and Environment). J. Agric. Eng. Res. 77, 7–38. doi:10.1006/jaer.2000.0525

Papadakis, G., Frangoudakis, A., Kyritsis, S., 1992. Mixed, forced and free convection heat transfer at the greenhouse cover. J. Agric. Eng. Res. 51, 191–205.

Papadakis, G., Manolakos, D., Kyritsis, S., 1998. Solar Radiation Transmissivity of a Single-Span Greenhouse through Measurements on Scale Models. J. Agric. Eng. Res. 71, 331–338. doi:10.1006/jaer.1998.0331

Papadopoulos, A.P., Hao, X., 1997. Effects of greenhouse covers on seedless cucumber growth, productivity, and energy use. Sci. Hortic. (Amsterdam). 68, 113–123. doi:10.1016/S0304-4238(96)00961-2

Pieters, J.G., Deltour, J.M.R., 1997. Performances of Greenhouses with the Presence of Condensation on Cladding Materials. J. Agric. Eng. Res. 68, 125–137. doi:http://dx.doi.org/10.1006/jaer.1997.0187

Pietzsch, M., Meyer, J., 2008. Use of reject heat from biogas power plants for greenhouse heating, in: Acta Horticulturae. pp. 719–724. doi:10.17660/ActaHortic.2008.801.83

Popovski, K., 1986. Location of heating installations in greenhouses for low temperature heating fluids. In: Bartzanas et al. (eds). Influence of the heating method on greenhouse microclimate and energy consumption. Biosyst. Eng. 91, 487–499.

Portree, J., 1996. Greenhouse vegetable production guide for commercial growers.Ministry of Agr., Fisheries and Food, Province of British Columbia, Ext. Systems Branch. Victoria, BC,

Canada.

Professional Plastics, 2017. Thermal Properties of Plastic Materials [WWW Document]. Prof. Plast. INC. URL https://www.professionalplastics.com/professionalplastics/ThermalPropertiesofPlasticMaterials.pdf (accessed 4.20.17).

Pucar, M.D., 2002. Enhancement of ground radiation in greenhouses by reflection of direct sunlight. Renew. Energy 26, 561–586. doi:10.1016/S0960-1481(01)00155-0

Qaisar, S., Fonk, A., Bartus, K., Pope, C., Min Nam, K., Alvarez, M., Zorra, I., 2010. Power Plant Waste Heat Utilization for Greenhouse Applications.

Rahman, M.M., Rasul, M.G., Khan, M.M.K., 2010. Energy conservation measures in an institutional building in sub-tropical climate in Australia. Appl. Energy 87, 2994–3004. doi:10.1016/j.apenergy.2010.04.005

Raunkiaer, C., 1934. The life forms of plants and statistical plant geography; being the collected papers of C. Raunkiaer. Oxford: Clarendon Press.

Rebuck, S.M., Aldrich, R.A., White, J.W., 1977. Internal curtains for energy conservation in greenhouses. Trans Am. Soc. Agric Eng 4, 732–734.

Rincón, V.J., Páez, F., Sánchez-Hermosilla, J., Pérez, J., Callejón, Á., 2012. Estimation of leaf-area index in greenhouse tomato crop to determine the volume rate to spray, in: Power and Machinery. International Conference of Agricultural Engineering-CIGR-AgEng 2012: Agriculture and Engineering for a Healthier Life. Valencia, Spain, p. 402.

Roberts, W., Mears, D., Simpkins, J., Cipolletti, J., 1981. Movable thermal insulation for greenhouses. Proc. the... Natl. Agric. Plast. Congr.

Roberts, W.J., Mears, D.R., 1978. Energy conservation in greenhouses in USA. In Aberkani et al. (eds): Energy saving achieved by retractable liquid foam between double polyethylene films covering greenhouses. Trans Am. Soc. Agric. Eng. 54, 275–284.

Rorabaugh, P., Jensen, M., Giacomelli, G., 2002. Introduction to Controlled Environment Agriculture and Hydroponics. Control. Environ. Agric. Cent. 1–130.

Runkle, E., Both, A., 2012. Greenhouse energy conservation strategies. Michigan State Univ. Bul. 1.

Sallanbus, H., Durceylan, E., Yelboga, K., 1987. Utilization of solar energy in greenhouse. In: Sethi & Sharma (eds). Survey and evaluation of heating technologies for worldwide agricultural greenhouse applications. Sol. Energy 82, 832–859.

Sanford, S., 2011. Reducing greenhouse energy consumption—An overview. ENERGY 3907: 01, University of Wisconsin–Extension. University of Wisconsin–Extension.

Santamouris, M., Argiriou, A., Vallindras, M., 1994. Design and operation of a low energy consumption passive solar agricultural greenhouse. Sol. Energy 52, 371–378.

doi:10.1016/0038-092X(94)90114-H

Santamouris, M.I., 1993. Active Solar Agricultural Greenhouses. the State of the Art. Int. J. Sol. Energy 14, 19–32. doi:10.1080/01425919308909793

Sarkar, M.N.I., 2016. Estimation of solar radiation from cloud cover data of Bangladesh. Renewables Wind. Water, Sol. 3, 1–15. doi:10.1186/s40807-016-0031-7

Schepens, G., Mahy, D., Buis, H., Palz, W., 1987. Solar energy in agriculture and industry: Potential of solar heat in European agriculture, an assessment. In: Beshada et al.(eds). Winter performance of a solar energy greenhouse in southern Manitoba. Can. Biosyst. Eng. 48, 1–8.

Semple, L., Carriveau, R., Ting, D.S.K., 2017. Assessing heating and cooling demands of closed greenhouse systems in a cold climate. Int. J. Energy Res. doi:10.1002/er

Semple, L.M., Carriveau, R., Ting, D.S.K., 2016. Potential for large-scale solar collector system to offset carbon-based heating in the Ontario greenhouse sector. Int. J. Sustain. Energy 6451, 1–15. doi:10.1080/14786451.2016.1270946

Sengar, S., Kothari, S., 2008. Thermal modeling and performance evaluation of arch shape greenhouse for nursery raising. African J. Math. Comput. Sci. Res. 1, 1–9.

Sethi, V.P., 2009. On the selection of shape and orientation of a greenhouse: Thermal modeling and experimental validation. Sol. Energy 83, 21–38. doi:10.1016/j.solener.2008.05.018

Sethi, V.P., Lal, T., Gupta, Y.P., Hans, V.S., 2003. Effect of greenhouse micro-climate on the selected summer vegetables. J. Res. (India)-PAU.

Sethi, V.P., Sharma, S.K., 2008. Survey and evaluation of heating technologies for worldwide agricultural greenhouse applications. Sol. Energy 82, 832–859. doi:10.1016/j.solener.2008.02.010

Sethi, V.P., Sharma, S.K., 2007. Thermal modeling of a greenhouse integrated to an aquifer coupled cavity flow heat exchanger system. Sol. Energy 81, 723–741. doi:10.1016/j.solener.2006.10.002

Sethi, V.P., Sharma, S.K., 2007. Greenhouse heating and cooling using aquifer water. Energy 32, 1414–1421. doi:10.1016/j.energy.2006.10.022

Sethi, V.P., Sumathy, K., Lee, C., Pal, D.S., 2013. Thermal modeling aspects of solar greenhouse microclimate control: A review on heating technologies. Sol. Energy 96, 56–82. doi:10.1016/j.solener.2013.06.034

Sharan, G., Prakash, H., Jadhav, R., 2004. Performance of Greenhouse Coupled to Earth-Tube-Heat-Exchanger in Closed-Loop Mode.

Sheard, G.F., 1977. Shelter and the effect of wind on the heat loss from greenhouses, in: Symposium on More Profitable Use of Energy in Protected Cultivation. pp. 357–360.

Short, T.H., Shah, S.A., 1981. A portable polystyrene-pellet insulation system for greenhouses. Trans. ASAE 24, 275–284.

Shukla, A., Tiwari, G.N., Sodha, M.S., 2006a. Thermal modeling for greenhouse heating by using thermal curtain and an earth – air heat exchanger. Build. Environ. 41, 843–850. doi:10.1016/j.buildenv.2005.04.014

Shukla, A., Tiwari, G.N., Sodha, M.S., 2006b. Energy Conservation Potential of Inner Thermal Curtain in an Even Span Greenhouse. Trends Appl. Sci. Res. 1, 542–552.

Sigrimis, N., Anastasiou, A., Rerras, N., 2000. Energy saving in greenhouses using temperature integration: A simulation survey. Comput. Electron. Agric. 26, 321–341. doi:10.1016/S0168-1699(00)00083-1

Singh, D., Basu, C., Meinhardt-wollweber, M., Roth, B., 2015. LEDs for energy ef fi cient greenhouse lighting. Renew. Sustain. Energy Rev. 49, 139–147. doi:10.1016/j.rser.2015.04.117

Singh, G., Singh, P.P., Lubana, P.P.S., Singh, K.G., 2006. Formulation and validation of a mathematical model of the microclimate of a greenhouse. Renew. Energy 31, 1541–1560. doi:10.1016/j.renene.2005.07.011

Singh, R.D., Tiwari, G.N., 2010. Energy conservation in the greenhouse system: A steady state analysis. Energy 35, 2367–2373. doi:10.1016/j.energy.2010.02.003

Singh, R.D., Tiwari, G.N., 2000. Thermal heating of controlled environment greenhouse: A transient analysis. Energy Convers. Manag. 41, 505–522. doi:10.1016/S0196-8904(99)00095-3

Snyder, R.G., 1992. Greenhouse tomato handbook. Publication-Cooperative Extension Service, Mississippi State University (USA).

Solar Energy Laboratory, 2014a. TRNSYS 17 Manual, Volume 1. Madison.

Solar Energy Laboratory, 2014b. TRNSYS 17 Manual, Volume 5, 75-76, 147,165-166, 181-182. Madison.

Sorensen, B., 1989. Experiments with energy storage in a high-latitude greenhouse. Sol. Energy 42, 293–301.

Spanomitsios, G.K., 2001. Temperature control and energy conservation in a plastic greenhouse. J. Agric. Eng. Res. 80, 251–259. doi:10.1006/jaer.2001.0738

Spencer, J.W., 1971. Fourier series representation of the position of the sun. Search 2, 172–172.

Spencer, R., 2009. Starting a commercial greenhouse business in Alberta [WWW Document]. URL http://www1.agric.gov.ab.ca/$department/deptdocs.nsf/all/opp11207 (accessed 7.12.16).

Spokas, K., Forcella, F., 2006. Estimating hourly incoming solar radiation from limited meteorological data. Weed Sci. 54, 182–189. doi:10.1614/WS-05-098R.1

Stanciu, C., Stanciu, D., Dobrovicescu, A., 2016. Effect of Greenhouse Orientation with Respect to E-W Axis on its Required Heating and Cooling Loads. Energy Procedia 85, 498–504.

doi:10.1016/j.egypro.2015.12.234

Statistics Canada, 2015. Statistical-overview-of-the-Canadian-greenhouse-vegetable-industry [WWW Document]. doi:http://www.agr.gc.ca/eng/industry-markets-and-trade/market-information-by-sector/horticulture/horticulture-sector-reports/statistical-overview-of-the-canadian-greenhouse-vegetable-industry-2015/?id=1468861362193

Statistics Canada, 2008. Greenhouse, Sod and Nursery Industries. Statistics Canada [WWW Document]. doi:22-202-XWE

Stone, P., Youngsman, J., 2006. Gas-fired infrared heating for greenhouses. Buffalo, NY.

Stone, R.J., 1993. Improved statistical procedure for the evaluation of solar radiation estimation models. Sol. Energy 51, 289–291. doi:10.1016/0038-092X(93)90124-7

Supit, I., van Kappel, R.R., 1998. A simple method to estimate global radiation. Sol. Energy 63, 147–160. doi:10.1016/S0038-092X(98)00068-1

Swinbank, W.C., 1963. Long-wave radiation from clear skies. Q. J. R. Meteorol. Soc. 89, 339–348.

Swinkels, G.L.A.M., Sonneveld, P.J., Bot, G.P.A., 2001. Improvement of Greenhouse Insulation with Restricted Transmission Loss through Zigzag Covering Material. J. Agric. Eng. Res. 80, 283–292. doi:10.1006/jaer.2001.0732

Taki, M., Ajabshirchi, Y., Ranjbar, S.F., Rohani, A., Matloobi, M., 2016. Modeling and experimental validation of heat transfer and energy consumption in an innovative greenhouse structure. Inf. Process. Agric. 3, 157–174. doi:10.1016/j.inpa.2016.06.002

Tantau, H.J., 1998. Energy saving potential of greenhouse climate control. Math. Comput. Simul. 48, 93–101. doi:10.1016/S0378-4754(98)00145-1

Tantau, H.J., Meyer, J., Schmidt, U., Bessler, B., 2009. Low energy greenhouse-a system approach, in: International Symposium on High Technology for Greenhouse Systems: GreenSys2009 893. pp. 75–84.

Teitel, M., Peiper, U.M., Zvieli, Y., 1996. Shading screens for frost protection. Agric. For. Meteorol. 81, 273–286. doi:10.1016/0168-1923(95)02321-6

Teitel, M., Segal, I., Shklyar, A., Barak, M., 1999. A Comparison between Pipe and Air Heating Methods for Greenhouses. J. Agric. Eng. Res. 72, 259–273.

Teitel, M., Shklyar, A., Elad, Y., Dikhtyar, V., Jerby, E., 2000. Development of a microwave system for greenhouse heating, in: In International Conference and British-Israeli Workshop on Greenhouse Techniques towards the 3rd Millennium 534. pp. 189–196.

Teitel, M., Tanny, J., 1998. Radiative heat transfer from heating tubes in a greenhouse. J. Agric. Eng. Res. 69, 185–188.

Tesi, R., 2001. Medios de protección para la hortofruticultura y el viverismo. In: Castila (eds) Greenhouse Technology and Management.2nd edition, Cabi.

Thomas, Y., Wang, L., Denzer, A., 2017. Energy Savings Analysis of a Greenhouse Heated by Waste Heat, in: Proceedings of the 15th IBPSA Conference. San Francisco, CA, USA, Aug. 7-9, pp. 2512–2517.

Tian, W., 2013. A review of sensitivity analysis methods in building energy analysis. Renew. Sustain. Energy Rev. 20, 411–419. doi:10.1016/j.rser.2012.12.014

Tiwari, G.N., 2003. Greenhouse Technology for Controlled Environment. Alpha Science International Ltd., Pangbourne, England.

Tiwari, G.N., Akhtar, M.A., Shukla, A., Khan, M.E., 2006. Annual thermal performance of greenhouse with an earth – air heat exchanger : An experimental validation. Renew. Energy 31, 2432–2446. doi:10.1016/j.renene.2005.11.006

Tiwari, G.N., Din, M., Srivastava, N.S.L., Jain, D., Sodha, M.S., 2002. Evaluation of solar fraction (Fn) for the north wall of a controlled environment greenhouse: an experimental validation. Int. J. Energy Res. 26, 203–215. doi:10.1002/er.776

Tiwari, G.N., Gupta, A., 2002. Performance evaluation of greenhouse for different climatic zones of India. J Sol. Energy Soc. India 22, 15–20.

Tiwari, G.N., Gupta, A., Gupta, R., 2003. Evaluation of solar fraction on north partition wall for various shapes of solarium by Auto-Cad. Energy Build. 35, 507–514. doi:10.1016/S0378-7788(02)00158-5

Tong, G., Z., Che, Z., Bai, Y., Yamaguchi., T., 2008. Air exchange rate calculation for solar greenhouse using thermal balance. J. Shenyang Agric. Univ. 39, 459–462.

Tong, G., Christopher, D.M., Li, B., 2009. Numerical modelling of temperature variations in a Chinese solar greenhouse. Comput. Electron. Agric. 68, 129–139. doi:10.1016/j.compag.2009.05.004

Tong, G., Christopher, D.M., Li, T., Wang, T., 2013. Passive solar energy utilization: A review of cross-section building parameter selection for Chinese solar greenhouses. Renew. Sustain. Energy Rev. 26, 540–548. doi:10.1016/j.rser.2013.06.026

Tong, G., Christopher, D.M., Tianlai, L., Tieliang, W., 2008. Temperature variations inside Chinese solar greenhouses with external climatic conditions and enclosure materials. Int. J. Agric. Biol. Eng. 1, 21–26. doi:10.3965/j.issn.1934-6344.2008.02.021-026

Trigui, M., Barrington, S., Gauthier, L., 2001. SE—Structures and environment: A Strategy for Greenhouse Climate Control, Part I: Model Development. J. Agric. Eng. Res. 78, 407–413. doi:10.1006/bioe.2001.0020

Trnka, M., Žalud, Z., Eitzinger, J., Dubrovský, M., 2005. Global solar radiation in Central European lowlands estimated by various empirical formulae. Agric. For. Meteorol. 131, 54–76. doi:10.1016/j.agrformet.2005.05.002

Truffault, V., Fifel, F., Longuenesse, J.J., Vercambre, G., Le Quillec, S., Gautier, H., 2015. Impact of Temperature Integration under Greenhouse on Energy Use Efficiency, Plant Growth and

Development and Tomato Fruit Quality Depending on Cultivar Rootstock Combination, in: II International Symposium on Horticulture in Europe. pp. 95–100.

Tunc, M., Venart, J.E.S., Sollows, K., 1985. Bivalent (hybrid) heat pump-oil heating systems for greenhouses. J. heat Recover. Syst. 5, 483–491.

Tzivanidis, C., Antonopoulos, K.A., Gioti, F., 2011. Numerical simulation of cooling energy consumption in connection with thermostat operation mode and comfort requirements for the Athens buildings. Appl. Energy 88, 2871–2884. doi:10.1016/j.apenergy.2011.01.050

Urban, L., 1997. Introduction to greenhouse production. In: Castilla (eds). Greenhouse Technology and Management.2nd edition, Cabi.

Vadiee, A., 2011. Energy Analysis of the Closed Greenhouse concept. PhD thesis, KTH Royal Institute of Technology.

Vadiee, A., Martin, V., 2013. Energy analysis and thermoeconomic assessment of the closed greenhouse - The largest commercial solar building. Appl. Energy 102, 1256–1266. doi:10.1016/j.apenergy.2012.06.051

Van't Ooster, A., Van Henten, E.J., Janssen, E.G.O.N., Bot, G.P.A., Dekker, E., 2008. Development of concepts for a zero-fossil-energy greenhouse. Acta Hortic. 801 PART 1, 725–732. doi:10.17660/ActaHortic.2008.801.84

Van Beers, D., Biswas, W.K., 2008. A regional synergy approach to energy recovery : The case of the Kwinana industrial area , Western Australia. Energy Convers. Manag. 49, 3051–3062. doi:10.1016/j.enconman.2008.06.008

Van Berkel, N., Verveer, J.B., 1984. Methods of CO2 enrichment in the Netherlands. In: Castilla (eds). Greenhouse Technology and Management.2nd edition, Cabi.

Vanthoor, B.H.E., Stanghellini, C., Van Henten, E.J., De Visser, P.H.B., 2011. A methodology for model-based greenhouse design: Part 1, a greenhouse climate model for a broad range of designs and climates. Biosyst. Eng. 110, 363–377. doi:10.1016/j.biosystemseng.2011.06.001

Victoria, N.G., Kempkes, F.L.K., Van Weel, P., Stanghellini, C., Dueck, T.A., Bruins, M., 2012. Effect of a diffuse glass greenhouse cover on rose production and quality, in: Acta Horticulturae. pp. 241–248.

Villeneuve, J., De Halleux, D., Gosselin, A., Amar, D., 2005. Concept of dynamic liquid foam insulation for greenhouse insulation and the assessment of its energy consumption and agronomic performances, in: Acta Horticulturae. pp. 605–610.

Vreugdenhil, H., Mittleider, J.F., 2009. Economic Feasibility of Utilizing Waste~ Water Heat in Commercial Greenhouses in North Dakota.

Weimann, G., 1986. Investigations on new plastic film greenhouse design. In: Papadakis et al. (eds). Review Paper (SE—Structures and Environment): Radiometric and thermal properties of, and testing methods for, greenho. J. Agric. Eng. Res. 77, 7–38.

Wells, O.S., 1980. Conserving energy in plastic greenhouses with liquid foam insulation. In Aberkani et al. (eds): Energy saving achieved by retractable liquid foam between double polyethylene films covering greenhouses. Trans Am. Soc. Agric. Eng. 54, 275–284.

Whillier, A., 1967. Design factors influencing solar collector performance. Low Temp. Eng. Appl. Sol. Energy 27–40.

White, J.W., Sherry, W.J., 1981. High intensity lighting and reflective thermal blanket combination for economy of energy, in: II International Symposium on Artificial Light in Horticulture 128. pp. 119–130.

Wollaeger, H., 2015. Why should greenhouse growers pay attention to vapor-pressure deficit and not relative humidity? Michigan State University Extension.

Wong, H.Y., 1977. Heat transfer for engineers. Longman, New York, USA.

Worley, J.W., 2009. Greenhouses: heating, cooling and ventilation.The University of Georgia.

Xiao, S., van der Ploeg, A., Bakker, M., Heuvelink, E., 2004. Two Instead of Three Leaves Between Tomato Trusses: Measured and Simulated Effects on Partitioning and Yield. Acta Hortic. 303–308. doi:10.17660/ActaHortic.2004.654.35

Xu, F., Li, S., Ma, C., Zhao, S., Han, J., Liu, Y., Hu, B., Wang, S., 2013. Thermal environment of Chinese solar greenhouses: Analysis and simulation. Appl. Eng. Agric. 29, 991–997. doi:10.13031/aea.29.10205

Yang, S., Gu, C., Ashtiani-araghi, A., Yong, J., Yong, J., 2015. Heat gain and contribution to heating from supplemental lighting in greenhouse. Eng. Agric. Environ. Food 8, 67–71. doi:10.1016/j.eaef.2015.04.001

Yang, S., Son, J., Lee, S., Cho, S., Ashtiani-araghi, A., 2016. Surplus thermal energy model of greenhouses and coefficient analysis for effective utilization 14, 1–15.

Younes, S., Muneer, T., 2007. Comparison between solar radiation models based on cloud information. Int. J. Sustain. Energy 26, 121–147. doi:10.1080/14786450701549824

Yu, H., Chen, Y., Hassan, S.G., Li, D., 2016. Prediction of the temperature in a Chinese solar greenhouse based on LSSVM optimized by improved PSO. Comput. Electron. Agric. 122, 94–102. doi:10.1016/j.compag.2016.01.019

Zhang, J., Li, J., 1966. Ways and measures to optimize the performance of solar greenhouse structure (upper part). In: Tong et al. (eds). Passive solar energy utilization: A review of cross-section building parameter selection for Chinese solar greenhouses. Renew. Sustain. Energy Rev. 26, 540–548.

Zhang, L., Hu, Z., Fan, J., Zhou, D., Tang, F., 2014. A meta-analysis of the canopy light extinction coefficient in terrestrial ecosystems. Front. Earth Sci. 8, 599–609. doi:10.1007/s11707-014-0446-7

Zhang, X.H., Chen, Q.Y., Qv, M., Yu, F., 2008. Heating effects of source heat pump on sun-light

greenhouse. J. Shanghai Jiao Tong Univ. 26, 436–439.

Zhang, Y., Gauthier, L., Halleux, D. De, Dansereau, B., Gosselin, A., 1996. Effect of covering materials on energy consumption and greenhouse microclimate. Agric. For. Meteorol. 82, 227–244.

Zheng, W., Shi, H., Chen, S., Zhu, M., 2009. Benefit and cost analysis of mariculture based on ecosystem services. Ecol. Econ. 68, 1626–1632. doi:10.1016/j.ecolecon.2007.12.005

Zhou, N., Yu, Y., Yi, J., Liu, R., 2017. A study on thermal calculation method for a plastic greenhouse with solar energy storage and heating. Sol. Energy 142, 39–48. doi:10.1016/j.solener.2016.12.016

Zou, W., Yao, F., Zhang, B., He, C., Guan, Z., 2017. Verification and predicting temperature and humidity in a solar greenhouse based on convex bidirectional extreme learning machine algorithm. Neurocomputing 249, 72–85. doi:10.1016/j.neucom.2017.03.023